The University Of Sheffield.

In vivo imaging and analysis of host-pathogen interactions of intracellular pathogens

By: Josie F Gibson

A thesis submitted in partial fulfilment of the requirements for the degree of Doctor of Philosophy

The University of Sheffield
Department of Infection, Immunity & Cardiovascular disease

Submission Date: September 2017

Abstract

Cellular and extracellular host-pathogen interactions are important in the progression of infection. Extracellular survival and growth can be significant for pathogen dissemination. Equally, intracellular pathways, such as autophagy, can be employed in host cell defence. Autophagy is a cellular self-degradation process that recycles cellular components through lysosomal degradation. Primarily for regulating starvation and housekeeping pathways, autophagy is also important for degradation of invading intracellular pathogens. Selective autophagy receptors can also target pathogens for autophagic degradation. However, some intracellular pathogens are able to subvert or block host cell autophagy. *Cryptococcus neoformans* and *Staphylococcus aureus* represent fungal and bacterial pathogens which can reside either intracellularly or extracellularly. The role of host cell autophagy in *C. neoformans* and *S. aureus* infection is unclear. Infection of zebrafish with *C. neoformans* or *S. aureus* enabled *in vivo* imaging of host-pathogen interactions, to examine infection growth dynamics and dissemination, in addition to cellular level imaging of pathogen interactions with host cell autophagy components.

Cryptococcal infection can cause cryptococcal meningitis, frequently associated with cerebral infarcts. Analysis of cryptococcal proliferation during infection suggested that formation of intravascular cryptococcal masses precedes invasion of surrounding tissue. Vessel integrity analysis highlighted cryptococcal-mediated vascular damage, potentially providing a route for tissue dissemination. Vasculature damage may explain the origin of cortical infarcts in disease.

Autophagy mutant zebrafish were generated to analyse host autophagy in pathogen infection. Characterisation of mutant larvae revealed a clear survival and growth defect, indicating autophagy is required for larval development. Autophagy mutants were subsequently used to analyse the role of autophagy during infection through analysis of pathogenic burden and pathogen association with autophagosome marker LC3-II. LC3-II recruitment to pathogens was reduced in autophagy mutant neutrophils. Additionally, selective autophagy receptor p62 was recruited to *S. aureus* and *C. neoformans* within neutrophils, highlighting the involvement of host cell autophagy during infection.

Acknowledgements

I would like to thank my supervisors, Dr Simon Johnston, Prof Stephen Renshaw and Prof Philip Ingham, for their advice, encouragement and support throughout my PhD, in many aspects of my PhD including scientific ideas and technique, training, critical thinking, presentation and scientific writing. I would like to thank my personal tutor Dr Heather Wilson for her advice and support. Special thanks to Adam Pyrah, my family and friends for their support and encouragement over the last four years.

I would like to thank the entire D31 lab, the Johnston, Renshaw and Elks groups for their support, advice and friendship. Thanks to Aleksandra Bojarczuk for her support and for training in cryptococcal zebrafish infection and to Justyna Serba and Nelly Wagner for training in staphylococcus zebrafish infection.

I am thankful to Ingham and Carney groups for their welcoming into the lab, support and advice. Many thanks to Abraha Gebregziabher, Raymond Lee, and Jia Jia Ma, for advice, scientific chats and friendship. Additionally I would like to thank many new friends I met after moving to Singapore for all the fun times and for their help in integrating into a new place.

I would like to thank the aquarium staff, both at The University of Sheffield aquarium and the Institute of Molecular and Cell Biology fish facility (Singapore), particularly for their help in sending fish overseas, in use of the quarantine facility and for fish welfare. I would like to thank Darren Robinson and Felix Ellett for training and help with imaging.

I am very thankful to the University of Sheffield and A*Star graduate academy for funding my project, enabling me to conduct research and complete my PhD.

TABLE OF CONTENTS

Abbreviations

ADAM10 a disintegrin and metallopeptidase domain 10, ***agr*** Accessory gene regulator, **AIDS** acquired immune deficiency syndrome, **AMPK** AMP-dependent protein kinase, **AMP** adenosine monophosphate, **ATP** adenosine triphosphate, **APC** antigen presenting cell, **ATG3** autophagy related 3**, ATG** Autophagy-related genes, **ATG5** autophagy related 3, **BHI** Brain heart infusion, **BLAST** Basic Local Alignment Search Tool, **bp** Base pair**, CA-MRSA** community acquired methicillin-resistant *Staphylococcus aureus*, **cDNA** complementary DNA, **ClfA** Clumping factor proteins A, **ClfB** Clumping factor proteins B, **CFU** colony forming units, **CMA** Chaperone mediated autophagy, **CM** cryptococcal meningitis, **CRISPR** Clustered Regularly Interspaced Short Palindromic Repeat, **DAMP** danger associated molecular pattern, **DC** Dendritic cell, **DNA** deoxyribonucleic acid, **Dpf** days post fertilisation, **Dpi** days post infection, **Eap** extracellular adherence protein, **EET** eosinophil extra-cellular trap, **Efb** extracellular fibrinogen-binding protein, **ER** endoplasmic reticulum, *ETs* ***exfoliative toxins,*** **FcR** receptor to the Fc region of antibodies, **FnBPA** Clumping factor proteins A, **FnBPB** Clumping factor proteins B, **GABARAP** GABA Type A Receptor-Associated Protein, **GATE-16** Golgi-associated ATPase enhancer of 16 kDa, **GalXM** galactoxylomannan, **GAL4** galactose responsive transcription factor, **GFP**: Green fluorescence protein, **GXM** glucuronoxylomannan, **HA-MRSA** hospital acquired methicillin-resistant *Staphylococcus aureus*, **Het** Heterozygous, **Hom** Homozygous, **Hsc70** heat shock cognate protein of 70 kDa, **HIV** Human immunodeficiency virus, **Hpf** Hours post fertilisation, **Hpi** Hours post infection, **HUVECs** Human umbilical vein endothelial cells, **IFN-γ** interferon gamma, **Ig** immunoglobin, **IL** interleukin, **LAMP-2A** lysosome-associated membrane protein type 2A, **LAP** LC3 associated phagocytosis, **LB** Luria Bertani medium, **LC3** Microtubule-Associated Protein 1 Light Chain 3**, LIR** LC3 interacting region, **LPS** lipopolysaccharide, **LTA** lipoteichoic acid, **LTB4** leukotriene B4, **MEFs** mouse embryonic fibroblasts **MHC-I** major-histocompatibility complex class I molecule, **MHC-II** major-histocompatibility complex class II molecule, **MMP-2** metalloproteinase-2, **MPO** myeloperoxidase, **MPs** mannoproteins, **MRSA** methicillin-resistant *Staphylococcus aureus*, **mTOR** mammalian target of rapamycin, **mTORC1** mammalian target of rapamycin complex 1, **mTORC2** mammalian target of rapamycin complex 2, **MyD88** myeloid differentiation primary response 88, **NBR1** neighbour of Brca1 gene, **NDP52** nuclear dot protein 52, **NETs** neutrophil extracellular traps, **NF-kB** nuclear factor kappa-light-chain-enhancer of activated B cells**, NK** Natural killer cell, **NLR** NOD-like receptors, **PAMP** pathogen associated molecular pattern, **PAS** pre-autophagosomal structure, **PB1** (Phox/Bem 1p) domains, **PBS** Phosphate buffered saline, **PCR** Polymerase chain reaction, **PE** phosphatidylethanolamine, **PGN**

peptidoglycan, **PI3K** phosphatidylinositol 3-kinase, **Plb** phospholipase B, **PRIP** phospholipase C-related catalytically inactive protein, **PRR** Pattern recognition receptors, **p62/SQTSM1** sequestosome one. **RLR** RIG-like receptors, **RNA** ribonucleic acid, **ROS** reactive oxygen species, **rpm** revolutions per minute, **SAGs** super antigens, **SAR** selective autophagy receptor, **SEs** staphylococcal enterotoxins**, SD** standard deviation, **SEM** Standard error of the mean **S1P** sphingosine-1-phosphate, **SK1** sphingosine kinase, **SNPs** single nucleotide polymorphisms, **TALENs** transcription activator-like effector nucleases, **TAX1BP1** Tax1 Binding Protein 1, **TLR** Toll-like receptor, **TNF-α** tumour necrosis factor alpha, TSST **toxic shock syndrome toxin, UAS** Upstream activation sequence**, UBA** ubiquitin-associated, **UBD** ubiquitin-binding domain**, UTR** untranslated region, **VRSA** vancomycin-resistant *Staphylococcus aureus*, **WT** wild type, **ZFN** Zinc-finger nucleases, **3-MA** 3-methyladenine, **°C** degrees Celsius.

List of tables

List of figures

Chapter 1: Introduction

Autophagy is a conserved homeostatic process activated in response to starvation or damage. It enables cells to recycle the components of proteins and organelles following their degradation (Mizushima et al. 2008; Tanida 2011). An autophagosome is characterised by a double membrane vesicle, which surrounds the cargo selected for degradation. Fusion of lysosomes, containing lysosomal hydrolases, leads to the degradation of the contents of the autophagosome (Mizushima 2007). In addition to its homeostatic function, autophagy plays a fundamental role in immunity (Crotzer & Blum 2010). Intracellular pathogens can be targeted to the autophagic pathway, whereby pathogens inside the cell are degraded (Levine et al. 2011). Both *Cryptococcus neoformans* and *Staphylococcus aureus* can survive as intracellular pathogens, and as such, may be targeted to the autophagy pathway.

Diverse survival strategies are used by pathogens to infect and replicate inside a host cell. Unsurprisingly, pathogens also have different means to block or subvert the autophagy pathway, allowing their continuing survival (Mizushima 2007). Research into the role of autophagy employed by host cells in their defence against pathogens, and conversely how pathogens confront or evade host cell autophagy, may develop a greater understanding of how pathogens could be targeted therapeutically.

Investigating infection within a complete organism is useful in the study of immune response to infection. *In vivo* experiments provide an environment in which the pathogen interacts with multiple extracellular, cellular and sub-cellular host components, in conditions which exist in a living animal. These interactions are much more complex than the conditions that can be created in *in vitro* analysis, and enable analysis of how pathogens truly interact with a large range of host defence mechanisms. Consequently, a model organism is valuable to study the role autophagy plays within infection. Consideration of the many attributes of the zebrafish (*Danio rerio*) as an *in vivo* model, such as *in vivo* imaging potential, genetic manipulation and similarity of the immune system, highlights zebrafish as an ideal model organism for investigation of the immune response to infection in vertebrates (Renshaw & Trede 2012; Goldsmith & Jobin 2012). Therefore, the zebrafish model has been chosen for investigation of infection progression dynamics and the role of host cell autophagy in *Cryptococcus neoformans* and *Staphylococcus aureus* infection.

1.1 Innate immune system

1.1.1 Role of the innate immune system in infection

The innate immune system is involved in the first line of defence against pathogens that have invaded the host. The innate immune system is a non-specific defence against invading pathogens, and is comprised of: a physical barrier to infection, anti-microbial molecules and innate immune cells. The role of the innate immune system is to block access of pathogens from the host and to recognise invading pathogens and molecules related to the pathogen. The innate immune system can raise an appropriate anti-pathogen response, for example degrading the pathogen or promoting other immune responses, such as phagocyte cell recruitment, to block the spread of the pathogen throughout the host. The innate immune system provides a rapid and non-specific response, through generation of cytokines and chemokines, activation of phagocytes and other innate immune cells, and ultimately leads to the activation of the adaptive immune system. There are several components of the innate immune system which enable this.

1.1.2 Components of the innate immune system

The first line of host defence is the physical barring of pathogens from entry into the host tissue. Epithelial surfaces are potential routes of entry to pathogens, however also represent a major barrier to infectious particles. Tight-junctions between epithelial cells provide a continuous physical barrier between cells, for example in the skin, respiratory tract or gastrointestinal tract (Guttman & Finlay 2009; Anderson & Van Itallie 2009). Pathogens are able to invade the host when the epithelial layer is broken, for example in a skin wound, or are able to directly target tight-junctions. For example, *Clostridium perfringens*, a food poisoning causing bacteria, employs a toxin which binds to claudins, major tight-junction proteins, resulting in loss of tight junction integrity from epithelial cells (Sonoda et al. 1999). The physical barriers to infection are supported by antimicrobial molecules which help to prevent pathogen entry. For example, saliva, sweat, tears, stomach acid, secreted enzymes and antimicrobial proteins act to prevent pathogen access to host tissue. Mucus (and cilia movement) in the lung promote the expulsion of inhaled pathogens, by preventing interaction with the epithelial layer (Murphy 2012). Although physical barriers are generally effective in blocking pathogen access, where pathogens are able to gain entry into the host such as in injury or pathogen mediated mechanisms, further immune responses are required.

In cases where pathogens are able to access host tissues, rapid responses from innate immune cells are used as an initial defence. The innate cell types which first encounter invading pathogens recognise them through the use of pattern recognition receptors (PRRs). PRRs include Toll-like receptors (TLRs), RIG-like receptors (RLRs), and NOD-

like receptors (NLRs) which are located in cellular membranes (TLRs) or cytoplasm (RLRs and NLRs). PRRs recognise PAMPs (pathogen associated molecular patterns), specific pathogen antigens, and also DAMPS (danger associated molecular patterns), which may result from host cell damage caused by pathogens or inflammation. Cells which recognise PAMPS or DAMPS enable the activation of immune pathways responsible for pathogen degradation through signalling cascades which results in phagocytosis, cytokine secretion, immune cell chemotaxis and inflammation (Hato & Dagher 2015).

Phagocytic cells represent a large majority of innate cells and includes macrophages, neutrophils and dendritic cells. Neutrophils are the most abundant white blood cells, and effectively kill and degrade phagocytosed pathogens (discussed in section 1.1.4). Macrophages and dendritic cells (DCs), as professional antigen presenting cells, degrade foreign objects and later stimulate the adaptive immune response. Another phagocytic cell type, eosinophils, can phagocytose pathogens, but are largely involved in cytotoxic degradation of parasitic infections. Eosinophils also have an ability to co-ordinate the innate immune response (Shamri et al. 2011). Natural killer (NK) cells are not phagocytic, but act to kill infected host cells when “self-antigens” normally presented by cells are missing and no longer inhibit the NK cells from killing the host cells (Klas Kärre et al. 1986). Importantly, innate immune cells are able to release cytokines and influence the immune response after recognition and phagocytosis of pathogens.

The innate immune system has a non-specific route for promoting phagocytosis of foreign objects, the complement cascade. This cascade “complements” the host immune system, through improvement of phagocytosis, direct interactions with microbes and recruitment of phagocytic cells. There are three routes of activation of the complement cascade, classical, lectin and alternative. All three pathways can be activated in an innate immune response (Janeway et al. 2001d). The complement system is a cascade of proteolytic activation and cleavage. Pathogenic stimulation causes proteolytic cleavage of precursors of complement components, which are subsequently activated have their own proteolytic capabilities on further downstream components (Sim & Tsiftsoglou 2004). In each of the three activation pathways, C3 convertase is produced and subsequent complement components and fragments are created. For example C3b (complement fragment 3b), or iC3b (the proteolytic inactive form) are able to coat foreign objects as opsonins, and through binding of complement receptors on phagocytic cells promote phagocytosis (Merle et al. 2015). The complement system is not limited to increased phagocytosis. A membrane attack

complex is formed from multiple complement components, resulting in pore formation in the membrane of bacteria (Merle et al. 2015), highlighting that complement directly attacks pathogens. Complement can also attract immune cells to the infection site, C5a is important in the chemotaxis of neutrophils (Ehrengruber et al. 1994). Complement uses several mechanisms to target pathogens, and is therefore an important innate defence.

Phagocytosis of invading pathogens by innate immune cells results in pathogen degradation, cytokine release and antigen presentation. An important function of innate immune cells that have phagocytosed a foreign pathogen, is to alert other immune cells to the tissue invasion. Cytokine and chemokine release from infected innate immune cells promotes activation and recruitment of other innate immune cells. After phagocytosis, many cells (including lymphocytes and epithelial cells) are able to release cytokines, but macrophages play a primary role in releasing inflammatory cytokines including TNF-a, IL1, IL-6, IL-8 and IL-12 in addition to chemokines. Cytokine and chemokine secretion promote the influx of more inflammatory cells, the activation of macrophages and ultimately the correct immune response to pathogen invasion (Arango Duque & Descoteaux 2014). Additionally IL8 and TNF-α leads to activation of neutrophils (Janeway et al. 2001b). The role of cytokine secretion in the promotion of an immune response is key for the coordination of a correct host response.

The initial role of the innate immune system during invasion by a pathogen is to recognise the foreign object and if possible to degrade it. However, the innate immune system also acts to alert the adaptive immune system to pathogen invasion.

1.1.3 Innate immune system links to the adaptive immune system

Activation of the innate immune system can lead to the activation of the adaptive immune system. The adaptive immune system is the targeted response to specific invading pathogens. The adaptive immune system provides long lasting immune defences against (previously encountered) pathogens.

The adaptive immune system requires professional antigen presenting cells (APCs) such as macrophages or dendritic cells to phagocytose and degrade pathogens and to subsequently present pathogen antigens on major-histocompatibility complex class II (MHC-II) molecules (Al-Daccak et al. 2004). The APC may migrate to lymph nodes in order to activate CD4+ T helper cells (Itano & Jenkins 2003). CD4+ T cells specifically recognise antigens displayed on the MHC-II molecules, through T cell receptors leading to the activation of CD4+ T helper cells. Once active, CD4+ T cells are able to secrete pro-inflammatory cytokines and activate CD8+ cytotoxic T cells and B cells

(Janeway et al. 2001a). CD4+ T helper cells can be spilt into two groups: Th1 or Th2. The Th1 group secrete pro-inflammatory cytokines, IFN-γ (a potent macrophage activator). By contrast Th2 CD4+ cells promote an anti-inflammatory response through secretions of IL4, IL5 and IL10 (Romagnani 2000). In host defence against pathogens a Th1 profile is required, however excessive pro-inflammatory responses can be harmful for the host tissue and a Th1-Th2 balance is therefore needed (Romagnani 2000).

Non-professional APCs are important for the action of CD8+ cytotoxic T cells. Non-professional APCs present phagocytosed and degraded pathogen antigens on major-histocompatibility complex class I (MHC-I) molecules. Antigens presented by MHC-I molecules are recognised by CD8+ T cells which are then able to target and kill cells that contain pathogens (Janeway et al. 2001c).

An important part of the adaptive immune response is the production of antigen-specific antibodies. It is therefore important that B cells are activated to be able to produce antibodies. B cells can be activated by T helper cells, or through direct contact with foreign antigens (Janeway et al. 2001a). For B cells activated by T helper cells, initial internalisation of antigen leads to presentation (of antigen) on MHC-II molecules which stimulates CD4+ T helper cells. CD4+ T cells then provide B cells stimulus to produce antibodies (Janeway et al. 2001a).

The adaptive immune response provides long-lasting immune defence against pathogens, with a key role for CD4+ cells in the activation of further adaptive immune responses and in co-ordinating an appropriate pro-inflammatory response.

1.1.4 Phagocytic cells: macrophages and neutrophils

Macrophages and neutrophils represent important phagocytic cells. Both macrophages and neutrophils are of the myeloid lineage. Multipotent haematopoietic stem cells have the ability to generate multiple types of blood cells and can differentiate into myeloid progenitor stem cells or lymphoid progenitor stem cells. Lymphoid progenitor stem cells are able to differentiate into natural killer cells, T cells and B cells. Myeloid progenitor cells differentiate into erythrocytes, mast cells and myeloblast cells. Myeloblast cells are able to further differentiate into important innate immune cells basophils, neutrophils, eosinophils and monocytes, where monocytes are precursors to macrophage cells and dendritic cells (Kondo 2010; Kondo et al. 2003).

<u>Neutrophils</u>

Neutrophils are the most abundant white blood cells in the human body and, as a phagocytic cell, provide an important defence against invading pathogens. Neutrophils are polymorphonucelar cells, due to the multi-lobed nucleus, this enables neutrophils to squeeze through small spaces in the extracellular matrix, which may not be possible with a larger circular nucleus typical of most cells (Kondo et al. 2003). Usually circulating in the blood, neutrophils respond to cytokine and chemokine signalling and migrate to sites of damage or infection. Recognition of pathogens through TLRs leads to phagocytosis by neutrophils (Hayashi et al. 2003). Phagocytosis by neutrophils leads to pathogen degradation, through generation of reactive oxygen species (ROS). Furthermore, granules (vesicles which are specialised lysosomes) which contain antimicrobial molecules and degradative enzymes are used by neutrophils to degrade pathogens (Kumar & Sharma 2010). Granules fuse with phagosomes containing the pathogen leading to degradation. Additionally, neutrophils undergo a specialised form of cell death (termed NETosis) which releases nuclear genomic material, antimicrobial molecules and granules into the extracellular environment, in a process leading to the formation of neutrophil extracellular traps (NETs). NET formation traps extracellular pathogens and can also lead to their degradation (Brinkmann et al. 2004).

In addition to their important role as effector cells in pathogen degradation neutrophils also play a role in immune system activation and modulation. The role of immune system regulation by neutrophils has been reviewed in detail elsewhere, but includes secretion of chemokines and cytokines, which may be pro- or anti- inflammatory, provide help to B-cells and the modulation of the activity of macrophage and dendritic cells (Selders et al. 2017; Jaillon et al. 2013; Perobelli et al. 2015).

Macrophages

Monocytes develop into macrophages after leaving the blood stream, following chemokine signalling (Auffray et al. 2007). Tissue resident macrophages are localised to certain tissues to provide rapid responses, particularly in organs or tissues which may experience pathogen invasion often, such as the lungs or gut. Some tissue resident macrophages which are not derived from monocyte lineage are self-renewing, and are specialised to certain tissues, for example microglial cells in the brain, and alveolar macrophages (Yona et al. 2013).

Macrophages are phagocytic cells that actively monitor and search the tissue for pathogens. Macrophages recognise pathogens or pathogen associated damage through PRRs, including TLRs (Weiss & Schaible 2015). Macrophages are able to degrade pathogens through degradative enzymes. After phagocytosis, the phagosome (vesicle containing the pathogen formed from plasma membrane in phagocytosis)

fuses with other cellular vesicles, endosomes, lysosomes and autophagosomes resulting in an acidic pH (in the phagosome). Degradation of pathogens by hydrolases occurs, which are delivered to the pathogen vesicle by lysosome and late endosome fusion (Weiss & Schaible 2015). Therefore macrophages play an important role in the recognition and clearance of pathogens.

Macrophages may become activated and secrete cytokines to alert the immune system and recruit additional immune cells. Macrophages are activated by multiple stimuli, which can lead to specialisation of activation sate, broadly leading two activation groups, classically activated macrophages (M1), and alternatively activated macrophages (M2), reviewed elsewhere. M1 and M2 are named to match with Th1 pro-inflammatory, or Th2 anti-inflammatory subsets of T helper cells. As such, M1 macrophages are pro-inflammatory, important in pathogen killing whereas M2 are generally immunomodulatory, but still useful for pathogen killing (Martinez & Gordon 2014).

Macrophages also promote the activation of the adaptive immune system as professional antigen presenting cells, through presentation of pathogen antigens on MHC-II molecules to T-cells (Weiss & Schaible 2015). This leads to the activation of the adaptive immune response, as introduced above.

1.2 Cryptococcus neoformans

1.2.1 *C. neoformans* microbiology

Cryptococcus neoformans is an encapsulated yeast of the Cryptococcus genus, in the phylum basidiomycota within the kingdom of fungi. There are two variants of *C. neoformans* species, var. *neoformans* and var. *grubii*, containing 3 serotypes; A (var. *grubii*), D (var. *neoformans*) and a hybrid AD (Kwon-Chung et al. 1978). *C. gattii*, a related species, was initially included, but after genetic analysis, a clear difference between variants was found and it was proposed as a separate species (Kwon-Chung et al. 2002). *C. neoformans* has been detected in soil, pigeon excrement and in rotting vegetables and wood (Voelz et al. 2010) and is found globally. In contrast *C. gattii* is almost exclusively found in tropical and subtropical areas (Voelz & May 2010).

C. neoformans is a basidiomycetous yeast (spore forming) and as such has a sexual, in addition to an asexual form during its life cycle. The sexual stage requires contact between two fungal mating types, a and α, for reproduction (Kwon-Chung 1976). In the much more common, asexual stage, *C. neoformans* is in a yeast form. The yeast reproduces through budding and this is the form that has been isolated from human infection.

1.2.2 Route of *C. neoformans* infection

C. neoformans (var. grubii) is a human fungal pathogen which is found in the environment globally (Bovers et al. 2008). *C. neoformans* infection of healthy individuals can be controlled by the host immune system. *C. neoformans* infection is not controlled in immuno-compromised individuals and can lead to life-threatening disease.

Initial infection occurs through inhalation of environmental spores deep into the lung. It is thought that initial infection occurs in childhood since an antibody profile appears with age, indicating latent or repeated infection (Goldman et al. 2001). After inhalation of cryptococcal spores, they are believed to be encountered and phagocytosed by alveolar macrophages (Nicola et al. 2012). In healthy individuals, an immune response (discussed in section 1.2.4) is generated which can result in granuloma formation and ultimately clearance of cryptococcal cells (Shibuya et al. 2005). Cryptococcal cell survival within granulomas was shown in *C. neoformans* infection in a rat model (Goldman et al. 2001). Evidence of re-activation of cryptococcal infection was investigated through comparison of the geographical location of cryptoccocal strains and their occurrence in new locations. It was shown that individuals who were in the original location several years before had infection in new locations caused by the strain from the original location (Garcia-Hermoso et al. 1999). Indicating the cryptococcal cells were surviving within individuals overtime before causing clinical infection. *C. neoformans* infection in immuno-competent individuals can therefore lead to a subclinical infection; a latent stage.

In immunocompromised individuals, initial infection is not efficiently controlled. In these cases, pulmonary infection is likely to be followed by systemic spread where *C. neoformans* is able to escape the lung, and gain access to the blood stream. A potential mechanism of this extra-pulmonary dissemination is via an alveolar macrophage “Trojan horse”, in a similar manner to *B. anthracis* spores. Spores rather than yeast may be more likely to leave the lung in this way due to the ease of which cryptococcal spores are phagocytosed, in comparison to cryptococcal fungal cells (Guidi-Rontani 2002; Botts & Hull 2010). *C. neoformans* has a tropism towards the central nervous system (CNS), particularly to the brain. Cryptococcal cells in the blood stream are able to migrate into the brain parenchyma, although exactly how *C. neoformans* targets the CNS is unknown. Several mechanisms of how *C. neoformans* is able to cross the BBB have been described (discussed in section 1.2.5). Life-threatening diseases such as cryptococcal meningitis, and meningoencephalitis are caused when *C. neoformans* is able to invade the CNS.

1.2.2 *Cryptococcus gattii*

C. neoformans causes infection primarily in immunocompromised patients. On the other hand *C. gattii* is known to infect otherwise healthy individuals. There are four molecular subtypes of *C. gattii*, VGI, VGII, VGIII and VGIV. Subtypes VGIII and VGIV primarily infect immunocompromised hosts. However, subtypes VGI and VGII are known to infect immunocompetent individuals, causing infection in the CNS (VGI) and pulmonary infection (VGII).

C. gattii differs from *C. neoformans* by exhibiting a reduced ability to replicate within macrophages (Voelz et al. 2014) and a slower replication rate in the blood (Ngamskulrungroj et al. 2012). Furthermore, using a murine infection model *C. gattii* is shown to more often cause pulmonary infection than a CNS infection via inhalation, but could cause severe cryptococcal meningitis through intravenous infection (Ngamskulrungroj et al. 2012). These data suggest that through the inhalation infection route, *C. gattii* is not able to efficiently escape out of the lung to cause CNS invasion. *C. gattii* was also shown to invoke a reduced immune response from the host, including reduced neutrophil recruitment and reduced pro-inflammatory cytokines, in comparison to *C. neoformans* (Cheng et al. 2009). This reduced immune response may represent immune evasion by *C. gattii*, and it was suggested that this may enable infection of immunocompetent hosts through increased persistence. In contrast to this, a strain of *C. gattii* responsible for infection of immunocompetent people in the Vancouver Island outbreak was shown to have an increased ability to replicate within macrophages. It was determined that cryptococcal mitochondria can become tubular, which may protect against fungal cell death, and additionally is directly proportional to intracellular proliferation (Ma et al. 2009). Perhaps a reduced immune response associated with an increase in *C. gattii* persistence in immunocompetent hosts, coupled with increased intracellular proliferation provides the ability of outbreak strains to cause infection in otherwise healthy individuals.

1.2.3 Pathology of cryptococcosis

Cryptococcus neoformans is an opportunistic fungal pathogen, causing infection primarily within immunocompromised individuals. *C. neoformans* is therefore an important pathogen for HIV/AIDs patients, where infection is responsible for high mortality rates, for example up to 70% mortality in sub-Sharan Africa (Park et al. 2009; Mitchell & Perfect 1995). Indeed, 15% of HIV/AIDs related deaths worldwide are caused by cryptococcal meningitis (Rajasingham et al. 2017). Very different infection outcomes occur between immunocompromised and healthy individuals after initial infection with *C. neoformans*, with infection controlled in healthy individuals. It is thought that as immune efficiency declines in HIV-associated cryptococcal infection,

the host immune defence is unable to either eradicate or suppress infection, leading to clinical disease (Bovers et al. 2008).

Cryptococcus neoformans has a tropism to the CNS. Exactly how fungal cells target the CNS is not established, however the cryptococcal cells do employ several virulence factors which help the fungal cells to cross the BBB. If cryptococcal cells invade the brain, life-threatening cryptococcal meningitis or meningoencephalitis occurs. Cryptococcal meningitis (CM) is a subacute meningoencephalitis, where infection/inflammation occurs in the meninges (three layers of membrane surrounding and protecting the brain) and in the subarachnoid spaces (fluid filled spaces between the meninges). CM is caused by the invasion of cryptococcal cells into the meninges or subarachnoid spaces (Williamson et al. 2017). In HIV associated CM, cryptococcal cells are observed in the brain parenchyma and meninges often in large masses. By contrast in non-HIV associated CM, cryptococcal cells are observed in perivascular spaces and meninges, in most cases with fewer cryptococci present (Lee et al. 1996).

Differences in cryptococcal infection outcome between HIV associated and non-HIV associated CM are caused by different immune profiles and responses. The vast majority of cryptococcal infection occurs in immunocompromised individuals, such as HIV positive patients, with a reduced number of CD4+ T cells. It is known that CD4+ T cells are key in the control of cryptococcal infection (Jarvis & Harrison 2007). CD4+ cells can be grouped into Th1 pro-inflammatory, or Th2 anti-inflammatory subsets. The CD4+ cell profile changes over time in HIV/AIDS patients, becoming predominantly Th2 (Altfeld et al. 2000). It was later demonstrated that the CD4+ profile is important in the outcome of HIV associated cryptococcal meningitis, with a pro-inflammatory profile associated with increased survival and reduced fungal burden (Jarvis et al. 2013). The lack of control of cryptococcal infection in immunocompromised patients enables continued cryptococcal growth and eventual progression to CM.

Non-HIV associated CM occurs often in immunocompromised individuals, such as organ transplant receivers, who also have reduced CD4+ cell counts (Taylor et al. 2005). Most non-HIV CM cases have underlying illness, with ~40% being immunocompromised (Pappas 2013; Taylor et al. 2005). Of note some apparently healthy individuals still had cryptococcal infection, occurring in ~12% of a retrospective study (Kiertiburanakul et al. 2006). However, in healthy patients, cryptococcal infection is likely to remain as a pulmonary infection. In healthy individuals, CM is rare (Li et al. 2010), due to the ability of the immune system to control cryptococcal infection, therefore there is limited data on the normal response to cryptococcal infection.

Cryptococcal meningitis is the major cause of death in *C. neoformans* infection. Clinical studies have shown that in a proportion of cryptococcal meningitis cases, vascular damage results in infarcts, areas of necrotic tissue caused by a lack of blood supply (Mishra et al. 2017). Furthermore, the incidence of cortical infarcts is non-trivial, occurring in 30.3% of cryptococcal meningitis patients, most often observed in severe cases (Mishra et al. 2017). The physiological cause of infarcts in CM is currently unknown. Of note, cerebral infarcts are also observed in tuberculosis meningitis (Lan et al. 2001). This may suggest that in infective meningitis, blood vessels in the brain become damaged, potentially through physical damage or through toxins from the pathogen. For tuberculous meningitis, vascular damage is suggested to be caused by direct interaction of the bacterium and vessel wall, in addition to immune mediated damage (Lammie et al. 2009). Recent clinical studies and case reports have highlighted a potential role of blood vessel damage resulting from infection with *C. neoformans.* This may provide some understanding of the cause of infarcts in CM, that cryptococcal infection leads to vasculitis and brain vasculature damage and may ultimately result in infarcts (Aharon-Peretz et al. 2004; Rosario et al. 2012; Leite et al. 2004). Additionally, clinical dissection reports show cryptococcal cells invading the brain, observed both in the perivascular spaces and located next to brain capillaries which have cryptococcal cells present (Lee et al., 1996; Loyse et al., 2010). This may represent dissemination across the BBB, potentially at sites of vascular damage.

1.2.4 Host defence interactions with *C. neoformans*

The interactions that occur between the host and pathogen are key to the outcome of infection. The host response to *C. neoformans* infection involves both innate and adaptive immunity.

Cryptococcal spores are initially located in the lungs. The lungs provide some first line defences against *C. neoformans*. Firstly, adaptations of the lung enable particles larger than 2µm to be expelled, for example mucus and mucocilary transport and coughing (Nicod 2005). For this reason it is thought that the infectious propagule of *C. neoformans* is the cryptococcal spore, which is smaller at ~2-2.5µm than the fungal cells at ~4-8µm (Velagapudi et al. 2009).

Surfactant is a film of proteins and lipids which provides surface tension for alveoli. The presence of surfactant in the lung additionally promotes trafficking of particles (or pathogens) towards the alveoli, therefore promoting interactions with immune cells, such as alveolar macrophages (Schurch et al. 1992). Proteins within the surfactant are known to directly interact with *C. neoformans*. Surfactant protein A (SPA) and

surfactant protein D (SPD) acts to opsonise pathogens, therefore promoting their phagocytosis by neutrophils and macrophages (Kishore et al. 2005; Wright 2004). SPD has been shown to bind to *C. neoformans* and in particular to promote phagocytosis of acapsular cryptococcal cells (Geunes-Boyer et al. 2009). However, it was later demonstrated that mice lacking SPD had a reduced severity of cryptococcal infection, suggesting that SPD is useful for cryptococcal pathogenesis (Geunes-Boyer et al. 2012).

After alveolar macrophage phagocytosis of cryptococcal cells, an immune response generates formation of a granuloma (Haugen & Baker 1954). This encloses cryptococcal infection within a well organised structure composed of immune cells. The function of granulomas is to contain and resolve *C. neoformans* infection. *C. gattii* infection also induces pulmonary granuloma formation (Torda et al. 2001). In healthy patients, cryptococcal granulomas are usually located in the lung. Interestingly, using a rat cryptococcal intravenous infection, intravascular granulomas were observed, likely composed of monocytes, rather than alveolar macrophages (Yamaoka et al. 1996).

Cryptococcal granulomas are composed of (alveolar) macrophages, multi-nucleated giant cells (formed by fusion of macrophages or monocyte cells), and an outer layer of CD4+ T cells (Shibuya et al. 2005). Macrophages and multi-nucleated giant cells which contain cryptococcal cells are centrally located in the granuloma, observed in limited case reports (Takata et al. 2011; Haugen & Baker 1954; Izumikawa et al. 2008). Pulmonary *C. neoformans* infection using a rat model demonstrated infection is controlled in the lung through recruitment of macrophages and lymphocytes contributing to granuloma formation, ultimately resulting in a reduced fungal burden (Goldman et al. 2001). Together, these data suggest that granuloma formation in healthy individuals resolves cryptococcal infection.

In immunocompromised patients, cryptococcal granulomas are not composed of the same types of innate cells and the location of granulomas are not limited to the lung. A case study reports granulomas located in the brain in an immunocompromised patient (Taneja et al. 2008). In these cases, granulomas are composed of macrophages and multi-nucleated giant cells, (which contain proliferative cryptococcal cells) but importantly are lacking the outer layer of CD4+ T cells (Shibuya et al. 2005). Incomplete granuloma response, due to the lack of CD4+ T cells in immunocompromised patients, may account for the lack of pulmonary infection control in these cases.

Several molecules have been implicated in promoting the formation of a cryptococcal granuloma. Monocyte chemoattractant protein 1 (MCP-1) has previously been linked to

induced granuloma formation in rats, where alveolar macrophages provide a source of MCP-1 (Flory et al. 1993). MCP-1 production from alveolar macrophages occurs before granuloma formation. It was later demonstrated that phagocytosis of *C. neoformans* induced MCP-1 production by alveolar macrophages (He et al. 2003). Therefore, phagocytosis of cryptococcal cells results in further macrophage recruitment and may initiate the granuloma formation. A requirement of host sphingosine kinase 1 (SK1) in order to form a proper granuloma response to exclusively intracellular resident cryptococcal cells, was demonstrated using a murine model (McQuiston et al. 2010), although this was not seen in "wild-type" cryptococcal cells which can survive extracellularly. SK1 phosphorylates sphingosine to sphingosine-1-phosphate (S1P). S1P is able to induce immune cell activation and migration. This may enable recruitment of immune cells for the generation of a granuloma (Farnoud et al. 2015; McQuiston et al. 2010).

Two mouse models have been established, which illicit either a Th1 or Th2 response after *C. neoformans* inoculation. In a Th1 response, granuloma formation occurs. It was then demonstrated that metalloproteinase-2 (MMP-2) was highly expressed in the murine lung only in a Th1 response. It was therefore suggested that MMP-2 expression, (which provides immune cells help in terms of movement by degradation of extra-cellular matrix components) therefore may be associated with granuloma formation in healthy individuals (Majka et al. 2002).

Unsurprisingly, the common aspect which is involved in granuloma formation, is to allow recruitment of immune cells to generate a granuloma. Some factors which promote innate cell recruitment, such as MCP-1, are released after initial host interactions with cryptococcal cells. This host response and subsequent innate immune cell attractant release may be key in co-ordinating the correct granuloma formation response to cryptococcal infection.

The role of complement in *C. neoformans* infection

The complement system, (as described above) improves innate cell phagocytosis, has direct interactions with microbes and promotes the recruitment of phagocytic cells. In *C. neoformans* infection, the alternative pathway is used to activate complement as a host defence (Kozel et al. 1991). In each of the three activation pathways, C3 convertase and C3b is produced, and subsequently C5a and C5b components are created. Both C5 and C3 components are implicated in *C. neoformans* infection. C5 is important in the chemotaxis of immune cells. C5 deficient mice are more susceptible to cryptococcal infection (Rhodes et al. 1980), as may be expected by a lack of immune

cell recruitment. C3 is accumulated on the cryptococcal capsule, which aids in the phagocytosis of the fungal cell. However, to promote phagocytosis C3 is required to be at the surface of the capsule. If C3 is dispersed through the entire capsule structure there is a reduction in the help C3 provides in phagocytosis (Gates & Kozel 2006; Zaragoza et al. 2003). As with other innate immune responses, *C. neoformans* has strategies it uses to avoid the complement system. *C. neoformans* can reduce C3 deposition in the capsule through the use of lactonohydrolase, a hydrolytic enzyme produced by cryptococcal cells (Park et al. 2014). Additionally, as mentioned below complement has useful roles in neutrophil phagocytosis and killing of *C. neoformans.*

C. neoformans interactions with macrophages

In the host innate defence, the initial response to infection with *Cryptococcus neoformans* include phagocytosis, primarily by alveolar macrophages. The complement cascade also acts to promote phagocytosis (Voelz & May 2010). Despite this, cryptococcal cells are able to survive, replicate and escape from macrophages.

The macrophage response to phagocytosis of microbes is to acidify the cryptococcal phagosome to enable degradation. However, as a fungal pathogen, a low pH is preferable for cryptococcal growth, and the low pH of a phagosome is not detrimental. When cryptococcal phagosome acidification is blocked, there is a reduction in cryptococcal replication (Levitz et al. 1997), demonstrating that an acidic intracellular environment is preferable for cryptococcal proliferation. Despite this, in some cases the phagocytosed *C. neoformans* is presumed to be degraded within the phagocyte. The fungicidal activity of macrophages is dependent on the activation status of the macrophages. Through *in vitro* treatment of cytokines on macrophages, it was demonstrated that Th1 and Th17 type macrophages have improved fungicidal activity in comparison to Th2 macrophages (Voelz et al. 2009). Macrophages, primarily classically activated (Th1), are able to degrade *C. neoformans* through oxidative and nitrosative molecules (Alspaugh & Granger 1991). Macrophages are also able to kill extracellular *C. neoformans*. IFNγ treated macrophages (Th1) were shown to reduce growth of, and kill extracellular cryptococcal cells, and that this was likely mediated by secreted proteins (Flesch et al. 1989). Macrophages are therefore important phagocytes in the control of cryptococcal infection.

Although *C. neoformans* did not evolve to be a human pathogen, it exhibits many virulence factors (as discussed in section 1.2.5) and attributes which enable its survival during human infection. A key attribute is the ability for *C. neoformans* to survive, replicate and even escape from within macrophages. Cryptococcal cells were first

shown to be able to replicate within macrophages. *In vitro* studies showed that macrophages did not kill phagocytosed cryptococcal cells and in fact intracellular cryptococcal growth occurred (Diamond & Bennett 1973). Cryptococcal cells have been shown to survive intracellularly within phagolysosomes (Levitz et al. 1999), and may be able to gain access to the cytoplasm (Tucker & Casadevall 2002). Replication within the host cell has been suggested as a route of cryptococcal macrophage escape, by causing physical damage to the plasma membrane of the macrophage (Tucker & Casadevall 2002). Host macrophage lysis can allow cryptococcal escape from the macrophage and from there enable dissemination throughout the host.

C. neoformans can also utilise a phagosome emptying (into extracellular space) mechanism, termed "vomocytosis", in which the cryptococcal cell and macrophage remain alive after cryptococcal escape. Vomocytosis occurs frequently, with 29.9% of cryptococcal cells being able to escape *in vitro* and 44% *in vivo* (Nicola et al. 2011). However, the macrophage does employ an actin-cage blocking mechanism against vomocytosis (Johnston & May 2010). *C. neoformans* has also been observed to move from one macrophage to another *in vitro* (Alvarez & Casadevall 2007), although the whether this is a host defence, or fungal mediated evasion is unclear, but does allow the fungal cell to avoid the extracellular space.

In addition to routes of escape from macrophages, after phagocytosis, *C. neoformans* alters the macrophage/phagosome environment for its own end (Rahman & McFadden 2011). Several host macrophage factors are manipulated by cryptococcal cells, including the actin cytoskeleton, cell surface signalling molecules, vesicle transport and autophagy (Qin et al. 2011). Within the host cell, *C. neoformans* influences these factors to promote its own survival and replication. Like other pathogens, intracellular *C. neoformans* is able to prevent activation of the host macrophage through manipulation of the NF-kB pathway (Hayes et al. 2016). This will help prevent a larger host immune response to infection. Interestingly, phagolysosomal damage, which occurs increasingly with intracellular cryptococcal growth, was suggested to be beneficial for *C. neoformans*, through a self-perpetuating cycle of phagosome damage increasing cryptococcal growth (Davis et al. 2015). Additionally, reports that *C. neoformans* manipulates phagosome maturation, for example incomplete acidification and altered Rab protein association (Smith et al. 2015) suggest that *C. neoformans* is manipulating the host environment, although the mechanism behind this is unclear. Other fungal pathogens, including *Candida albicans* and *Histoplasma capsulatum,* are able to alter the phagosome maturation process (Kasper et al. 2014; Strasser et al. 1999), similar mechanisms may be present between these fungal pathogens to promote fungal survival.

C. neoformans interactions with neutrophils

Neutrophils are able to phagocytose and degrade cryptococcal cells, however, unlike macrophages, neutrophils do not play a key role in the control of cryptoccocal infection. Neutrophils are not considered important in the control of *C. neoformans* infection due to the lack of clinical evidence of any increased susceptibility to cryptococcal infection in neutrophil disorders, such as neutropenia. Furthermore, in mice depleted of neutrophils no change in fungal burden was observed after pulmonary infection in comparison to mice which had neutrophils (Wozniak et al. 2012). This suggests that neutrophils are not key in the clearance of cryptococcal cells.

Neutrophils, are however, very much capable of degrading *C. neoformans*. There is evidence that *in vivo*, neutrophils play a key role in the degradation of cryptococcal cells in the brain vasculature, as when neutrophils were depleted in a murine model, the fungal burden in the brain increased (Zhang et al. 2016). Neutrophils employ oxidative and non-oxidative strategies to kill cryptococcal cells. Oxidative killing of phagocytosed cryptococcal cells was demonstrated by blocking myeloperoxidase function (an enzyme involved in production of microbicidal hypochlorous acid) which led to reduced fungicidal activity of neutrophils (Diamond et al. 1972). Neutrophils also use non-oxidative methods to kill *C. neoformans*. Calprotectin may mediate fungistatic effects through nutritional zinc depravation and is abundantly present in neutrophils. Defensins present in neutrophil granules also promote fungal killing (Mambula et al. 2000).

C. neoformans is also able to defend against neutrophil killing. *C. neoformans* uses mannitol to protect against oxidative species, where mannitol acts to scavenge oxidative species. Furthermore the amount of mannitol produced during infection is proportional to the fungal load (Chaturvedi et al. 1996; Wong et al. 1990). *C. neoformans* is able to reduce the killing ability of neutrophils, likely through a secreted cryptococcal factor, although the mechanism for this is currently unknown (Qureshi et al. 2011). Another demonstration of cryptococcal modulation of neutrophils was shown *in vitro* where cryptococcal capsule inhibits neutrophil NET formation (Rocha et al. 2015).

There is an emerging role of complement (described above) in neutrophil phagocytosis of cryptococcal cells. *In vitro* and *ex vivo* studies have demonstrated that complement (C5) signalling is important in neutrophil movement towards cryptococcal cells and is required for phagocytosis and killing by neutrophils (Sun et al. 2016b). In a murine model, neutrophil swarming in the lungs in response to *C. neoformans,* is dependent

on complement activation and subsequent leukotriene B4 (LTB4, immune cell attractant) release from neutrophils which have encountered cryptococcal cells (Sun & Shi 2016). It is suggested that complement (specifically C5) which is required for intravascular recruitment of neutrophils, could be targeted therapeutically, to promote neutrophil clearance of cryptococcal cells in the brain (Sun et al. 2016a). Due to the effective killing of cryptococcal cells by neutrophils, if complement activation were targeted therapeutically, it may represent a promising approach to target cryptococcal cells in human infection.

C. neoformans interactions with other innate immune cells

Eosinophils can degrade *C. neoformans*, and are able to activate the adaptive immune response, despite not being professional antigen presenting cells. In a rat *in vitro* model of cryptococcal infection, eosinophils up regulated MHC-II molecules (after cryptococcal phagocytosis), and stimulate T cells to adopt a Th1 profile, suggesting these cells are important in the formation of an adaptive immune response (Garro et al. 2010). It was later shown *in vivo* that cryptococcal activation promotes eosinophil migration to lymph nodes, where they can interact with T cells to initiate an appropriate adaptive immune response. It was also demonstrated that this incurred long lasting immunity to cryptococcus in rats later re-infected with *C. neoformans* (Garro et al. 2011). These data suggest that eosinophils have a role in organising the correct Th1 response and induce long lasting adaptive immunity in *C. neoformans* infection.

Dendritic cells (DCs) are also involved in the immune response to cryptococcal infection. DCs phagocytose, degrade and present pathogen antigen to T cells of the adaptive immune system, linking together innate and adaptive immune systems. DCs are the most important antigen presenting cell in *C. neoformans* infection, despite the key role of alveolar macrophages early in infection (Syme et al. 2002). However, DCs require opsonins, such as complement molecules or antibodies, to efficiently phagocytose cryptococcal cells (Kelly et al. 2005). DCs are able to phagocytose and degrade *C. neoformans* using oxidative and non-oxidative methods. After phagocytosis, cryptococcal particles are displayed on MHC-II molecules to enable activation of T cells and promote a suitable adaptive immune response. A murine model highlighted that DCs are able to phagocytose cryptoccocal cells *in vivo*, and that these DCs were subsequently able to activate T cells *in vitro* (Wozniak et al. 2006). Overall, DCs have an important role in coordinating the adaptive immune response to *C. neoformans*.

The adaptive immune system in *C. neoformans* infection

The adaptive immune system plays a key role in response to cryptococcal infection. The adaptive immune response is clearly implicated in *C. neoformans* infection, through the existence of antibodies against *C. neoformans* and the known link between individuals with reduced CD4+ T cell numbers and their increased susceptibility to *C. neoformans*. After initial innate immune cell interactions with *C. neoformans*, antigen presentation leads to adaptive immune response, which enable T cells and B cells to play important roles.

T cells are lymphocytes which are involved in cell mediated immune responses, and have a variety of types including, T helper cells (CD4+), T memory cells, natural killer T cells or cytotoxic T cells (CD8+). HIV positive patients increased susceptibility to infection is caused by a reduction in the number of CD4+ T cells (Jarvis & Harrison 2007). The role of T helper cells in *C. neoformans* infection in particularly important in helping activate innate immune cells to effectively kill *C. neoformans*. T helper cells recognise antigens displayed by APCs (such as macrophages or DCs), and subsequently release cytokines to induce a different immune responses, such as a Th1 or Th2 profile. CD4+ T cells are key in the control of cryptococcal infection.

B cells are lymphocytes which can produce antibodies against specific antigens when they are activated. Antibodies against *C. neoformans* are present from a young age, indicating that an adaptive immune response occurs after encountering environmental cryptococcal cells (Goldman et al. 2001). It has been demonstrated with an *in vivo* murine model that B cells are responsible for antibody production in response to pulmonary cryptococcal challenge, and that depletion of B cells causes enhanced susceptibility and reduced survival (Rivera et al. 2005). Furthermore, a reduction in memory B cells (IgM+) is associated with a higher risk of cryptococcal disease in HIV/AIDS patients (Subramaniam et al. 2009). Together these studies demonstrate that B cells and antibody production are important in preventing cryptococcal infection.

1.2.5 *C. neoformans* virulence factors and pathogenesis

To counteract the host innate and adaptive immune responses *C. neoformans* has several virulence factors which promote its survival. Of high importance is the ability of pathogens to be able to live and reproduce within the host in order to survive. The ability of *C. neoformans* to survive and replicate at 37ºC is key to enabling infection of humans (Perfect 2006).

The cryptococcal capsule is an important virulence factor for *C. neoformans* which surrounds the cryptococcal cell. The capsule consists of polysaccharides, glucuronoxylomannan (GXM), and galactoxylomannan (GalXM). In addition

mannoproteins (MP) may be associated with the capsule. Capsule size varies depending upon conditions (e.g. capsule size is upregulated in infection conditions) and is a known required virulence factor for infection. In mice acapsular yeast have a reduced ability to cause infection (Chang & Kwon-Chung 1994; Fromtling et al. 1982). An increase in capsule size may present a challenge for phagocytosis. The capsule allows the yeast to avoid phagocytosis, with acapsular yeast more frequently and easily phagocytosed than yeast possessing a capsule (Kozel & Mastroianni 1976). The cryptococcal capsule has multiple immunomodulatory effects, as reviewed by Coelho et al. 2014, which include a reduction in immune cell migration, reduced MHC presentation and reduced cytokine secretion (Coelho et al. 2014). The capsule also functions to prevent ROS from reaching the cryptococcal cell. Together these studies demonstrate the importance of the capsule in promoting cryptococcal infection, especially by preventing phagocytosis.

If the cryptococcal cell is phagocytosed, nutrients are required for the fungal cell to survive. As mentioned above, *C. neoformans* replicates preferentially at an acidic pH, and therefore can reside within a phagosome, or phagolysosome (Levitz et al. 1997). However, how cryptococcal cells obtain nutrients for growth (from within the phagosome) in not fully understood. *C. neoformans* up-regulates autophagy pathways to enable increased re-cycling of host cell components to provide nutrients for growth (Palmer et al. 2008). It has also been shown that the phagolysosome membrane becomes damaged due to cryptococcal growth. This may represent a route for cryptococcal cell to access cytoplasmic nutrients (Tucker & Casadevall 2002). It is likely that several mechanisms of nutrient acquisition are used by cryptococcal cells within the host cell.

C. neoformans utilises secreted factors to promote its survival. Melanin, an antioxidant, which is able to scavenge radicals, is a key virulence factor which protects the yeast from oxidative damage (Wang et al. 1995). Laccase, another cryptococcal virulence factor, is responsible for promoting the synthesis of melanin and as such is important in the protection of *C. neoformans* from oxidative species. Additionally, laccase is capable of immuno-modulation, through promotion of a Th2 rather than the host protective Th1 profile (Qiu et al. 2012). Another secreted virulence factor is urease, which reduces the pH of the surrounding environment through hydrolysis of urea, although in *C. neoformans* infection this does not appear to be necessary. In *C. neoformans* infection, urease promotes the trapping of cryptococcal cells in micro-capillary vessels, (Shi et al. 2010), potentially important in the tropism of fungal cells to the brain. Virulence factors phospholipase B (Plb) and associated secretion factor, Sec14, are required for dissemination and vomocytosis (Chayakulkeeree et al. 2011). Plb1 is utilised by *C.*

neoformans for degradation of phospholipids (Chen et al. 2000), it is suggested that this may enable degradation of the cryptococcal vesicle and allow access to nutrients in the host cell cytoplasm. Interestingly, Plb1 is required for the cryptococcal escape from macrophages through vomocytosis (Chayakulkeeree et al. 2011), highlighting a potential role of Plb1 in cryptococcal dissemination.

Well studied virulence factors have been described here, this list is non-exhaustive, many more cryptococcal virulence factors exist including multiple secreted molecules, which are reviewed elsewhere (Coelho et al. 2014; Buchanan 1998).

C. neoformans invasion of the brain

In order for *C. neoformans* to cause cryptococcal meningitis, cryptoccocal cells are required to migrate from the site of infection, the lungs, to the brain. When infection in the lungs is not controlled, cryptococcal cells are able to escape into the blood stream, and gain access to the brain. This means that the cryptococcal cells must cross the blood brain barrier (BBB). Cryptococcal passage across the BBB has been described to occur by several mechanisms.

Firstly, a “Trojan-horse” mechanism whereby cryptococcal cells residing within a macrophage are transported across the BBB and subsequently escape in the brain. This was demonstrated *in vivo* when depletion of macrophages in mice led to a reduced fungal burden in the brain (Charlier et al. 2009). Recently, the Trojan-horse macrophage mechanism was shown to enable passage of cryptococcal mutants which cannot cross through other mechanisms. Furthermore it was demonstrated that the macrophages pass through trans-endothelial pores in the BBB (Santiago-Tirado et al. 2017). Another route for *C. neoformans* to cross the BBB is via an intercellular mechanism. Evidence to support this was shown when tight-junction protein occludin was damaged in the presence of *C. neoformans,* suggesting that tight-junctions between endothelial cells in the BBB are broken (Chen et al. 2003). Finally, *in vitro* data suggests that *C. neoformans* can actively transcytose through cells in the BBB. Cryptococcal cells were able to pass through a layer of human brain microvascular endothelial cells (Chen et al. 2003). Together these mechanisms of cryptococcal cells crossing the BBB highlight that *C. neoformans* is first present in the blood stream before invasion of the brain.

1.3 Staphylococcus aureus

1.3.1 Microbiology of *S. aureus*

Staphylococcus aureus is a bacteria of the *Staphylococcus* genus in the bacteria kingdom. *S. aureus* is a gram-positive bacterium, with a 1µm diameter and a spherical shape. *S. aureus* is a facultative anaerobe, aerobic respiration is used under normal circumstances, but the bacteria are also able to survive and replicate in environments where oxygen is absent. During replication *S. aureus* can from "clumps" of bacteria. These "grape-like" clusters are created when *S. aureus* replicates through binary fission where daughter cells do not fully separate. Bacteria replicate in a pre-determined format and are (partially) separated by enzymes, which results in the grape-like cluster formation (Koyama et al. 1977). *S. aureus* is found globally, colonising the nasal passage and skin in 20% of the human population (Kluytmans et al. 1997). In these cases *S. aureus* are found commensally, and do not result in infection or disease.

1.2.2 *S. aureus* route of infection

S. aureus is found commensally in the nasal passage, persistently so in 20% of the human population, and intermittently in 60% (Kluytmans et al. 1997). *S. aureus* spreads person to person, however, rather than directly via aerosols, it is spread through nasal secretions, contaminated clothing and skin, which can then be spread when disturbed (Hare & Thomas 1956). Interestingly, improved cleaning of a university gym drastically reduced the presence of *S. aureus* on the students and gym environment (Oller et al. 2010), indicating that presence of *S. aureus* in the environment causes colonisation of individuals.

Colonised individuals have an increased risk of developing pathogenic *S. aureus* infection. Indeed, in a hospital based study of the source of *S. aureus* in bacteraemia, it was found that for 82% of patients, the bacteria in the blood was from the nares within the same individual, suggesting that the commensal bacteria was the source of infection (von Eiff et al. 2001). It is suggested that commensal *S. aureus* becomes pathogenic when gene expression alters the virulence factors expressed by bacteria, resulting in a pathogenic bacteria (Jenkins et al. 2015). These changes may occur when bacteria gain entry into the host, from their commensal sites, for example into the blood stream through skin injury.

1.2.3 *S. aureus* disease and significance

S. aureus colonises the human respiratory tract, primarily in the nasal passage but also on the skin, and causes infection when the skin or mucosal barriers are broken allowing access into the host tissue. *S. aureus* infection causes a large range of infections, from largely superficial infections such as skin lesions and abscesses, and more serious infections such as food poisoning, meningitis or pneumonia, to life-threatening infections, caused by bacteraemia such as sepsis, endocarditis, or toxic shock (Lowy 1998).

Bacteraemia (where *S. aureus* gains access to the blood stream) is a common, and important *S. aureus* infection. The incidence rate of *S. aureus* bacteraemia is non-trivial, with a range of 19-50 cases per 100,000 people, varying by country (van Hal et al. 2012). The mortality rate associated with *S. aureus* bacteraemia is high, 20-30% of bacteraemia patients do not survive (van Hal et al. 2012). Although this is reduced from the pre-antibiotic era where bacteraemia mortality was 80%. As noted by van Hal et al. 2012, *S. aureus* bacteraemia is responsible for more deaths than AIDs, tuberculosis and viral hepatitis related deaths together. Bacteraemia caused by *S. aureus* is therefore a significant human infection.

Treatment of *S. aureus* infection is usually completed through antibiotic courses. However, evolution of antibiotic resistant *S. aureus* has led to the development of methicillin-resistant *Staphylococcus aureus* (MRSA) and vancomycin-resistant *Staphylococcus aureus* (VRSA). Both MRSA and VRSA present a major hurdle in the successful treatment of *S. aureus* infections, particularly as more strains become resistant to antibiotics (Foster 2005). Indeed the mortality rate associated with bacteraemia caused by MRSA is increased in comparison to antibiotic-susceptible strains as demonstrated in a hospital based study (Yilmaz et al. 2016).

A large number of MRSA infections occur within the hospital environment. MRSA has been a known hospital acquired infection since the 1960s. Risk factors of infection, such as a urinary catheter, a central line or exposed site of surgery, which may be more likely during lengthy hospital stays, make certain individuals more susceptible to hospital acquired MRSA (HA-MRSA) (Carnicer-Pont et al. 2006). These risk factors may allow the bacteria passage into the host tissue. Therefore long and/or frequent hospital visits are associated with an increased chance of *S. aureus* exposure which may increase the risk of bacterial infection.

Blocking *S. aureus* transmission in hospitals is particularly important in MRSA infection. *S. aureus* present in the environment, or present on people who work in the hospital may facilitate bacterial transmission within the hospital. This highlights the requirement

of improved methods for the treatment and containment of *S. aureus* infection. It was suggested that abolishing commensal nasal *S. aureus* (through nasal antibiotic treatment) in patients before surgical procedures can help to reduce the likelihood of *S. aureus* infection post-surgery (Wenzel et al. 1995).

More recently since the 1990s, MRSA is causing infection outside of hospital sites, known as community acquired MRSA (CA-MRSA). It is likely that many CA-MRSA strains originate from hospital environments (Rollason et al. 2008). A retrospective study in a Californian medical centre compared CA-MRSA to HA-MRSA infections. It was demonstrated that 45% of MRSA infections were community acquired, but that most infections were skin/soft tissue lesions. It was noticed that the risk factors for contracting each type of MRSA was different, with CA-MRSA linked to injection drug use in at least 49% of cases (Huang et al. 2006). These data suggest that CA-MRSA is spread largely by intravenous drug users.

Overall, it is clear that *S. aureus* causes a wide range of infections, some of which are life-threatening. Evolution of antibiotic resistant strains, which may be hospital or community acquired represent a hurdle for the treatment of *S. aureus*.

1.3.4 *S. aureus* host-pathogen interactions

S. aureus causes pathogenic infection when it gains access host tissue, for example, in an injury where the skin layer is exposed. The host immune system has several defences to stop the invasion and spread of bacteria within the host. The first step in the response is recognition of the pathogen.

The innate immune system is able to recognise *S. aureus* through several PRRs, each able to recognise different bacterial components or secreted molecules. Toll-like receptors (TLRs) are important in host recognition of *S. aureus*. TLR signalling, via MyD88, results in NF-kB translocation to the nucleus which causes altered gene expression and leads to cytokine release, important in the formation of an immune response. An increase in susceptibility to *S. aureus* infection, and a decrease in survival was observed in mice lacking TLR2, and in mice lacking MyD88 (part of the TLR signalling pathway) (Takeuchi et al. 2000). TLR2 recognises peptidoglycan (PGN) and lipoteichoic acid (LTA), both components of gram-positive bacteria such as *S. aureus*, as PAMPs (Schwandner et al. 1999). Furthermore TLR2 is important in recognition of *S. aureus* lipoproteins. Generation of bacterial mutants demonstrated that lipoprotein recognition was important in host immune responses particularly, in blocking abscess formation (Wardenburg et al. 2006). Therefore TLR2 is important in the recognition of extracellular *S. aureus*, and promoting an immune response.

Nod-like receptors (NLRs) sense PAMPs in the cytoplasm, and cause pro-inflammatory cytokine release through the NF-kB pathway signalling. Nod2 recognises peptidoglycans isolated from *S. aureus* in macrophages (Girardin et al. 2003). This demonstrates further how the host pro-inflammatory response is dependent on the sensing of bacterial presence.

The complement system promotes phagocytosis of *S. aureus*. It was demonstrated that complement is activated in *S. aureus* bacteraemia in clinical studies (Hallett & Cooper 1980). It was also demonstrated that complement is also involved in blocking the attachment of *S. aureus* to endothelial cells, important in reducing the pathogenesis of bacteria in the blood stream. *In vitro, S. aureus* was able to bind less efficiently to endothelial cells when exposed to complement, in comparison to when complement molecules were absent (Cunnion & Frank 2003). This demonstrates that complement is acting as host defence and reduces the bacteria's ability to bind to endothelial cells. However, in the same study it was shown that complement activation by *S. aureus*, also increases endothelial cell susceptibility to *S. aureus* adherence. A potential explanation for this could be that *S. aureus* uses a secreted protein Efb (extracellular fibrinogen-binding protein) which can bind to C3 and therefore reduce complement mediated opsonisation (Lee et al. 2004). Another staphylococcal secreted protein Eap (extracellular adherence protein) is able block C3 activation and therefore stop binding by complement opsonins (Woehl et al. 2014). Indeed several staphylococcal factors target complement activation. Together these studies demonstrate that although complement may have a useful role as an opsonin for *S. aureus*, complement is also targeted by *S. aureus* to evade this important host response.

Intracellular handling of *S. aureus*

Phagocytosis of *S. aureus* allows bacterial clearance and degradation. Both neutrophils and macrophages are able to phagocytose *S. aureus*. In the zebrafish model it was demonstrated that macrophages represent the major type of phagocytic cell which responds to *S. aureus* infection. Individual macrophages can phagocytose more *S. aureus* in comparison to neutrophils, but that neutrophils represent an intracellular niche in which *S. aureus* can reside (Prajsnar et al. 2008; Prajsnar et al. 2012). It was demonstrated in the zebrafish model that a population bottle-neck is mediated by neutrophils, whereby a small number of bacteria which successfully evade neutrophil degradation eventually replicate and cause uncontrolled infection (Prajsnar et al. 2012). Evidence of this occurring in macrophages also exists. *In vitro* macrophage studies have shown that *S. aureus* promotes the survival of its host cell, through upregulation

of anti-apoptotic genes (Koziel et al. 2009), this may represent another intracellular survival strategy. By promoting host macrophage survival, or residing within a neutrophils, *S. aureus* gains time to replicate before being exposed to the extracellular environment.

Neutrophil phagocytosis of *S. aureus* is aided with the binding of complement and antibodies which can then be recognised by complement receptors and FcRs (receptors to the Fc region of antibodies) respectively. After phagocytosis, neutrophils are required to degrade the bacteria. In order to kill and degrade the bacteria, neutrophils utilise the fusion of granules to the phagosome. Granules contain anti-bacterial molecules, for example myeloperoxidase, (MPO). MPO generates hypochlorous acid which is efficient at killing bacterial pathogens (Klebanoff et al. 2013). When lysosomes fuse with the bacterial phagosome an acidic phagolysosome is formed. In these conditions lysozymes (delivered by the lysosome) are able to activate auto-lytic enzymes found in the bacterial cell wall, to promote digestion (Wecke et al. 1982). However, it has been demonstrated that *S. aureus* uses a membrane protein OatA to block lysozyme effects, demonstrated with increased sensitivity to lysozyme in OatA deficient bacteria (Bera et al. 2004).

Neutrophils also use ROS mediated mechanisms to degrade phagocytosed *S. aureus*. ROS mediated bacterial damage is very important in bacterial killing, individuals with dysfunctional phagocyte NADPH oxidase, have an increased susceptibility to bacterial pathogens (Heyworth et al. 2003). Neutrophils use phagocyte NADPH oxidase to generate the production of superoxide, and subsequently other reactive oxygen species. ROS are very toxic to *S. aureus*, and can therefore lead to bacterial degradation. However, *S. aureus* has strategies to overcome ROS mediated degradation. Superoxide dismutase and catalase production help to remove ROS, by degrading superoxide and hydrogen peroxide respectively (Mandell 1975). In addition to other virulence factors which defend against ROS (discussed in section 1.3.5). This demonstrates that although the neutrophil uses diverse bacterial killing strategies, *S. aureus* has defences which allow continued survival with the neutrophil.

S. aureus is able to survive, replicate and eventually escape from within neutrophils, or other host cells, for example macrophages or endothelial cells (Bhakdi & Tranum-Jensen 1991; Vandenesch et al. 2012; Heyworth et al. 2003; Schröder et al. 2006; Bayles et al. 1998). *S. aureus* is able to replicate within the phagosome or cytoplasm of host cells. In macrophages *S. aureus* is able to replicate within the phagosome (Heyworth et al. 2003). In endothelial cells, *S. aureus* can replicate within the lysosome (Schröder et al. 2006). Additionally *S. aureus* can replicate in the cytoplasm, following phagosomal escape, shown using epithelial cells (Bayles et al. 1998). Exactly how the

phagosome is escaped by *S. aureus* is unknown, but likely caused by toxins or membrane rupture due to growth. Once in the cytoplasm, hemolysins (discussed in section 1.3.5) are able to cause the lysis of phagocytic cells, and ultimately allow the escape of *S. aureus* into the extracellular environment (Bhakdi & Tranum-Jensen 1991; Vandenesch et al. 2012).

S. aureus interactions with innate immune cells

In addition to neutrophils and macrophages, the host defence includes other innate immune cells. *S. aureus* is known to be phagocytosed and killed by eosinophils. In a human blood assay, where phagocytes were exposed to *S. aureus*, phagocytosis by eosinophils occurred at ~50% of the rate in comparison to neutrophils. Additionally, eosinophils were capable of killing *S. aureus,* but only after phagocytosing 15 or more bacteria (Yazdanbakhsh et al. 1986). It was suggested this is because eosinophils required further activation to be able to release sufficient ROS. However, like other elements of the immune system, *S. aureus* is able to attack eosinophils to promote bacterial survival. *S. aureus* is able to effectively kill eosinophils. The supernatant of *S. aureus* cultures induced eosinophil death, but not the death of neutrophils. It was demonstrated that the bacterial factor causing eosinophil death was α-hemolysin, as an α-hemolysin deficient bacterial strain was unable to cause eosinophil death (Prince et al. 2012). Interestingly, increased eosinophil death through lysis may lead to formation of eosinophil extra-cellular traps (EETs), including granules which are useful in degradation of extracellular *S. aureus* (Persson 2015; Ueki et al. 2013). Eosinophils represent another cellular host defence which degrade *S. aureus*.

Dendritic cells (DCs) are also implicated as a host defence in *S. aureus* infection. The role of DCs in the host immune response to pathogens is to activate the adaptive immune system, after encountering a pathogen. Immature DCs sample the host environment for pathogens, and when they encounter a pathogen, DCs mature and migrate to lymph nodes to activate T cells and consequently the adaptive immune system. In a comparison of phagocytosis rates, immature DCs were able to phagocytose at a similar rate to neutrophils, whereas mature DCs had a reduced ability phagocytose *S. aureus*. Furthermore, while neutrophils were able to effectively degrade phagocytosed *S. aureus*, both immature and mature DCs did not, and in fact the bacteria was able to replicate within DCs (Nagl et al. 2002). This is indicative of the role DCs play in comparison to neutrophils in host defence. DCs are required to phagocytose in the immature state, but once a pathogen has been encountered the DCs are required to alert the adaptive immune system. In contrast, neutrophils are required to clear infection. After *S. aureus* phagocytosis, DCs have been shown to activate type I interferon expression (cytokines which affect immune regulation) through

TLR9 signalling. However, in TLR9 deficient mice, the bacterial burden was reduced after pulmonary *S. aureus* infection. This suggests that DCs type I interferon production is actually detrimental to the host (Parker & Prince 2012). This may suggest that *S. aureus* subverts DC function to promote pathogenesis and highlights how DCs are able to influence the immune response to infection.

DCs are important regulators in the co-ordination of the immune response to *S. aureus*. *In vitro* human blood assays highlighted that a subset of peripheral blood DCs are able to release pro-inflammatory cytokines, including IL-1β and TNF-α after phagocytosis of *S. aureus*. Furthermore this DC subset is able to efficiently activate T cell production of IFN-γ (Jin et al. 2014), an important pro-inflammatory cytokine used in infection resolution. DCs therefore may represent an important immune cell type involved in the generation of a Th1 response in *S. aureus* bacteraemia infection. In a mouse model of bacteraemia, depletion of DCs led to increased bacterial burden, and increased mortality. It was suggested that reduced neutrophil bactericidal activity (despite increased neutrophil recruitment) may have been caused by a lack of (DC derived) IL-12 (Schindler et al. 2012). Indeed, IL-12 is known to activate neutrophils (Moreno et al. 2006). This suggest that DCs can provide IL-12 which is able to promote a Th1 profile, important in host defence and key in the coordination of the correct immune response. DCs therefore represent an important role in the regulation of the activation of the adaptive immune system.

The adaptive immune system in *S. aureus* infection

Neutrophil and complement-assisted phagocytosis act as a primary innate host defence. The adaptive immune system has the ability to enhance innate immune cell activity, and to coordinate the immune defence against *S. aureus*.

T cells are able to influence *S. aureus* infection in a variety of ways. Firstly, cytotoxic T cells (CD8+) can directly kill infected host cells to release bacteria surviving intracellularly. T helper cells (CD4+) are able to recruit and active phagocytic cells. T helper cells are also used to help active B cells to produce antibodies and subsequently increase phagocytosis by opsonisation of the bacteria. Additionally T cells are important in dampening the inflammation response, important after bacterial infection has been cleared (Bröker et al. 2016). Memory Th1 cells are important in the production of IFN-γ, as shown when a successive inoculum of *S. aureus* led to a greater Th1 response and IFN-γ production in a murine model, in comparison to the initial inoculum which did cause limited IFN-γ production (Brown et al. 2015). This suggests that T cells provide lasting immunity against *S. aureus*. However, like many

host defences, *S. aureus* has strategies to overcome T cell interactions. While early in *S. aureus* infection T cells are effective at *S. aureus* killing and required to contain infection, T cells become unresponsive to *S. aureus* antigen presentation after longer exposure (e.g. in persistent infection) (Ziegler et al. 2011). Whether this is a *S. aureus* mediated defence, a host mediated prevention of inflammation damage, or a combination of both is unknown.

The role of B cells in *S. aureus* infection is not clear cut. Antibodies against a *S. aureus* cytotoxin (LukAB) were present in a child (Thomsen et al. 2017), and IgM, IgA and IgG antibodies (against *S. aureus*) are present in individuals from childhood. Antibodies are produced on exposure to *S. aureus* antigens in healthy and currently infected individuals (Dryla et al. 2005), indicating that B cells produce antibodies in response to *S. aureus* exposure.

Interestingly, within infected individuals, specific antibodies for *S. aureus* antigens were missing. These missing antibodies were present in healthy individuals (Dryla et al. 2005). This may suggest that some B cells are a target of *S. aureus* attack. A reduction of B cell binding of *S. aureus*, (in comparison to *Staphylococcus epidermis)* was caused by secreted *S. aureus* virulence factors (Nygaard et al. 2016). In mice it was shown that *S. aureus* superantigen protein A mediates a B cell specific attack, by directly binding to antigen receptors on the B cell surface. This results in B cell apoptosis and reduced antibody production (Silverman et al. 2000; Goodyear & Silverman 2003). In humans, Protein A is suggested to act as an immunodominant antigen, through binding a high percentages of B cells, and therefore blocking B cell recognition of other *S. aureus* antigens (Pauli et al. 2014). *S. aureus* is therefore capable of influencing the adaptive immune response through blocking B cell antibody production.

1.3.5 *S. aureus* virulence factors and pathogenesis

S. aureus can cause pathogenic infection in the same individual it commensally inhabits. It is suggested that when *S. aureus* gains access to host tissue, perhaps through puncture of the skin, that *S. aureus* undergoes gene expression changes which includes upregulation of virulence factor expression. *S. aureus* utilises varied virulence factors during infection. These include a polysaccharide capsule and extracellular enzymes and toxins. Virulence factor expression was compared between *S. aureus* clinical samples from the nares, blood stream, and from lesions in the heart, chosen to represent commensal bacteria, and pathogenic bacteria from two sites. Virulence factors, including for toxins and immune evasion, were up-regulated in

pathogenic bacterial locations in comparison to commensal bacteria location (Jenkins et al. 2015). For example, in bacteraemia *S. aureus* increases expression of factors required for adhesion, most likely to increase binding with endothelial cells in the vasculature (Jenkins et al. 2015). Exactly how these gene expression changes occur upon entry into host tissue is unknown, but it is likely in response to the bacterium's new environment.

Bacterial cell surface factors

The *S. aureus* capsule is composed of hexosaminuronic acids and polysaccharides. Highly encapsulated *S. aureus* strains are often found in human disease (O'Riordan & Lee 2004). The *S. aureus* capsule, much like *C. neoformans*, benefits *S. aureus* by reducing bacterial phagocytosis (Lee et al. 1987). Reduced phagocytosis enables more bacterial survival within the host. Staphyloxanthin is a carotenoid pigment produced by *S. aureus*, resulting in its characteristic golden colour. However this pigment also acts as an antioxidant, useful in the prevention of damage from host cell oxidative species, which helps facilitate evasion of degradation by a neutrophil (Liu et al. 2005).

Protein A, is a surface protein, which remains attached to *S. aureus.* Protein A is capable of binding to the Fc region of immunoglobin G (IgG), and IgM, blocking the opsonising potential of these antibodies and reducing the rate of phagocytosis (Forsgren & Nordström 1974; Falugi et al. 2013). Some Protein A does not remain attached to the bacterial cell. *In vitro* studies of co-culture of *S. aureus* with non-surface associated Protein A and white blood cells (whole human blood) show white blood cells had a reduced phagocytic ability (O'Halloran et al. 2015), indicating that non-surface associated Protein A is able to reduced host neutrophil phagocytosis. However, in humans deficient in B cells or antibody production, there is no increased susceptibility to *S. aureus* infection, suggesting that infection is not controlled by antibody production.

S. aureus also expresses several binding proteins which promote bacterial binding to host components. Fibronectin in an extracellular glycoprotein which binds to integrins, collagen and extracellular molecules. Fibronectin binding proteins A and B (FnBPA and FnBPB) enable to adhesion and invasion of integrin (the host fibronectin receptor) expressing host cells, such as endothelial and epithelial cells (Sinha et al. 1999). This is important in the pathogenic ability of *S. aureus* to invade host tissue. Indeed it was shown that FnBPA and FnBPB are sufficient to enable invasion of tissue, when both proteins were coated onto inert beads, which when coated were subsequently able to invade epithelial cells (Sinha et al. 2000).

Clumping factor proteins A and B (ClfA and ClfB) enable *S. aureus* clumping and binding to fibrinogen (a blood clotting factor), in the presence of fibronectin (Ní Eidhin et al. 1998; McDevitt et al. 1994). ClfA is also able to reduce phagocytosis of *S. aureus* by polymorphonuclear leucocytes (Higgins et al. 2006). Additionally, ClfA can bind to human platelets directly (Siboo et al. 2001), this may improve bacterial survival during infection. FnBPA, FnBPB, ClfA and ClfB, are all under the regulation of Sortase A (which in involved in the retention of these proteins on the bacterial surface). Sortase A expression may reduce the spread of bacteria in the host. Bacteria which lack Sortase A, a hyper-spreading phenotype was observed, (measured by growth on TSB agar plates). This suggests that when these proteins (FnBPA, FnBPB, ClfA and ClfB) are absent, increased bacterial spreading occurs (Tsompanidou et al. 2012). This may represent a bacterial response to loss of adhesion, or simply the lack of adhesion leads to increased spreading.

Together, *S. aureus* cell surface factors reduced phagocytosis, reduces oxidative damage, promote cellular adhesion and promote invasion of cells/tissues. These varied host defence mechanisms contribute to the pathogenesis of *S. aureus*.

S. aureus enzyme and toxin virulence factors

Extracellular enzymes and toxins are released from the bacteria, including haemolysins, nucleases, lipases and proteases, which promote the pathogenesis of *S. aureus* through escape of host cells and spreading through infected tissues (Dinges et al. 2000).

S. aureus is capable of damaging the host cell plasma membrane through several secreted factors. α-hemolysin is able to form transmembrane pores in the plasma membrane of red blood cells (and other blood cells), which results in osmotic mediated host cell lysis (Bhakdi & Tranum-Jensen 1991). Forming pores in the plasma membrane is not the only tactic used by *S. aureus* for membrane damage. β-hemolysin, does not form pores, but actively degrades plasma membrane component sphingomyelin (Vandenesch et al. 2012). Plasma membrane damage can also be caused by peptides, including γ-hemolysin, however the mechanism of this membrane degradation is currently not clear (Vandenesch et al. 2012). Together, these toxins cause plasma membrane damage which leads to host cell lysis and bacterial escape.

S. aureus produces enzymes used to promote bacterial survival and invasion in the host. For example, two coagulase enzymes are produced by *S. aureus*, which induces clotting of the blood (McAdow et al. 2012). This may be useful for bacteria in formation

of lesions and evading phagocytic cells. Hyaluronidases are enzymes which breaks down hyaluronate (an extracellular glycosaminoglycan), and are expressed by *S. aureus* as a virulence factor (Hynes & Walton 2000), thought to be important in the spreading of bacteria throughout tissue. In addition *S. aureus* uses lipase, and nuclease enzymes to degrade lipids and DNA respectively. Lipase is important in biofilm formation, and nucleases are used to evade NETs (Kiedrowski et al. 2014; Hu et al. 2012). In addition, *S. aureus* uses staphylokinase, this enzyme indirectly results in the digestion of fibrin networks (often used by the host to contain infection), which further enables the spreading of bacteria (Bokarewa et al. 2006).

Toxins released by *S. aureus* are important in bacterial pathogenesis, particularly in sepsis outcome (where an excessive host immune defence response becomes detrimental for the host). *S. aureus* releases super antigens (SAGs) which are able to cause massive activation of T cells. Importantly, SAG mediated T cell activation is non-specific, and results in activation of up to 20% of the T cells within the host (Li et al. 1999). Over activation of T cells leads to massive cytokine production, deregulation of the adaptive immune system and ultimately leads to life-threatening host outcomes, for example food poisoning, toxic shock syndrome, or organ failure (Llewelyn & Cohen 2002). *S. aureus* releases several SAGs, including toxic shock syndrome toxin (TSST), staphylococcal enterotoxins (SEs), and exfoliative toxins (ETs) (Bukowski et al. 2010; Dinges et al. 2000). SAGs promote *S. aureus* survival and spread within the human host.

1.4 Autophagy

Autophagy is a conserved, intracellular self-degradation pathway which recycles cellular components including, long-lived proteins, damaged organelles and damaged proteins, through trafficking to the lysosome (or vacuole in yeast/plants) for degradation (Mizushima et al. 2008; Tanida 2011). In fact the term “autophagy” means self-eating and was first used to describe cellular components being degraded by lysosomes in mammalian cells (Ashford & Porter 1962). Important studies and screens primarily using budding yeast, *Saccharomyces cerevisiae*, have led to the rapid identification of multiple autophagy genes, and their role in autophagy regulation, initiation and function (Nakatogawa et al. 2009).

There are three autophagic pathways in mammalian cells. These include macroautophagy, microautophagy, and chaperone mediated autophagy (CMA) (Figure 1.1) which use distinct pathways to target cargo for degradation (Boya et al. 2013; Glick et al. 2010). Macroautophagy is characterised with the formation of a double

membrane vesicle, termed “autophagosome”, which engulfs cargo for degradation and subsequently fuses with lysosomes. Microautophagy is the engulfment of cargo directly into the lysosome. Chaperone mediated autophagy is mediated by a chaperone protein which brings cargo to the lysosome which ultimately results in cargo translocation within the lysosome. All three autophagy pathways result in the lysosomal degradation of cargo.

In addition, within the macroautophagy (and microautophagy) pathway, there are also a number of selective pathways for the degradation of specific cellular components. In macroautophagy, selective autophagy pathways include mitophagy, aggrephagy and ribophagy, which target damaged mitochondria, protein aggregates and ribosomes respectively, to the autophagosome for degradation (Kubli & Gustafsson 2012; Lamark & Johansen 2012; Bakowska-Zywicka & Tyczewska 2009).

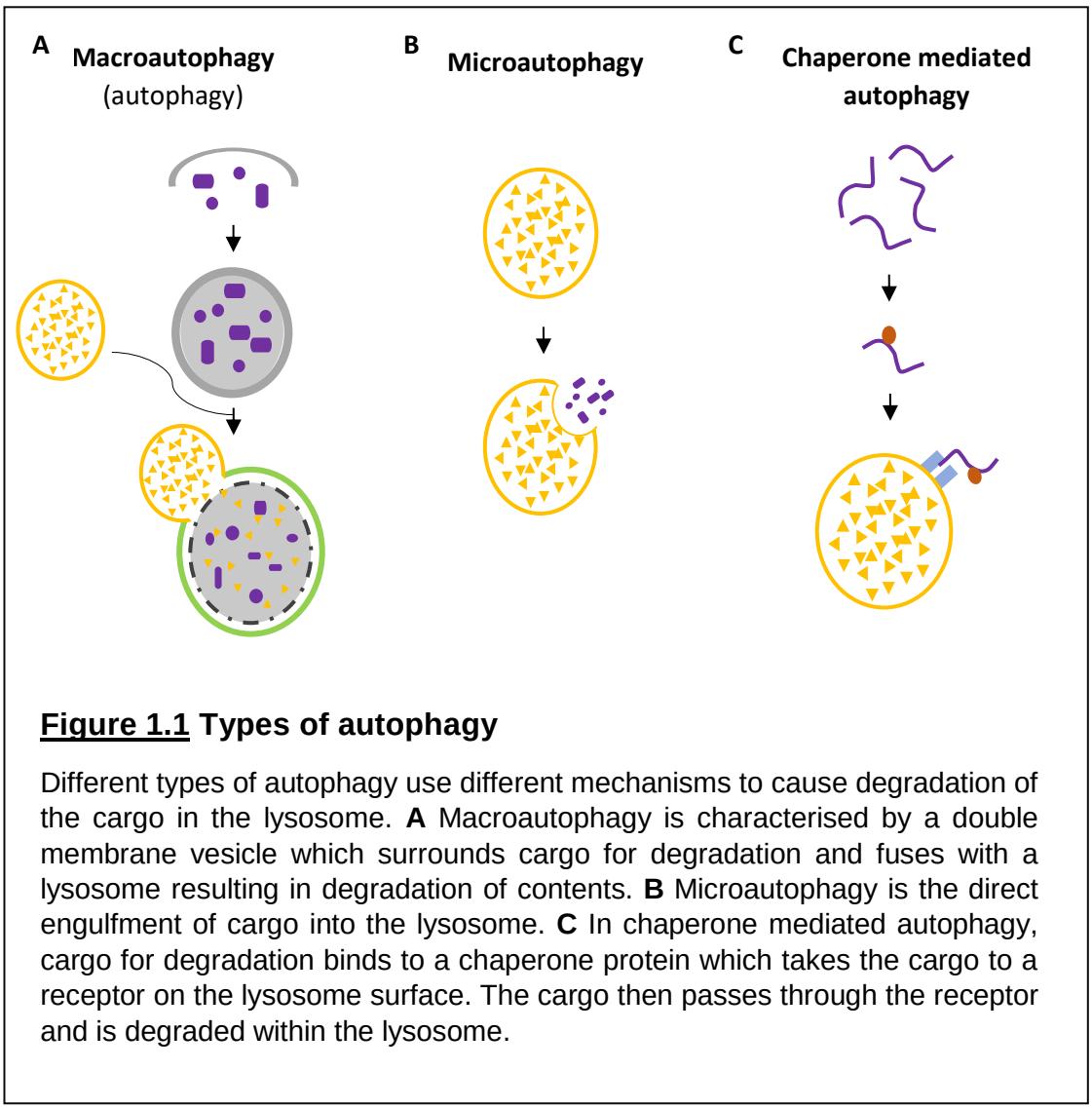

Figure 1.1 Types of autophagy

Different types of autophagy use different mechanisms to cause degradation of the cargo in the lysosome. **A** Macroautophagy is characterised by a double membrane vesicle which surrounds cargo for degradation and fuses with a lysosome resulting in degradation of contents. **B** Microautophagy is the direct engulfment of cargo into the lysosome. **C** In chaperone mediated autophagy, cargo for degradation binds to a chaperone protein which takes the cargo to a receptor on the lysosome surface. The cargo then passes through the receptor and is degraded within the lysosome.

1.4.1 The role of macroautophagy

Macroautophagy (hereafter termed autophagy) is the most studied autophagic pathway. Autophagy is a non-selective cellular degradation system, which can degrade a wide array of cellular components. This is in contrast to the other major cellular degradation processes completed by proteasomes, which degrade ubiquitinated proteins in a selective manner (by ubiquitination). The non-selective autophagy pathway enables autophagy to have multiple cellular roles.

It is thought autophagy evolved in order to allow cells to adapt and survive in starvation conditions. Autophagy, through degradation of cellular components, creates new material for the cell to use, significant in starvation situations (Mizushima et al. 2008). A cellular reduction in nutrients, for example amino acids or ATP can induce autophagy. After cargo is degraded by lysosomal hydrolases, the degraded components can be recycled back into the cytoplasm for alternative use by the cell. Transfer of components back into the cytoplasm (out of the lysosome) can occur through lysosomal permeases. For example, a probable sugar efluxer, Spinster, may promote passage of sugars into the cytoplasm (Rong et al. 2011). In yeast, autophagy gene ATG22 has been shown to be an amino acid efluxer (Yang et al. 2006), although an equivalent mammalian mechanism to transfer amino acids has not been identified. Autophagic cellular recycling, induced under starvation conditions, may also be important in enabling synthesis of proteins specifically required by cells in starvation conditions (Onodera & Ohsumi 2005).

Autophagy is not only used for recycling of cellular components under basal and starvation conditions. Autophagy is used to degrade damage-causing cellular components, such as damaged mitochondria or protein aggregates. In these cases, autophagy promotes cellular survival. Furthermore autophagy provides degradation of long-lived proteins, used for cellular homeostasis, which are no longer required (Mizushima et al. 2008). Autophagy is also important in development, highlighted by fact that the majority of murine knock-out models in autophagy genes lead to lethality at the embryonic or neonatal stages (Mizushima et al. 2010). Furthermore, autophagy has roles in regulation of the immune system, for example in the release of IL1-β (Dupont et al. 2011) and in loading of the MHC-II molecules in DC and epithelial cells (Schmid et al. 2007).

Since autophagy has multiple important cellular roles, when autophagic components or pathways do not function properly, cells are unable to maintain homeostasis, and this can lead to disease. A role of dysfunctional autophagy is promoting cancerous cell

survival, where autophagy may prevent necrotic cell death, has been demonstrated (Degenhardt et al. 2006). However evidence exists that the role of autophagy in cancer can be beneficial or detrimental for cancerous cells, differences may be caused by specific tumour cell types. Autophagy is also important in the clearance of protein aggregates, and dis-functional autophagy therefore is implicated in neurodegenerative diseases. In Alzheimer's disease, impaired autophagy induction and autophagosome formation may result in a lack of clearance of protein aggregates (Orr & Oddo 2013).

In other human diseases single nucleotide polymorphisms SNPs in *ATG5* have been linked to auto-immune diseases, such as asthma and systemic lupus erythematosus (López et al. 2013; Poon et al. 2012). Furthermore, SNPs in autophagy receptor p62 (sequestosome 1, or SQSTM1) and other autophagy genes including *ATG5* and *ATG16* increases the likelihood of Paget's disease, a bone disease (Usategui-Martín et al. 2015; Chamoux et al. 2009). Interestingly, a lack of human diseases associated with complete loss of function in core autophagy genes indicates that autophagy genes are necessary for human development. The important role of autophagy in infectious disease is discussed in section 1.4.6. Several pathogens are targeted to the autophagosome, resulting in pathogen degradation, providing an important host defence against pathogens.

1.4.2 Microautophagy and chaperone mediated autophagy

Microautophagy and chaperone-mediated autophagy have not been as well studied as macroautophagy, although both also result in the lysosomal degradation of cellular components. Microautophagy is the engulfment of cargo directly into the lysosome, where invagination of the lysosomal membrane enables small proportions of the cytoplasm to be degraded in a non-selective manner (Marzella et al. 1981). However, selective microautophagy occurs for organelles, including micro-mitophagy, micro-pexophagy (peroxisome degradation), and in micro-nucleophagy (Mijaljica et al. 2011; Sahu et al. 2011).

Chaperone mediated autophagy is facilitated by a chaperone protein which transports cargo to the lysosome. This ultimately results in cargo translocation across the lysosome membrane for degradation. In CMA, only soluble proteins are targeted for degradation. The chaperone protein is heat shock cognate protein of 70 kDa (Hsc70), which recognises proteins for degradation via a KFERQ sequence (Dice 1990; Chiang et al. 1989). The lysosome-associated membrane protein type 2A (LAMP-2A) is a receptor for Hsc70 (Cuervo & Dice 1996), which leads to the protein for degradation being translocated into the lysosome and degradation.

1.4.3 The macroautophagy pathway

The autophagy pathway is a complex pathway involving many proteins, however the pathways can be broken into four key steps: vesicle nucleation, vesicle elongation, lysosome fusion, and lysosomal degradation of cargo (Tanida 2011; Mizushima 2007). A general overview of the pathway begins with the generation of a double membrane vesicle, which engulfs cargo for degradation forming an autophagosome. A lysosome then fuses with the autophagosome and releases acid hydrolases which cause degradation of the contents. A diagram of the autophagy process is shown in figure 1.3. The autophagy pathway is highly regulated, resulting in a complex pathway involving several key proteins (Table 1.1).

The first step, vesicle nucleation, begins after autophagy induction signals cause inactivation of a key negative regulator of autophagy, mammalian target of rapamycin (mTOR) (Crotzer & Blum 2010). This leads to the activation of the protein kinase ULK-1 complex, which itself is normally inhibited by mTOR (Hosokawa et al. 2009). The ULK-1 complex then binds to the phosphatidylinositol 3-kinase (PI3K) complex, which is known to form a pre-autophagosomal structure (PAS) in yeast, which is also thought to occur in mammals (Mizushima et al. 2011). The next step is the formation of an omegasome from the endoplasmic reticulum (ER) which is regulated by the PI3K complex (Axe et al. 2011; Crotzer & Blum 2010). The omegasome is named after the similarity in shape to the Greek omega symbol. The isolation membrane is subsequently formed from the omegasome and is released from the ER (Mizushima et al. 2011). The source of the membrane used in autophagosome formation is not fully understood. It is thought that membrane from the Golgi, endosomes, plasma membrane or mitochondria may also be used (Chan & Tang 2013).

Vesicle elongation starts at this point, utilising two protein ubiquitin-like conjugation systems the ATG12-ATG5-ATG16 complex and the LC3-lipidation system (Mizushima et al. 2001). The ATG12-ATG5-ATG16 complex locates on the isolation membrane (Mizushima et al. 2001), as the vesicle membrane surrounds cargo for degradation. In addition, the product of the LC3 lipidation, LC3-II, localises to the autophagosome, on both the inner and outer membranes (Weidberg et al. 2010). LC3-II on the outer membrane is removed by ATG4 after autophagosome formation (Yu et al. 2012), whereas LC3-II is degraded on the inner membrane after lysosomal fusion.

The ATG12-ATG5-ATG16 complex is created when ubiquitin-like ATG12 is covalently conjugated to ATG5, using E1-like enzyme ATG7, and E2-like enzyme ATG10 (Mizushima et al. 2001). ATG16 associates with the ATG12-ATG5 complex. The second ubiquitin-like conjugation system leads to the lipidation of LC3-I (or lipidation of homologues GABARAP and GATE-16). LC3-I is conjugated to

phosphatidylethanolamine (PE), by E1-like enzyme ATG7, and E2-like enzyme ATG3 (Ichimura et al. 2000). Additionally, the ATG12-ATG5-ATG16 complex acts as a scaffold E3-like enzyme in this lipidation process (Mizushima et al. 2007). A schematic of both conjugation processes is shown in Figure 1.2.

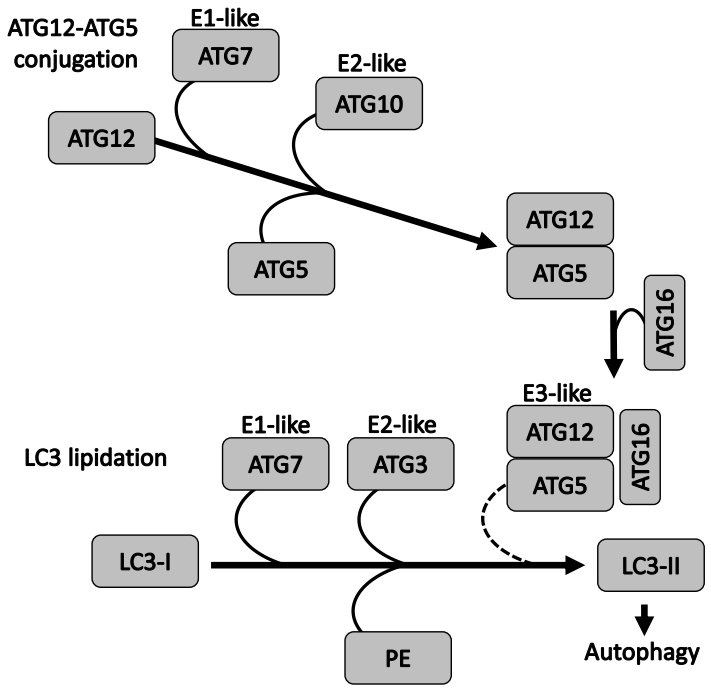

Figure 1.2 Ubiquitin-like conjugation systems in LC3-II lipidation

ATG12-ATG5 covalent conjugation requires E1-like ATG7 and E2-like ATG10. ATG12-ATG5 associates with ATG16. Lipidation of LC3-I with phosphatidylethanolamine (PE), requires E1-like ATG7 and E2-like ATG3, and the ATG12-ATG5-ATG16 complex acts as an E3-like scaffold to promote lipidation

Both conjugation systems may promote membrane elongation, however are thought to be more important in the closure of the autophagosome. When elongation is nearly complete the ATG12-ATG5-ATG16 complex departs from the membrane (Mizushima et al. 2001). Each side of the elongating vesicle membrane is joined by membrane scission (Knorr et al. 2015). Once circularisation is complete an autophagosome, with a characteristic double membrane, is formed, harbouring enclosed cargo for degradation.

The next stage of the autophagy pathway is the fusion of a lysosome to the outer membrane of the autophagosome, forming an autolysosome. In mammals an extra step can occur before lysosomal fusion, autophagosomes can fuse with early or late endosomes forming amphisomes (Strømhaug & Seglen 1993). This adds another layer of complexity through linking the endosomal and autophagic pathways. It is currently unknown exactly how autophagosomes dock with lysosomes, although in yeast it is shown that SNARE proteins are involved in trafficking to the vacuole (Fischer von

Mollard & Stevens 1999). The vacuole is comparable to a mammalian lysosome. In addition, in a study using *Drosophila melanogaster*, a SNARE protein, Syntaxin 17 has been identified on autophagosome membranes (Krämer 2013), indicating SNARE protein involvement. Until recently it was thought that the ATG12-ATG5-ATG16 and LC3 conjugation systems were required for autophagosome elongation. Interestingly, autophagosomes have been observed in cells deficient of the autophagy conjugations systems, (using syntaxin 17 as an autophagosome marker rather than LC3-II). However, these autophagosomes (formed without the conjugation system) had a reduced rate of degradation of the inner autophagosomal membrane. This suggests the conjugation systems are required for efficient degradation of the inner membrane after lysosomal fusion (Tsuboyama et al. 2016).

The final step of the pathway is the degradation of cargo. This occurs with the release of acid hydrolases from the lysosome which gain access to the cargo after degradation of the former autophagosome inner membrane (Klionsky 2007). The acid hydrolases then degrade the contents of the autolysosome (Tanida 2011). After degradation the autolysosome components are recycled. Vesicles from the autolysosome bud off and can become mature lysosomes (Yu et al. 2010). In terms of the fate of degraded cargo, Atg22 has been shown to be an amino acid efluxer in yeast (Yang et al. 2006). Spinster is a potential sugar efluxer, which is additionally required for re-formation and acidification of lysosomes (Rong et al. 2011).

Regulation of macroautophagy induction

The autophagy pathway is highly regulated, and can be induced for example in starvation conditions, by sensing of a reduction in cellular nutrition and increased cellular stress. The protein kinase mTOR, as described above, is a regulator of autophagy induction, which is found in two complexes, mTOR complex 1 (mTORC1) and mTORC2, however, mTORC1 is important in starvation induced autophagy induction. The nutrients available in the cellular environment are monitored by sensing of amino acid availability, where Rag GTPases regulate mTORC1 activity (Sancak et al. 2008). Additionally, a reduction in cellular energy levels, in terms of ATP and AMP, causes the activation of (AMP-dependent protein kinase) AMPK, which indirectly leads to inhibition of mTOR, leading to autophagy induction (Shaw et al. 2004). In addition to nutrients, cellular stress is also monitored. Insulin signalling negatively regulates autophagy induction through mTORC1 (Naito et al. 2013). Another cellular stress, hypoxia induces autophagy through mTORC1 signalling, although the pathway which includes REDD2, is not completely understood (Sofer et al. 2005). Together these reports highlight how a wide variety of signals of cellular energy and health are monitored and used to induce/inhibit autophagy through mTOR dependent pathways.

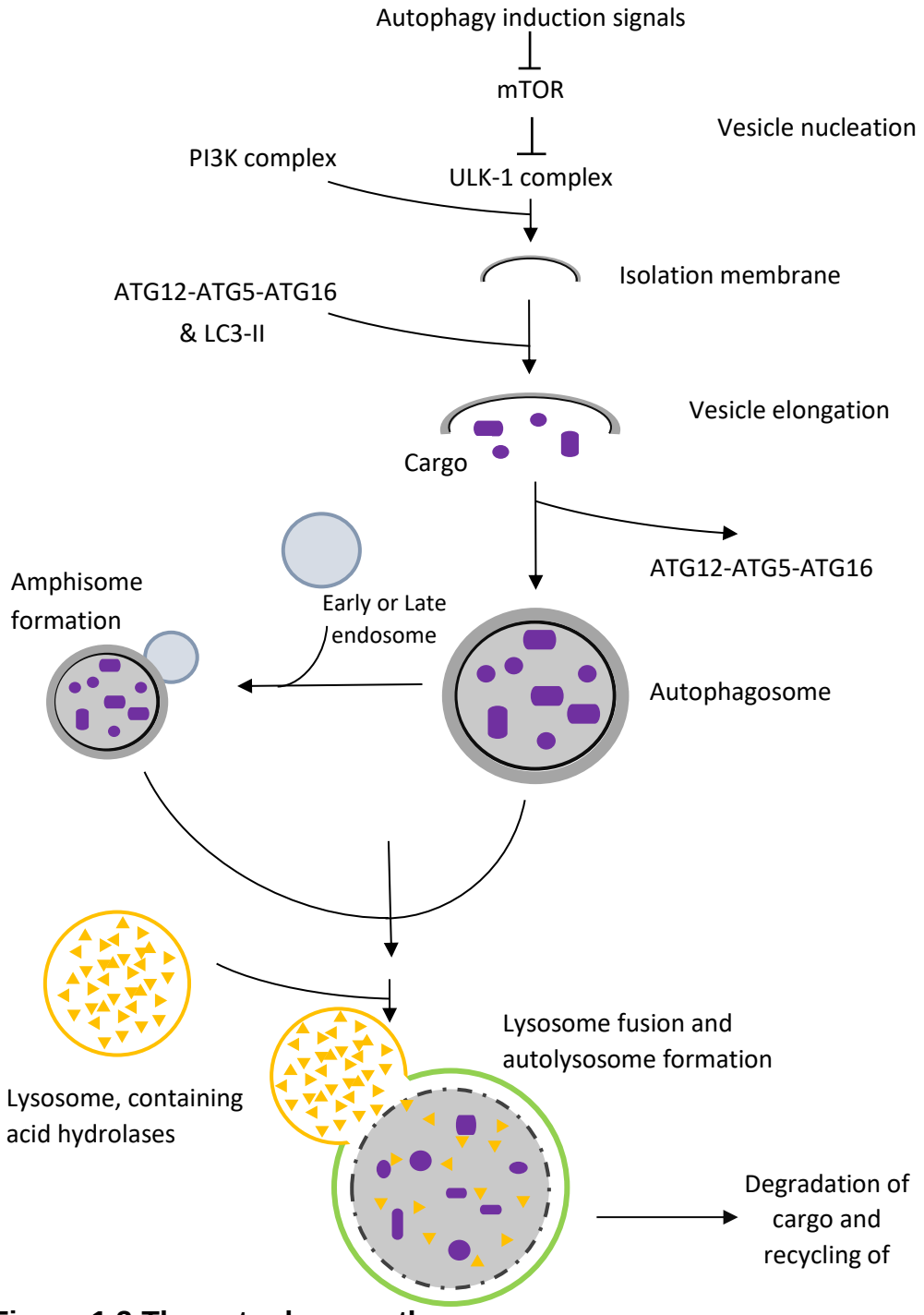

Figure 1.3 The autophagy pathway

Autophagy induction signals lead to the activation of the ULK-1 complex through inhibition of mTOR. The ULK-1 complex then binds to the PI3K complex, leading to the formation of an isolation membrane. Elongation of the characteristic double membrane requires both the ATG12-ATG5-ATG16 and LC3 conjugation systems, which engulfs cargo for degradation, eventually resulting in the formation of an autophagosome. The autophagosome can fuse with early or late endosomes to form amphisomes, then both autophagosomes and amphisomes can fuse with lysosomes to form an autolysosome. Acid hydrolases are released from the lysosome which degrade the inner membrane and cargo which can then be recycled, in addition to the autolysosome constituents.

Table 1.1: Autophagy proteins, interactions and their role in autophagy

Protein	Interactions	Role in autophagy
mTOR	- ULK-1: inhibitor of ULK-1 complex activation	Negative regulator of autophagy which can be activated or inactivated by autophagy inducers or inhibitors. Inhibition leads to autophagy.
ULK-1 complex	- mTOR: which inhibits activation - PI3K complex	Usually inhibited by mTOR, so when mTOR inhibition ceases the complex becomes activated - Complex includes; ULK-1, FIP200, Atg13 and Atg101
PI3K complex	- ULK-1 complex	Binds to ULK-1 complex after activation. May form a PAS structure in mammals. - Complex includes; Class IIIPI3K/Vsp34, p150/Vsp15, Beclin 1, Atg14(L) and AMBRA1
ATG12-ATG5-ATG16 complex	Binds to the isolation membrane	Elongation of the isolation membrane
LC3 lipidation complex	LC3-II (the product of the complex) binds to the isolation membrane	Elongation of the isolation membrane
SNARE proteins	Potentially provide interactions between the lysosome and the autophagosome	Potentially involved in lysosomal fusion

Table 1.1: Table highlights key proteins and protein complexes used in the autophagy pathway which are described in detail in this section 1.4.3. The interactions of each complex/protein with other autophagy proteins and the role in autophagy induction is described.

1.4.4 Selective autophagy

Autophagy is largely a non-specific pathway induced by starvation, however within macroautophagy, there is also the capacity for selective autophagy where specific cargo, pathogens, protein aggregates or organelles are directly targeted for degradation. In selective autophagy, autophagy receptor proteins interact with both autophagic machinery and the specific ubiquitinated cargo, to initiate autophagic degradation. Autophagy receptors recognise and bind cargo through ubiquitin-binding domains (UBDs). Selective autophagy requires ubiquitination of cargo for degradation. This is mediated by ubiquitin ligase, for example the role of parkin in mitophagy (Popovic & Dikic 2012). Autophagy receptors can then also bind to autophagosome marker LC3, through LC3 interacting regions (LIRs). Therefore, autophagy receptors selectively collect and transport cargo towards LC3 marked autophagosomes for degradation (Popovic & Dikic 2012; Rogov et al. 2014). Multiple autophagy receptors have been described, including p62 (also known as sequestosome 1, SQSTM1), optineurin (OPTN), nuclear dot protein 52 (NDP52) and neighbour of Brca1 gene (NBR1). A well-studied example of selective autophagy is mitophagy, whereby parkin, a ubiquitin ligase, is recruited to damaged mitochondria by Pink1, and here parkin can ubiquitinate the mitochondria, which leads to autophagy receptor, p62 recruitment, and ultimately autophagic degradation of the mitochondria (Popovic & Dikic 2012).

Pathogens resident in the cytoplasm may be ubiquitinated and therefore become targets of selective autophagy. An interesting example is *Salmonella enterica*, here phosphorylation of autophagy receptor optineurin (OPTN), led to its increased LC3 binding affinity, and therefore an increased capacity to induce autophagy and ultimately limit cytosolic bacterial replication and survival. Indeed, optineurin deficiency in HeLa cells led to increased *Salmonella* proliferation (Wild et al. 2011). In addition it was shown that autophagy receptor NDP52 is used as a host-defence against *S. enterica* to promote pathogen degradation (Thurston et al. 2009). Therefore, multiple autophagy receptors may be utilised against the same ubiquitin coated pathogen.

In another example, ubiquitin ligase SMURF1 is important in the ubiquitination of *Mycobacterium tuberculosis*, leading to NBR1 and LC3 recruitment. In mice deficient in *Smurf1*, a higher bacterial load and mortality were seen following *M. tuberculosis* infection (Franco et al. 2017). Both p62 and NDP52 autophagy receptors have been shown target *Shigella flexneri* and *Listeria monocytogenes* for autophagy degradation, but in bacterial specific pathways. *Shigella* is dependent on septin and actin mediated mechanisms, (whereby host cell septin caging limits pathogen actin based mobility and recruits autophagy machinery to the pathogen), whereas *Listeria* targeting did not

require septin or actin (Mostowy et al. 2011; Mostowy et al. 2010). This is suggestive that different pathogens are able to induce alternative selective autophagy pathways. It is clear that selective autophagy has an important role in cell mediated clearance of unwanted or damaged cargo, and in pathogen clearance.

1.4.5 Canonical and non-canonical autophagy

Canonical autophagy is autophagy which employs the use of autophagy proteins to assemble the double membrane autophagosome (as described in section 1.4.3). On the other hand, non-canonical autophagy is the creation of an autophagosome, without the use of all the core autophagy proteins, this can include loss of Beclin (in the PI3K complex), ATG5/ATG7, LC3 or ULK1 (Codogno et al. 2011).

ATG5 and ATG7 independent autophagy has been described, where formation of autophagosome and autolysosomes could occur without either protein. *In vitro* studies determined that autophagosome formation occurred in ATG5 or ATG7 deficient MEFs, and that this ATG5-independent autophagy responded to autophagy influencing drugs and starvation in a similar manner as conventional autophagy. Importantly, the lack of ATG5 or ATG7 resulting in a blockage in the creation of LC3-II (LC3-I lipidation) (Nishida et al. 2009). Therefore, autophagy processes are not entirely dependent on core autophagy genes, perhaps enabled through distinct signalling pathways or high redundancy in the autophagy system. A recent report highlighted the importance of ATG5-independent autophagy in mitochondrial clearance (Ma et al. 2015). Furthermore, ATG5-independent autophagy has been implicated in pathogen clearance. *Mycobacterium marinum* is targeted to autophagosomes lacking LC3-II marking, in an ATG5-independent manner (Collins et al. 2009). Furthermore, ATG5-independent autophagy promotes clearance of pathogenic bacteria within intestinal cells (Ra et al. 2016).

ATG3-independent autophagy is suggested by the formation of autophagosome-like structures in *atg3*-/- mice (Sou et al. 2008). ATG3/ATG7-independent autophagy has been demonstrated in Drosophila melanogaster, specifically in mid-gut cell shrinkage (which occurs in development). ATG8 (LC3-II) was not lipidated in this system, and it was shown that E1-like enzyme UBA-1 is required for mid-gut cell shrinkage, but is not involved in lipidation of ATG8 (LC3-I) (Chang et al. 2013).

Both ATG5 and ATG3 independent autophagy appear to function without lipidation of LC3. This has been confirmed in a recent report highlighting that autophagosome and autolysosome formation can occur when autophagy conjugation systems are not present (Tsuboyama et al. 2016). Together these studies demonstrate that ATG3 and

ATG5 are not essential for autophagy, and that LC3-II does not always mark autophagosomes.

1.4.6 Host-pathogen interactions in macroautophagy

Pathogens often target or subvert specific parts of the immune response for their own survival and autophagy is no exception. Autophagy has a role in the host-pathogen interactions with bacterial, viral, fungal and protozoan pathogens (Kuballa et al. 2012). There are several methods host cells use to recognise and induce autophagy, through activation of pathogen recognition receptors (PRRs), such as Toll-like receptors (TLRs; which recognise pathogen associated molecular patterns (PAMPs)), through damage associated molecular patterns (DAMPs), and directly through pathogen receptors. One example is TLR4, which recognises lipopolysaccharide (LPS), found in bacterial cell walls. When TLR4 is activated this can inhibit the bacterial mediated arrest of phagosome maturation, and bacteria are subsequently targeted to autophagosomal degradation (Xu et al. 2007). Furthermore, TLR4 (among other TLR) signalling, has been shown to increase Beclin-1 levels (part of the PI3K complex, Table 1), thus inducing autophagy (Shi & Kehrl 2008). Therefore, autophagy can be induced through recognition of pathogens.

Autophagy induction plays a crucial role in the front-line innate defence against pathogens. Mutations in ATG proteins increase the risk of infection by intracellular pathogens (Levine et al. 2011). *S. aureus* is demonstrated to be degraded through autophagy (Amano et al. 2006), and ATG proteins appear to be involved in the ability of *C. neoformans* to cause infection within the host (Qin et al. 2011). This highlights a link with both *C. neoformans* and *S. aureus* with autophagy, which is discussed in detail in section 1.4.7 and 1.4.8.

The interaction between bacterial pathogens and the autophagy pathway are well studied. Autophagy is an effective strategy to eliminate bacteria, however is some cases this may be limited to an early time point in infection, before bacteria begin to replicate in the cytosol (Py et al. 2007). Bacteria block autophagy for their own end using several methods such as, inhibiting autophagy induction, remaining in the phagosome by preventing maturation, preventing lysosomal fusion, and concealing themselves from the autophagy pathway, as reviewed by Deretic and Levine 2009. There is remarkable diversity in the different strategies employed by bacteria to subvert or induce autophagy in these circumstances. Some gram-negative bacteria, including *Porphyromonas gingivalis*, and *Brucella abortus* hide and replicate within vacuoles (lysosomes) of the host cell, which are shown to have autophagic marking (Dorn et al. 2001; Pizarro-Cerdá et al. 1998). It is suggested that remaining in the vacuole (lysosome) provides bacteria access to degraded contents such as amino acids,

therefore these bacteria may inhabit a niche within the autophagy pathway (Colombo 2005). Another interesting mechanism is seen in *Legionella pneumophila, Coxiella burnetii* and *Salmonella enterica* serovar typhimurium infections. Each of these pathogens utilise a secretion system to promote autophagy, by injecting autophagy inducing proteins into the host cell (Amer & Swanson 2005; Hernandez et al. 2003; Gutierrez et al. 2005). From these studies, reviewed in Colombo 2005, it is clear that bacteria utilise the autophagic pathway for their own survival.

Unlike bacteria, fungal pathogens have not been studied at depth in relation to autophagy, however there is some evidence of the involvement of autophagy. *Aspergillus fumigatus* phagosomes were shown to be marked with LC3, in Lc3-assocaited phagocytosis (Martinez et al. 2015). A loss of autophagy, specifically ATG5 in myeloid cells, in mice infected with *Candida albicans* led to increased susceptibility of infection (Nicola et al. 2012). Therefore, autophagy (or autophagic machinery) is employed in response to fungal infections.

1.4.7 Autophagy in *S. aureus* infection

S. aureus interactions with host cell autophagy have been described for several cell types, due to the range of cells *S. aureus* interacts with during infection, for example phagocytes after tissue invasion, or keratinocytes during infection of the skin.

It was demonstrated using HeLa cells that *S. aureus* resides in an autophagosome, as determined through marking of LC3 on a double membrane vesicle, but that the autophagosome does not become marked with LAMP-2 or become acidified (Schnaith et al. 2007). This suggests that the maturation of the staphylococcal autophagosome is inhibited. It was concluded that *S. aureus* later escapes from the autophagosome into the cytoplasm causing host cell death. The host cell death was shown to be autophagy dependent, specifically requiring *Atg5* (this was not apoptosis due to a lack of caspase involvement) (Schnaith et al. 2007). This represents evidence that host cell autophagy is beneficial for *S. aureus* during infection. Where bacteria have escaped the autophagosome and reside in the cytoplasm, selective autophagy can result in autophagosome enclosure. This occurs for *S. aureus*, but the bacteria can escape autophagosomes, in a manner which results in autophagosome membrane damage (Neumann et al. 2016).

S. aureus has been shown to subvert host cell autophagy to promote its own survival. In mouse embryonic fibroblasts (MEFs) deficient in *Atg5*, a reduction of both bacterial replication and the ability to kill the host cell was observed (Schnaith et al. 2007), indicating that host *Atg5* is helpful for bacterial survival. However the exact opposite results were recently found where an increase in bacterial replication occurs in *Atg5*

deficient MEFs (Neumann et al. 2016). This suggests that multiple factors, for example bacterial strain, may affect autophagy induction. Interestingly, it was determined that in MEFs, which are non-professional phagocytes, PRIP (phospholipase C-related catalytically inactive protein) can bind to LC3 and that PRIP is required for autophagy mediated degradation of *S. aureus*. Loss of PRIP promoted bacterial survival and proliferation within an LC3 marked vesicle (Harada-Hada et al. 2014). This highlights that different cell types may handle *S. aureus* through different mechanisms.

In vitro studies on murine macrophages (RAW264.7 cells) determined that TLR2 is important in the phagocytosis and activation of autophagy. Using siRNA to target TLR2 reduces both *S. aureus* phagocytosis and cell autophagy (Fang et al. 2014). Similarly, microglial cells, which are tissue resident macrophages in the CNS, also have increased autophagy expression in response to *S. aureus*. TLR2 is used to sense bacterial peptidoglycan (PGN) which results in autophagy dependent host cell death. This was demonstrated with injection of PGN into murine brains which led to microglial cell death (Arroyo et al. 2013). This suggests that for macrophages, autophagy induction is detrimental for the cell survival.

The importance of the *agr* locus is clear. The *agr* locus controls *S. aureus* virulence factor expression in host autophagy activation. It appears that *agr* virulence factors are required to induce autophagy involvement since bacteria deficient in *agr* were not targeted into autophagosomes and did not cause host cell death (Schnaith et al. 2007). Similarly in DCs, *agr* is required to increase autophagosome formation, enabling bacterial survival and eventual cellular escape (O'Keeffe et al. 2015), further suggesting that autophagy promotes bacterial survival. Interestingly, loss of *agr* in MRSA strains enables persistent infection of keratinocytes, however in this case autophagy was induced and was associated with degradation of inflammasomes (Soong et al. 2015), perhaps enabling *S. aureus* to evade keratinocyte mediated damage. This highlights that autophagy strategies employed by *S. aureus* differ between infection site/host cell.

Host cell autophagy can also be beneficial for the host cells. The staphylococcal virulence factor, α-hemolysin, creates pores in the plasma membrane of infected cells and results in the loss of ATP and amino acids. Autophagy activation may occur in two ways. Firstly, through cellular energy sensor AMPK activity which inhibits mTORC1, resulting in autophagy. Secondly, eIF2α-kinase GCN2 which acts a nutrient sensor, perhaps sensing a lack of amino acids, which results an increase in autophagy (Kloft et al. 2010; von Hoven et al. 2012). By blocking autophagy with 3-MA, cells had a reduced ability to recover from non-lethal *S. aureus* infection (Kloft et al. 2010), suggesting that autophagy promotes host cell survival from *S. aureus* α-hemolysin

damage. Interestingly, it is suggested that host cell autophagy is able to reduce the effects of α-hemolysin through dysregulation of ADAM10 (a disintegrin and metallopeptidase domain 10) which is a α-hemolysin receptor (Maurer, Torres, et al. 2015; Maurer, Reyes-Robles, et al. 2015). Furthermore, IFNγ has been demonstrated to induce autophagy to protect keratinocytes from α-hemolysin, through a reduction in ADAM10 expression (Brauweiler et al. 2016). This may add another host cell defence mechanism towards survival of *S. aureus* infection.

Overall the interaction between host cell autophagy and *S. aureus* is complex. Different outcomes may be expected in different cell types, in response to specific bacterial strain virulence expression or in different stages of infection.

1.4.8 Autophagy in *C. neoformans* infection

C. neoformans has been shown to survive, replicate and even escape from inside macrophages, indicating macrophages are a key intracellular niche, important in the pathogenesis of cryptococcal infection. Therefore, the limited publications which investigate the role of autophagy in cryptococcal infection focus solely on macrophage autophagy.

Autophagy was first linked to cryptococcal infection when capsule components, GalXM and GXM, were shown to induce autophagosome formation in murine macrophages (Villena et al. 2008), however, this did not reveal whether host macrophage autophagy was beneficial to the host or for the cryptococcal cells. Interestingly, it was next shown that autophagy proteins, including ATG2a, ATG5 and ATG9, are required for *C. neoformans* growth, through RNAi analysis in murine macrophages, which reduced both the uptake, and replication of intracellular cryptococci (Qin et al. 2011), thus implicating an autophagy role beneficial for cryptoccocal cells. However, a similar RNAi strategy resulting in *atg5* deficiency led to reduced macrophage fungistatic ability, suggesting that autophagy is important as a host defence (Nicola et al. 2012). In contrast, in myeloid specific *atg5* deficient mice no increase in susceptibility to cryptococcal infection is observed (Nicola et al. 2012), suggesting that myeloid cells do not control cryptococcal infection through autophagy *in vivo*. It was recently demonstrated in a murine model that cryptococcal infection leads to an increase in phosphorylation of both AMPKα and ULK-1, both proteins which induce autophagy. However, deletion of AMPKα in myeloid cells in mice leads to a reduction in fungal burden following cryptococcal infection (Pandey et al. 2017) suggesting that AMPKα, and therefore autophagy induction in myeloid cells increases susceptibility to cryptococcal infection. Contradictory evidence means that further analysis is required.

Furthermore, autophagosome marker LC3 has been shown to localised to antibody opsonised cryptococcal cells, however, currently no data showing the yeast within a double-membrane, only within a single membrane structure exists, despite autophagosomes being seen in close proximity (Nicola et al. 2012; Pandey et al. 2017). Due to the overlapping roles of autophagy components in different types of autophagy, for example between classical, *atg5*-independent autophagy and in LAP, further analysis is required to determine the precise roles autophagic components have in the handling and outcome of cryptococcal infection.

In both *S. aureus* and *C. neoformans* infections, the role of host cell autophagy in infection outcome is unclear. Analysis so far has determined contradicting roles of autophagy as both beneficial and detrimental for each pathogen. Therefore the role of host cell autophagy in infection is unknown and warrants further investigation. It is important to determine whether interactions with autophagy components occur with pathogens, and what affect these interactions have of the outcome of autophagy, this may be completed through imaging. *In vivo* analysis in mammals does not enable good cellular level imaging, equally *in vitro* analysis does not provide an environment which matches what the pathogens encounter in real infection. For these reasons a different model organism was required.

1.5 Zebrafish

1.5.1 Zebrafish as a model organism

To study immune function and host-pathogen interactions within vertebrates, *Danio rerio* (zebrafish), make an apt model organism which circumvents limitations of murine and *in vitro* methods. Zebrafish are a worthy model primarily for three key reasons: similarity of immune system with vertebrates, genetic manipulation and imaging potential, in addition to high genetic homology and high fecundity (Renshaw & Trede 2012; Goldsmith & Jobin 2012; Meijer et al. 2014; Torraca et al. 2014).

1.5.2 Zebrafish transgenic reporter lines

The *in vivo* imaging potential of zebrafish is particularly convenient as embryos have translucent skin, and zebrafish lines without pigmentation are available, allowing imaging within whole, live organisms (Goldsmith & Jobin 2012). This factor was initially exploited for study of development, but also allows study of host cell-pathogen interactions (Renshaw & Trede 2012; Goldsmith & Jobin 2012). Fluorescent strains of pathogens can be imaged within the live larvae. Importantly, zebrafish can be manipulated specifically for the research at hand to enable fluorescent labelling/tagging

of specific tissues, cell types or proteins within individual larvae, allowing cellular interactions to be visualised in real time. For example fluorescence can be induced in specific cells/tissues through the Gal4-UAS system, whereby a promoter specific to the required cell type (e.g. neutrophils) drives Gal4 expression in larvae. When crossed to a reporter line, which has a reporter (e.g. GFP) downstream of the UAS enhancer site, Gal4 is able to bind to the UAS site (the binding motif of Gal4) and induces GFP fluorescence within the promoter specific tissue (Asakawa & Kawakami 2008). Another useful tool is the Gateway^{TM} and Tol2 transgenesis system. The Gateway system allows efficient cloning of vectors (which may include tissue specific promotors, reporter constructs, or fluorescently tagged proteins) into specifically designed expression clones which include Tol2 transgenesis sites (Kwan et al. 2007). The relative ease, and speed (due to zebrafish high fecundity and low sexual maturity age), mean zebrafish is an excellent model for imaging of cellular, sub-cellular and host-pathogen interactions.

1.5.3 Genetic manipulation of Zebrafish

Significantly, the zebrafish genome is fully sequenced and zebrafish have a high genetic homology, 70%, with the human genome (Howe et al. 2013) providing good translational potential. Accordingly, zebrafish are well placed for genetic study. Genetic manipulation, through diverse methods allows gene function to be thoroughly examined (Renshaw & Trede 2012; Goldsmith & Jobin 2012). For example, transient gene knock-down can be achieved through the use of Morpholinos (phosphorodiamidate Morpholino oligomers), short ~25bp oligomer molecules which are designed to bind and block access to RNA resulting in inhibition of protein production (Summerton & Weller 1997).

For more permanent effects, mutagenesis can be performed. Zinc-finger nucleases (ZFN), which cause double stranded DNA breaks, can be customised to insert a frame-shift mutation. Through customisation of a zinc finger array (specific DNA sequences targeted for mutagenesis) which is fused to the nuclease, site specific mutants can be created (Foley et al. 2009). Another method of mutagenesis is through the use of TALENs (transcription activator-like effector nucleases). Similar to ZFN, sequence specific repeats fused to a nuclease enable site specific DNA double stranded breaks (Moore et al. 2012). For both ZFN and TALEN mutagenesis DNA breaks are repaired by non-homologous end joining, which can result in mutations.

A recent mutagenesis method is the CRISPR-Cas9 system, whereby Cas9 an endogenous bacterial nuclease is directed to specific DNA targets through the use of site specific guide RNAs (Hwang et al. 2013). Alternatively, the CRISPR/Cas9 system can be used to knock-down gene expression through CRISPR interference (CRISPRi).

Here non-functional Cas9 which binds to the target site, but cannot cut the DNA, blocks gene expression (Qi et al. 2013). Overall, several efficient methods for genetic manipulation exist for zebrafish, enabling gene function to be examined.

1.5.4 Drug treatment in zebrafish

In addition to mutagenesis and transgenic approaches, zebrafish can also be treated with drugs. Drugs can be administered via immersion, where drugs are added to the larvae water, or can be administered through injection. Zebrafish have successfully been used for drugs screens (Parng et al. 2002). Importantly, drug treatment enables further routes of analysis on zebrafish, useful in varied settings.

1.5.5 The zebrafish innate immune system

The zebrafish immune system has high similarity to other vertebrates, including humans. Zebrafish have both adaptive and innate immune systems. The innate immune system is responsible for initial interactions with invading pathogens, and subsequently initiating an appropriate adaptive immune response. The zebrafish model enables study of the innate system alone, which is not confounded by adaptive immunity because innate and adaptive immune systems develop at different rates. Innate cells are present at one day post fertilisation, whereas adaptive immunity does not fully develop until 3 weeks post fertilisation (Willett et al. 1999; Herbomel et al. 1999).

The zebrafish immune system contains macrophages, neutrophils, lymphocytes, eosinophils, dendritic cells and natural killer cells (Renshaw & Trede 2012) all cells are also found within vertebrate immune systems. Both macrophages and neutrophils are observed in the blood stream at 1dpf (Lieschke et al. 2001). Importantly, phagocytic cells are able to phagocytose and successfully degrade a variety of pathogens.

To enable recognition of pathogens, the zebrafish immune system senses pathogens through pattern recognition receptors (PRRs) as in vertebrates. PPRs recognise PAMPs (pathogen associated molecular patterns), from pathogen presence, and also DAMPS (danger associated molecular patterns), which may result from damage caused by pathogens or inflammation. PRRs recognition of PAMPS or DAMPS results in the activation of immune pathways responsible for pathogen degradation. Zebrafish have similar PPRs to humans, including Toll-like receptors (TLRs) identified through BLAST searches (Jault et al. 2004), RIG-like receptors (RLRs) which respond to viral infection (Zou et al. 2015), and NOD-like receptors are shown to be important in *Salmonella* resolution in the zebrafish model (Oehlers et al. 2011). Of note, the zebrafish does have some altered specificity and number of PPRs (Li et al. 2017). An additional arm of the innate immune system is the complement pathway (as discussed

in 1.1.2). The complement pathway exists in the zebrafish, indeed all components of the mammalian complement system have identified orthologues in the zebrafish (Zhang & Cui 2014). Together, these similarities between the innate immune system of humans and zebrafish suggest that zebrafish is a good model for vertebrate innate immunity.

In addition to the attributes of zebrafish in vertebrate immunity study, it is important to acknowledge the drawbacks of the zebrafish immune model. Although the immune system is similar to humans, they are not identical. Additionally the normal human response to infection would involve both the innate and adaptive immune systems, however, due to differential development rates, and the fact most zebrafish work is done under the age of 5 days, adaptive immunity is missing from infection models. Therefore translating data from zebrafish studies to humans is difficult, despite providing a good basis from which to begin human study. Furthermore, consideration of the temperature at which pathogens invade the human body is required. Zebrafish live at a temperature of 28°C, not the human body temperature pathogens have evolved to infect at. Thus in the study of human pathogens in zebrafish there may be differences in pathogen survival and the outcome of disease. Overall however, there are many significant factors in favour of the use of zebrafish as a model of vertebrate immunity, given interpretation of data, especially in a translational context is carefully examined.

The innate immune cells which are important in controlling *C. neoformans* and *S. aureus* infections are macrophages and neutrophils respectively (Feldmesser et al. 2000; Rigby & DeLeo 2012). The study of the innate immune response in zebrafish, to both *C. neoformans* or *S. aureus* challenge is neatly separated from the adaptive immunity, because innate and adaptive immune systems develop at different rates, (Willett et al. 1999; Herbomel et al. 1999). Thus zebrafish make a good model of innate vertebrate immunity for *C. neoformans* and *S. aureus* infection study.

1.5.6 Study of autophagy in zebrafish

In choosing a useful and relevant model for *in vivo* study, it is important to consider which experimental tools and procedures useful for study of autophagy function can be used in zebrafish. Importantly, autophagy, as a conserved cellular mechanism is known to take place in zebrafish. For 70% of human genes, orthologous gene(s) have been identified in zebrafish (Howe et al. 2013). Indeed, for core autophagy genes, at least one orthologous gene exists (Mathai et al. 2017). Autophagy genes can therefore be targeted for the study of gene function and expression, as mentioned above (section 1.5.2 and 1.5.3).

LC3-II is commonly used to analyse autophagy, due to its localisation to autophagosomes. The yeast Atg8 protein has multiple homologues in mammals, MAP1LC3 (LC3), GABARAP and GATE-16. Humans have four LC3 genes, two GABARAP genes and one GATE-16 gene. On the other hand, zebrafish have four Lc3 genes, three GABARAP genes and one GATE-16 gene (Shpilka et al. 2011). Most autophagy studies focus on MAP1LC3B (LC3B), as it is the most studied, and consequently often first examined due to the abundance of tools readily available. Autophagy genes (particularly LC3C) are maternally expressed in zebrafish, indicating a requirement of autophagy during development. Zygotic expression of genes, including autophagy genes (particularly LC3B), begins at ~3.5 hours post fertilisation (Kane & Kimmel 1993; Mathai et al. 2017)

Several methods exist to study autophagy in mammals for example: electron microscopy of vesicle structure, analysis of degradation of long-lived proteins, analysis of delivery of selected material to the lysosome, autophagy marker LC3 localisation, and LC3-I to LC3-II lipidation (Mizushima 2004; Mizushima et al. 2010). These methods do not include mRNA or protein expression assays. Mizushima et al. 2010 make a very significant point that although autophagy genes are up-regulated in response to autophagy cues, there is no evidence to show that the actual process of autophagy (autophagic flux) is up-regulated. Thus, methods such as imaging LC3 localisation, lipidation and function are more robust than mRNA or protein levels measurement, and will provide information on the level of autophagy when carefully controlled (Mizushima et al. 2010). It is highly important to consider the level of autophagic flux during autophagy measurements, rather than simply the levels/amount of autophagy components present. The use of drugs which can block lysosomal fusion to the autophagosome are very useful as controls in helping determine changes to autophagic flux.

Several methods have been proven and used specifically for the study of autophagy in zebrafish including, generation of reporter lines, microscopy, Lc3 western blots and lysotracker staining (He & Klionsky 2010), these methods fit neatly with genetic manipulation, adding another dimension to these techniques.

Lc3 is widely used as an autophagy marker in zebrafish. Lc3 is dispersed cytosolically until autophagy induction, where autophagosomes (or Lc3 associated vesicles) can be visualised by puncta formation. The imaging of Lc3 localisation to autophagosomes is visualised through Lc3 being fluorescently tagged or stained (He & Klionsky 2010). Lc3 microscopy is particularly useful in host pathogen interactions as pathogens can also be fluorescently marked allowing conclusions to be drawn on the location of pathogens in relation to autophagosomes (or Lc3 marked vesicles). Lysotracker dye can be used

to visualise autolysosomes, through the drop in pH after autophagosome fusion with a lysosome (He & Klionsky 2010). It is important to note that lysotracker is not autolysosome specific, and will stain other acidic compartments too. Therefore when using lysotracker, visualisation of Lc3 using another method is also required. Double tagging (GFP and RFP) of Lc3 enables the generation of “traffic-light” Lc3 constructs, which are useful in assessing autophagic flux. When expressed *in vivo*, the GFP tag is quenched under acidic conditions. Lc3 experiences acidic conditions when lysosomal fusion to the autophagosome occurs. Therefore, comparison of double GFP/RFP fluorescence to RFP alone, enables conclusions to be drawn on autophagic flux and degradation. Generation of Lc3 tagged zebrafish lines enable cell specific expression of tagged Lc3. Of particular interest, phagocytes expressing traffic-light Lc3 were generated (PhD thesis Serba, 2016).

Overall, imaging techniques using autophagy constructs, largely Lc3 based, provide analysis of autophagic flux, localisation and dynamics. Lc3 western blots are used to monitor the Lc3-I to Lc3-II lipidation process, using Lc3-II production as a marker of functional autophagy. An increase in the amount of Lc3-II may indicate increased autophagy induction when properly controlled for autophagic flux (He & Klionsky 2010). Additionally, p62 is also assessed by western blot, with a loss of p62 protein suggesting an increase in autophagy, since p62 is degraded through autophagy (Bjørkøy et al. 2009).

1.5.8 Using the zebrafish model to study infection

In vitro infection studies enable insight into host-pathogen interactions. However, the *in vitro* situation is very different to an *in vivo* setting, which may have implications for host-pathogen interactions, for example much more complex cytokine signalling or steric interactions may alter how pathogens are degraded or are able to survive within a host. In order to have improved understanding of the immune response to pathogen infection, an *in vivo* model is favoured. *In vivo* infection models, such as the mouse offer greater understanding of host-pathogen interactions, but have limitations such as reduced imaging potential and reduced genetic tools. Zebrafish provide a good animal model for infection studies due to their genetic tractability, imaging potential and similarity of immune system to humans. The ability to conduct high quality imaging, with regulation of gene expression provides an ability to visualise infection dynamics and host-pathogen interactions throughout an entire vertebrate organism. As such, multiple infection models have been established in zebrafish including bacteria, fungus and virus models.

Importantly, many useful zebrafish transgenic lines have been established to enable visualisation of cellular interactions. Of note macrophage and neutrophil lines are used

to determine whether pathogens are phagocytosed, and if so whether pathogens are degraded, or able to escape the phagocyte and survive extracellularly or survive intracellularly. Additionally granuloma formation may be observed. Furthermore, in order to observe where pro-inflammatory signalling is occurring, perhaps at sites of infection, fluorescent molecules, driven by promoters of molecules such as NF-kB or IL1-B, allow visualisation of sites of inflammation (Kanther et al. 2011; Nguyen-Chi et al. 2014). Visualisation of cellular interactions, or signalling molecules enables host-pathogen interactions to be investigated in detail, within an entire organism.

Relevant to the study of pathogens using zebrafish, several successful infection models have been established. For example, *Mycobacterium marinum*, a bacterium related to *Mycobacterium tuberculosis*, is a natural pathogen of fish. As such, *M. marinum* is well placed as a translational model of mycobacterial disease being proven to replicate within, and cause acute and chronic infection of zebrafish (Prouty et al. 2003). Another example of a bacterial zebrafish infection model is the model of *Shigella flexneri*, which is further relevant due to the study focus of autophagy. Here *S. flexneri* is shown to infect and cause disease in zebrafish, in addition to causing the induction of autophagy (Mostowy et al. 2013). The fungal pathogen *Candida albicans* was shown to induce NF-kB signalling at mucosal epithelial surfaces in the zebrafish model in severe infection, although at low infection doses infection is controlled by phagocytes (Gratacap et al. 2013). Recently, the route of viral entry to the central nervous system was compared between two viruses, (chikungunya and Sindbis) which although were related, showed preferential routes via separate pathways, additionally showing that the viral tropism to the CNS was conserved in zebrafish (Passoni et al. 2017). The listed pathogens mentioned here are not definitive, many more pathogens such as *Salmonella typhimurium*, *Staphylococcus aureus, Cryptococcus neoformans, Aspergillus fumigatus, Streptococcus pneumoniae* and more have been established in a zebrafish infection model. However, the range of pathogen infection models established in zebrafish highlight that a diverse range of human (and zoonotic) pathogens can be used in the zebrafish model, and can provoke similar pathologies and immune responses which occur in human disease. These examples highlight the versatility and potential of the zebrafish as an infection model.

1.5.9 Zebrafish as an infection model for *S. aureus*

The *Staphylococcus aureus* zebrafish infection model has previously been well established (Prajsnar et al. 2008; Prajsnar et al. 2012). Larvae are infected at 1dpf into the yolk sac circulation valley with *S. aureus* suspended in sterile PBS. A range of inoculum doses can be used, with higher doses reducing larval survival more than

lower doses, indicating that *S. aureus* is responsible for larvae death (Prajsnar et al. 2008), importantly this was completed at 28ºC. Furthermore, using reduced virulence *S. aureus* strains for infection increased larval survival.

It was determined that phagocytes control *S. aureus* infection and are responsible for clearing infection. This was determined through depletion of myeloid cells, which resulted in uncontrolled growth of bacteria. (Prajsnar et al. 2008). In the same model it was later shown that neutrophils are a likely intra-cellular niche from which a small population of bacteria survive, replicate and ultimately escape to cause an uncontrolled infection, in a population "bottle-neck" (Prajsnar et al. 2012). Interestingly, a study comparing injection site into the zebrafish indicates that injection into the blood stream is more lethal in comparison to localised sites. It was shown that macrophages phagocytose more *S. aureus*, but that the majority of phagocytes which respond are neutrophils (Li & Hu 2012). Together these studies highlight that as a model of *S. aureus* bacteraemia, the zebrafish model enables study of the innate immune responses, of which neutrophils are particularly important. In contrast to other *in vivo S. aureus* infection models, such as the mouse, the zebrafish offers the opportunity to study bacterial growth dynamics, and cellular-bacterial interactions in the entire organism, through greater imaging capabilities.

1.5.10 Zebrafish as an infection model for *C. neoformans*

The *Cryptococcus neoformans* zebrafish infection model has previously been established by two groups concurrently. Larvae are infected at 2dpf into the yolk sac circulation valley with *C. neoformans* suspended in sterile polyvinylpyrrolidone (PVP) in phenol red. *C. neoformans* was shown to be responsible for increased larval death when infected with higher doses, and conversely reduced larval death was observed at lower doses (Bojarczuk et al. 2016).

Several aspects of human cryptococcal infection are recapitulated in the zebrafish, including a key role of macrophage phagocytosis in controlling early infection, intracellular proliferation within macrophages, and importantly the ability of cryptococcal cells to cross into the brain from the blood stream (Tenor et al. 2015; Bojarczuk et al. 2016). Furthermore, observations made in other models have been confirmed in zebrafish. Using a cryptococcal mutant fnx1Δ, which had previously been shown in mice to have reduced ability to invade cross the BBB, infection of zebrafish also highlighted a reduced ability of cryptococcal invasion into the brain (Tenor et al. 2015). Together, these publications demonstrate that the zebrafish is a valid and useful model for *C. neoformans* infection studies. Interestingly, a zebrafish model where

cryptococcal spores and fungal cells are injected to compare cryptococcal growth dynamics, demonstrated that both types of inoculum cause fungemia and display an ability to cross the BBB (Davis et al. 2016). Furthermore, the role of macrophages, (and to a smaller extent in endothelial cells for spore inocula), were confirmed to act as intracellular niches which led to eventual cryptococcal escape. The role of endothelial cells in enabling intracellular spore survival, at sites away from the brain is a novel finding demonstrated in the zebrafish model.

Mammalian cryptococcal infection models have been established, The mammalian inhalation infection models do provide a useful route of infection, similar to the infection route seen in humans (Price et al. 2011). Non-mammalian invertebrate cryptococcal models have also been established, but lack the similarity of vertebrate immune system, or susceptibility to infection mean findings may have to be proven in a separate model (Harwood & Rao 2014). The zebrafish offers the ability to visualise cellular and subcellular interactions and growth dynamics within an entire organism, with an innate immune system similar to humans.

1.6 Introduction summary

The selection of zebrafish as a model organism for the study of host cell autophagy during infection is well supported through immune system similarity with vertebrates, genetic manipulation and imaging potential. Furthermore, the presence of orthologous autophagy genes in zebrafish is significant, allow investigation of relevant, and potentially translational, research questions.

Autophagy is known to play a role in host-pathogen interactions, applicable to both *C. neoformans* and *S. aureus*. Since the autophagy pathway has several key steps which can be blocked or subverted by pathogens for their own end, it is interesting to question how *C. neoformans* and *S. aureus* may avoid or utilise the pathway during infection, an area which is yet to be fully defined.

S. aureus is known to be targeted for degradation through the autophagy pathway whilst conversely having a capability to subvert the pathway. This indicates a niche within the autophagy pathway that *S. aureus* can utilise to promote survival. Identifying which part of the autophagy pathway *S. aureus* can block or subvert may lead to translational uses in the treatment of infection, in addition to understanding why the same mechanism is not always used or successful, although this may be dependent on the cell type and bacterial strain.

For *C. neoformans* the role of autophagy and interactions of *C. neoformans* with the pathway are not well defined. Particularly because no data has been published describing *C. neoformans* within an autophagosome. It is therefore interesting to investigate whether *C. neoformans* either being degraded by, or subverting, the autophagy pathway. Or alternatively whether non-canonical autophagy may lead to the interaction of cryptococcal cells with autophagic machinery.

To conclude, the many attributes of the zebrafish model will be central in the study of autophagy as a host defence against both *S. aureus* and *C. neoformans*. Despite both pathogens being implicated in a pathogen-host interaction with autophagy, the interactions with autophagy are yet to be fully defined, providing an exciting area for investigation.

1.7 Thesis aims

Important and non-trivial diseases are caused by *C. neoformans* and *S. aureus* in human infection. Cryptococcal infection is responsible for 15% of AIDS related deaths worldwide and can cause cryptococcal meningitis (Rajasingham et al. 2017). In addition bacteraemia caused by *S. aureus* infection has a mortality rate of 20-30% (van Hal et al. 2012). Understanding how pathogen infection progresses is important in enabling targeted treatment during infection.

The physiological cause of cortical infarcts in cryptococcal meningitis is unknown, and finding the cause may provide a therapeutic target. Limited clinical reports have suggested that vascular damage occurs in cryptococcal infection (Aharon-Peretz et al. 2004; Rosario et al. 2012; Leite et al. 2004), which may develop at locations of intravascular cryptococcal growth (Lee et al. 1996; Tenor et al. 2015). Therefore, I hypothesised that cryptococcal proliferation may play a role in vascular damage in cryptococcal meningitis.

Similarly, the role of host cell autophagy in the handling of both *C. neoformans* and *S. aureus* is unclear, but may provide a potential therapeutic target in the treatment of these infections. As described above, host autophagy appears to have both beneficial and detrimental effects for intracellular *C. neoformans* or *S. aureus.* Variations in the role of host cell autophagy may be may be dependent on the host cell type and the virulence of the pathogen strain. It is therefore worthwhile investigating the role of host cell autophagy, both macroautophagy and selective autophagy, in handling of these pathogens.

The aims of this thesis are to:

1. Investigate the role of cryptococcal proliferation in infection dynamics, vascular damage and tissue invasion
2. Characterise and use zebrafish autophagy mutants to analyse the role of host cell autophagy in *C. neoformans* or *S. aureus* infection
3. Generate a p62 zebrafish reporter line to analyse the role of selective autophagy in *C. neoformans* and *S. aureus* infection

Chapter 2 Materials and Methods

2.1 Materials

2.1.1 Zebrafish

The Zebrafish lines used in this study are shown in table 2.1, for wild-type, transgenic and mutant lines. The reason the line was used, and the origin of each line.

Table 2.1: Zebrafish lines

Line	Use	Origin
AB	Wild-Type	
Nacre	Wild-type with loss of pigment cells	
atg3^{sh371}	Mutation in *atg*3 gene	Kind gift from Lore Lambein) (unpublished)
atg5	Mutation in *atg*5 gene	Kind gift from Ingham lab (unpublished)
Tg(lyz:RFP.GFP.ZFLc3)^{SH383}	Neutrophil specific traffic light Lc3 (GFP and RFP)	Kind gift from Justyna Serba (unpublished)
Tg(lyz:GFP.p62)	Neutrophil specific tagged p62 (GFP)	(This study)
*Tg(GalFFCadh)** *Tg(UAS:TEAL)* ^{uq13bh}	Vascular endothelial cadherin (TEAL)	Kind gift from Tim Chico (UAS made by Anne Lagendijk unpublished, Gal4 (Bussmann & Schulte-Merker 2011))
Tg(lyz:nfsB.mCherry)^{sh260}	Neutrophil specific nitroreductase and mCherry expression	Renshaw lab (Elks et al. 2011; Pisharath et al. 2007)
Tg(kdrl:mCherry)^{S916}	Marker of endothelial vascular cells	Johnston lab (Krueger et al. 2011)

2.1.2 *Cryptococcus neoformans*

2.1.2.1 *C. neoformans* strains

The *C. neoformans* strains used in this study are shown in table 2.2

Table 2.2: *Cryptococcus neoformans* var *grubii* strains used in zebrafish infection

Cryptococcus neoformans	Description	Origin
KN99	Wild-type strain	(Nielsen et al. 2003)
KN99 GFP	GFP fluorescence	(in submission, Gibson et al. 2017)
KN99 mCherry	mCherry fluorescence	(in submission, Gibson et al. 2017)
H99	Wild-type strain*	(Bojarczuk et al. 2016)
Ure-1 (KN99)	Urease mutant	** (unpublished)
Sec14 (KN99)	Mutant in secretion factor 14	** (unpublished)
Pho4 (KN99)	Pho4 mutant (phosphate acquisition)	** (unpublished)

*Use of H99 was swapped to KN99 due to a consensus in the field that H99 was not representative of wild-type *C. neoformans*.

** From a cryptococcal (KN99) deletion library (University of California, San Francisco, 2015, Madhani plates)

2.1.2.2 Media used for cryptococcal work

YPD: Cultures were grown in yeast peptone dextrose (YDP), (Sigma-Aldrich Y1375). 50g in 1 litre of distilled water. Autoclaved before use.

PVP in phenol red: Cryptococcal cultures were re-suspended in PVP in phenol red (10% Polyvinylpyrrolidone (PVP) Sigma-Aldrich, 0.5% Phenol Red Sigma-Aldrich in PBS), where PVP is a polymer which prevents needle blockage in cryptococcal injection. Autoclaved before use.

YDP agar plates: Cryptococcal cultures were stored on YDP agar plates at 4ºC. YPD made as above, Agar (Oxoid number 1) was used at 2%. Autoclaved before use.

2.1.3 *Staphylococcus aureus*

2.1.3.1 *S. aureus* strains

The *S. aureus* strains used in this study are shown in table 2.3, showing the strain and description and required antibiotic.

Table 2.3: *Staphylococcus aureus* strains used

Staphylococcus aureus	Description	Origin	Required antibiotic
SH1000	Wild-type strain	Foster lab *	n/a
SH1000-pMV158-mCherry	mCherry fluorescence	(SJF4308) Foster lab *	Tetracycline
SH1000-pMV158-GFP	GFP fluorescence	(SJF4405) Foster lab *	Tetracycline

* The University of Sheffield

2.1.3.2 Media used for Staphylococcal work

Brain heart infusion: *S. aureus* was cultured in Brain heart infusion (BHI) (Oxoid), 37.5g in 1 litre distilled water. Autoclaved before use.

LB: At IMCB, *S. aureus* was cultured (and plated) using Luria Bertani medium (LB) (Sigma-Aldrich). 20g in 1 litre distilled water Autoclaved before use.

BHI or LB agar plates: *S. aureus* cultures were stored on LB or BHI agar plates at 4ºC. Agar (Oxoid number 1) was used for BHI or LB agar plates. LB or BHI made as above, Agar was used at 2%. Autoclaved before use

2.1.4 Media

2.1.4.1 Phosphate buffered Saline

Three types of phosphate buffered saline (PBS) used, due to working in two locations, and also the concentration of PBS that was available.

1. 1x Phosphate buffer saline, (Life technologies 20012-027).
2. 10x Phosphate buffer saline: (Life technologies AM9625). Diluted to 1x with distilled water before use.
3. PBS tablets: (Oxoid, BR0014G). A single tablet is dissolved per 100ml of distilled water, and autoclaved to sterilise before use.

2.1.4.2 E3

A 10x stock of E3 (NaCl 5mM, KCl 170µM, $CaCl_2$ 330µM, $MgSO_4$ 330µM) was provided by the aquarium. Distilled water was used to make a 1x dilution, and methylene blue (0.00005%) was added. 1x E3 was stored at 28.5ºC

2.1.4.3 Methyl cellulose

A 3% methyl cellulose (Sigma-Aldrich) in E3 for solution was used for larvae injection. Stored at -20ºC until shortly before use when it was stored at 28.5ºC

2.1.5 Antibiotics

The antibiotics listed below are used at the working concentration for inside growth media (LB or BHI) for liquid cultures and agar plates, for both *S. aureus* and *E. coli* (competent cell) cultures.

Table 2.4: Antibiotics used in this study

Antibiotic	Working concentration
Tetracycline	5µg/ml
Chloramphenicol	10µg/ml
Ampicillin	50µg/ml
Kanamycin	50µg/ml

2.1.6 Western blot solutions

2.1.6.1 Protein extraction buffer

0.3M NaCl, 2.5mM EDTA pH8.0, 50mM Tris-HCl pH7.4, 1% octylglucoside, 1 Complete mini tablet, 1 PhosSTOP tablet, up to 20ml with sterile water

2.1.6.2 Laemmli buffer

2x Laemmli buffer: 65.8mM Tris-HCl pH 6.8, SDS (2.1%), Glycerol (26.3%), and Bromophenol blue (0.01%). Stored at 4ºC. 50µl BME added to 950µl of 2x Laemmli buffer on use. Or, 4x Laemmli buffer: Biorad (1610747)

2.1.6.3 Running buffer and Transfer Buffer

10x running buffer: 30.3g Trizma base, 144g glycine, 10g SDS, up to 1 litre with distilled water. 1x solution made with distilled water.

10x transfer buffer: 30.3g Trizma base, 144g glycine, up to 1 litre with distilled water, 1x solution made with distilled water.

2.1.6.4 SDS-PAGE gels

Stack gel (6%): 1ml Acrylamide (30%, Biorad, #1610154), 1.25ml 0.5M Tris-HCL pH6.8, 50µl Sodium dodecyl sulphate (SDS) (10%, Biorad #1610416), 3ml distilled water, 30µl Ammonium persulfate (APS) (Biorad, #1610700, 10% made fresh in distilled water at time of use), 15ul TEMED (Biorad #1610801).

Resolving gel (12%): 10ml Acrylamide (30%, Biorad, #1610154), 6.25ml 0.5M Tris-HCL pH8.8, 250µl Sodium dodecyl sulphate (SDS) (10%, Biorad #1610416), 8.2ml distilled water, 250µl Ammonium persulfate (APS) (Biorad, #1610700, 10% made fresh in distilled water at time of use), 25µl TEMED (Biorad #1610801).

2.1.6.5 Protein concentration measurement

To measure the protein concentration of protein lysate the Bio-Rad Protein Assay Dye Reagent Concentrate (#500-0006). A standard curve was made using 10mg/ml BSA serial dilutions. BSA dilutions and protein lysate were added to the assay dye and absorbance measured at 595nm.

2.1.6.6 Other western blot reagents

1. Amersham ECL Prime Western Blotting Detection Reagent (RPN2232)
2. Amersham hyperfilm (28906836)
3. PBST: 1x PBS (as above) with 0.1% Tween 20 (Biorad #170653)
4. Blotting membrane: 0.2um pore size polyvinylidene fluoride (PDVF) membrane (Amersham #10600021)

2.1.7 Drugs used in treatment of Zebrafish

Drug treatments given to zebrafish to manipulate autophagy were used in several experiments. The table below lists the drug, the concentration used and the effect the drug has on autophagy. Stock solutions were stored at 4ºC or -20ºC, and diluted in E3 for use. All autophagy drugs were sourced from Sigma-Aldrich.

Table 2.5: Drug treatments for autophagy manipulation

Drug	***Concentration used for treatment***	***Autophagy inducer or inhibitor***	***Mechanism of action***
Chloroquine	2.5 µM	Inhibitor	Blocks lysosomal fusion to autophagosome

NH_4Cl	100mM	Inhibitor	Prevents acidification of lysosomes
Bay-K 8644	1 µM	Inhibitor	Calcium channel agonist
Rapamycin	1µM	Inducer	Inhibits mTOR
3-methyladenine (3-MA)	10mM	Inhibitor	Inhibits PI3K

2.1.8 Microscopes

1. Spinning disc confocal microscope: UltraVIEW VoX spinning disk confocal microscope (Perkin Elmer, Cambridge, UK). 405nm, 445nm, 488nm, 514nm, 561nm and 640nm lasers were available for excitation. A 40x oil lense (UplanSApo 40x oil (NA 1.3)) was used for cellular level imaging. GFP, TxRed emission filters were used and bright field images were acquired using a Hamamatsu C9100-50 EM-CCD camera. Volocity software was used.

2. Nikon custom widefield: A custom-build wide-field microscope, Nikon Ti-E with a CFI Plan Apochromat λ 10X, N.A.0.45 objective lens, a custom built 500 µm Piezo Z-stage (Mad City Labs, Madison, WI, USA) and using Intensilight fluorescent illumination with ET/sputtered series fluorescent filters 49002 and 49008 (Chroma, Bellow Falls, VT, USA). NIS software was used.

3. LSM 700 confocal microscope: Zeiss LSM700 AxioObserver, with an EC Plan-Neofluar 10x/0.30 M27 lense. 488nm and 639nm lasers were used for excitation. GFP, mCherry emission filters were used, and bright field images were also acquired. Zeiss zen black software was used.

2.1.9 Software

1. Graph pad Prism software (version 7.02) was used for all statistical analysis, as described in individual figure legends.

2. ApE - A plasmid Editor v2.0.45 was used to analyse construct restriction site digests

3. Lasergene molecular biology suite, a software package was used for sequences alignments (MegAlign), sequence editing (SeqBuilder) and sequencing result analysis (SeqMan Pro).

4. Volocity software was used to acquire and analyse imaging (spinning disk confocal microscope).

5. NIS elements software was used to acquire and analyse imaging (Nikon widefield microscope).

6. Zen black software was used to acquire and analyse imaging (spinning disk LSM700 microscope).

7. Image J (FIJI) was used for quantification of fluorescence imaging, RFP or GFP vesicles in traffic light Lc3 analysis and for GFP pixel counts in fungal or bacterial burden.

8. EMBL-EBI pairwise sequence alignment, an online sequence alignment tool (http://www.ebi.ac.uk/Tools/psa/) used for protein sequences alignment

2.2 Methods

2.2.1 Zebrafish Procedures

2.2.1.1 Zebrafish husbandry

Zebrafish were kept according to UK home office standards with a 14-10 hour light-dark cycle at within home office approved aquariums at the University of Sheffield. In Singapore adult zebrafish were kept according to established standards, with 14-10 hour light-dark cycle, in the Institute of Molecular and Cell Biology (IMCB), A*Star. Zebrafish larvae are kept at 28°C in E3 solution with added methylene blue, and anaesthetised with tricaine before experimental techniques where the fish is required to be anaesthetised and/or immobilised. Zebrafish lines used throughout this study are shown in table 2.1. Culling of protected animals (>5.2dpf) was completed through a home office approved method at the University of Sheffield. All zebrafish larvae used in experiments ending at 5.2 days post fertilisation (dpf), were disposed through a home office approved method at the University of Sheffield. 10dpf was used as an end point at IMCB, unless otherwise stated.

2.2.1.2 Zebrafish anaesthesia

Tricaine was used as an anaesthetic before zebrafish experimental work. Larvae were anesthetised by immersion in 0.168 mg/mL tricaine in E3 until larval movement was no longer observed. Larvae would be maintained in tricaine in E3 until the end of experimental procedure. Where required, larval recovery was completed through replacing medium with fresh E3 which did not contain tricaine.

2.1.1.3 Zebrafish line maintenance

Adult zebrafish lines were maintained by out-crossing to AB wild-types (or in some cases nacre wild-type) to ensure zebrafish lines were not inbred. Out-crossing would be completed when adults were 1-2 years old to ensure the zebrafish line was continued. Where required, fin-clipping of adult zebrafish was completed and subsequent genotyping/screening enabled grouping of adult fish by genotype/transgenic reporter, important for experimental procedures.

2.2.2 *Staphylococcus aureus*

2.2.2.1 *S. aureus* storage:

S. aureus strains were stored for one month at 4°C after a frozen stock was streaked in sterile conditions on to BHI or LB agar plates and grown at 37°C for two days. If required the correct antibiotic would be added to the BHI or LB agar before pouring the plates (table 2.3). Frozen stocks are kept at -80°C.

2.2.2.2 *S. aureus* cultures:

A single *S. aureus* SH1000 colony was picked from a plate (brain heart infusion (BHI) agar or LB), and was cultured in 10ml BHI medium or LB overnight at 37°C, 250rpm. 500µl of this overnight culture was then added to 45ml of BHI/LB medium and incubated at 37°C, 250rpm until an acceptable optical density (at 600nm) was reached (between OD_{600} 0.5 and 1), typically after 1 hour and 40 minutes. If required antibiotics were added to both the overnight and used cultures. The bacteria were then pelleted at 4500rpm, 4°C for 15 minutes. The bacteria were then re-suspended in PBS, using a volume to dilute at the required dose, with 2500cfu/nL being standard. Bacteria were then incubated on ice for a short period until use.

2.2.2.3 *S. aureus* inocula calculation

In order to determine the approximate inoculum of the bacteria, an approximate concentration was calculated using the OD at 600nm. Previously calculated standard curves enabled the bacteria to be re-suspended in a volume of PBS required to attain the correct inocula.

To calculate the exact dose injected into larvae, the same needle as used for injections was sued to inject 4nl into 1ml of sterile PBS. After vortexing, 10µl drops would be placed onto BHI or LB agar plates (with antibiotics if required). The bacteria were left to grow at 37ºC overnight. An average of the colony forming units grown in each 10µl drop would be used to calculate a more accurate estimated injected dose.

2.3 *Cryptococcus neoformans* cultures

2.3.1 *C. neoformans* Storage*:*

C. neoformans strains were stored for one month at 4°C, after a frozen stock was streaked on YPD agar plates and grown at 28°C for two days. Frozen stocks were kept at -80°C.

2.3.2 *C. neoformans* Culture:

C. neoformans var. *grubii* strains (table 2.2, above), were cultured in 2ml yeast peptone dextrose (YPD) medium overnight, for 16-18 hours, in a rotator at 28°C, (30°C

shaker in Singapore). 1 ml of this culture was then pelleted 6,000rpm, RT for 1 minute and re-suspended in 1ml of PBS. This was then diluted in PBS 1:20, and the number of *C. neoformans* cells were counted using a haemocytometer. The same 1ml was then then pelleted 6,000rpm, RT for 1 minute and re-suspended in the correct volume of polyvinylpyrrolidone (PVP) in phenol red, for 1000cfu/nL. If required, dilutions of 1000cfu/nL, to make 500cfu/nL, 100cfu/nL and 10cfu/nL were made.

2.4 Zebrafish microinjection of pathogens

Zebrafish larvae were de-chorionated (manually the chorion of the embryo was carefully removed, using forceps to pull it apart) before micro-injection and anaesthetised using tricaine (0.168 mg/mL tricaine in E3). Zebrafish larvae were injected into the circulation valley with *C. neoformans* at ~48 hours post fertilisation (hpf), whereas larvae were ~30hpf when injected with *S. aureus* (Prajsnar et al. 2008; Bojarczuk et al. 2016). Larvae were place onto 3.5% methylcellulose in E3 prior to injection. Pulled glass needles were then loaded with the correct dose of pathogen, placed onto the micromanipulator apparatus and the needle tip broken. The injection dose was then determined through use of a graticule, allowing a 1nL drop size to be fixed, through manipulation of Pneumatic PicoPump (PV 820P). Larvae were then injected with 1nL of the required pathogen dose, and placed into fresh E3 solution and kept at 28°C (28.5ºC for *S. aureus*).

2.5 Drug treatments

Where larvae were treated with autophagy inducers and inhibitors, either with or without additional pathogen injection, zebrafish were immersed in E3 medium. The drugs were then added to the E3 to the correct dose concentration (table 2.5) at 28°C for the required length of time. Zebrafish were not anaesthetised for immersion drug treatments.

2.6 Survival analysis

Larvae which had undergone either injection, drug treatment, both or were non-injected controls may have been subject to survival analysis. Zebrafish larvae were checked every 24hrs for their survival or mortality. Dead fish were removed, and if required stored at -20°C for subsequent genotyping. All zebrafish larvae used in experiments were under 5.2 days post fertilisation (dpf) at The University of Sheffield, at which point the zebrafish were disposed through a home office approved method. However those injected with *S. aureus*, which were housed at 28.5°C were disposed of by 5dpf. All survival analysis of infection at IMCB in A*Star was completed by 10dpf, unless otherwise stated, and were kept at 28°C.

2.7 Imaging and analysis

Imaging was utilised to visualise fluorescent, *C. neoformans* or *S. aureus* within infected zebrafish. Furthermore, fluorescent zebrafish lines, allow visualising of cell types and proteins within transgenic zebrafish and additionally co-localisation of pathogens with these cells or proteins. Imaging was completed through use of either a custom wide-field fluorescence Nikon microscope, or a spinning disk confocal microscope at Sheffield University. A LSM700 microscope was utilised in IMCB. Zebrafish were anaesthetised before mounting in 0.8% agarose in 96 glass bottom plates, glass bottomed culture dishes or glass slides. E3 with added tricaine was placed on top of the fish once mounted.

Fungal/bacterial burden: Analysis of fluorescent pathogens/cellular components was completed using ImageJ/FIJI. NIS images were opened in FIJI. A threshold was set to remove background and leave only true signal (completed by eye and all groups were blinded). The number of pixels where GFP signal was present were then measured using FIJI to give a GFP positive pixel area which could be used for comparison.

Cryptococcoma definition: Larvae were infected at 2dpf with 25cfu of GFP and mCherry cryptococcal cells and a single z-stack image acquired daily until 10dpf. A cryptococcoma was defined as a mass of cryptococcal cells and visually determined. A mass consisted of at least 3 cryptococcal cells observed in one location in a single z-stack.

Larval size analysis: The size of larvae was measured in two locations (Sheffield and Singapore). To enable the same method to be used, an image was taken of larvae placed within 96 well plates (or similar such as 24 well plate used for older larvae) with a ruler in the field of view (using a mobile phone camera). Using ImageJ, the number of pixels in a 1cm line was measured for each picture. Lines were drawn to the same size of individual larvae and pixel count recorded and size later calculated using the pixel count for the 1cm line.

Heart rate: For analysis of the heart rate of autophagy mutant larvae, the GFP heart marker was imaged (using an in-cross of the traffic-light Lc3 line crossed to either *atg3* or *atg5* lines). In this case larvae were not given tricaine, and were placed in a small volume of E3 for imaging, all completed before 5.2dpf. The heart was imaged at a fast speed for a timelapse of 20 to 60 seconds (dependent on whether larvae swam out of the field of view). Timelapse videos were analysed on NIS elements and heart beat counted for a 20 second period.

Blood vessel width: The blood vessel width of intersegmental blood vessels in larvae was imaged, the tail section of larvae included ~20 blood vessels per larvae. Analysis

was completed using NIS elements, using the measure tool, where the software calculates size based on the length of a drawn line. The blood vessel width were measured at the widest point of the blood vessel or at the site of cryptococcal cells/beads. The average size of infected or non-infected blood vessels was calculated as a mean for individual larvae for analysis.

2.8 Genotyping

Adult zebrafish were fin-clipped and kept in separate tanks whilst genotyping took place. The DNA was extracted from the finclips through NaOH (50mM) boiling, and after neutralisation with 1M Tris-HCL pH8, the finclips were centrifuged 4000rpm, for 30mins at 4°C. To amplify the DNA, a PCR of each mutant, *atg3* and *atg5* using primers shown in table (2.6) was completed, using GoTaq G2 Green master mix (Promega #M7823). Zebrafish larvae micro-finclips were also genotyped using the same method, in smaller volumes.

Table 2.6: Primers used for genotyping autophagy mutant fish

Mutant line	Forward primer	Reverse primer
atg3^{SH171}	GGCATCTGGAGAAGAAGCAA	CCGAGTTATGAAAGGTGTCCA
atg5	TTTCTTTCTGTCAATCTGTCAGC	CCTCTGCCTTCATGACTTTGAG

Genotyping primers for *atg3* and *atg5* mutant lines, which have 10bp and 23bp deletions respectively, were designed to enable the PCR product sizes of wild-type and mutation containing sequences to be discriminated by size through electrophoresis on 4% or 2.5% agarose gels. Using the different band sizes and patterns the genotype of each fish was determined. Band sizes corresponding to each genotype, wild-type, heterozygous and homozygous were confirmed with sequencing. *atg3* genotyping is described in Chapter 4, and *atg5* genotyping has been previously established (PhD thesis Lambein 2015).

2.9 Western blotting

After de-chorionating and de-yolking, zebrafish larvae were homogenized, using a T10 ULTRA-TURRAX handheld homogenizer, in protein extraction buffer. Debris within the samples were pelleted at 14,000rpm, 30s, 4°C, after which the supernatant, containing extracted protein, was removed to a fresh Eppendorf, repeated three times. Samples were mixed with an equal volume of Laemmli buffer, and heated at 95°C for 10 minutes. Samples were then loaded into the gel and run at 85V for 25 minutes and then 150V for approximately 45 minutes, in running buffer. After 15 minutes incubation in transfer buffer, the gel, methanol-activated PVDF and filter paper were assembled in

a Trans-blot SD semi-dry transfer cell, at 25V for 25 minutes, or alternatively wet transfer kit was used at 110V for 150 minutes.

The PVDF membrane was then checked for protein with Ponceau S solution, where a positive result led to blocking the membrane in 2.5% non-fat milk powder in PBST for at least 2 hours or overnight. After washing with PBST, primary antibody diluted in 2.5% milk in PBST was placed in a falcon tube with the membrane and rolled overnight. Again, after washing with PBST, the secondary antibody in PBST was placed on the membrane and rocked at room temperature for 1 hour. Washing of the membrane then lead to the application of ECL reagent and the membrane was placed in a Hypercassette and covered with Amersham hyperfilm for appropriate time periods. The film was developed using an Optimax 2010 x-ray film processor.

Table 2.7: Antibodies used for western blots

Antibody	Company	Primary concentration	Secondary concentration
ATG5	Novus Biologicals NB110-53818	1/4000	1/10,000 (Rabbit)
LC3	Novus Biologicals NB100-2220	1/4000	1/10,000 (Rabbit)
β-actin	Cell signalling Technology 4967S	1/ 3000	1/50,000 (Rabbit)
GFP	Abcam 6556	1/4000	1/10,000 (Rabbit)
HRP-conjugated anti-rabbit secondary antibody (Sheffield)	Bethyl Laboratories INC: A120-101P	-	1/10,000
HRP-conjugated anti-rabbit secondary antibody (IMCB)	Amersham NA934	-	1/10,000

2.10 Reverse Transcription PCR

Zebrafish embryos at different stages from 1 cell through to 30 dpf, were collected of AB wild-type, ATG3+/- and ATG5+/- lines and placed into TRIzol (Ambion 15596018). Following homogenisation, RNA was extracted following the TRIzol protocol, re-suspended in RNAse free water, and stored at -80°C. RNA quality and concentration

was measured by Nanodrop (ND-1000) and gel electrophoresis. Synthesis of cDNA was completed with the Invitrogen Superscript III kit, with the same concentration of RNA used for individual samples within each experiment, typically 400ng RNA in a 20ul reaction. Reverse transcription PCR was completed using equal volumes of the cDNA generated using GoTaq G2 Green master mix (M7823).

Two pairs of primers were designed for both *atg3* and *atg5* zebrafish genes. The first pair with both primers located downstream of the mutation site. The second pair the forward primer covered the mutation site. Each set of primers have one primer covering an exon-exon junction, to ensure amplification of cDNA only.

Table 2.8: Primers used for reverse transcription PCR
Underlined sequence represents part of mutation site covered by mutation (see appendix 3 for cDNA and primer sites)

Sequence	Forward primer	Reverse primer
atg3 after mutation	ATGAGCTGGAGGCCATCATA	ATTCTTCCATGTCTGCCGCC
atg3 covering mutation	AAGCCCTATCTGCCCAATGAC	TCACCCCTGTAACACCCGA
atg5 after mutation	TGGATGGGTCTGCAGAATGATAA	CCTCCCTCTTCGGTGGGATA
atg5 covering mutation	CCTCCCACGGGTCAGTTAC	CTTTGGCTCATCCTCAATGGC

2.11 Traffic light Lc3 DNA injection

Zebrafish embryos of heterozygous in-crosses of *atg3* and *atg5* lines, in addition to AB wild-type, were injected at the one cell stage with 30ng of traffic-light Lc3 DNA construct (pDest395CMV.ZFLc3.polyA), a kind gift from Dr Katherine Henry and Dr Angeleen Fleming, pME(RFP.GFP.Lc3) was a kind gift from Dr Angeleen Fleming, Dr Katherine Henry performed the recombination reaction to produce pDest(CMV:RFP GFP.Lc3) plasmid). The embryos were screened for green fluorescence the following day to select successful injections. Importantly fluorescence observed of any kind was picked out, due to the possibility of down regulation of the construct within autophagy mutant lines. Half of the fish were treated with rapamycin and chloroquine, (table 2.5) overnight, and re-treated the following morning. All fish were imaged using the LSM

700 scanning confocal, with consistent laser and microscope settings maintained throughout all repeats. RFP, GFP and DIC images were taken of the 5th half somite, above the yolk.

Analysis of images was completed using ImageJ. Images were first exported from ZEN black software into Tagged Image Format (TIF). For both RFP and GFP channels an individual 16-Bit monochrome image was created. The threshold was set to best observe only true signal, 0 – 12,800 for the RFP channel and 0-19,700 for the GFP channel, and converted to mask. The area corresponding to the half somite was selected. Particles were counted based on size 1.6 pixels to infinity, corresponding to 1um equal to 3.2 pixels, adjusted to start counting from the smallest size being equivalent of autophagosome size from 0.5um. Images and genotyping data were not matched together until after image analysis of each fish was completed, to ensure this analysis was completed blinded to genotype.

2.12 Generation of transgenic zebrafish line

The generation of the *Tg(lyz:GFP.p62)* line was completed through use of the Gateway™ system in combination with Tol2 transgenesis. This is described in full detail in Chapter 6 and Appendix 1.

2.13 Statistical analysis

Statistical analysis was completed using GraphPad Prism software (version 7.02) in all cases. Unless mentioned within individual figure legends, “n” refers to the number of repeats an entire experiment was completed, which includes multiple zebrafish larvae in each repeat. Standard deviation is represented by SD.

Survival analysis: The Log-Rank Mantel-Cox test was used to compare the trend of survival between different populations.

T-tests: Mann-Whitney T-tests were used to test if data are from the same population when the data is not a normal distribution (observed by data scatter). Wilcoxon matched pairs T-test was used to test if data are from the same population when the data is not a normal distribution (observed by data scatter) between two paired data sets (e.g. before and after time scale).

Linear regression: Line of best fit for data points. R^2 (between 0 and 1) value represents the percentage of points which line on the line, where 1 represents 100% of all points lie on the line.

Contingency table analysis: The (Pearson's) Chi-squared test was used to compare categorical data of three or more groups. Where low numbers were observed (less than 5), or for comparing categorical data in groups of two, the Fischer's exact test was used.

Analysis of variance: One way ANOVA was used to determine the difference of means between two or more groups, with Kruskal-Wallis test for non-parametric data. Two way ANOVA was used to determine the difference of means between two or more groups, which two variables. Tukey's test was added to this to compare each mean to every other mean.

Chapter 3: Results Chapter 1:

The role of clonal expansion in *C. neoformans* infection dynamics

3.1 Introduction

C. neoformans is a human fungal pathogen which has a tropism for the brain, ultimately leading to life-threatening cryptococcal meningitis (CM). After inhalation of fungal spores, cryptococcal cells are able escape the lung into the blood, and from the blood cross the blood brain barrier (BBB) to gain access to the brain parenchyma.

C. neoformans is able to cross the BBB using a variety of mechanisms. *In vitro* data demonstrate that *C. neoformans* is able to actively transcytose through microvascular endothelial cells (Chen et al. 2003). It is also suggested that cryptococcal cells are also able to pass between tight junctions in the vessel wall, by determining that damage occurs to tight junctions through analysis of occludin, a major tight junction transmembrane protein, in the presence of *C. neoformans* (Chen et al. 2003). On the other hand, *C. neoformans* can utilise host defence responses to promote dissemination across the BBB. As has been demonstrated through *in vivo* murine studies, cryptococcal cells are able to cross the BBB from within a macrophage, which acts as a "Trojan horse" (Charlier et al. 2009; Santiago-Tirado et al. 2017). It is clear that a range of methods enable *C. neoformans* to disseminate across the BBB. Of note, in each mechanism described, the cryptococcal cells are within the brain blood vessels, highlighting that during infection, cryptococcal cells are present in the brain vasculature, and therefore that dissemination occurs when *C. neoformans* is in close contact to the BBB.

Recent clinical studies have highlighted a potential role of blood vessel damage resulting from infection with *C. neoformans*. A limited number of case reports describe cases in which cryptococcal infection and meningitis lead to vasculitis and brain vasculature damage, and can ultimately result in infarcts (necrotic tissue resulting from a lack of blood supply), (Aharon-Peretz et al. 2004; Rosario et al. 2012; Leite et al. 2004). Interestingly, cerebral infarcts are observed in meningitis caused by tuberculosis, in addition to CM (Lan et al. 2001). This indicates that in infective meningitis, blood vessels in the brain are becoming blocked or damaged, potentially through physical damage or through toxins released by the pathogen. Furthermore, the incidence of cortical infarcts is non-trivial, occurring in 30.3% of cryptococcal meningitis cases, most often observed in severe cases (Mishra et al. 2017). This highlights the frequent occurrence of infarcts in cryptococcal meningitis. Nevertheless, the physiological cause of infarcts in *C. neoformans* infection is not characterised.

Murine models of cryptococcal infection have shown that cryptococcal cells can become trapped in brain blood vessels (Shi et al. 2010), suggesting that cryptococcal cells cross the BBB after they become trapped in the brain vasculature. Indeed, this hypothesis is supported by observations from CM post-mortems showing that cryptococcal cells are seen in the brain parenchyma adjacent to brain vessels containing cryptococcal cell masses (Lee et al. 1996). The presence of several cryptococcal cells in vessels within the brain, located right next to cryptococcal cells in the brain parenchyma is suggestive that cryptococcal cells are proliferating in the brain vasculature and then disseminating from that location. Furthermore, in the zebrafish *C. neoformans* infection model, dissemination into the brain occurs more often from individual brain vessels with high fungal burdens (Tenor et al. 2015). These data suggest that cryptococcal proliferation may be involved in cryptococcal cell ability to cross the BBB. The role of cryptococcal proliferation as a mechanism of vessel damage and dissemination has hitherto not been investigated. It could be hypothesised that cryptococcal proliferation from cryptococcal cells trapped in the brain vasculature, is causing physical vessel damage leading to dissemination.

A population “bottleneck” has been described in bacterial pathogenesis, including *S. aureus* and *S. enterica* (Prajsnar et al. 2012; Grant et al. 2008) . In *S. aureus* infection, the majority of bacteria are efficiently degraded by the host, but a small proportion evade host defence mechanisms and reside in an intra-phagocyte niche. Bacteria are able to replicate within a neutrophil, escape the neutrophil and eventually lead to overwhelming infection in the host (Prajsnar et al. 2012). A population “bottleneck” in infection refers to the small proportion of pathogens which ultimately become the fatal infectious burden responsible for the uncontrolled infection. The role of a cryptococcal population “bottleneck” has not been established. The zebrafish cryptococcal infection model demonstrates that cryptococcal cells are able to proliferate within macrophages (Bojarczuk et al. 2016). It is possible that a small proportion of cryptococcal cells which are not efficiently degraded, reside within macrophages, proliferate and eventually lead to uncontrolled infection.

To investigate the role of clonal expansion and dynamics of cryptococcal infection as a mechanism behind vasculature damage and dissemination, an inoculum of two fluorescently labelled cryptococcal strains was used to monitor growth dynamics, and to determine whether a population bottleneck exists in cryptococcal infection. Furthermore, to investigate a role of localised expansion in the vasculature, cryptococcal growth in addition to the integrity of the vessel walls was investigated, with the aim to discover whether cryptococcal clonal expansion may be involved in a mechanism to cross the BBB.

Hypothesis 1: *C. neoformans* infection has a population "bottleneck"

Hypothesis 2: Vasculature damage is caused by cryptococcoma formation

Chapter aims:

1) To determine if cryptoccocal expansion dynamics from a single or small number of cryptococcal cells control infection outcome
2) To determine if cryptococcal cells become trapped in the vasculature in the zebrafish model
3) To determine if cryptococcal clonal expansion in vasculature leads to dissemination into the surrounding tissue
4) To determine if cryptococcal clonal expansion in the vasculature causes blood vessel damage

3.2 Cryptococcal infection progresses without passing through a population bottleneck

A population bottleneck in cryptococcal infection may be present because *C. neoformans* is able to survive and replicate within macrophages. Cryptococcal cells which are present in the macrophage niche may be responsible for cryptococcal proliferation and uncontrolled infection, and could represent a population bottleneck.

The dynamics of *C. neoformans* infection were examined, in regards to a potential population bottleneck. A 25cfu mixed inocula of 5:1 GFP:mCherry *C. neoformans* was injected into the circulating blood of AB (wild-type) larvae. A low dose infection was used with the aim of determining whether a single or small number of cryptococcal cells are responsible for overwhelming infection, expected if a population bottleneck does occur in cryptococcal infection. I therefore predict that the majority of fish would be majorly infected by a single colour strain if a population bottleneck occurs in cryptococcal infection.

Co-infection with a mixture of two cryptococcal strains (a genetically identical parental strain with two different fluorescent markers) demonstrated that multiple fungal cells contribute to the progression of infection. In 51.6% of all fish infected, an overwhelming infection outcome was determined within 7dpi. In fish which did not reach an overwhelming infection, infection may have been effectively cleared, the larvae may have died due to handling or infection may have been likely to reach overwhelming infection after the experimental time course. The overwhelming infection outcomes reached were either predominantly GFP *C. neoformans*, predominantly mCherry *C. neoformans,* or mixture of GFP and mCherry *C. neoformans*, as shown in Figure 3.1 A-

C. The presence of mixed strain overwhelming infection indicates that a single cryptococcal cell is not responsible for the final infection outcome. Where overwhelming infection was seen, this was composed of predominantly GFP positive cryptococci in 56.25% of cases, predominantly mCherry positive cryptococci in 6.25% of cases, and a mixture of GFP and mCherry positive cryptococci in 37.5% of the cases. (Fig. 3.1 D). These results are unexpected if a single or very small number of cryptococcal cells were responsible, where a single colour outcome may expected more often. Therefore it is likely that a larger number of individual cells divide and contribute to the final fatal burden.

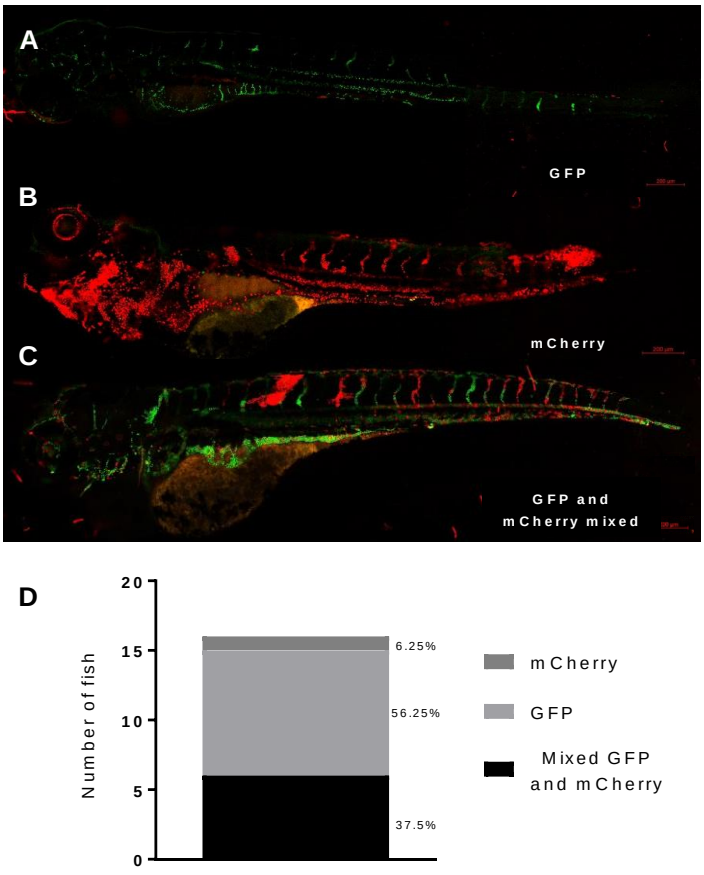

<u>Figure 3.1</u> A single cryptococcal cell is not responsible for fatal fungal burden

Infection of 2dpf AB larvae with 25cfu of a 5:1 ratio of GFP:mCherry KN99 *C. neoformans*. Larvae were imaged until 8dpf, or death (n=3, in each repeat 7, 10 and 12 larvae were used) **A-C** Larvae which have reached a final fatal infection outcome from a predominantly GFP and/or mCherry *C. neoformans* infection, red scale bar represents 200µm **A** Predominantly GFP *C. neoformans* infection outcome **B** Predominantly mCherry *C. neoformans* infection outcome **C** Mixed GFP and mCherry *C. neoformans* infection outcome. **D** Proportion of each overwhelming infection outcome observed, GFP, mCherry or mixed (n=3, 12, 7, and 12 larvae were used in each repeat).

3.3 Injected inoculum ratio does not determine uncontrolled infection outcome

To investigate whether the actual number of *C. neoformans* from either the GFP or mCherry strain injected into each larvae led to differential infection outcomes, the injected strain ratio was calculated through counting of individual cryptococcal cells present in each larvae from images acquired at 2hpi. Although a 5:1 ratio of GFP to mCherry was prepared for infections, the actual ratios observed within 2 hours of infection were varied (Fig. 3.2 A), and in most cases a lower GFP:mCherry ratio was observed. Comparing the injected ratios between each final infection outcome determined there was no difference in inoculum ratio, (Fig. 3.2 B), indicating that the injected ratio does not determine the final infection outcome. Indeed, no significant relationship was observed between the injected strain ratios compared with the strain ratios at the final infection outcome (Fig. 3.2 C). Taken together these data demonstrate that the injected ratio does not determine the final infection outcome.

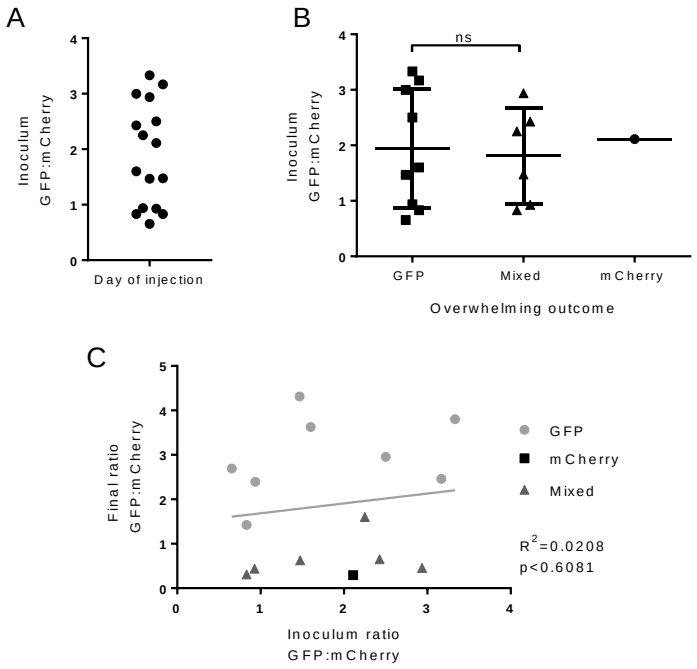

Figure 3.2 ***C.neoformans*** **inoculum ratio does not determine uncontrolled infection**

Infection of 2dpf AB larvae with 25cfu of a 5:1 ratio of GFP:mCherry KN99 *C. neoformans*. Larvae were imaged until 8dpf, or death (n=3, in each repeat 7, 10 and 12 larvae were used) **A** Actual injected ratios of GFP:mCherry KN99 *C. neoformans* at 2hpi **B** Actual injected GFP:mCherry ratios for each overwhelming outcome (n=3, +/- standard deviation, Man-Whitney t-test ns= not significant, 16 larvae) **C** Inoculum ratio of GFP:mCherry, against final GFP:mCherry ratio at overwhelming infection stage (Linear regression R^2=0.0208, p<0.6081, n=3, 15 larvae).

3.4 Cryptococcoma formation in infection progression

The ratio between GFP and mCherry cryptococci in the injected inoculum ratio does not determine uncontrolled infection. Therefore time point images of infection were studied, and it was observed that cryptococcoma (cryptococcal mass) formation clearly preceded progression of infection to a higher fungal burden. The term “cryptococcoma” means a mass composed of both cryptococci and immune cells and is generally used to refer to cryptococcal granulomas. However in the zebrafish model we often see intravascular masses composed of cryptococci, which are best described by the term cryptococcoma

Cryptococcal masses form within the larvae and these precede overwhelming infection, as shown in Figure 3.3 A (AI-AII). This example of pathogen growth over time clearly demonstrates that initial infection causes the occurrence of small cryptococcal masses early in infection. Indeed, in this example, cryptococcal masses of both GFP and mCherry are observed at 1dpi, two days before a final overwhelming mixed infection is observed at 3dpi.

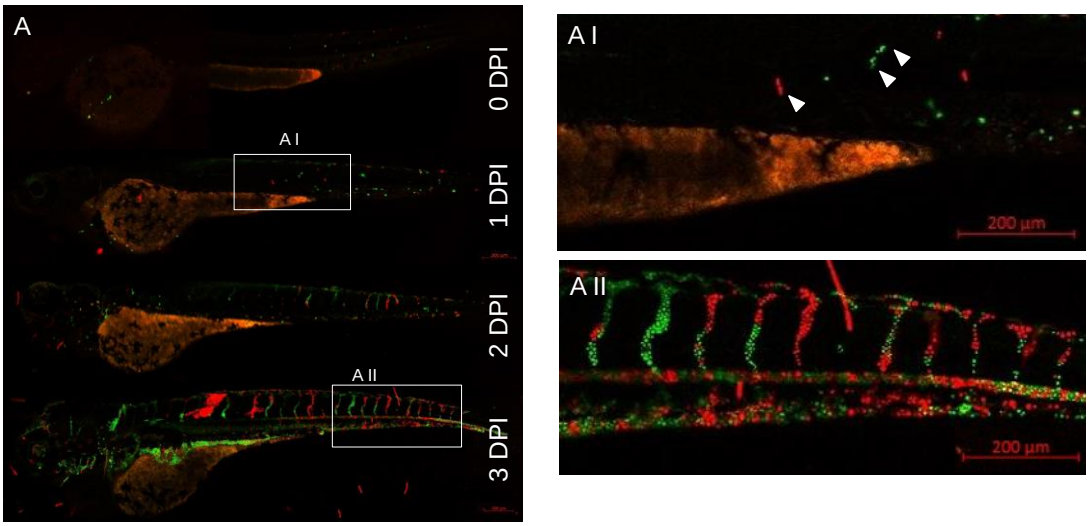

<u>Figure 3.3</u> Cryptococcoma formation in *C.neoformans* zebrafish infection

Infection of 2dpf AB larvae with 25cfu of a 5:1 ratio of GFP:mCherry KN99 *C. neoformans*. Larvae were imaged until 8dpf, or death (n=3, in each repeat 7, 10 and 12 larvae were used) **A** Representative infection of AB wild-type larvae with 5:1 ratio of GFP:mCherry KN99 *C. neoformans*, at 0dpi, 1dpi, 2dpi and 3dpi **A I** Formation of cryptococcal masses (white arrows) at 1dpi **A II** Final infection outcome of high fungal burden at 3dpi. All scale bars represent 200um.

3.5 Cryptococcoma formation precedes uncontrolled infection

It was noticed that cryptococcoma formation appeared to occur before progression to uncontrolled infection. To determine whether cryptococcoma formation is likely involved in the progression of infection to a higher fungal burden, the time between formation of cryptococcomas and subsequent uncontrolled infection was investigated.

Cryptococcoma formation infection precedes uncontrolled infection by approximately 2 days. Cryptococcoma formation was found to occur before overwhelming infection in every case, in addition to forming approximately 2 days prior to final infection (Fig. 3.4 A). This was truly independent of the predominant strain colour of the cryptococci in the final infection (Fig. 3.4 B). In fact, no significant difference was observed in the speed (between cryptococcoma formation and overwhelming infection outcome) between uncontrolled infection outcomes of predominantly GFP, mCherry or mixed *C. neoformans* (Fig 3.4. C). These data suggest that cryptococcoma formation is important in infection dynamics and may be responsible for infection outcome.

If cryptococcomas are responsible for infection outcome, it may be expected that a greater number of these cryptococcal masses would lead to an increased speed in infection progression. Therefore the number of cryptococcal masses present within individual fish was examined. In agreement, a higher number of cryptococcomas was associated with a decreased time for overwhelming infection to occur (Fig. 3.4 D). Cryptococcal replication is an exponential rate of doubling every 3.2 hours *in vitro* (Park et al. 2010). Therefore infection growth dynamics which follow an exponential decay (i.e. a higher number of cryptococcomas decreases the time of infection progression and vice versa) was expected. Overall these data suggest that cryptococcoma formation is associated with infection progression and lead to overwhelming infection.

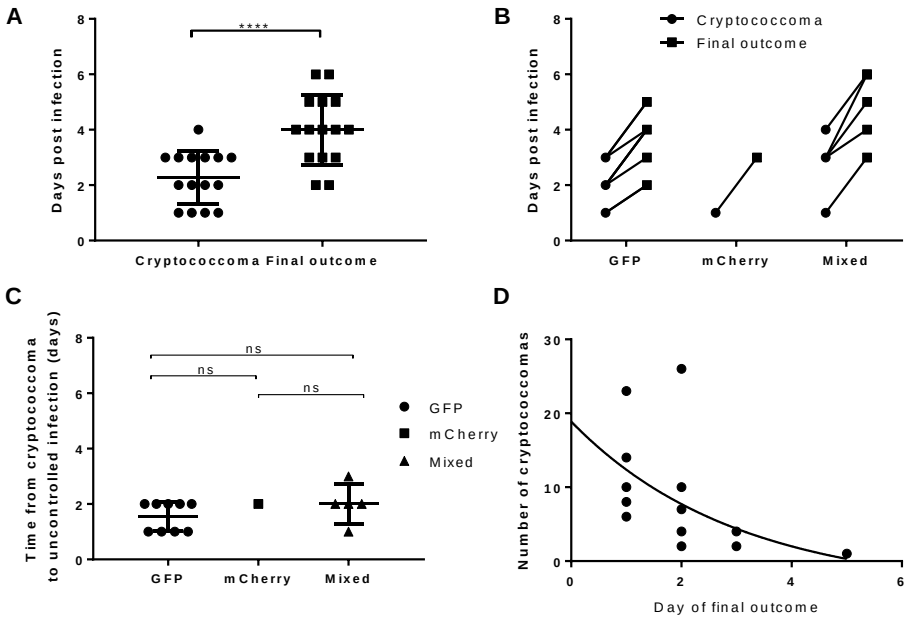

Figure 3.4 Cryptococcoma formation precedes overwhelming infection

Infection of 2dpf AB larvae with 25cfu of a 5:1 ratio of GFP:mCherry KN99 *C. neoformans*. Larvae were imaged until 8dpf, or death (n=3, in each repeat 7, 10 and 12 larvae were used) **A** Day post infection that cryptococcoma was observed and when final uncontrolled infection outcome is observed (n=3, 15 larvae, +/- SD, Wilcoxon matched pairs test, ****p<0.0001) **B** Day post infection when cryptococcoma is first observed and the final outcome, grouped by final outcome **C** Days between cryptococcoma formation and final outcome grouped by final outcome (n=3, 15 larvae, +/-SD, One-way ANOVA, ns= not significant) **D** The number of cryptococcomas observed within individual larvae in comparison to the day final overwhelming infection was reached (n=3, 15 larvae, non-linear regression, one-phase exponential decay)

3.6 Cryptococcoma formation leads to uncontrolled infection

To determine whether cryptococcoma formation is important in determining the infection outcome, the strain colour of *C. neoformans*, either GFP or mCherry, within individual cryptococcomas was compared with the predominant strain colour of *C. neoformans* in the resultant uncontrolled infection. I hypothesised that if a cryptococcoma is important in progression of infection, *C. neoformans* will be of matching fluorescent strains in the initial cryptococcoma(s) observed, as the predominant *C. neoformans* colour in the uncontrolled outcome, within individual larvae.

C. neoformans within cryptococcomas are likely responsible for uncontrolled infection. A clear relationship was observed between cryptococcal cell colour in a cryptococcoma

and the predominant colour of *C. neoformans* in the final uncontrolled outcome, with individual cryptococcoma formation indicative of the final outcome, (Fig. 3.5 A). Indeed, a single coloured cryptococcoma is significantly more likely to lead to a single coloured final outcome, and conversely, mixed colour cryptococcomas are most likely to cause a mixed final outcome (Fig. 3.5 B), further suggesting that cryptococcoma formation is important, and may be responsible for infection progression and outcome.

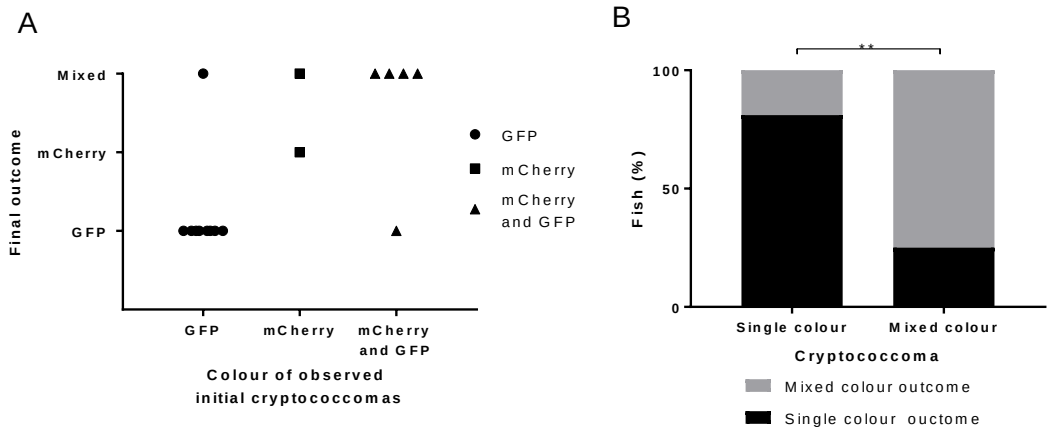

<u>Figure 3.5</u> Cryptococcoma is predictive of overwhelming infection

Infection of 2dpf AB larvae with 25cfu of a 5:1 ratio of GFP:mCherry KN99 *C. neoformans*. Larvae were imaged until 8dpf, or death (n=3, in each repeat 7, 10 and 12 larvae were used) **A** Comparison of the colour (either GFP, mCherry or mixed strains) of *C. neoformans* in cryptococcomas, in relation to the final outcome predominant *C. neoformans* strain colour **B** Comparison of the colour, either single colour or mixed, and the colour of final outcome (n=3, 15 larvae **p<0.01, Fischer's exact test).

3.7 Localised clonal growth of cryptococci leads to cryptococcoma formation and dissemination

It is likely that *C. neoformans* within cryptococcomas represent the population of cryptococcal cells which are responsible for the final infection outcome. Therefore the formation of cryptococcomas was next examined. It was hypothesised that cryptococcoma formation is likely caused by localised clonal expansion since it was noticed that most cryptococcomas were a single coloured fluorescent strain of *C. neoformans*. In fact, a majority of single coloured cryptococcomas, as shown with 11 of 16 cryptococcomas observed were a single colour (Fig. 3.5 A, above).

By analysing how infection progresses over time, it appears that cryptococcomas (likely in the vasculature) form through localised clonal expansion (Fig. 3.6). Early in infection, a single or few cryptococcal cells appear to become trapped within the vasculature. The trapped cryptococcal cells appear to proliferate throughout infection (1dpi to 3dpi)

and form a cryptococcoma. Finally, I observed that cryptococcal cells appear to spread from the vasculature into the surrounding tissue late in infection, when an uncontrolled infection outcome is also observed (4dpi) (Fig. 3.6).

This is a potentially important observation, which suggests that clonal expansion may be involved in cryptococcoma formation. Furthermore, the observation that the cryptococcal cells are able to invade surrounding tissue suggests that cryptococcal proliferation may be involved in cryptococcal dissemination.

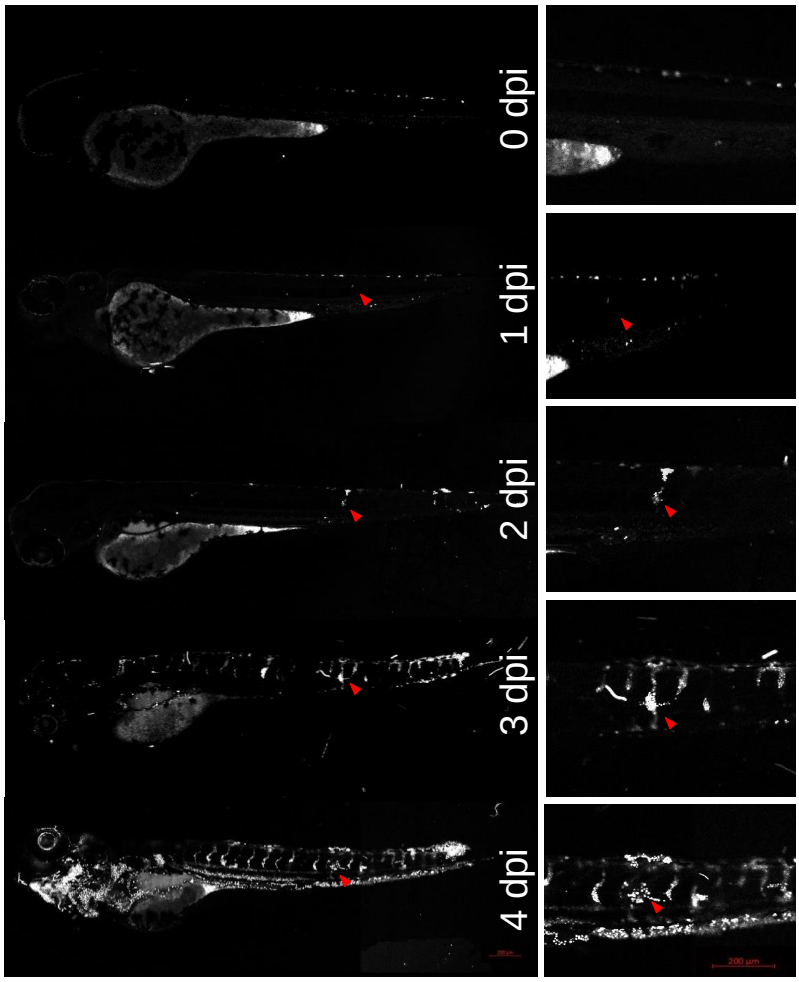

Figure 3.6 Cryptococcoma formation leading to dissemination

Infection of 2dpf AB larvae with 25cfu of a 5:1 ratio of GFP:mCherry KN99 *C. neoformans*. Larvae were imaged until 8dpf, or death (n=3, in each repeat 7, 10 and 12 larvae were used). This representative example highlights a predominantly mCherry *C. neoformans* overwhelming infection reached at 4dpi, with only mCherry *C. neoformans* shown in this figure. Infection progression from 0dpi (day of infection imaged 2hpi), until 4dpi. Red arrows follows an individual cryptococcoma formation and dissemination, panel on the right are a zoomed in on the area of cryptococcoma formation, red scale bar represents 200um.

3.8 Cryptococcal cells become trapped in intersegmental vessels

The next overarching aim was to determine whether localised clonal expansion at sites within the vasculature may lead to dissemination, due to the observation that dissemination from inter-segmental vessels into the surrounding somite can occur at sites of cryptococcomas.

However, in order to demonstrate that cryptococcal cells were able to disseminate out of the blood vessels, perhaps through formation of cryptococcoma via clonal expansion, it was first necessary to show that cryptococcal cells were becoming trapped in blood vessels. It has already been demonstrated that cryptococcal cells can become trapped within similarly sized brain blood vessels, stopping suddenly, in the same manner as inert beads of a similar size using the murine model (Shi et al. 2010), likely due to becoming stuck based on size. This indicates that blood vessel size is important in trapping of cryptococcal cells.

To determine if a similar trapping mechanism is observed in zebrafish intersegmental vessels, time lapse analysis of larvae was completed immediately after infection with 25cfu *C. neoformans*, using the KDRL blood marker line. Indeed, individual cryptococcal cells were observed becoming stuck in the vasculature, stopping in a similar way as described in the murine model (Shi et al. 2010), moving at a similar speed to blood flow and becoming trapped and therefore stopping instantaneously (Fig 3.7).

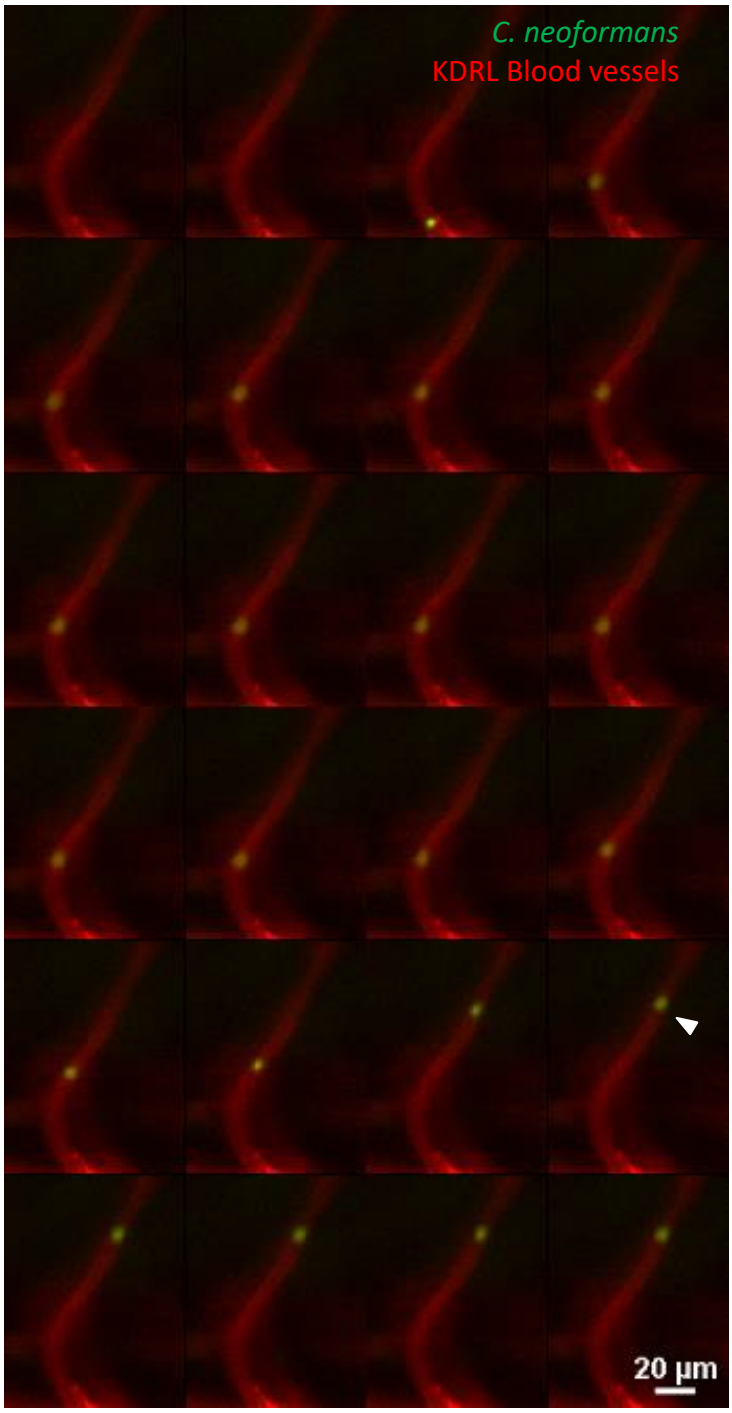

Figure 3.7 Individual cryptococcal cell trapped in the vasculature

Infection of KDRL mCherry blood marker transgenic line with 25cfu GFP KN99 *C. neoformans*, imaged immediately after infection **A** Single cryptococcal cell becomes trapped in the vasculature (white arrow), after moving from the bottom of the vessel to toward to top (left to right, time points 0.6 seconds),white arrow points at location of trapping, n=1.

Although a single cryptococcal cell which is trapped in a blood vessel could lead to formation of a cryptococcoma by clonal expansion, it is also plausible that cryptococcal cells could be sequentially trapped behind an original cryptococcal cell which was

trapped initially. It might be hypothesised that this would be more likely to occur at higher fungal loads, so larvae infected with a higher inoculum of 200cfu were imaged immediately after infection. Indeed, it was observed that after a single cryptococcal cell became trapped in the vasculature, another two cryptococcal cells became subsequently trapped (Fig. 3.8). Importantly, cryptococcal masses were observed soon after infection at higher inoculum, indicating a separate mechanism of cryptococcoma formation within the vasculature, through a build-up of cryptococcal cells, at high fungal burdens.

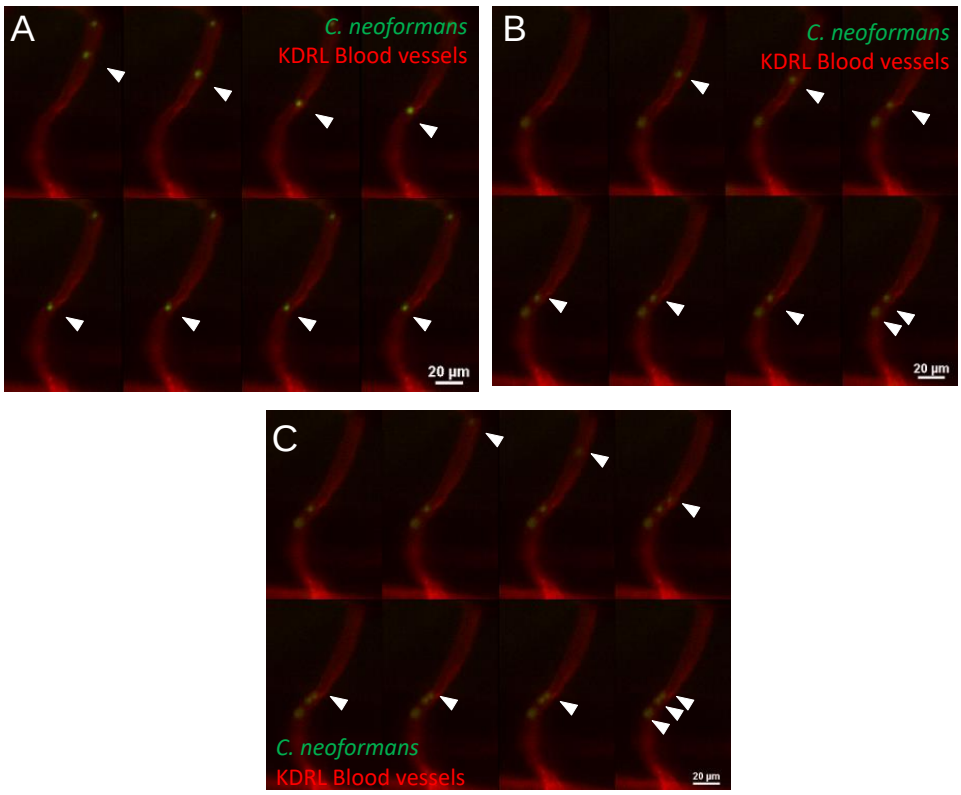

Figure 3.8 Cryptococcal blockage and build up in the vessels

Infection of KDRL mCherry blood marker transgenic line with 200cfu GFP *C. neoformans*, imaged immediately after infection **A** Initial Cryptococcal cell becomes trapped (white arrow) **B** 72 seconds later, a second cryptococcal cell becomes trapped behind the initial one **C** A further 117 seconds later, a third cryptococcal cell becomes trapped behind the first and second (left to right, time points 0.6 seconds), white arrows track individual cryptococcal cells, n=1.

However, in larvae infected with a low cryptococcal inocula (25cfu), in mixed cryptococcal fluorescent strain infection experiments, the majority of cryptococcomas were a single colour. This suggests that, at lower fungal burdens, a single or very small number cryptococcal cells are responsible for cryptococcoma formation. This is because, at a higher inocula where cryptococcal cells become trapped behind each other mixed cryptococcoma formation may be expected to occur frequently, since the

cryptococcal cells which get stuck could be compromised of both cryptococcal fluorescent strains. Taken together, these data suggest a potential role of cryptococcal clonal expansion in cryptococcoma formation, particularly at low fungal burdens.

3.9 Cryptococcal clonal expansion in small blood vessels

After determining that cryptococcal cells are trapped in the intersegmental blood vessels, I hypothesised that a higher proportion of cryptococcomas would be present in narrower blood vessels, where cryptococcal cells are able to become trapped and therefore replicate.

Indeed, 80.36% of cryptococcomas were observed within narrow blood vessels in the brain, or intersegmental (between somites) vessels (Fig. 3.9 A), in comparison to the larger (wider) sized vessels, such as the caudal vein. In this case, brain and intersegmental vessels are of a similar diameter to cryptococcal cells, whereas the caudal vein is significantly wider than cryptococci. These data further support the observation that cryptococcal cells form cryptococcomas after initial trapping, is favoured in narrow blood vessels, followed by localised clonal expansion.

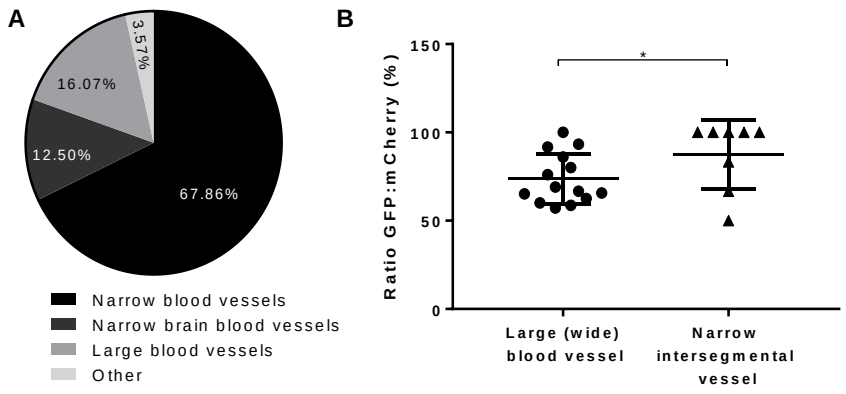

Figure 3.9 Cryptococcoma formation favoured in narrow blood vessels

Infection of 2dpf AB larvae with 25cfu of a 5:1 ratio of GFP:mCherry KN99 *C. neoformans*. Larvae were imaged until 8dpf, or death (n=3, in each repeat 7, 10 and 12 larvae were used). **A** Proportion of cryptococcomas observed in small inter-somal blood vessels, small brain blood vessels, large caudal vein or in other locations e.g. yolk, (n=3). **B** The ratio of GFP:mCherry *C.neoformans* in the large caudal vein in comparison to the fifth intersegmental blood vessel (n=3, *p<0.05, +/-SD, paired t-test).

Cryptococcoma formation occurs in the early stages of infection. To investigate whether clonal expansion is also favourable in smaller blood vessels later in the infection, the ratio of GFP:mCherry *C. neoformans* was compared between narrow intersegmental vessels, and the larger (wider) caudal vein, at the final uncontrolled infection stage. As shown in Fig. 3.3 A-II (above), it is clear that groups/blocks of single coloured strain of cryptococcus are seen in intersegmental vessels, in comparison to the mixture of cryptococcal strains in the large caudal vein, in uncontrolled infection. Indeed, the ratio of GFP:mCherry was higher in the small vessels, in comparison to the large vessels, (Fig. 3.9 B), indicating that a single block of GFP cryptococcal cells was most likely to occur in narrow blood vessels. This further supports localised clonal expansion occurs in narrow blood vessels, both in early and late stages of infection, after a single or small number of cryptococci are trapped in the vasculature.

3.10 Cryptococcal proliferation as a route of dissemination

To determine if clonal expansion at sites of cryptococcomas is associated with invasion of surrounding tissue, the strain colour of *C. neoformans* located at tissue invasion events were compared to the colour of nearby cryptococcomas in the blood vessels (in the original 25cfu mixed infection experiments). Clear examples of cryptococcal tissue invasion from the vasculature into the surrounding somite is demonstrated (Fig. 3.10 A). In every case, the strain colour of *C. neoformans* in a tissue invasion event was the same strain colour as cryptococcal cells in the cryptococcoma at the closest location in the vasculature (Fig. 3.10 B). Therefore it is highly probable that cryptococcal masses are the source of *C. neoformans* which invade the surrounding tissue.

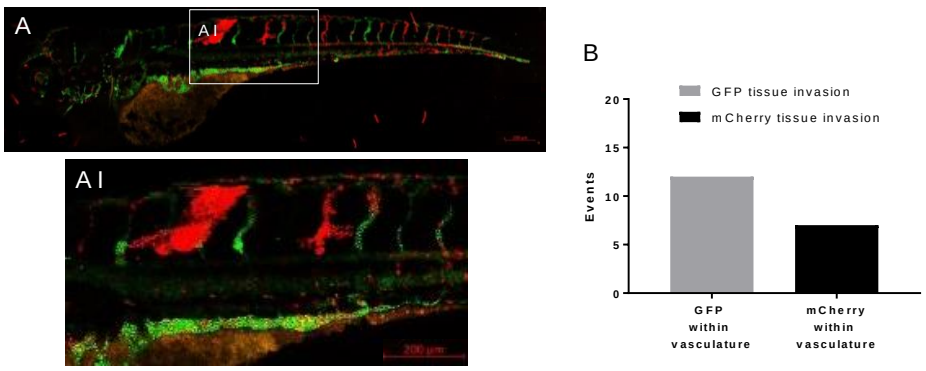

Figure 3.10 ***C. neoformans*** **dissemination events**

Infection of 2dpf AB larvae with 25cfu of a 5:1 ratio of GFP:mCherry KN99 *C. neoformans*. Larvae were imaged until 8dpf, or death (n=3, in each repeat 7, 10 and 12 larvae were used). **A** (and **AI**) representative example of dissemination of *C. neoformans* (mCherry) into the somite surrounding existing mCherry cryptococcomas **B** Comparison of strain colour of *C. neoformans* in the vasculature (GFP or mCherry), and the corresponding colour of nearby (or in the same position), dissemination events (n=3, 15 larvae). Red scale bars represent 200um.

3.11 Cryptococcomas cause physical vessel damage

Cryptococcomas close to dissemination events are the likely source of cryptococcal cells found in the surrounding tissue, so the mechanism of exactly how *C. neoformans* is able to get out of the vasculature was next investigated. Several mechanisms have been demonstrated of how *C. neoformans* is able to escape the vasculature enabling crossing the BBB. These include transcytosis through vascular endothelial cells and use of macrophages as Trojan horses.

Data shown below, indicate that cryptococcal masses present in the blood stream are directly responsible for increased vessel width (Fig. 3.13). Localised clonal expansion was shown to be associated with formation of cryptococcoma (Fig. 3.6), which are located at sites of dissemination (Fig. 3.10). Therefore I next investigated a potential route of cryptococcal dissemination whereby clonal expansion in the vasculature leads to vessel wall damage through physically pushing and damaging the vessel wall.

Vessel integrity at sites of tissue dissemination was examined using a 1000cfu high dose infection to enable sufficient visualisation of dissemination events, in the KDRL blood vessel marked line. At some sites of dissemination, the vessel wall appeared to remain intact, despite *C. neoformans* being present in the surrounding tissue (Fig. 3.11 A). This may represent transcytosis events. However, some sites of dissemination show damage to the structure of the vessel wall (Fig 3.11 B), resembling bursting of the vessel. Indeed, this damage could be caused by physically pushing and damaging the vasculature until rupture. Or perhaps a cryptococcal blockage in the vessel causes a build-up of pressure leading to bursting close to, or at the site of the cryptococcoma. This suggests dissemination events are being caused by both (likely) transcytosis, and vessel damage.

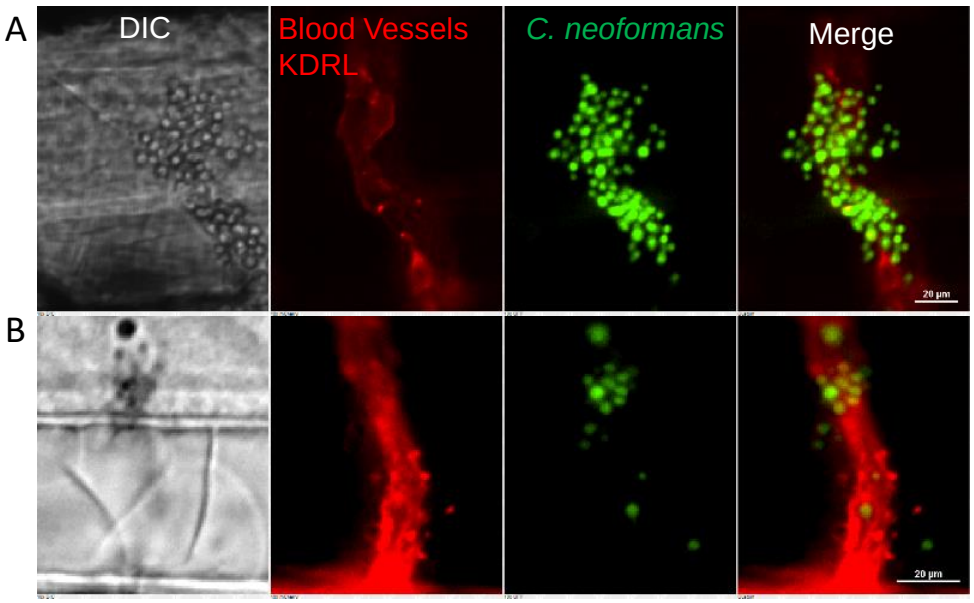

Figure 3.11 Vasculature dissemination at sites of cryptococcoma

Infection of KDRL mCherry blood marker transgenic line with 1000cfu GFP *C. neoformans* imaged at 3dpi (n=3, 17 larvae) **A** Representative image of Intact blood vessel, with *C. neoformans* in the surrounding tissue **B** Representative image of Damaged blood vessels with *C. neoformans* in surrounding tissue.

3.12 Disruption of vascular endothelial cell-cell junctions at sites of cryptococcomas

To further investigate whether the vessel walls are physically damaged, infection of 1000cfu mCherry *C. neoformans* into a transgenic vascular endothelium (VE) cadherin line was used to determine whether damage occurs between cell-cell junctions in the vessel endothelium.

Similar to the KDRL lines, the VE-Cadherin line highlighted transcytosis events, in addition to vessel damage as routes of dissemination. Vessel damage was shown at sites of dissemination, where a clear line resembling the endothelium is not seen on one side of the vessel, indicating damage to the endothelial layer (Fig. 3.12 A, B). Equally, transcytosis events were demonstrated where the vessel wall (VE-Cadherin expression) remains intact despite *C. neoformans* being outside the vasculature (Fig. 3.12 C, D). Comparison of (likely) transcytosis and vessel damage events demonstrate that both routes of dissemination occur at similar rates, with an equal number of 3 events observed each. Of note, all dissemination events occurred at sites of cryptococcal masses.

Overall, these data suggest that a previously un-characterised mechanism of cryptococcal dissemination occurs at sites of localised clonal expansion, leading to vessel damage and escape from the vasculature.

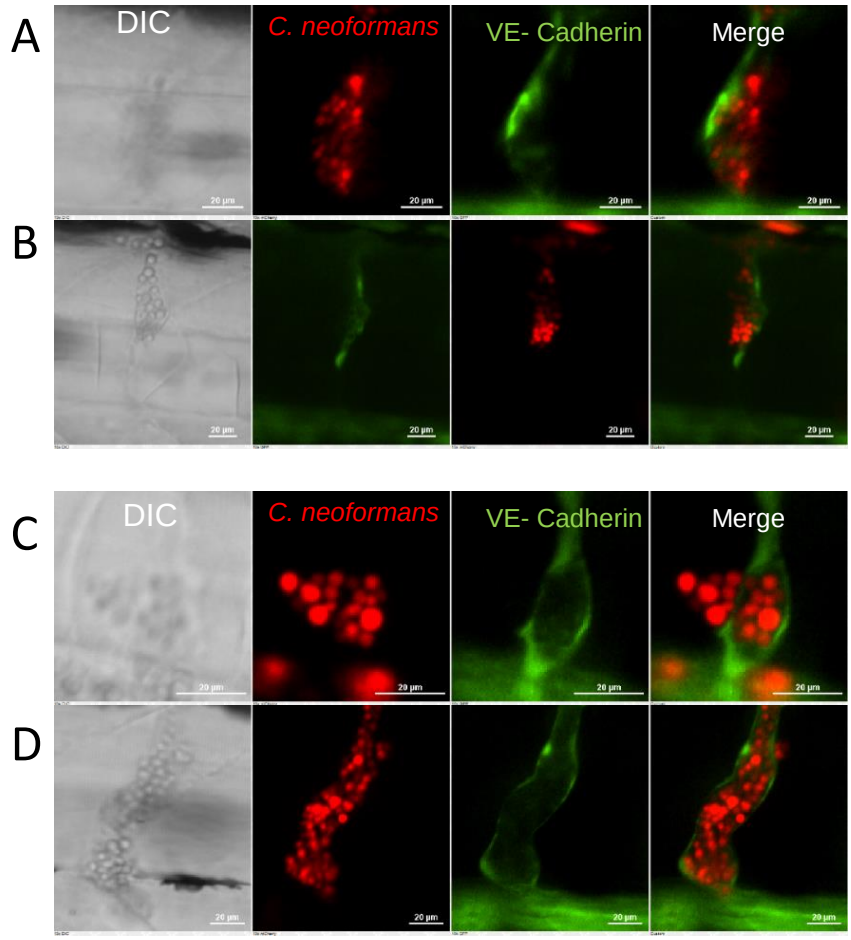

Figure 3.12 Disruption of cell-cell junction integrity at cryptococcoma sites

Infection of vascular-endothelium cadherin GFP cell-cell junction (blood vessel marker) transgenic line with 1000cfu mCherry *C. neoformans* imaged at 3dpi (n=2, 11 larvae) **A**-**B** Representative images **of** damaged cell-cell junctions in the blood vessel endothelial layer at sites of cryptococcoma. **C-D** Representative images of intact cell-cell junctions in the blood vessel endothelial layer, with *C. neoformans* in the surrounding tissue. All scale bars represent 20um.

3.13 Clonal expansion results in vasculature damage

Vessel damage occurs at sites of cryptococcomas. Cryptococcal cells can become trapped in narrow blood vessels and proliferate forming a cryptococcoma. It may be

possible that this localised clonal expansion at sites within the vasculature may lead to reduced vessel integrity. I hypothesised that vessel damage occurs due to increasing size of the cryptococcal mass, due to localised expansion.

Due to the low occurrence of dissemination events (19 events) at low inocula of 25cfu, a large inoculum of 1000cfu *C. neoformans* was injected into larvae, to enable more frequent cryptococcoma formation. Firstly the width of blood vessels in infected larvae, with and without *C. neoformans* masses within were compared at 2hpi, and subsequently at 3dpi, to determine whether the presence of a cryptococcoma increases the width of the vessel. At 2hpi there is a small but significant increase in blood vessel width at the site of cryptococcal masses (Fig. 3.13 A). Furthermore at 3dpf a clearly visible and significant increase in size is observed for blood vessels containing a cryptococcal mass (Fig. 3.13 B). This provides clear evidence that the cryptococcal masses are increasing the size of blood vessels, and this increases over time as cryptococcal cells proliferate.

To determine if the increase in blood vessel width is caused by the presence cryptococcal masses, the width of the cryptococcal mass in relation to the vessel width (it was located in) was compared. Indeed at both 2hpi and 3dpi, the vessel width was proportional to the cryptococcal mass size, (Fig. 3.13 C, D). Furthermore, comparison of the sizes of cryptococcal masses, at 2hpi and 3dpf clearly highlight cryptococcal mass increases over time. Together these data indicate that cryptococcal masses directly influence the blood vessel size, perhaps through physically pushing and damaging the vessel wall as localised expansion increases the size of the cryptococcoma.

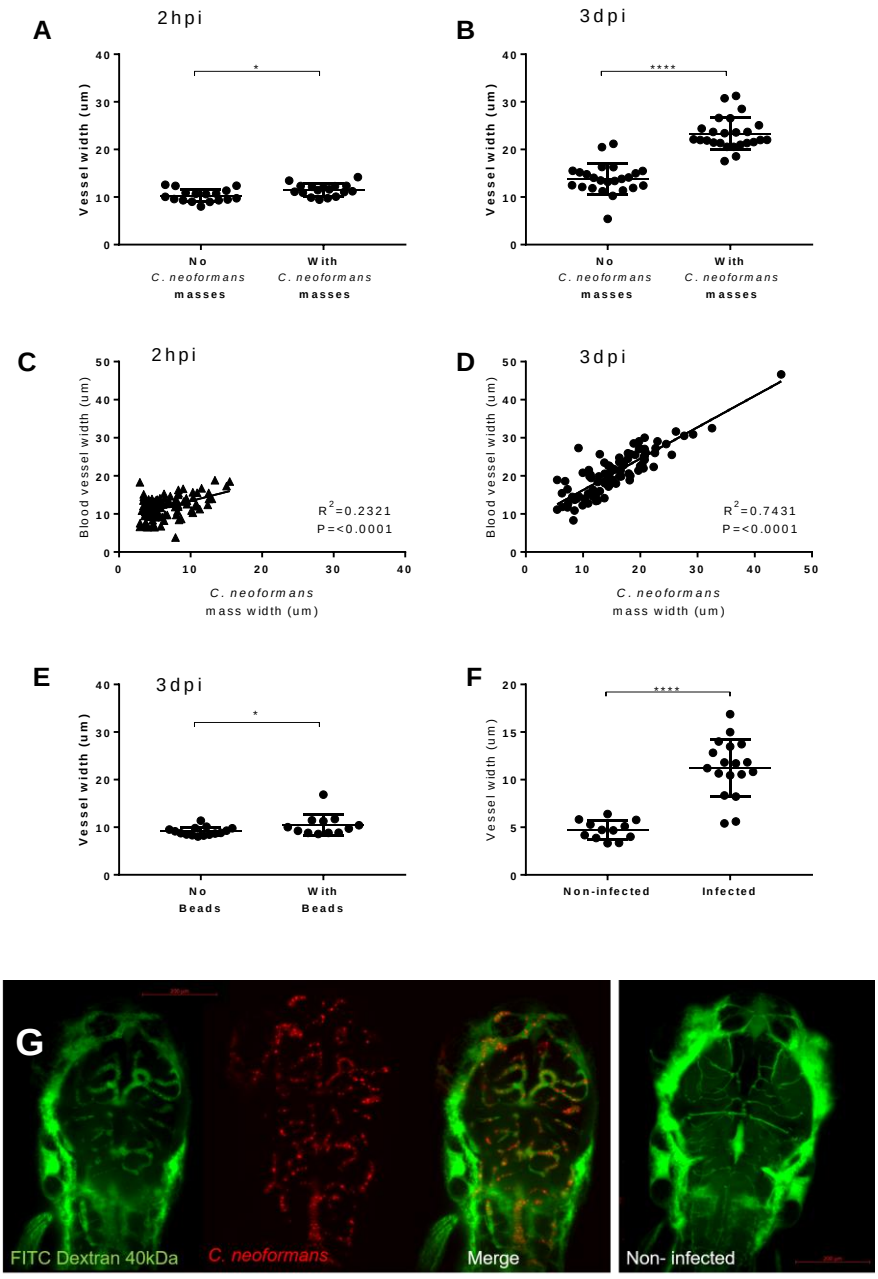

Figure 3.13 Cryptococcal proliferation causes damage to the vasculature

A-E: Infection of KDRL mCherry blood marker transgenic line with 1000cfu GFP *C. neoformans* **A** Average vessel width with and without cryptococcal masses at 2hpi (n=3, *p<0.05, unpaired t-test, 17 larvae) **B** Average vessel width with and without cryptococcal masses at 3dpi (n=3, ****p<0.0001, unpaired t-test, 26 larvae) **C** Relationship between *C. neoformans* mass and vessel width at 2hpi (n=3, linear regression, 17 larvae) **D** Relationship between *C. neoformans* mass and vessel width at 3dpi (n=3, linear regression, 26 larvae) **E** Average vessel width with and without beads present at 3dpi (n=3, *p<0.05, unpaired t-test, 15 larvae). F-G: Infection of mCherry *C. neoformans* with 40kDa FITC Dextran to mark blood vessels **F** Comparison of infected brain vessels width to non-infected corresponding brain vessels (three infected fish analysed, +/- SD, ****p<0.0001, paired t-test) **G** Representative image of infected and non-infected brain vessels (Dr Robert J Evans), red scale bars represent 200um.

To further demonstrate that proliferation of cryptoccocal cells, rather than a blockage in the blood vessels was responsible for the an increase in blood vessel size and resulting vessel integrity damage, inert beads of a similar size (4.5µm) to cryptococcal cells were injected into larvae as a control which cannot proliferate. At 3dpf, inert beads were observed in intersegmental blood vessels, with a small but significant increase in blood vessel size shown (Fig. 3.13 E). Of note, in comparison to *C. neoformans* infection at 3dpi, the average blood vessel width is ~22µm, whereas with beads, an average blood vessel width of 10µm is observed, very similar to the 2hpi *C. neoformans* data. This shows that while both beads and cryptococcal cells can become trapped in blood vessels, only *C. neoformans* is able to replicate and form larger masses. Cryptococcal growth most likely directly physically interacts with the blood vessels, pushing against the vessel wall resulting in damage and increased width of blood vessels.

Finally, blood vessel widening was also observed in the brain. I analysed images of larvae injected with *C. neoformans* in addition to the 40kDa Dextran (to observe the blood vessels, experiment performed by Dr Robert J Evans). Similar to the intersegmental vessel data, equivalent blood vessels in the brain were enlarged under infection conditions (Fig. 3.13 F, G). Importantly this highlights that vessel damage is occurring in the brain vasculature, an important site in *C. neoformans* pathogenicity, implicating vascular damage mediated tissue invasion as a route of crossing the BBB.

3.14 Blood vessel width increase at sites without cryptococcoma

I noticed that blood vessels which were not colonised by *C. neoformans* at 3dpi, within infected larvae, appeared to be larger in width than the size of the non-colonised blood vessels at 2hpi (Fig. 13 A, B above). This may suggest that cryptococcal presence perhaps virulence factors, could influence the entire vasculature, in addition to physical damage at cryptococcoma locations.

The vessel width in non-infected larvae was compared with the vessel width of non-colonised vessels in larvae which had been infected with *C. neoformans*. This was to determine if intersegmental blood vessel width was enlarged in vessels not colonised with cryptococci, but within infected larvae. At 0dpi, no significant difference between blood vessel size was shown (Fig 3.14 A), however, at 3dpi, a significant increase in non-colonised vessel width (from infected larvae) in comparison to non-infected larvae was shown (Fig 3.14 B). This suggests cryptococcal presence affects the entire vasculature. In agreement, larvae injected with inert beads showed no change in vessel with at 0dpi (Fig. 3.14 C), and at 3dpi, with a small but significant decrease in

vessel width in non-bead-colonised vessels in comparison to non-injected larvae (Fig 3.14 D).

The bead injection data suggest blockage alone of some intersegmental blood vessels does not increase the vessel width of non-blocked vessels. This suggests that the increase observed in vessel width of non-colonised vessels (in *C. neoformans* infection) may be caused by other cryptococcal factors.

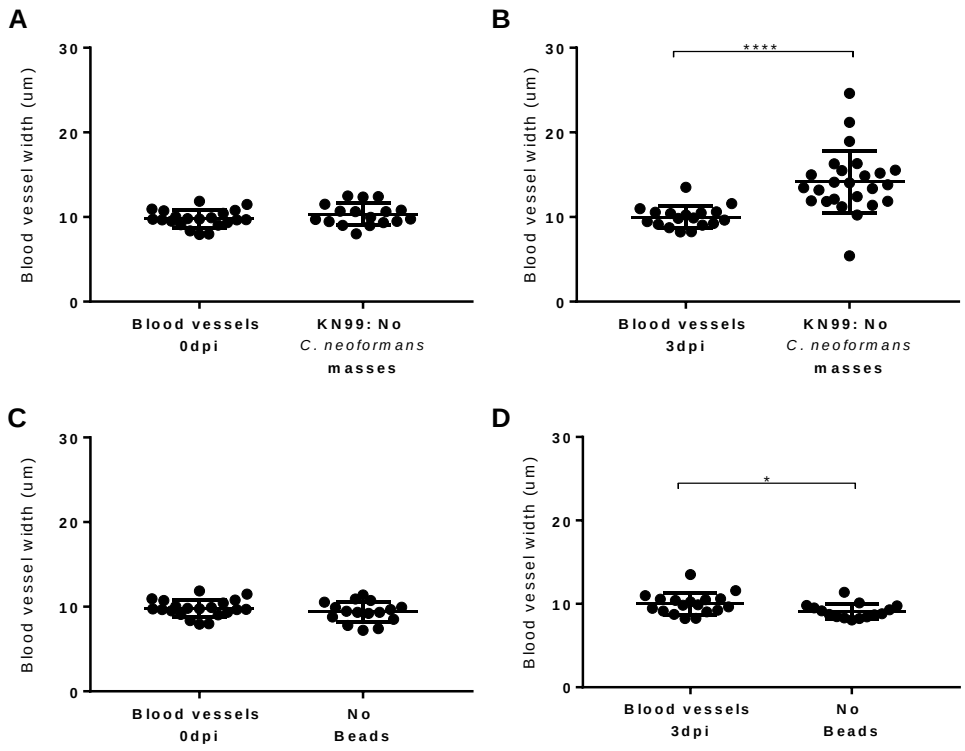

<u>Figure 3.14</u> Cryptococcal infection increases width of non-colonised intersegmental blood vessels

KDRL mCherry blood marker transgenic line with 0cfu or 1000cfu GFP *C. neoformans* **A** Average vessel width without injection, or without cryptococcal masses at 2hpi within (n=3, ns Student's t-test, 21 non-injected larvae, 17 injected larvae) **B** Average vessel width without injection, or without cryptococcal masses at 3dpi within (n=3, ****p<0.0001, Student's t-test, 18 non-injected larvae, 26 injected larvae) **C** Average vessel width without injection, or without inert bead masses at 2hpi within infected larvae (n=3, ns Student's t-test, 21 non-injected larvae, 16 injected larvae) **D** Average vessel width without injection, or without inert bead masses at 3dpi within infected larvae (n=3, *p<0.05, Student's t-test, 18 non-injected larvae, 15 injected larvae)

3.15 Blood vessel width increase in *C. neoformans* infection lacking virulence factors

An increase in non-colonised intersegmental vessels within *C. neoformans* infected, but not inert bead injected, suggest that cryptococcal factors are damaging the vasculature perhaps through virulence factor mediated damage. Three cryptococcal mutants deficient for cryptococcal virulence factors, *Ure-1* deficient in Urease, *Pho4* deficient in phosphate sensing and acquisition and *Sec14* deficient in secretion factor 14, which is required for secretion of enzymes including virulence factor phospholipase b, were chosen for analysis.

Each cryptococcal mutant has previously been linked to vasculature mediated dissemination. Urease is suggested to be important in the trapping of cryptococci in blood vessels, and in the transmigration across the vasculature (Shi et al. 2010; Olszewski et al. 2004). *Pho4* is important for cryptococcal pathogenicity, and in dissemination into the brain from the blood stream (Lev et al. 2017). Finally, *Sec14* is required for the secretion of enzymes, including virulence factor phospholipase b (plb) (Chayakulkeeree et al. 2012), which itself is required for cryptococcal dissemination to the brain (Noverr et al. 2003). I hypothesised that cryptococcal cells which are deficient in dissemination through the vasculature, may be unable to cause vasculature damage, due to reduced viability in the bloodstream

To determine if colonisation of intersegmental cells, in these cryptococcal mutants, also leads to vessel damage in a similar mechanism as KN99 *C. neoformans*, the vessel width was compared between blood vessels containing either KN99 (wild-type data as above), *Sec14*, *Pho4* or *Ure-1* strains and corresponding non-colonised blood vessels within infected larvae. Indeed, for each strain, a significant increase in the vessel width was found at 3dpi in colonised blood vessels in comparison to non-colonised blood vessels (Fig. 3.15 A-D). These data suggest that *Sec14*, *Pho4* and Urease are not required by the cryptococci to damage blood vessels through cryptococcal proliferation.

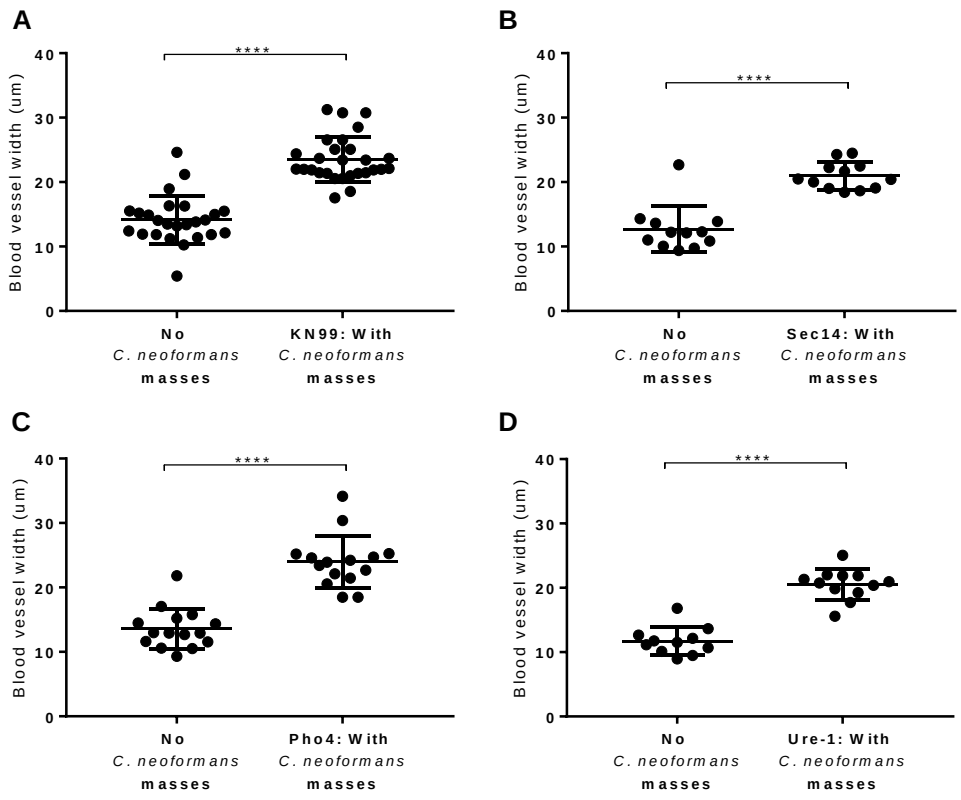

<u>Figure 3.15</u> Cryptococcoma increases blood vessel width when infected with mutant cryptococcal stains

KDRL mCherry blood marker transgenic line with 1000cfu GFP *C. neoformans* **A** Average vessel width with or without cryptococcal masses in KN99 infection at 3dpi within (n=3, ****p<0.0001, Student's t-test, 26 injected larvae) **B** Average vessel width with or without cryptococcal masses in *Sec14* infection at 3dpi within (n=3, ****p<0.0001, Student's t-test, 13 injected larvae) **C** Average vessel width with or without cryptococcal masses in *Pho4* infection at 3dpi within (n=3, ****p<0.0001, Student's t-test, 15 injected larvae) **D** Average vessel width with or without cryptococcal masses in *Ure-1* infection at 3dpi within (n=3, ****p<0.0001, Student's t-test, 15 injected larvae).

I hypothesised that if either of these virulence factors are involved in vasculature damage, away from the physical site of trapping or cryptococcoma, the vessel width in non-colonised intersegmental vessels would not be increased at 3dpi. However, in KN99 (wild-type data same as above), in addition to *Sec14*, *Pho4* and *Ure-1*, a significant increase in the vessel width in non-colonised intersegmental vessels from infected larvae was shown in comparison to non-infected larvae (Fig 3.16 A-D). These data suggest that urease, Pho4 or Sec14 deficient cryptococcal cells are able to increase non-infected vessel width, despite deficiency in cryptococcal virulence factors.

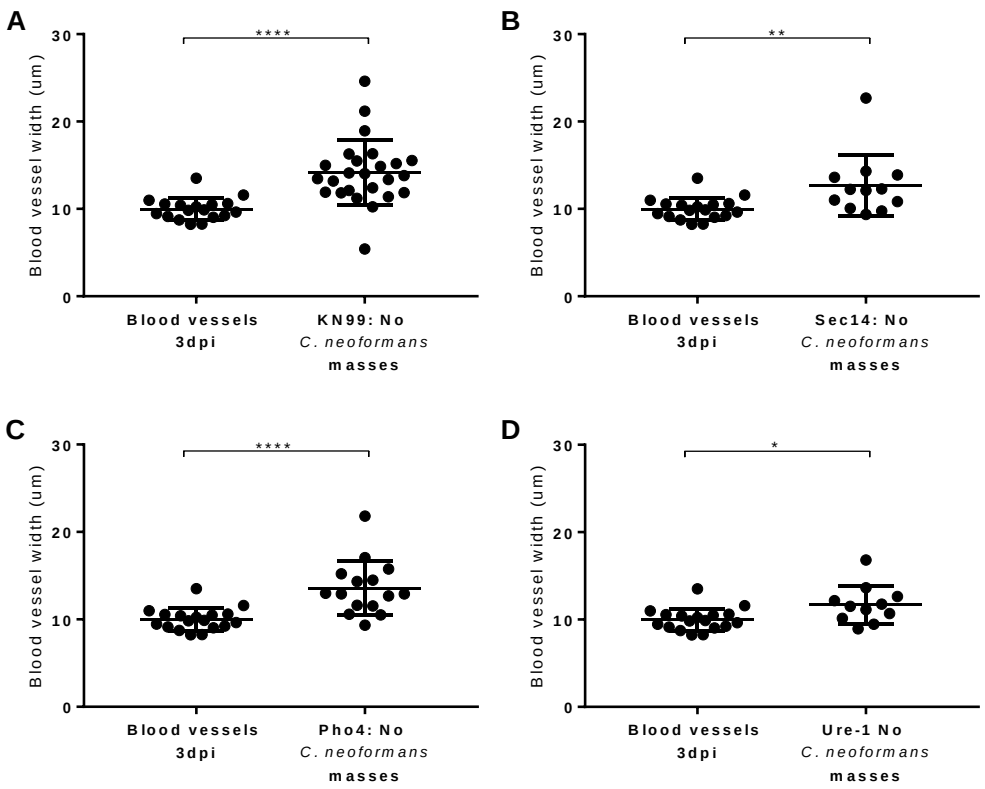

Figure 3.16 Increased non-colonised blood vessel width by mutant cryptococcal strains

KDRL mCherry blood marker transgenic line with 0cfu or 1000cfu GFP *C. neoformans* **A** Average vessel width without cryptococcal masses in KN99 infection at 3dpi within (n=3, ****p<0.0001, Student's t-test, 18 non-injected larvae, 17 injected larvae) **B** Average vessel width without cryptococcal masses in *Sec14* infection at 3dpi within (n=3, **p<0.01, Student's t-test, 18 non-injected larvae, 13 injected larvae) **C** Average vessel width without cryptococcal masses in *Pho4* infection at 3dpi within (n=3, ****p<0.0001, Student's t-test, 18 non-injected larvae, 15 injected larvae) **D** Average vessel width without cryptococcal masses in *Ure-1* infection at 3dpi within (n=3, *p<0.05, Student's t-test, 18 non-injected larvae, 15 injected larvae)

Overall, these data suggest that blockage of some intersegmental vessels is not sufficient to cause increased width of non-colonised vessels. However, cryptococcal mutants in key virulence factors, which were able to inflict vessel damage in a similar manner to KN99 *C. neoformans,* were also able to cause an increase in vessel width in non-colonised vessels.

3.16 Chapter summary

I have shown a previously uncharacterised mechanism of cryptococcal dissemination. Through infection of a mixed ratio of GFP and mCherry *C. neoformans* strains, I demonstrated that the inoculum ratio of each fluorescent strain does not determine the predominant colour strain which is causes the fatal infection outcome. Cryptococcal masses, which are predictive of final infection outcome, are likely formed through entrapment in the vasculature followed by localised clonal expansion. The sites of clonal expansion, often in narrow vessels, appear to cause damage to the vasculature, which may be involved in progression to dissemination into the surrounding tissue. An interesting observation that non-cryptococcal-colonised blood vessel width was also increase in infected larvae, and this was shown to not be caused by vessel blockage. However analysis of cryptococcal mutants did not reveal a cryptococcal virulence factor responsible for increased non-colonised blood vessel width.

3.17 Discussion

3.17.1 Cryptococcal infection dynamics

The first aim of this chapter was to determine if cryptoccocal expansion from a single or small number of cryptococcal cells determines infection outcome. The role of clonal expansion in dissemination has not been studied in *C. neoformans* infection previously. However, clinical reports suggest that cryptococcal proliferation may be involved in cryptococcal dissemination across the BBB (Lee et al. 1996). It is also known that for both *S. aureus* and *S. enterica* infection, a small number of bacteria are responsible for overwhelming infection (Grant et al. 2008; Prajsnar et al. 2012). It was therefore hypothesised that a small number of cryptococcal cells may be responsible for infection outcome.

A 5:1 ratio of two fluorescently labelled *C. neoformans* strains (GFP: mCherry) were injected into larvae in order to examine infection dynamics, in regards to a potential population bottleneck. A low dose of 25cfu was chosen to highlight any clear growth dynamics. Three distinct outcomes were observed, uncontrolled infection compromised of *C. neoformans* predominantly of the GFP strain, the mCherry strain, or a mixed outcome. The presence of the mixed group, which occurred in 37.5% of cases, indicates that a single cryptococcal cell (and clonal progeny) is not responsible for the final infection outcome, and does support the suggestion that a small number of cells are not responsible. However, presence of mixed cryptococcal strain infection outcomes does not provide conclusive evidence that a small number of cryptococcal cells are not responsible for entire infection outcome, as seen in the *S. aureus* population bottleneck.

To further investigate the dynamics of infection, the initial inoculum ratio was calculated for individual larvae. Importantly, in each fish the inoculum ratio was not 5:1, but ranged from ~4.5:1 to ~1:1 (GFP:mCherry). This large range of ratios is likely due to the very low number of cryptococcal cells injected, of approximately 25cfu. Indeed, it is expected to observe a relatively large range in the number cryptococcal cells injected into larvae at small doses (Bojarczuk et al. 2016). To further characterise the clonal expansion, it may be informative to infect at different ratios, or a larger dose, in order to compare growth dynamics at a relatively more consistent inoculum ratio. Different inoculum ratios mean it is not possible to conclude whether clonal expansion from a small number of cryptococcal cells is responsible for final ratios based on the proportion of final outcome types (GFP, mCherry or mixed) observed alone.

Comparing initial inoculum with final outcome showed that the injected inoculum does not determine the final outcome, clearly demonstrating that the injected strain ratio is not responsible for the uncontrolled growth of cryptococcal strains, which results in a majority clonal strain of fungal cells. This suggests that only a few cryptococcal cells (and clonal progeny) are responsible for uncontrolled infection. However, I cannot exclude the possibility that the majority of cryptococcal cells are effectively controlled by the immune system, while a small number are not, leading to overwhelming infection. Due to the known extracellular proliferation of *C. neoformans* it may be likely that cryptococcal cells which are not phagocytosed by macrophages, cause uncontrolled infection through extracellular replication. In fact early macrophage control of *C. neoformans* infection has previously been demonstrated in zebrafish (Bojarczuk et al. 2016). In order to examine this, cryptococcal infection dynamics in larvae depleted of macrophages could be compared with larvae which have normal macrophage function.

A caveat of this study is that, due to the long time period (2dpf – 9dpf), confocal imaging was completed using a single plane (z stack plane) in the larvae, to allow the larvae to be as little affected by imaging to have no effect on infection progression. This may mean that actual injected ratios could be inaccurate, if some cryptococcal cells were not observed during imaging. However, the fluorescent cryptococcal strains are bright, so this is unlikely to have occurred often or at all. Of note, this may mean inoculum ratios are not truly accurate.

Only 51.6% of infected fish had cryptococcal infection which became fully systemic. In all other cases, fish had cryptoccocal infection, but died before infection became overwhelming. It is likely these fish died due to handling and repeated imaging, including repeated anaesthetic exposure over the time course, or even normal expected death observed at ~15% of a population, rather than cryptococcal infection.

For this reason these fish were excluded from the study, with only final overwhelming infections considered.

The first finding in the study of cryptococcal growth dynamics was that initial inoculum ratio does not determine the predominant strain which causes the fatal final infection outcome. Analysis of infection over time led to the observation that cryptococcal masses were present in larvae ~2dpf before final infection outcome. Furthermore, cryptococcomas were shown to be predictive of infection outcome in terms of the major strain colour (GFP or mCherry), additionally suggesting that clonal expansion from a small number of cryptococci are responsible for infection outcome. Finally, the number of cryptococcomas within an individual fish was proportional to the speed of infection.

These data suggest that a small number of cryptococcal cells, which initially form a cryptococcoma, are responsible for the overwhelming infection. This suggests similar infection dynamics which are seen in bacterial infection occur in cryptococcal infection, where a small number of cryptococcal cells results in localised proliferation leading to overwhelming infection. For *S. aureus* infection, bacterial lesions which are formed through clonal expansion are observed in the established bottleneck infection (Prajsnar et al. 2012). In addition, in *Salmonella enterica* serovar *Typhimurium* infection of mice, localised clonal expansion is observed at separate locations within the animal (Grant et al. 2008). This suggests that dynamics of infection for *C. neoformans* infection also including a stage of localised proliferation.

Overall these data suggest that, the formation of cryptococcomas is an important stage of infection, and may be important in causing uncontrolled infection. Dissection reports highlighted that intravascular cryptococcoma (consisting of *C. neoformans* rather than in combination with immune cells) formation occurs in human infection, in addition to being observed in murine infection models (Lee et al. 1996; Olszewski et al. 2004). Indicating that cryptococcoma formation within the vasculature is seen in human clinical infection and occurs in both in murine and zebrafish models, and therefore could be important in progression of disease.

To understand how cryptococcomas determine infection outcome, formation of cryptococcomas and whether this is consistent with established mechanisms of cryptococcal infection, was investigated with the overarching aim to consider whether clonal expansion from these cryptococcal masses may be a mechanism of dissemination.

3.17.2 Cryptococcal cell trapping and cryptococcoma formation

To establish if cryptococcal cells can become stuck in the vasculature in the zebrafish model, trapping of cryptoccocal cells in intersegmental blood vessels was analysed to

confirm that trapping can occur in the same way as previously demonstrated in mice. Whereby cryptococcal cells become stuck in small/narrow blood vessels of a similar size to the cryptococci, when moving by blood flow throughout the vasculature (Shi et al. 2010). It is required that cryptococcal cells become trapped in the vasculature, before proliferation mediated dissemination can occur. This is supported in the observation that cryptococcoma formation occurred most often in small blood vessels. However, this is presumed in the low dose infections, because infection was directly into the blood stream. To determine whether this mechanism is truly occurring, it was required to observe this in a blood marker line.

Imaging of a recently infected larvae demonstrated that cryptococcal cells can become trapped in the larval intersegmental blood vessels. This was observed in the same manner as in the mouse model which demonstrated trapping of cryptococcal cells in blood vessels of a similar size to the cryptococcal cell (Shi et al. 2010). This is suggestive that cryptococcal cells become trapped in the vasculature and form cryptococcal masses through clonal expansion. Cryptococcal masses may not have been observed in mice, due to shorter imaging time periods. It was reasoned that another mechanism of cryptococcoma formation in the vasculature could be due to a build-up of cryptococcal cells behind an initial trapped cryptococci. Indeed, this was demonstrated using a higher inoculum, but was not observed at the low inoculum. Therefore, at low doses, a single cryptococcal cell becoming trapped and proliferating locally leads to cryptococcoma formation.

It is understandable that cryptococcal cells would become trapped in small blood vessels. Firstly, the size of the blood vessels, in this case intersegmental vessels, are of a similar size (~0.4-10um) to cryptococcal cells (~4-8um). This can explain why fewer cryptococcal cells become trapped in the larger caudal vein. Furthermore, *in vitro* and *in vivo* studies confirmed that *C. neoformans* becomes “instantaneously trapped” rather than undergoing rolling and adhesion steps, which is the mechanism immune cells use to stop within the vasculature (Shi et al. 2010).

Additionally, polystyrene spheres of matching size to cryptococcal cells, and *S. cerevisiae* were observed to become trapped in a similar manner to *C. neoformans*, (Shi et al. 2010) suggesting size may be more important than virulence factors in the trapping of cryptococcal cells in brain micro-capillaries. Similarly, inert beads of 4.5µm size used in this study were observed stuck within the intersegmental vessels. In comparison to cryptococcal cells, fewer beads were trapped in the vasculature, perhaps suggesting that cryptococcal factors do promote trapping within vessels in some part. However, the cryptococcal cell size is varied, from ~4-8um, and larger cells with a width greater than 10um were observed. Injection with larger sized inert beads

may lead to increased trapping, and would be an interesting experiment for the future. Despite this, is it clear that cryptococcal cells become trapped in the vasculature largely based on cell size (the potential role of cryptococcal factors is discussed below).

An alternative factor may be that macrophages are present in greater numbers in the caudal haematopoietic tissue, at the site of the caudal vein. Any cryptococcal cells that become trapped in this area may have a greater chance of being phagocytosed and degraded than in intersegmental vessels and nearby tissues. Interestingly, in zebrafish infection models, immune cell responses appear less pronounced in the brain (or immune privileged sites), and it was suggested that capsule induction may enable improved immune evasion at later stages of infection (Tenor et al. 2015). It may be possible that cryptococcal cells in the caudal vein have a larger risk of macrophage interactions, than those in the intersegmental vessels, resulting reduced cryptococcoma formation. On the other hand, *C. neoformans* in the intersegmental vessels may largely evade macrophage interactions in early larvae development (due to lack of macrophage encounters), leading to their continued survival, by which time capsule induction may provide further evasion from immune cell interactions. Analysis of the location of macrophage-cryptococcal interactions would be required to confirm this possibility.

It is also possible that cryptococcal factors may have a role in trapping, despite evidence that inert beads (this study) and polystyrene spheres become trapped in the same manner as cryptococcal cells (Shi et al. 2010). The role of urease in trapping of cryptococcal cells in the vasculature is disputed. Analysis of cryptococcal cells lodged in vessels (within different organs) was compared soon after inoculation in mice, to avoid potential roles of cryptococcal proliferation. Cryptococcal cells lacking urease had reduced fungal burden in the brain and lung, which represent organs with closed capillary beds, in comparison to cryptococcal cells with functional urease activity (Olszewski et al. 2004). In contrast, it has been suggested that urease in most important in transmigration out of the vasculature, than being important in the trapping of cryptoccocal cells. Co-infection of urease deficient and expressing cryptoccocal strains had no difference in trapping in the brain soon after infection (Shi et al. 2010). A major difference in these experiments in the initial inocula. It is likely that any role of urease in fungal trapping is most important at lower fungal burdens. The reduction in brain cfu counts (between urease deficient and expressing strains of *C. neoformans*) is more pronounced at lower fungal burdens (Olszewski et al. 2004). Urease may therefore play a role in this project where very low inocula were used. It would be interesting to compare trapping and cryptococcoma formation between urease deficient and expressing cryptoccocal strains to determine this.

Following cryptococcoma formation, overwhelming infection occurs. To understand the importance of this, it is important to determine how cryptococcal masses are formed. A single or very small number of cryptococcal cells are observed to form a cryptococcoma, which is suggested to be localised clonal expansion from within the vasculature. Furthermore, later in infection dissemination from the site of the mass (presumably in the vasculature), into the surrounding tissue is observed. Firstly, this observation implicates localised clonal expansion resulting from a vasculature site as responsible for cryptococcoma formation, and resulting in dissemination, the first observation of clonal expansion directly leading to dissemination. Clinical dissection reports of *C. neoformans* in the brain parenchyma, located next to brain blood vessels, also containing cryptococcal cells (Lee et al. 1996) may be expected to have formed through this mechanism.

Evidence that cryptococcoma formation is caused by clonal expansion is presented where cryptococcoma formation is shown to be resultant of a single/small number of cryptococci. Additionally, most cryptococcomas are likely formed by clonal expansion from a single colour strain (GFP or mCherry *C. neoformans*). If multiple cryptococcal cells were responsible for cryptococcoma formation, it may be likely that more cryptococcomas would contain both GFP and mCherry strains. In bacterial infection in zebrafish, also inoculated with two fluorescently marked bacterial strains, single colour bacterial lesions formed, (Prajsnar et al. 2012) thought to be generated by a single bacterium, due to the lack of mixing. Furthermore, at later time points during infection, in small blood vessels, where cryptococcoma formation is likely as discussed above, blocks of colour are observed, in correlation to a more mixed colour seen in the larger vessels. In *Salmonella enterica* serovar *Typhimurium* infection in mice, localised clonal expansion is observed in distinct locations in the animal. These subpopulations undergo clonal expansion but eventually lead to mixing, due to expansion into the blood stream leading to bacteraemia (Grant et al. 2008). This is similar to the observation of the single strain (GFP or mCherry *C. neoformans*) groups/masses seen in intersegmental vessels, but where strains are mixed in the larger caudal vein. It may be possible a similar mechanism is causing this. Overall, there is clear evidence that localised proliferation of cryptococcal cells trapped in the vasculature form clonal cryptococcal masses. This appears to be the major mechanism, however as mentioned above, a build-up of cryptococcal cells may occur in some cases (more so at higher fungal burdens), and could be responsible for the mixed colour cryptococcomas.

Alternatively, cryptococcoma could be formed when macrophages lyse after phagocytosis of several cryptococcal cells, resulting in releasing several cryptococcal cells. Indeed, a neutrophil intra-phagocyte niche was demonstrated for *S. aureus*

(Prajsnar et al. 2012). Multiple pathogens are able to survive and replicate within macrophages, including *Mycobacterium tuberculosis* and *Legionella pneumophila* (Xu & Luo 2013; Schlesinger et al. 2002). Furthermore, it is established that *C. neoformans* can reside, replicate and eventually escape from macrophages. This mechanism has not been investigated, and may be informative, as it could be hypothesised that in places such as the larger caudal vein, this mechanism may be predominant. However, due to the observation of single or small numbers of cryptococcal cells primarily within the narrow blood vessels, it is likely that in most cases a trapping mechanism in the vasculature is responsible, especially keeping in mind this may be experienced in human infection in micro-capillaries the brain vasculature.

Intra-vascular *C. neoformans* masses have been shown to be predominantly cleared by neutrophils in mice (Sun et al. 2016a; Zhang et al. 2016). Similarly, neutrophils have been shown to have an important role in the killing of cryptococcal cells circulating in the blood in zebrafish (Davis et al. 2016). *C. neoformans* are able to become trapped in the vasculature in both the brain and lungs. It is shown that improved neutrophil recruitment to the lungs results in improved fungal clearance in mice. Furthermore, by inducing neutrophil recruitment to the brain (by LPS injection), fungal clearance was enhanced (Sun et al. 2016a). This may suggest neutrophil mediated clearance of intravascular resident cryptococcal cells could be a therapeutic target, which could ultimately reduce fungal dissemination into the brain.

To conclude, evidence of a mechanism of dissemination from within the vasculature, caused by trapping of a single, or small number of cryptococcal cells at each site, which then proliferate leading to cryptococcoma formation and eventual dissemination is presented. The mechanism of how localised clonal expansion results in dissemination was investigated.

3.17.3 *C. neoformans* dissemination through localised clonal expansion

To determine if cryptococcal clonal expansion in vasculature leads to dissemination, sites of tissue invasion from the 25cfu (5:1 GFP:mCherry) larval infections were investigated. Most likely due to the low infection dose, only 19 dissemination events were observed in all larvae (15 larvae) which reached an uncontrolled infection. Significantly, in all instances of tissue invasion, the colour of the *C. neoformans* in the surrounding tissue was the same colour as the nearby, or same location cryptococcoma. These data clearly demonstrate that cryptococcal cells in the sites of cryptococcomas are the source of *C. neoformans* which disseminate at these locations. As discussed above localised clonal expansion, which contributes to the formation of

cryptococcomas, are the source of cryptococcal cells which then invade surrounding tissue. Considering the suggested mechanism to this point, a clear role of localised clonal expansion in formation of cryptococcomas, and ultimately dissemination out of the vasculature is presented.

It has been shown that cryptococcal proliferation is not required to cross the BBB, using cryptoccocal strains deficient in proliferation still able to gain access to the brain parenchyma in mice (Shi et al. 2010), which suggests the proposal that cryptococcal proliferation vascular damage is one of multiple cryptococcal dissemination mechanisms. Firstly this could be because this study is examining intersegmental blood vessels, rather than the brain, although it is unlikely location of blood vessel would affect the ability of cryptococcal proliferation mediated dissemination, as demonstrated with the observation of vascular cryptococcal growth in the larvae brain. Importantly, this current presented clonal expansion mechanism is not the only route it is possible for *C. neoformans* to disseminate from. Indeed it is possible for cryptococcal cells to disseminate without the requirement of proliferation using other methods such as transcytosis or a macrophage as a Trojan horse. It is likely that clonal expansion as a dissemination mechanism is possible, but as is well established, other methods can occur in the absence of proliferation.

Therefore, a role of clonal expansion which results in dissemination is presented, which acts in complement with established mechanisms, leading to *C. neoformans* ability disseminate from the vasculature. The mechanism by which clonal expansion leads to dissemination is next examined.

3.17.4 Clonal expansion of *C. neoformans* causes vessel damage

I have demonstrated a role of localised clonal expansion of a single or few cryptococcal cells in the formation of a cryptococcoma which is subsequently associated with dissemination out of the vasculature. A logical hypothesis that vasculature damage is caused by cryptococcal masses physically damaging vessels was next examined, with the aim to determine if cryptococcal clonal expansion causes blood vessel damage as a mechanism of dissemination.

KDRL blood marker larvae infected with 1000cfu of *C. neoformans* were followed for 3dpi to examine whether presence of cryptococcal masses in individual intersegmental blood vessels may damage the blood vessel. Vessel width was increased in the presence of cryptococcoma at 2hpi. This increase was larger by 3dpi, consistent which localised clonal expansion and was not observed for inert beads. Importantly, the increased size of the vessel was directly proportional to the size of the cryptococcal

mass, demonstrating that the cryptococcal mass is responsible for the increased vessel width. This is the first report that the size of cryptococcal masses are able to directly influence the vasculature, however some evidence that this can occur has been suggested in previous studies. Vascular damage resulting in compression of vascular endothelial cells, and altered vessel structure caused by *C. neoformans* was observed in mice (Olszewski et al. 2004). Damage to brain blood vessels by *C. neoformans* has been observed in multiple studies, vasculitis is recorded in human dissection reports (Lee et al. 1996), vascular distension at sites of cryptococci in zebrafish (Tenor et al. 2015) and distended capillaries or blocked vessels in mice infection (Olszewski et al. 2004). These data suggest that the observed vessel damage in this present study is conserved in cryptococcal pathogenesis throughout multiple organisms. In fact, in other human pathogenic fungal infection clinical case reports vasculature damage occurs in *Arthrographis kalrae* infection and that vasculitis occurs in *Candida krusei* infection (Pichon et al. 2008; Kleinfeld et al. 2013). These reports may suggest that this mechanism of cryptococcal vessel damage may be employed by multiple pathogenic fungi.

This current study has focussed on intersegmental vessels of the zebrafish larvae. Despite this, it is reasonable that the mechanism of clonal expansion causing dissemination will also occur in the brain. Images kindly provided by Dr Robert Evans were analysed, demonstrating that blood vessels in the brain are enlarged when *C. neoformans* is present, suggesting that dissemination occurring by this proposed clonal expansion mechanism will also occur at the BBB. It would be informative to confirm this with further microscopy analysis in the future.

Vessel integrity was examined to determine whether any damage to blood vessels occurs, expected due to the large increase in width of infected blood vessels. Unsurprisingly damage was observed using the KDRL blood vessel marker, with damage suggesting the vessel was burst, caused by physical damage to the vessel wall. Or perhaps a cryptococcal blockage in the vessel causes a build-up of pressure leading to bursting close to, or at the site of the cryptococcoma. The fungus *Arthrographis kalrae* which can cause pathogenic human infections, was shown to cause a cortical infarct in a case study, furthermore, massive brain vessel damage was observed, including necrotising arteries containing massive fungal growth (Pichon et al. 2008). It may be likely that vessel damage was caused by physical damage to the brain vasculature. Furthermore, a case study of localised vasculitis in a leg ulcer caused by *Candida krusei* infection suggests that vasculature damage caused by pathogenic yeast is not limited to the brain (Kleinfeld et al. 2013). These data suggest physical damage to the vasculature is occurring in pathogenic fungal infection.

Therefore evidence of vessel damage directly due to presence of cryptococcomas is demonstrated. The KDRL-mCherry marker visualises the vascular endothelial growth factor receptor KDRL, present on endothelial cells in the vasculature. To further investigate the vessel wall damage, cell-cell junctions in the vessel walls were next investigates.

The vascular endothelial cell-cell junctions were investigated using the (vascular endothelial) VE-Cadherin line, to determine the integrity of potential gaps between endothelial cells. Similar to the KDRL line, at places of cryptococcal masses, a clear lack of signal (a lack of a clear vessel wall) indicates that vessels which possess cell-cell junctions are damaged, clearly demonstrating vessel wall damage. Equally, in some cases transcytosis was observed, with *C. neoformans* observed outside the vasculature, despite clearly intact cell-cell junctions. Of note, a matching incidence rate was observed, albeit at very low occurrences, indicating that transcytosis and vessel damage occur are similar levels, as routes of dissemination. Investigation of cell-cell junctions in cryptococcal infection has previously indicated that damage may be occurring to the vasculature, through demonstration of tight junctions are damaged due to the loss of occludin, a major tight junction protein (Chen et al. 2003). It is not surprising, therefore, to determine cell-cell junctions are damaged through loss of cadherin expression at sites of cryptococcoma in the vasculature. Importantly, both transcytosis and vessel damage occurred at sites of clonal expansion. This implicates cryptococcoma formation, in both transcytosis and vascular damage mediated cryptococcal dissemination out of blood vessels.

Transcytosis is not only dependent on trapping in the vasculature. As discussed above, cryptococcal urease expression is shown to increase transmigration, potentially more important at low fungal burdens (Shi et al. 2010; Olszewski et al. 2004). In addition to urease, another cryptococcal gene *FNX1* (facilitated nutritional exit 1) has been linked to transmigration, with a reduced ability to transmigrate *in vitro*, through human brain capillary endothelial cells (Tseng et al. 2012). *FNX1* deficient cryptococcal cells also had a reduced ability to migrate into the brain parenchyma in a zebrafish infection model (Tenor et al. 2015). It is important to acknowledge that multiple factors are likely important *C. neoformans* ability to disseminate into the brain. It would be useful to test at low inocula, the ability of urease and *FNX1* cryptococcal mutants' ability to invade tissue from the vasculature, in regards to proliferation mediated vasculature damage, to determine whether proliferation mediated dissemination provides an alternative route of dissemination when other routes (e.g. transcytosis), are not available.

Infarcts and vasculature damage are observed in cryptococcal meningitis (Mishra et al. 2017). However, the physiological cause of infarcts is not identified in cryptococcal meningitis. The common occurrence of infarcts, seen in ~30% of cases in one clinical study, make this an important research area (Mishra et al. 2017). The proposed mechanism of vasculature damage demonstrated here may be responsible for causing infarcts observed in these cases, through physical damage to the vessel wall, leading to loss of tissue blood supply. This may represent an important understanding of clinical infarct occurrence in *C. neoformans* infection, and may be valuable for future therapeutic care.

Infarcts are associated with cryptococcal meningitis, and in meningitis caused by bacterial pathogens, *S. pneumonia* and *M. tuberculosis* (Floret et al. 1989; Lan et al. 2001). It may be possible both fungal and bacterial pathogens share mechanisms causing infarcts, although bacteria are much smaller in size, bacteria grow faster and can form biofilms which may be similar to cryptococcoma formation. Therefore a mechanism dependent on trapping, proliferation resulting in vessel damage may occur in bacterial infection. In a clinical study comparing cryptococcal and tuberculosis caused meningitis, infarcts were observed in 32% and 47% of cases respectively (Lan et al. 2001). Both cryptococcal and tuberculosis meningitis cause vasculitis, and, similar to *C. neoformans*, bacterial lesions are sometimes observed (Rock et al. 2008). Similarly, a rabbit model of meningitis caused by *Streptococcus pneumoniae* leads to harmful inflammation and damage of the BBB. However, a reduction in inflammation was observed when leukocyte recruitment was inhibited (Tuomanen et al. 1989). This suggests that leukocyte recruitment can be detrimental in meningitis. Furthermore, mycobacterial infection in rabbits was associated with TNF-α expression (a pro-inflammatory cytokine), where higher TNF-α expression was linked to increased vascular damage in the CNS (Tsenova et al. 1999). BBB damage in bacterial meningitis may be linked to harmful inflammation responses. These studies suggest distinct mechanisms could be used by *C. neoformans* in comparison to bacterial pathogens, which results in meningitis. However, it may be interesting to study TNF-α in cryptococcal meningitis, as a role of inducing vasculitis which could provide a useful therapeutic target.

To conclude, at sites of cryptococcal masses in the vasculature, dissemination occurs, through damage to the vasculature, at a similar incidence rate to previously established transcytosis.

3.17.5 Non-colonised vascular alterations in cryptococcal infection

It was determined that intersegmental vessel width is increased in non-cryptococcal colonised vessels (within infected larvae) in comparison to intersegmental vessels in non-infected larvae. However, no increase in non-colonised vessels was observed within inert bead injected larvae. These data suggest that the increase in vasculature width, not at sites of colonisation, is caused by other cryptococcal factors and not due to vessel blockage alone.

Blockages in some intersegmental vessels, may mean that blood flow and pressure in adjacent (i.e. non-colonised vessels) is increased. This may lead to increased demand on the individual vessel to enable sufficient blood flow within the larva, leading to vessel growth, and therefore blood vessel widening. It has been shown that blood flow is essential for the development of blood vessels in mouse models, where blocking normal blood cell movement reduced blood vessel development (Lucitti et al. 2007). Since these current experiments were conducted until 5dpf, if might be expected that blood vessel development may promote the growth of un-obstructed vessels at this age. In zebrafish which have a blocked aorta, nearby vessels re-develop to enable sufficient blood flow (Gray et al. 2007). It would be interesting to determine whether blocking blood flow in multiple intersegmental blood vessels induces increased development on adjacent blood vessels, in a similar manner as in cryptococcal infection. If it is possible to occlude certain vessels, perhaps using a laser to seal vessels, analysis of blood vessel development may highlight this.

However, due to the data presented showing non-colonised blood vessels are not increased in width, within larvae infected with inert beads, it may be possible that cryptoccocal mediated factors induce the increased vessel width. Importantly, fewer inert beads were trapped in comparison to *C. neoformans*, and since only cryptococcal cells can proliferate, the blockages caused by inert beads were smaller. It is therefore possible that the lack of increase in width of non-colonised vessels in bead injected larvae, may be due to a reduced extent of blockages. In order to quantify this, using increased inocula and larger sizes of inert beads to produce much larger vessel blockages must be tested. It may be possible that the extent of vascular blockage is very important in this observation.

Cryptococcal mutants in urease, phosphate acquisition and secretion of enzymes including virulence factor phospholipase b, have all been linked to cryptococcal dissemination, and were therefore chosen for analysis of the ability to cause vasculature damage at the site of infection. These mutants were additionally analysed to determine whether loss of these virulence factors led to a reduced vessel width size in non-colonised vessels. Importantly, the strains used in these presented data were

taken from a cryptococcal (KN99) deletion library (University of California, San Francisco, 2015, Madhani plates), and were not tested to ensure the mutant was in fact deficient in the required virulence factor. The library was used, rather than existing mutants, to match the KN99 cryptococcal strain used in all experiments. It is very important to determine whether the cryptococcal mutants are true mutants by sequencing, and western blot analysis in order to prove these data are representative of each mutation. This makes it impossible to truly conclude any observations using these strains until this analysis is complete.

Each cryptococcal mutant was able to form masses in the vasculature, which led to increased vessel size at the site of the cryptococcoma. This is very interesting, because each mutant has previously been shown to have reduce ability to invade the brain, but importantly, this ability was never totally blocked. Transmigration ability of urease deficient cryptococcal cells across the murine BBB was roughly reduced to a fifth in comparison to cells with urease expression (Shi et al. 2010), suggesting that urease is useful but not required for dissemination out of the bloodstream. An extremely minimal number of Pho4 cryptococcal mutants were able to migrate into the brain in mice, in comparison to many cryptococcal cells (4 orders of magnitude) which were Pho4 competent (Lev et al. 2017), interestingly in these infections Pho4 cryptococcal mutants were not detected in the blood. In this study, dissemination can occur without Pho4, but it is likely that reduced fungal viability leads to reduced fungal burden during infection. Reduced viability of a Pho4 cryptococcal strain was previously demonstrated (Lev et al. 2017). In Sec14 mutant cryptococcal infection in mice, no dissemination into the brain occurred by 7dpf, whereas dissemination did occur for wild-type strains. However, by 19dpi, dissemination was observed after infection with a Sec14 deficient strain (Chayakulkeeree et al. 2012). Therefore, trapping in the vasculature, growth, physical vasculature damage and tissue dissemination, presents an alternative approach for cryptococcal cells to disseminate out of the blood stream. It appears that the varied mechanisms of cryptococcal dissemination into the brain enable dissemination even when some routes are unavailable.

Cryptococcal mutants were able to increase the vessel size of non-colonised vessels within infected larvae. This suggests that urease, phosphate acquisition and secretion of phospholipase b do not cause increased vessel width in non-colonised vessels, away from the cryptococcoma site. Urease may be linked to vasculature damage due to urease production of ammonia which may be damaging to the endothelial cells (Morrow & Fraser 2013), but this may be limited to the site of the cryptococcoma. It would be interesting to analyse the type of dissemination events in urease deficient cryptococcoma, in correlation with the type of vasculature damage. It may be likely that

transcytosis occurs more often due to a reduction in vessel damage. It is not surprising that Pho4 does not alter vasculature damage, as phosphate acquisition it is important in the viability of cryptococcal cells. Sec14 is important in the secretion of phospholipase b (Chayakulkeeree et al. 2012). Fungal cell wall integrity of *C. neoformans* is maintained by phospholipase b, which could decrease the ability of Sec14 cryptococcomas to inflict physical damage onto the blood vessel wall (Siafakas et al. 2007).

It may be possible that alternative cryptococcal virulence factors may directly target blood vessel walls, leading to vasculature damage. In pathogenic infection, vasculitis has been shown to occur from toxins. In fact when streptococcal and staphylococcal toxins were repeatedly injected into a rabbit's arteries, vasculitis was observed (Abe et al. 1998). In *Aspergillus fumigates* human infection, expression of virulence factor elastase can degrade blood vessel walls (Ben-Ami et al. 2010). In future, further analysis of alternative virulence factors of *C. neoformans*, may provide an explanation for the non-colonised vessel expansion.

3.18 Chapter summary

A previously unknown dissemination mechanism of *C. neoformans* infection is demonstrated. Through investigation of infection dynamics, the formation of cryptococcal masses, by clonal expansion after trapping in the vasculature was demonstrated. It was next shown that at sites of *C. neoformans* proliferation dissemination events occur, through vasculature damage.

Cryptococcal mediated damage to the vasculature was observed by cryptococcal mutants which may be unable to disseminate in established routes (e.g. transmigration). Therefore, cryptococcal dissemination through vasculature damage likely represents one of multiple route of dissemination.

Chapter 4: Results Chapter 2

Characterisation of zebrafish autophagy mutants

4.1 Chapter introduction

Autophagy mutants were created in two key autophagy genes, *atg3* and *atg5*. These genes were selected for mutagenesis due to their important role early in the formation of the autophagosome and due to the likely impact of their loss being significant in blocking autophagy downstream of autophagosome formation. As discussed previously (see section 1.6), these two genes are key in each of the two ubiquitin-like conjugation processes, important in the elongation of the autophagosome double membrane and are responsible for LC3-I lipidation. Indeed, according to current dogma, it would be expected that loss of either of these genes would abolish lipidation of LC3-I.

Corresponding mouse mutant models exist for both *Atg3* and *Atg5* genes. Both *Atg3*-/- and *Atg5*-/- mice are neonatal lethal (Kuma et al. 2004; Sou et al. 2008). The *Atg5*-/- mice exhibit a suckling defect however the life expectancy of these murine models can be extended through force feeding, but only by several hours (Kuma et al. 2004). Furthermore, LC3-II production is lost in *Atg3* null and *Atg5* null mice. These mouse models implicate both genes as important in development. In zebrafish, morpholino data suggests that a lack of nutrients, potentially caused by the knock-down of autophagy through *atg5*, leads to damaged cardiac tissue during development, and it may be this which ultimately leads to death of zebrafish larvae (Lee et al. 2014).

It is unknown what effect a deletion mutation in *atg3* or *atg5* will cause in the zebrafish. Due to the neonatal lethality following the loss of either *Atg3* or *Atg5*, in murine models, a similar survival phenotype may be expected in the zebrafish. Furthermore, the potential effects of lack of nutrients which could be caused by disruption of autophagy, especially during development, may affect the viability and growth of the larvae. For these reasons, characterisation of each mutation is very important to understand what mutation phenotypes exists, before infection studies could be interpreted.

Hypothesis: Autophagy is downregulated, or non-functional in *atg3-/-* and *atg5-/-* zebrafish.

Chapter aims:

1. Define the phenotype of mutants in autophagy genes *atg3* and *atg5*
2. Determine whether autophagy *atg3* "mutant" fish are deficient in *atg3* expression
3. Determine whether autophagy *atg5* "mutant" fish are deficient in *atg5* expression
4. Ascertain whether autophagy is reduced in the *atg3* and *atg5* mutant larvae

4.2 Characterisation of the autophagy mutant lines

Zebrafish lines with induced mutations in *atg3* and *atg5* were generated. Former lab members in the Ingham Lab at IMCB used Zinc Finger Nuclease technology to generate the *atg5*. Former PhD student Lore Lambein, in the Renshaw lab used TALEN mutagenesis to generate the *atg3*^{sh371}. These fish have genomic lesions disrupting the reading frame of *atg3* and *atg5* genes. However, genomic lesions generated in this way do not always lead to null phenotypes, due to alternative splicing or to genetic compensation. It is therefore critical to ensure mutant fish were truly deficient in autophagy and to determine whether absence of a key autophagy gene leads to a specific phenotype in zebrafish.

4.2.1 Analysis of predicted effect of autophagy mutations

atg3:

The zebrafish genome has one copy of the *atg3* gene found on chromosome 6, made up of 12 coding exons, which has a single transcript, coding for a protein which is comprised of 317 amino acids. The zebrafish *atg3* gene is orthologous to the human ATG3 gene. EMBL-EBI pairwise sequence alignment (using protein for the alignment) of the zebrafish Atg3 protein (ENSDARP00000041303.7) against human *ATG3* protein (ENSP00000283290.5) shows 83.6% identity between protein sequences (Fig. 4.1 A). The *atg3* mutant zebrafish line was previously made at Sheffield University through TALEN mutagenesis, which resulted in a 10bp deletion in exon 4. The predicted protein sequence resulting from the 10bp mutation site was aligned against the full *atg3* zebrafish protein, using MegAlign (Fig. 4.1 B), showing a predicted STOP within 21 bases of the mutation site. Thus, the *atg3* mutation is predicted to code for a truncated protein, only 71 amino acids long compared to 317 amino acids in the full length protein, suggesting it is unlikely to function normally.

atg5:

The zebrafish atg5 gene is on chromosome 16 and has 7 coding exons. The zebrafish genome has one copy of the *atg5* gene, which is orthologous to the human gene, and while the zebrafish has 2 transcripts, they both encode the same 275 amino acid protein sequence, with the difference in sequence in the UTR. An EMBL-EBI pairwise sequence alignment (using protein sequences for the alignment) of zebrafish Atg5 (ENSDARP00000124077.1) protein sequence against the human ATG5 (ENSP00000358072.3) protein shows 80.9 % identity (Fig. 4.2 A). The *atg5* zebrafish line was previously made in Singapore, IMCB, A*Star Labs, through zinc finger mutagenesis, which resulted in a 23bp deletion in exon 3. Since exon three is found in both coding transcripts, it is predicted the mutation would affect both transcripts. The predicted protein sequence resulting from the 23bp mutation site is aligned against the full *atg5* zebrafish protein, using MegAlign (Fig.4.2 B), highlighting a predicted STOP within 12 bases after the mutation site. Thus, the *atg5* mutation is also predicted to code for a truncated protein, 43 amino acids in length, shorter than the 275 seen normally, again suggesting this protein would not function.

A

Zebrafish Atg3 [ENSDARP00000041303.7] **83.6% identity**

Human ATG3 [ENSP00000283290.5]

```
Atg3 zebrafish     1 MQNVINSVKGTALGVAEFLTPVLKESKFKETGVITPEEFVAAGDHLVHHC
                     ||||||:|||.||.|||:||||||||||||||||||||||||||||||||
ATG3 human         1 MQNVINTVKGKALEVAEYLTPVLKESKFKETGVITPEEFVAAGDHLVHHC

Atg3 zebrafish    51 PTWKWASGEEAKVKPYLPNDKQFLLTRNVPCYKRCKQMEYSDELEAIIEE
                     |||:||:|||.|||.|||..||||:|:||||||||||||||||||||||
ATG3 human         51 PTWQWATGEELKVKAYLPTGKQFLVTKNVPCYKRCKQMEYSDELEAIIEE

Atg3 zebrafish   101 DDGDGGWVDTFHNSGVTGVTEAVREISLDNKDNMNMNVKTGACGNSGDDD
                     ||||||||||:||:|:||:||||:||:|:||||:.:...:..|   .:::
ATG3 human       101 DDGDGGWVDTYHNTGITGITEAVKEITLENKDNIRLQDCSALC---EEEE

Atg3 zebrafish   151 DDEEGEAADMEEYEESGLLETDDATLDTSKMADLSKTKAEAGGEDAILQT
                     |::|||||||||||||||||:|||||.|:.:..|.|.:||||||||||
ATG3 human       148 DEDEGEAADMEEYEESGLLETDEATLDTRKIVEACKAKTDAGGEDAILQT

Atg3 zebrafish   201 RTYDLYITYDKYYQTPRLWLFGYDEDRQPLTVDQMYEDISQDHVKKTVTI
                     ||||||||||||||||||||||||.|||||:.||||||||||||||||
ATG3 human       198 RTYDLYITYDKYYQTPRLWLFGYDEQRQPLTVEHMYEDISQDHVKKTVTI

Atg3 zebrafish   251 ENHPNLPPPAMCSVHPCRHAEVMKKIIETVAEGGGELGVHMYLLIFLKFV
                     ||||:||||.||||||||||||||||||||||||||||||||||||||||
ATG3 human       248 ENHPHLPPPPMCSVHPCRHAEVMKKIIETVAEGGGELGVHMYLLIFLKFV

Atg3 zebrafish   301 QAVIPTIEYDYTRHFTM    317
                     |||||||||||||||||
ATG3 human       298 QAVIPTIEYDYTRHFTM    314
```

B

Zebrafish Atg3 [ENSDARP00000041303.7]

Atg3 coding missing 10bp deletion= ATG3 predicted 10bp mutation protein sequence

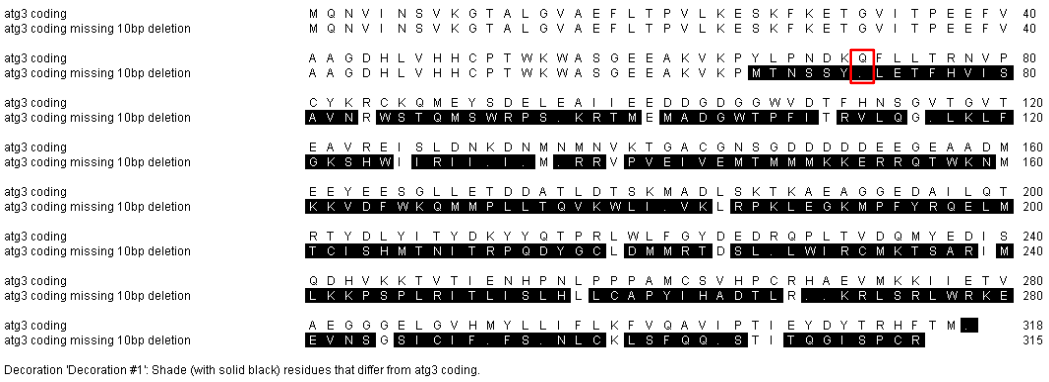

Decoration 'Decoration #1': Shade (with solid black) residues that differ from atg3 coding.

Figure 4.1 10bp deletion in *atg3* is predicted to code for truncated protein

A EMBL-EBI pairwise sequence alignment of zebrafish Atg3 protein against human ATG3 protein, showing the zebrafish protein has 83.6% identity to the human protein. **B** MegAlign protein alignment of zebrafish Atg3 against zebrafish ATG3 with 10bp mutation predicted sequence. Black shading indicates where the predicted mutation residues do not match the zebrafish atg3 residues. An early STOP, shown by a "." (red box), is predicted leading to a predicted protein of 71 amino acids.

A

Zebrafish Atg5 [ENSDARP00000124077.1] **80.9% identity**

Human ATG5 [ENSP00000358072.3]

```
Atg5 zebrafish     1 MIMADDKDVLRDVWFGRIPACFTLSPDETTEREAEPYYLLLPRVSYLTLV
                     |.|||||||||||||.||||..||.|||||||||||||||||||||
ATG5 human         1 --MTDDKDVLRDVWFGRIPTCFTLYQDEITEREAEPYYLLLPRVSYLTLV

Atg5 zebrafish    51 TDKVKKHFLKVMKAEDVEEMWFEHEGTPLKWHYPIGVLFDLHASNSALPW
                     ||||||||.|||:.||:.|:|||:||||||||||||:||||.||:|||||
ATG5 human         49 TDKVKKHFQKVMRQEDISEIWFEYEGTPLKWHYPIGLLFDLLASSSALPW

Atg5 zebrafish   101 NITVHFKNFPEQDLLHCSTNSVIEAHFMSCIKEADALKHKGQVINDMQKK
                     |||||||:|||:|||||.:...||||||||:|||||||||.||||:||||
ATG5 human         99 NITVHFKSFPEKDLLHCPSKDAIEAHFMSCMKEADALKHKSQVINEMQKK

Atg5 zebrafish   151 DHKQLWMGLQNDKFDQFWAMNRKLMEYPTEEGGFRYIPFRIYQTMSDRPF
                     ||||||||||||:||||||:||||||||.||.||||||||||||.::|||
ATG5 human       149 DHKQLWMGLQNDRFDQFWAINRKLMEYPAEENGFRYIPFRIYQTTTERPF

Atg5 zebrafish   201 IQTLFRPVSSEGQALTLGDLLKELFPAAI--EDEPKKFQVMIHGIEPLLE
                     ||.|||||:::||..||||||||:.|:||  ||..||.|||||||||:||
ATG5 human       199 IQKLFRPVAADGQLHTLGDLLKEVCPSAIDPEDGEKKNQVMIHGIEPMLE

Atg5 zebrafish   249 TPIQWLSEHLSHPDNFLHISIIPAPSD    275
                     ||:|||||||:||||||||||.|:|
ATG5 human       249 TPLQWLSEHLSYPDNFLHISIIPQPTD    275
```

B

Zebrafish Atg5 [ENSDARP00000124077.1]

Atg5 coding missing 23bp deletion= ATG3 predicted 23bp mutation protein sequence

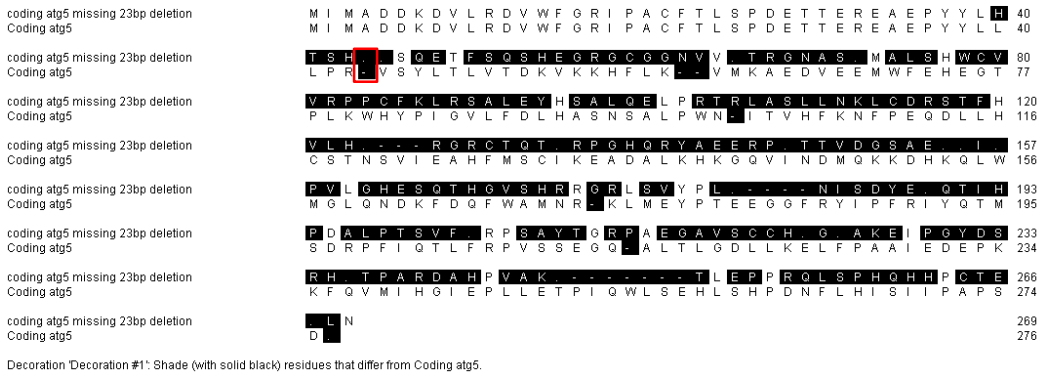

Figure 4.2 23bp deletion in *atg5* is predicted to code for truncated protein

A EMBL-EBI pairwise sequence alignment of zebrafish Atg5 protein against human ATG5 protein showing the zebrafish protein has 80.9% identity to the human protein. **B** MegAlign protein alignment of zebrafish Atg5 against zebrafish ATG5 with 23bp mutation predicted sequence. Black shading indicates where the predicted mutation residues do not match the zebrafish atg3 residues. An early STOP, shown by a "." (red box), is predicted leading to a predicted protein of 43 amino acids.

4.2.2 Optimising *atg3* genotyping

The *atg3* mutation causes a 10bp deletion. Previously established genotyping methods were unreliable so a new genotyping protocol was created. Primers were designed either side of the mutation site, leading to a total PCR product size of 245bp. Therefore the homozygous mutant would have a PCR product of 235bp, and heterozygous of both 245bp and 235bp. The PCR products were then run on a high percentage agarose gel (4%), to allow separation of the 10bp size. Examples of the PCR product band sizes expected for each genotype (Fig 4.3 A) were chosen for sequencing to determine if the band sizes were accurate in determining genotype. Sequencing data matched with expected band sizes for each genotype (Fig. 4.3 B). This genotyping protocol was used in following experiments. A genotyping protocol was previously established for the *atg5* mutation (PhD thesis Lambein, 2015), which was followed in this project.

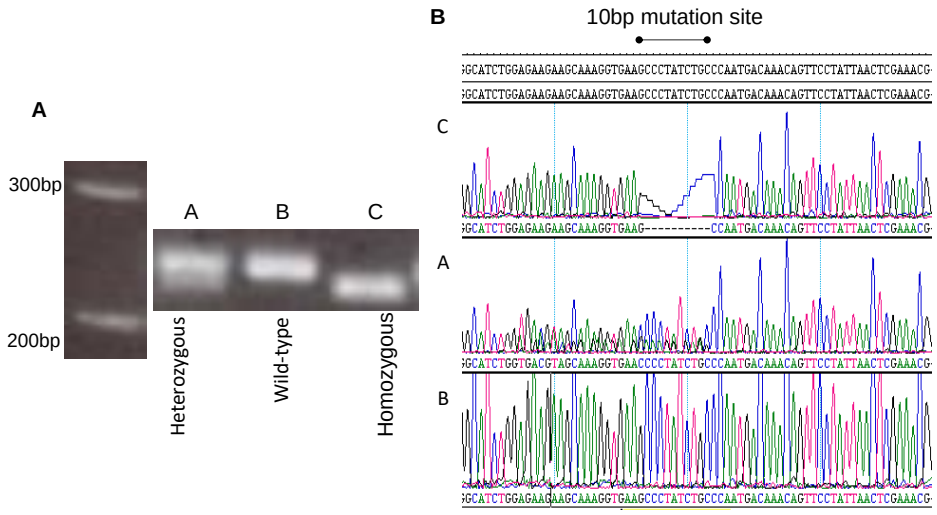

Figure 4.3 ***atg3*** **PCR genotyping correlates with sequencing**

A Expected band size for each genotype, 245bp as wild-type, and 235bp with the mutation present A-C is heterozygous, wild-type and homozygous **B** Corresponding sequencing data of the genotyped fish A-C, with the 10bp mutation site marked.

4.2.3 Survival of autophagy mutants

The survival of mutant fish was first investigated due to the noteworthy absence of adult homozygous fish resulting from the first raised heterozygous in-crosses, found for both *atg3* and *atg5* lines which had been raised to adulthood (Fig. 4.4 A). The survival of these fish had been monitored at 30dpf, before genotyping at 78dpf. Due to no change in survival from 30dpf until 78dpf, it was possible to conclude that no homozygous fish survived past 30dpf for *atg3* and *atg5* fish (Fig 4.4 B). Furthermore, the decrease in survival at 30dpf was greater than the expected normal loss rate of 15%, and was a further ~25% decreased, as shown in (Fig. 4.4 A), which suggests the homozygous fish did not survive as well as wild-type or heterozygous fish. Importantly, absence of homozygous adults suggests that both *atg3* and *atg5* are required for zebrafish survival. It was therefore necessary to determine how long, if at all, homozygous larvae are viable.

To confirm whether survival was reduced in homozygous mutants, survival of larvae from an in-cross of both *atg3*+/- or *atg5*+/- mutant fish was assessed at 5dpf to identify a potential additional reduction in survival of ~25% above expected death, perhaps due to the homozygous mutants dying according to Mendelian proportions (as indicated by the adult survival data). Survival of the *atg3* and *atg5* homozygous larvae until 5dpf does not show reduced survival more than normal expected loss (Fig. 4.4 C). This suggests that homozygous mutants are viable until 5dpf. To check *atg3* and *atg5* homozygous viability at 5dpf, fish were genotyped and grouped accordingly showing that homozygous mutants for both *atg3* and *atg5* are viable at 5dpf (Fig. 4.4 D), in addition they are present at Mendelian ratios. Homozygous survival at 5dpf and their absence by 30dpf suggests that homozygous fish lose viability between 5 and 30dpf.

Next, to compare larval survival between 5dpf and 30dpf, fish from either *atg3,* or *atg5,* in-crosses were placed into three groups, to be culled and genotyped at either 10, 20 or 30dpf. The comparison of the ratio of homozygous, heterozygous and wild-type siblings by genotype at these time points show a significant reduction in homozygous fish numbers over time for both *atg3* mutants from 20dpf (Fig. 4.4 E) and *atg5* mutants by 30dpf (Fig. 4.4 F), in comparison to expected Mendelian ratios while heterozygous survival is normal. Importantly, this decrease in survival may suggest that the autophagy genes which are missing are required for survival, but only at a later stage in development.

Interestingly, there are very rare viable *atg5* homozygous fish at 30dpf, indeed, only 2 viable homozygous adult fish have been found. In one case the *atg5*-/- fish has survived until at least 226 dpf, (at the time of writing). These fish may represent larvae

which have alternative genetic adaptations which enable survival past 30dpf, despite the loss of *atg5*.

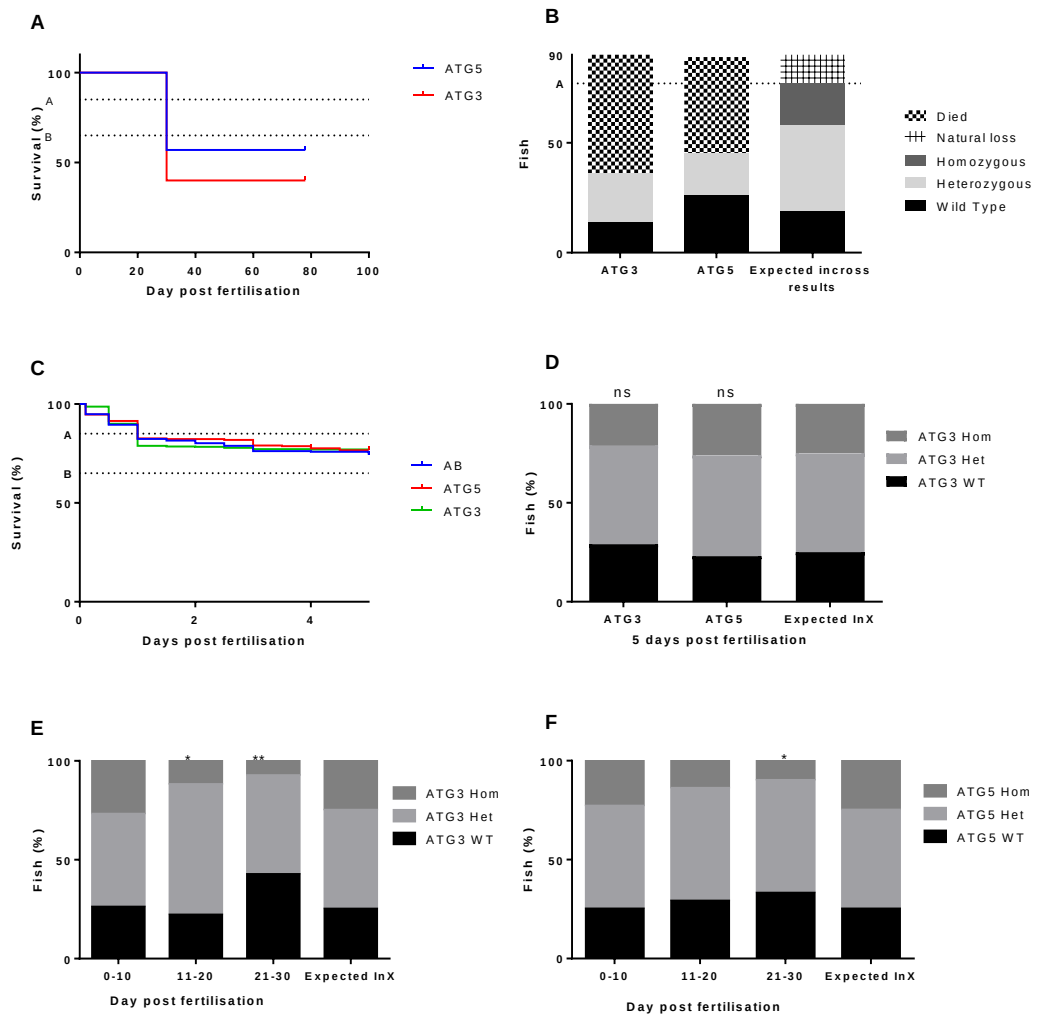

Figure 4.4 Autophagy mutant zebrafish have a survival defect

A Survival of 90 *atg3,* and 100 *atg5* larvae raised from heterozygous in-crosses. Line A represents normal expected loss, Line B represents a further 25% loss. **B** The genotype of raised fish of *atg3* and *atg5* mutants in comparison to expected in-cross (36 *atg3* larvae, and 45 *atg5* larvae). **C** Survival of *atg3*, *atg5* and AB wild-type larvae to 5dpf (n=3, 282 *atg3* and 1,430 *atg5* larvae). **D** Genotype of fish at 5dpf, where line A represents normal expected loss and line B represents a further 25% loss, (ns = no significant difference, Pearson's chi-squared test, n=3, 90 larvae for *atg3* and *atg5*). **E** Genotype of an ATG3 in-cross at three time points, 10, 20 and 30dpf, in comparison to the expected in-cross, (Pearson's chi-squared test, * $p<0.05$, ** $p<0.01$, n=3, 217 *atg3* larvae). **F** Genotype of an ATG5 in-cross at three time points, 10, 20 and 30dpf, in comparison to the expected in-cross, (Pearson's chi-squared test, * $p<0.05$, n=3, 221 *atg5* larvae).

The reduced survival of homozygous *atg3* and *atg5* mutant fish may be anticipated due to the essential roles of autophagy in cellular component re-cycling, development and cell homeostasis, so it is imperative to next determine whether these fish are truly deficient in autophagy and at what stage, in addition to investigating the cause of the mutant's death.

4.2.4 Maternal contribution of autophagy genes

Survival data suggests that in zebrafish, both *atg3* and *atg5* autophagy mutations are lethal, at a stage in development starting at 10-20dpf. Interestingly this is different to equivalent mouse models which are neonatal lethal (Kuma et al. 2004; Sou et al. 2008), and even further different from equivalent mouse models lacking maternal contribution which do not survive past the 4-8 cell stage (Tsukamoto et al. 2008). It therefore may be possible maternal contribution enables the viability of zebrafish homozygous mutants to a certain stage.

To determine whether maternal contribution of *atg3* and *atg5* mRNA occurs, larvae were grouped into developmental stages, total RNA was collected and cDNA was subsequently synthesised. This cDNA was then used for reverse transcription PCR analysis, where the occurrence of a PCR product indicates mRNA presence. Two sets of primers for each mutation were designed. One primer pair covered the site of the mutation, which would not be present in the homozygous mutants. The second primer pair was designed against a separate location in the each gene (*atg3* or *atg5*), distant from the mutation site. This pair was used as a control to ensure the collected mRNA and subsequently synthesised cDNA were good quality.

The first question addressed was whether maternal contribution occurs for both *atg3* and *atg5*. It is established that zebrafish zygotic transcription begins at ~3hpf (Kane & Kimmel 1993). Therefore, AB wild-type fish at very early developmental stages, before zygotic transcription begins, were used. The mRNA of *atg3* and *atg5* are both present from the one cell stage onwards, observed for both sets of primers (Fig 4.5 A-D), suggesting that both *atg3* and *atg5* mRNAs are maternally contributed. Presence of mRNA continues until 30dpf, showing that at no point during development mRNA is absent for these genes, with zygotic transcription starting before maternal mRNA is depleted.

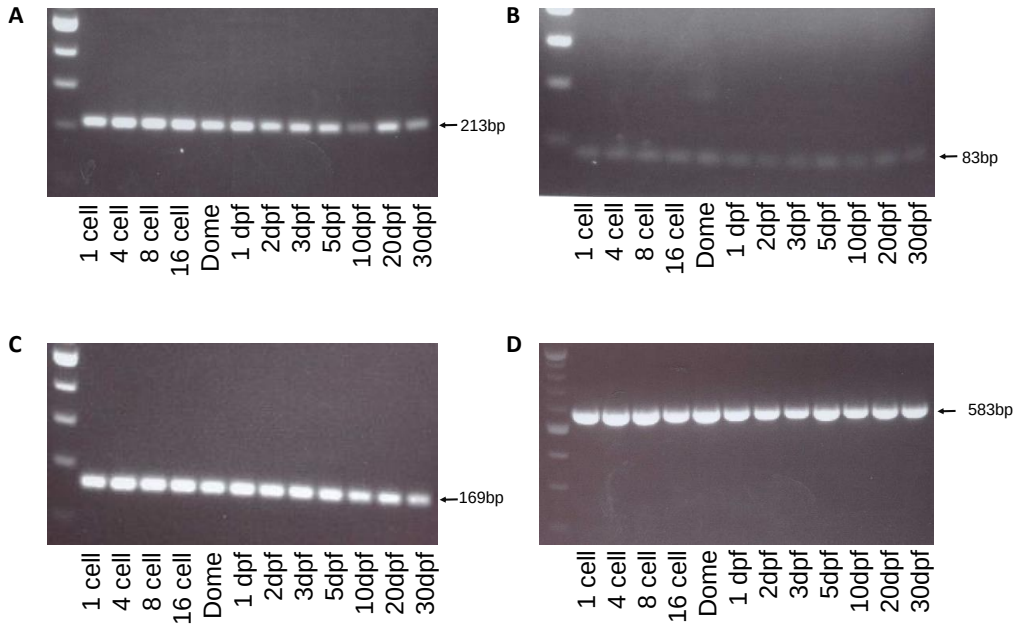

Figure 4.5 ***atg3*** **and** ***atg5*** **transcript is present in AB wild-types from the single cell stage**

Reverse transcription of cDNA synthesized from RNA extracted from AB wild-type fish at different ages, from 1 cell to 30dpf, ~20 larvae used for each time point for RNA extraction. **A** Reverse transcription of ATG3, using primers not at the mutation site. Correct expected band size of 213bp. **B** Reverse transcription of ATG5, using primers not at the mutation site. Correct expected band size of 83bp. **C** Reverse transcription of ATG3, using primers over the mutation site. Correct expected band size of 169bp. **D** Reverse transcription of ATG5, using primers over the mutation site. Correct expected band size of 583bp.

Zebrafish mutant lines were next examined to determine whether homozygous zebrafish experience the loss of *atg3* mRNA and *atg5* mRNA, after maternal contribution had ablated. The cDNA synthesised from RNA collected from homozygous mutants at 2, 5, 10, 20 and 30dpf was used for reverse transcription PCR analysis, with an AB wild-type 5dpf control used to ensure the PCR reaction worked. In addition, these experiments determine the age when wild-type maternal mRNA is lost. Wild-type mRNA for each gene is no longer present in homozygous mutants at 2dpf for *atg5* and 2dpf for *atg3* (Fig. 4.6 A, B). It therefore may be expected that deleterious survival effects of each mutation may become apparent after these ages in homozygous larvae, with the loss of ability to transcribe fresh protein from maternal mRNA. Survival data showing homozygous mutant survival is normal until 5dpf is consistent with this.

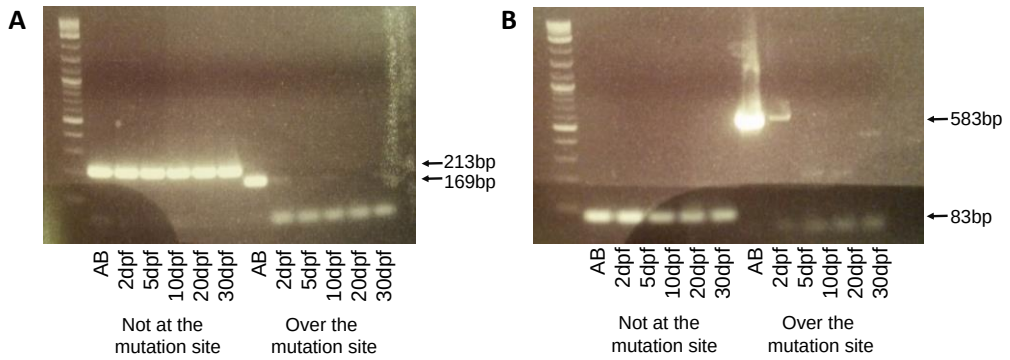

Figure 4.6 Transcript presence of *atg3* and *atg5* is lost in homozygous mutants

Reverse transcription of cDNA synthesized from RNA extracted from, ~10-20 larvae used for each time point **A** ATG3 homozygous fish, and **B** ATG5 homozygous fish, and control AB wild-type fish at different ages, from 2dpf to 30dpf. **A** Reverse transcription of ATG3, using primers not at the mutation site with correct expected band size of 213bp and primers over the mutation site with correct band size of 169bp. **B** Reverse transcription of ATG5, using primers not at the mutation site with a correct expected band size of 83bp and using primers over the mutation site with correct expected band size of 583bp.

4.2.5 Presence of Atg5 protein

The presence of Atg5 protein was examined to determine whether the *atg5* mutation was effective in resulting in loss of Atg5 protein, or produces a truncated and non-functional protein, as anticipated from expected mutation effects in Fig 4.2, above,

First, protein lysate from an *atg5* in-cross of wild-type siblings, heterozygous and homozygous fish at 8dpf was examined, a time-point chosen as a likely age that maternal contribution would have subsided. Atg5 protein was not present in the homozygous *atg5* fish (Fig. 4.7 A), indicating that by 8dpf homozygous fish are truly deficient of Atg5 protein.

Maternal mRNA is present at 2dpf in *atg5* null larvae. To determine whether maternally contributed mRNA transcribed by the zygote led to the presence of Atg5 protein, an earlier time-point of 2dpf was examined. At 2dpf Atg5 protein is present in the homozygous zebrafish (Fig. 4.7 B). Considering that maternally contributed mRNA is likely present at 2dpf (as suggested above in Fig 4.5 and 4.6), it is expected Atg5 protein is present at 2dpf in homozygous fish. The comparison of the presence of Atg5 protein at 8dpf and 2dpf demonstrate that the mutation is effective, with maternally encoded protein depleted by 8dpf, after maternal contribution has subsided. Taken together this protein analysis demonstrates that maternal contribution of Atg5 protein through synthesis of donated mRNA is concluded by 8dpf.

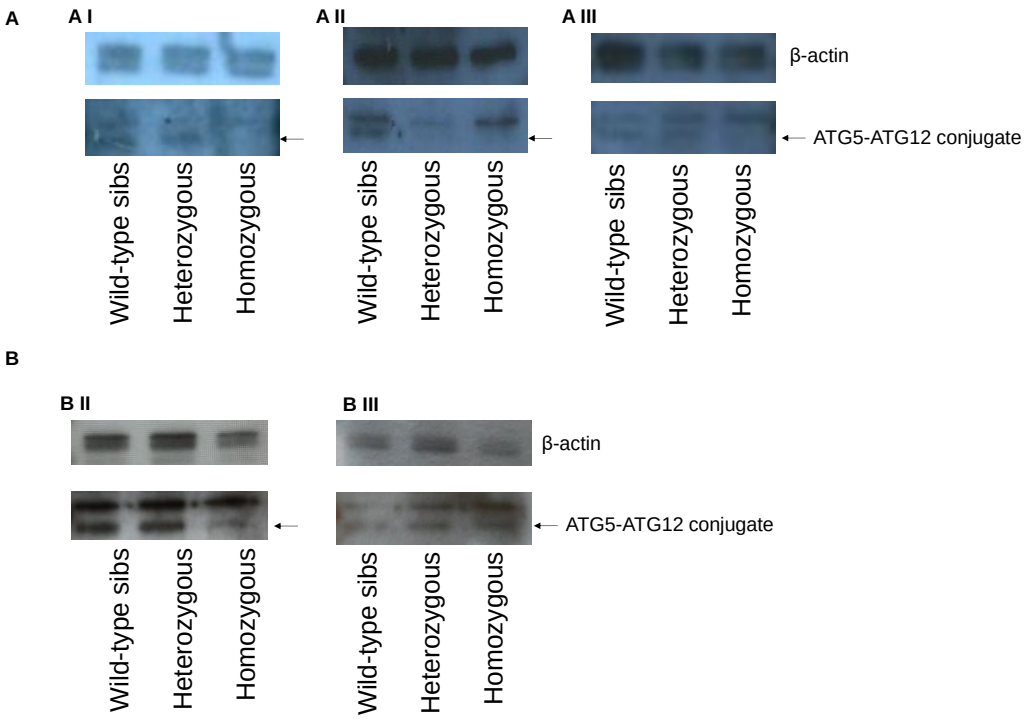

Figure 4.7 Atg5 protein is present at 2dpf, but lost at 8dpf

A ATG5 fish grouped by genotype at 8dpf, of three biological repeats AI-AIII. β-actin loading control and ATG5 antibody which recognises the ATG5-ATG12. **B** ATG5 fish grouped by genotype at 2dpf, with two biological repeats BI-BII. β-actin loading control and ATG5 antibody which recognises the ATG5-ATG12.

Unfortunately, there is currently no published antibody against *atg3* which works successfully on zebrafish lysate according to literature searches at the time of experimental work. Attempts using a human *atg3* antibody which was made against an antigen on the C-terminal of the protein, highly similar to the zebrafish protein, proved unsuccessful.

4.2.6 Measuring Lc3 levels in autophagy mutants

To determine if homozygous mutant fish have reduced autophagy function, Lc3 was chosen as a marker of functional autophagy machinery. Both *atg3* and *atg5* are involved in the production of Lc3-II from Lc3-I, it therefore might be expected that mutation of either *atg3* or *atg5* would reduce or stop Lc3-II production. Indeed, corresponding mouse models show a reduction in the presence of LC3-II (Kuma et al. 2004; Sou et al. 2008). Two methods of LC3-II detection were used; 1) imaging of mutant fish expressing “traffic-light Lc3” at 2dpf, and 2), western blot using fish lysate at a later age of 8dpf.

1. Traffic light Lc3 injections

The first method used to analyse autophagy function was through injection of “traffic-light” Lc3. The plasmid (pDEST395.CMV.ZFLc3.PolyA, a kind gift from Dr Angeleen Fleming and Dr Katherine Henry, pME(RFP.GFP.Lc3) was a kind gift from Dr Angeleen Fleming, Dr Katherine Henry performed the recombination reaction to produce pDest(CMV:RFP.GFP.Lc3) plasmid), containing Lc3 tagged with both GFP and RFP. The fluorescence of GFP is quenched in an acidic environment, which leads to a colour change with only RFP visible within the autolysosome or acidic vesicles. A change of GFP/RFP to RFP may be suggestive of fusion of autophagosomes with lysosomes, this colour change was used as a read-out of functional autophagy.

The plasmid was injected into a heterozygous in-cross of either *atg3* or *atg5* mutants at the one cell stage. Fish were then imaged after incubation overnight, with or without treatment of rapamycin and chloroquine. Rapamycin induces autophagy, whereas chloroquine blocks autophagosome maturation. This combination of drugs is commonly used to both induce autophagy and subsequently block autophagosome maturation, essentially trapping acidic vesicles from autophagic turnover. After imaging, fish were grouped according to genotype, after blinded analysis, whereby Lc3 associated vesicles, both GFP and RFP, were counted using ImageJ, to enable comparison of vesicle number.

First, in *atg3* fish not injected with the Lc3 construct as a control, neither RFP nor GFP vesicles were observed. In addition, this was consistent if the fish were pre-treated with rapamycin and chloroquine (Fig 4.8 A, B). For *atg3* larvae with construct injected, RFP vesicles were seen at a similar number in all genotypes. Furthermore, when pre-treated with rapamycin and chloroquine, no significant change in the number of RFP vesicles is observed (Fig 4.8 C). GFP vesicles observed in larvae in all *atg3* genotypes had a consistent number of vesicles (Fig. 4.8 D). No significant change in the number of *atg3* GFP vesicles in larvae treated with rapamycin and chloroquine was observed between any genotypes (Fig. 4.8 D).

Similarly, the *atg5* data show *atg5* fish not injected with the Lc3 construct have neither RFP nor GFP vesicles, and that this was observed with and without pre-treatment of rapamycin and chloroquine (Fig. 4.9 A, B). For *atg5* injected with the construct, RFP vesicles were seen at a similar number in wild-type, heterozygous and homozygous fish. For pre-treatment with rapamycin and chloroquine, no significant difference in the number of RFP vesicles are observed for all genotypes (Fig 4.9 C). *atg5* GFP vesicles in all genotypes were at a consistent number (Fig. 4.9 D), in agreement with this, *atg5* fish treated with rapamycin and chloroquine show similar numbers of GFP positive vesicles in all genotypes (Fig 4.9 D).

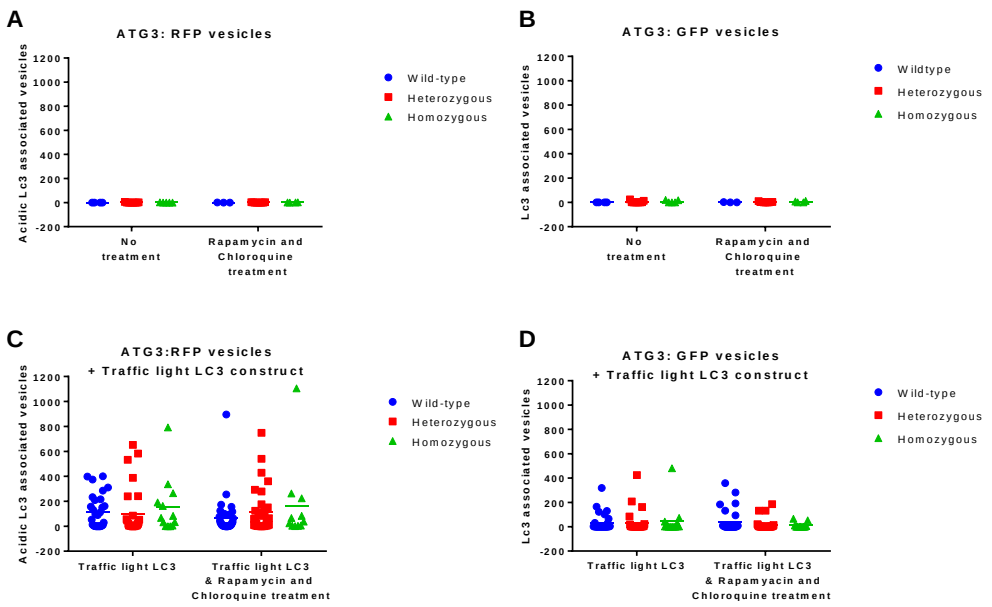

Figure 4.8 Lc3 vesicles are present in *atg3* mutants

A ATG3 fish with or without rapamycin and chloroquine treatment, grouped by genotype. Vesicles which were RFP positive were counted. (n=8, 73 larvae, not significant, Two-way ANOVA Tukey's test). **B** ATG3 fish with or without rapamycin and chloroquine treatment, grouped by genotype. Vesicles which were GFP positive were counted. (n=8, 73 larvae, not significant, Two-way ANOVA Tukey's test). **C** ATG3 fish which had been injected with a traffic light Lc3 construct, with or without rapamycin and chloroquine treatment, grouped by genotype. Vesicles which were RFP positive were counted. (n=8, 73 larvae with treatment, 77 larvae without treatment, not significant, Two-way ANOVA Tukey's test). **D** ATG3 fish which had been injected with a traffic light Lc3 construct, with or without rapamycin and chloroquine treatment, grouped by genotype. Vesicles which were GFP positive were counted. (n=8, 73 larvae with treatment, 77 larvae without treatment, not significant, Two-way ANOVA Tukey's test).

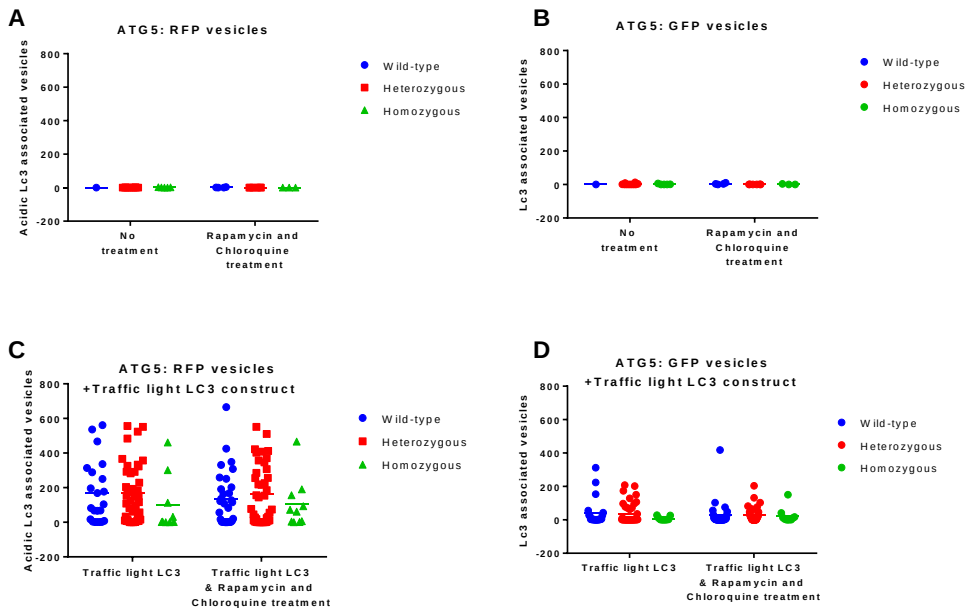

Figure 4.9 Lc3 vesicles are present in *atg5* mutants

A ATG5 fish with or without rapamycin and chloroquine treatment, grouped by genotype. Vesicles which were RFP positive were counted. (n=3, 16 larvae, not significant, Two-way ANOVA Tukey's test). **B** ATG5 fish with or without rapamycin and chloroquine treatment, grouped by genotype. Vesicles which were GFP positive were counted. (n=3, 13 larvae not significant, Two-way ANOVA Tukey's test). **C** ATG5 fish which had been injected with a traffic light Lc3 construct, with or without rapamycin and chloroquine treatment, grouped by genotype. Vesicles which were RFP positive were counted. (n=7, 71 larvae with treatment, 80 larvae without treatment, not significant, Two-way ANOVA Tukey's test). **D** ATG5 fish which had been injected with a traffic light Lc3 construct, with or without rapamycin and chloroquine treatment, grouped by genotype. Vesicles which were GFP positive were counted. (n=7, 71 larvae with treatment, 80 larvae without treatment, not significant, Two-way ANOVA Tukey's test).

I did not identify any differences between GFP or RFP vesicles between any genotype, with or without pre-treatment of autophagy enhancing and blocking drugs. Therefore, these traffic-light Lc3 DNA injection data suggest that Lc3 associated vesicles are formed to a similar extent in both *atg3* and *atg5* homozygous mutants as heterozygous and wild-type siblings, and suggests that Lc3-II is present within homozygous mutants at 2dpf. At 2dpf, a non-significant difference in autophagy function may be expected, due to the known presence of maternal mRNA and protein present in the larvae.

Analysis of RFP or GFP alone was completed to determine whether a complete loss of Lc3-II lipidation was observed in autophagy mutant larvae. To compare autophagic flux, the ratio of RFP (acidic) and GFP vesicles was compared. This is useful to determine whether autophagy is functional in comparison to analysis of RFP or GFP

vesicles alone, as it considers autophagic flux. As above rapamycin and chloroquine treatment was used to monitor autophagic flux. A higher ratio of RFP:GFP vesicles indicates that autophagy is functional, as most Lc3 associated vesicles have become acidic. On the other hand a low RFP:GFP ratio indicates that most Lc3 associated vesicles are not acidic and therefore suggests that autophagy is not functioning as expected. The RFP:GFP ratio was not-significantly different between *atg3* homozygous, heterozygous or wild-type siblings with or without rapamycin and chloroquine treatment (Fig 4.10 A). Similarly, no significant difference between the RFP:GFP ratio for *atg5* homozygous, heterozygous or wild-type siblings with or without rapamycin and chloroquine treatment (Fig 4.10 B). This may be caused by the young age of these larvae, which at 2dpf at the day of imaging still have maternally contributed mRNA which may enable normal autophagy function.

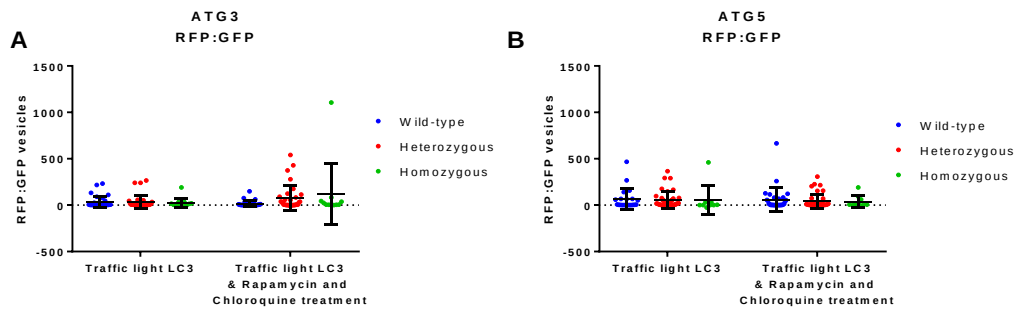

<u>Figure 4.10</u> The ratio of RFP to GFP Lc3 vesicles is not altered in *atg3* or *atg5* mutants

A *atg3* fish with or without rapamycin and chloroquine treatment, grouped by genotype. The ratio of RFP positive vesicles to GFP vesicles in individual fish was calculated (n=8, 73 larvae with treatment, 77 larvae without treatment, Two-way ANOVA (Tukey's test) not significant). **B** *atg5* fish with or without rapamycin and chloroquine treatment, grouped by genotype. The ratio of RFP positive vesicles to GFP vesicles in individual fish was calculated (n=7, 71 larvae with treatment, 80 larvae without treatment, Two-way ANOVA (Tukey's test) not significant).

2. Western blots:

Western blot analysis of Lc3-II was used to determine if mutant fish were deficient in autophagy at 8dpf. The 8dpf time point was chosen as an age where the maternal effects may be expected to have diminished and residual autophagy proteins depleted.

Micro fin-clipping (Wilkinson et al. 2013) of in-crosses of *atg3* and *atg5* lines at 5dpf enabled genotyping to be completed by 8dpf, where fish were grouped by genotype, either wild-type siblings, heterozygous or homozygous, and protein extracted. In

addition to these groups, wild-type AB controls with and without NH_4Cl treatment were used. NH_4Cl treatment blocks lysosomal fusion to autophagosomes through change in the pH of lysosomes and has been demonstrated to be effective on zebrafish (Hart & Young 1991), acting as a positive control of increased Lc3-II levels. Human embryonic kidney 293 (HEK293) cells were used as an additional control between human and zebrafish lysate.

Western blots with an LC3 antibody designed against human LC3 is expected to recognise both lipidated and non-lipidated forms of LC3. However, the antibody does not easily recognise zebrafish Lc3-I, but does identify Lc3-II. Confirmation that the zebrafish protein was Lc3-II rather than Lc3-I was highlighted by the use of human cell lysate, which does identify both LC3-I and LC3-II, with the LC3-II the same size at the zebrafish Lc3-II. To further confirm the zebrafish lysate Lc3-II band is truly the lipidated form, the NH_4Cl treated group have a larger band indicating an increase in Lc3-II levels. For these reasons, the lower band recognised by the antibody is likely to be Lc3-II. The loading control used was β-actin.

atg3 western blots, demonstrate that Lc3-II is present in homozygous mutants at 8dpf in three separate biological repeats (Fig. 4.11 A, B, C). Quantification to adjust for slightly unequal protein loading allowed calculation of the relative Lc3-II levels, showing that Lc3-II is on average increased in the *atg3* homozygous mutants in relation to the wild-type siblings and heterozygous larvae (Fig. 4.11 D). Similarly, *atg5* western blots, with an *atg5* in-cross grouped by genotype, demonstrate that Lc3-II is present in homozygous mutants at 8dpf, in three separate biological repeats (Fig. 4.11 E, F, G). Calculation of the relative Lc3-II levels show that Lc3-II is slightly increased in the *atg5* homozygous mutants, in relation to the wild-type siblings and heterozygous larvae (Fig. 4.11 H), but to a lesser extent than *atg3* homozygous larvae.

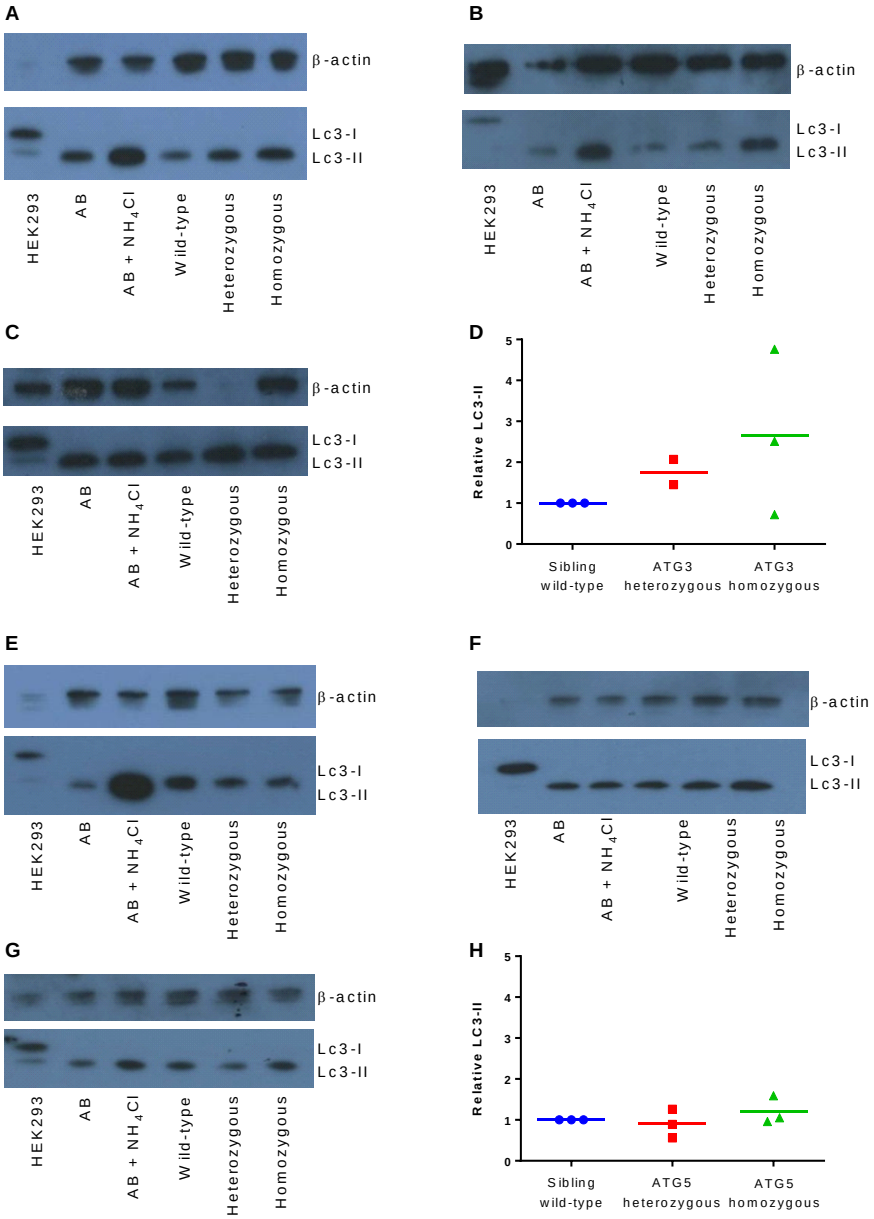

Figure 4.11 Lc3-II is present in *atg3* and *atg5* mutants

A-C Three biological repeats of ATG3 western blots using β-actin as a loading control and LC3 antibody to detect fish Lc3-II. **D** Relative Lc3-II levels in ATG3 heterozygous and homozygous larvae, compared to wild-type siblings and accounting for un-equal loading. **E-G** Three biological repeats of ATG5 western blots using β-actin as a loading control and Lc3 antibody to detect fish Lc3-II. **H** Relative Lc3-II levels in ATG5 heterozygous and homozygous larvae, compared to wild-type siblings and accounting for un-equal loading.

Despite either an *atg3* or *atg5* mutation being present, Lc3-II presence in the 8dpf zebrafish western blots, regardless of genotype, raised an interesting question of the mechanism of lipidation of Lc3. According to recent literature, and importantly corresponding mutant mouse models, Lc3 would not be expected to be lipidated

without these core autophagic components (Kuma et al. 2004; Sou et al. 2008). However, an increase in Lc3-II levels can be due to an increase in Lc3-II synthesis, or be due to reduced autophagic turnover. For this reason, autophagy enhancing and blocking drugs were used to assess autophagic flux.

4.2.7 Autophagic turnover of Lc3-II in zebrafish mutants

It is unexpected that Lc3-II levels would be the same or increased in homozygous fish at 8dpf, a time when Atg3 or Atg5 protein is expected to be depleted. Autophagy components are degraded in the process of autophagy, meaning that autophagic flux must be considered. Double treatment with rapamycin and chloroquine enable autophagic flux to be examined. Rapamycin acts to induce and therefore increase autophagy, whereas chloroquine blocks lysosomal fusion, acting to block autophagy. It would be expected that a fish able to produce more Lc3-II (wild-type) would have more Lc3-II than fish unable to produce more Lc3-II (homozygous) in treatment conditions. To see if this holds true in terms of Lc3-II protein in fish, Lc3 western blots were performed with or without rapamycin and chloroquine treatment in all genotype groups (Fig 4.12).

Levels of Lc3-II in *atg3* fish showed a slight reduction in Lc3-II levels in wild-type and heterozygous fish with rapamycin and chloroquine treatment than without, whereas a small increase in Lc3-II levels were seen for homozygous treated fish (Fig 4.12 A-D). This supports that Lc3-II is present in *atg3* homozygous fish. Of note, the wild-type and heterozygous Lc3-II levels did not increase as expected with drugs treatment. This may suggest autophagic turnover is occurring, which is not observed for homozygous larvae, suggestive that autophagy function is impaired in *atg3* null mutants.

In *atg5* fish, Lc3-II was slightly increased following rapamycin and chloroquine treatment in all genotypes (Fig. 4.12 E-H). This provides further evidence that *atg5* homozygous fish have Lc3-II present. Again, wild-type and heterozygous fish did not have an increase in Lc3-II levels as expected in two repeats, but a large increase was seen for one repeat in each genotype, but not seen in homozygous fish. High variability is hard to explain, but may suggest that *atg5* homozygous fish have defects in regulation of autophagy.

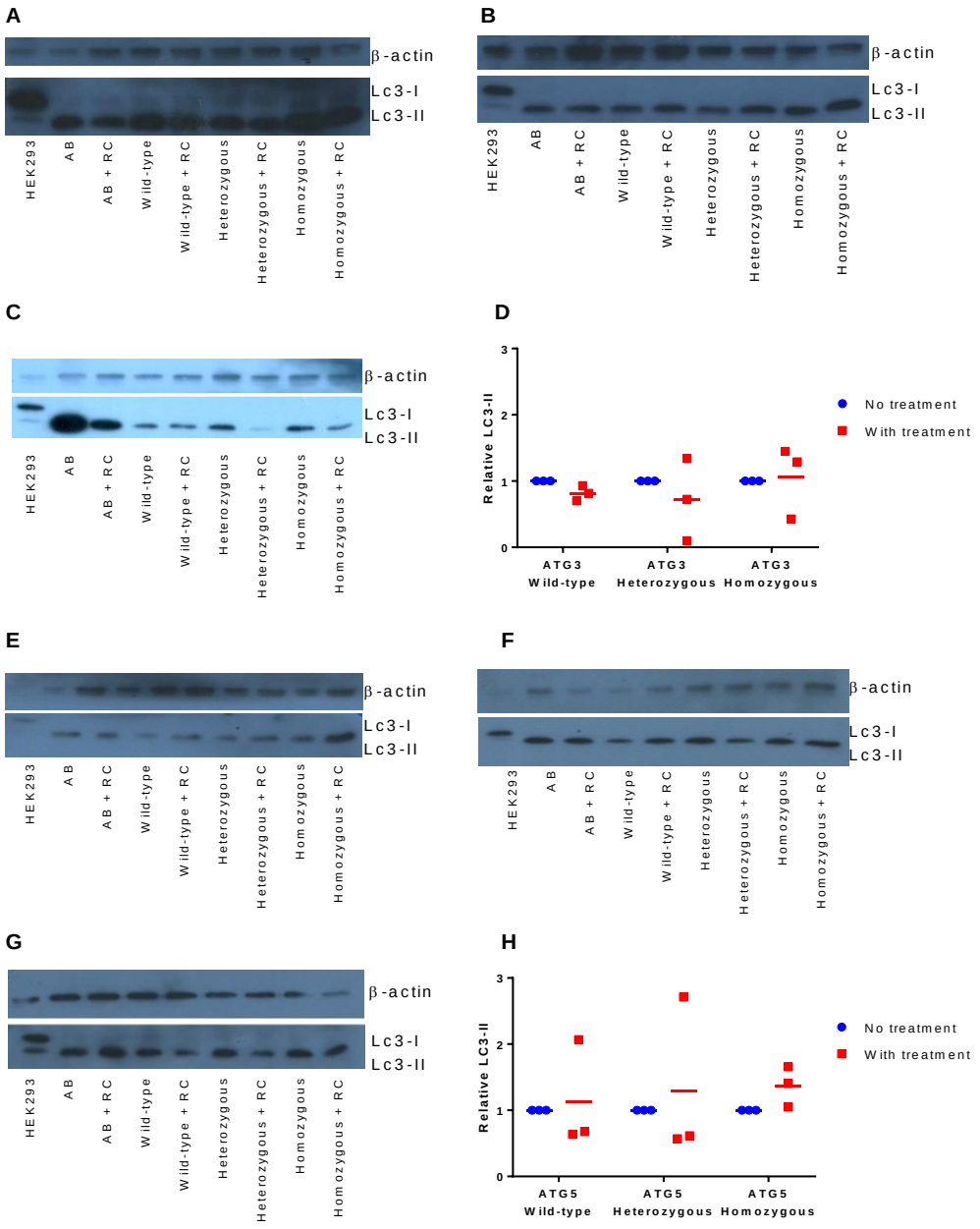

Figure 4.12 Lc3-II is present in *atg3* and *atg5* mutants following autophagy induction

RC: rapamycin and chloroquine treated **A-C** Three biological repeats of ATG3 western blots using β-actin as a loading control and LC3 antibody to detect fish Lc3-II **D** Relative Lc3-II levels in ATG3 heterozygous and homozygous larvae, compared to corresponding genotype without RC treatment, and accounting for un-equal loading. **E-G** Three biological repeats of ATG5 western blots using β-actin as a loading control and LC3 antibody to detect fish Lc3-II. **H** Relative Lc3-II levels in ATG5 heterozygous and homozygous larvae, compared to corresponding genotype without RC treatment, and accounting for un-equal loading.

4.2.8 Phenotype analysis of autophagy mutant fish

Observations of a substantial survival defect in *atg3* and *atg5* homozygous mutants indicate that each autophagy mutation has a significant effect on zebrafish health. Furthermore, for *atg5* mutants, the lack of Atg5 protein is likely responsible for this increased mortality. Further characterisation of the autophagy mutants was undertaken with the aim to ascertain the cause of death for homozygous mutants.

Firstly, the size of zebrafish was used as an indicator of the ability of the zebrafish to grow normally in addition to ability to feed, due to the comparable mouse autophagy mutant models which display a suckling defect. Furthermore, size may also be an indication of the ability of the zebrafish to recycle cellular components, if homozygous fish were able to feed normally. Zebrafish were measured at time points, 2dpf, 5dpf, 10dpf, 20dpf and 30dpf, and subsequently genotyped and grouped. Importantly data was collected in IMCB in Singapore, and some in Sheffield, UK. The aquarium at IMCB is thought to have a higher pathogenic load in comparison to Sheffield University (Dr Claire Allen, personal communication), so data is represented separately.

Data collected at IMCB, which represent single groups of larvae raised in individual tanks highlight a clear size defect at 30dpf in *atg3* and *atg5* homozygous mutants (Fig. 4.13 and Fig. 4.14 respectively), but no significant difference in size at 2dpf, 5dpf, 10dpf or 20dpf. Heterozygous mutants do not have a reduced size at any time point, in keeping with their normal survival data. Furthermore, these data further support the homozygous survival defect through lack of viable mutants, as shown through reduced homozygous numbers available to study, from time points 10dpf and later. In order to consider growth over time, the average size of larvae, grouped by genotype at each time point is shown in Figure 4.13 F and Figure 4.14 F, for *atg3* and *atg5* respectively. Growth appears to be at matching rates for homozygous mutants, wild-type siblings and heterozygous mutants until 10dpf, where growth appears to arrest for homozygous mutants only.

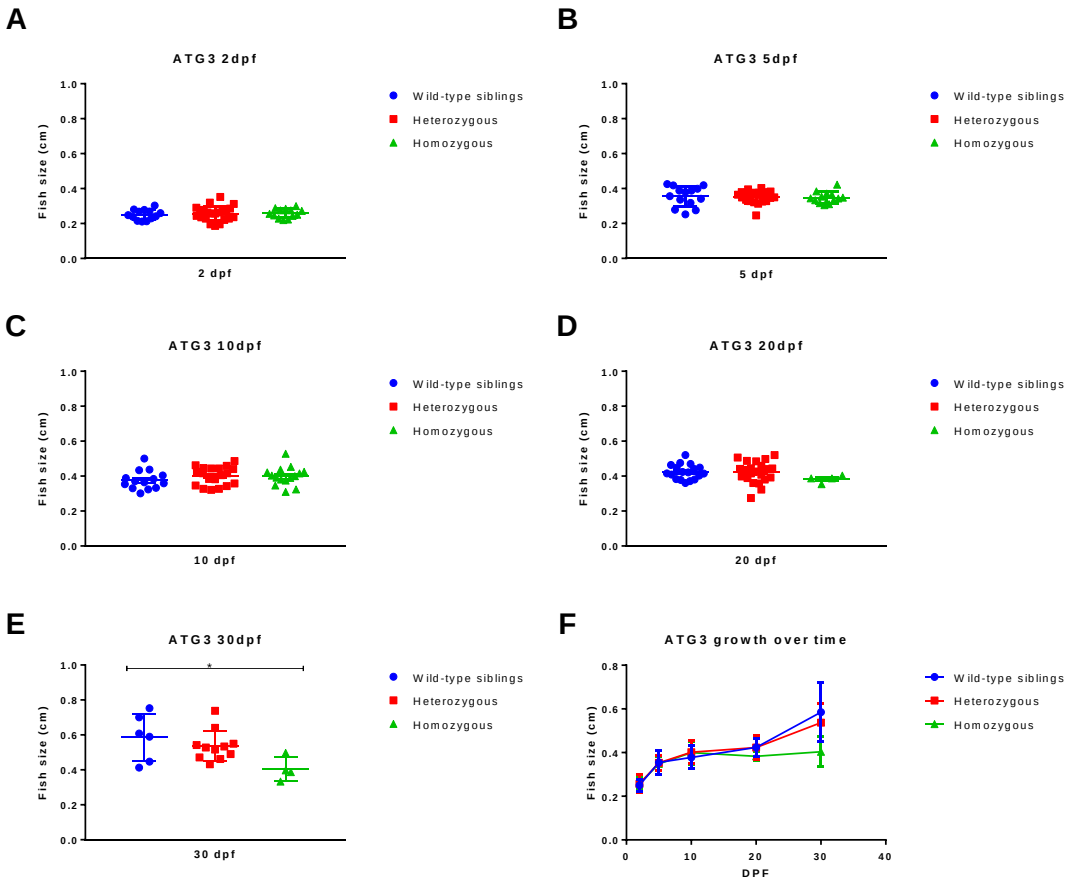

<u>Figure 4.13</u> Autophagy *atg3* mutant zebrafish have a reduced size

The size of individual zebrafish larvae grouped by ATG3 genotype at different time points: **A** 2dpf (48 larvae), **B** 5dpf (48 larvae), **C** 10dpf (48 larvae), **D** 20dpf (47 larvae), **E** 30dpf (21 larvae), (Data collected in Singapore, n=1, Mann-Whitney T-test *p<0.05, error bars +/-SD). **F** Average size of zebrafish grouped by genotype over time (Data collected in Singapore, n=1, error bars +/- SD).

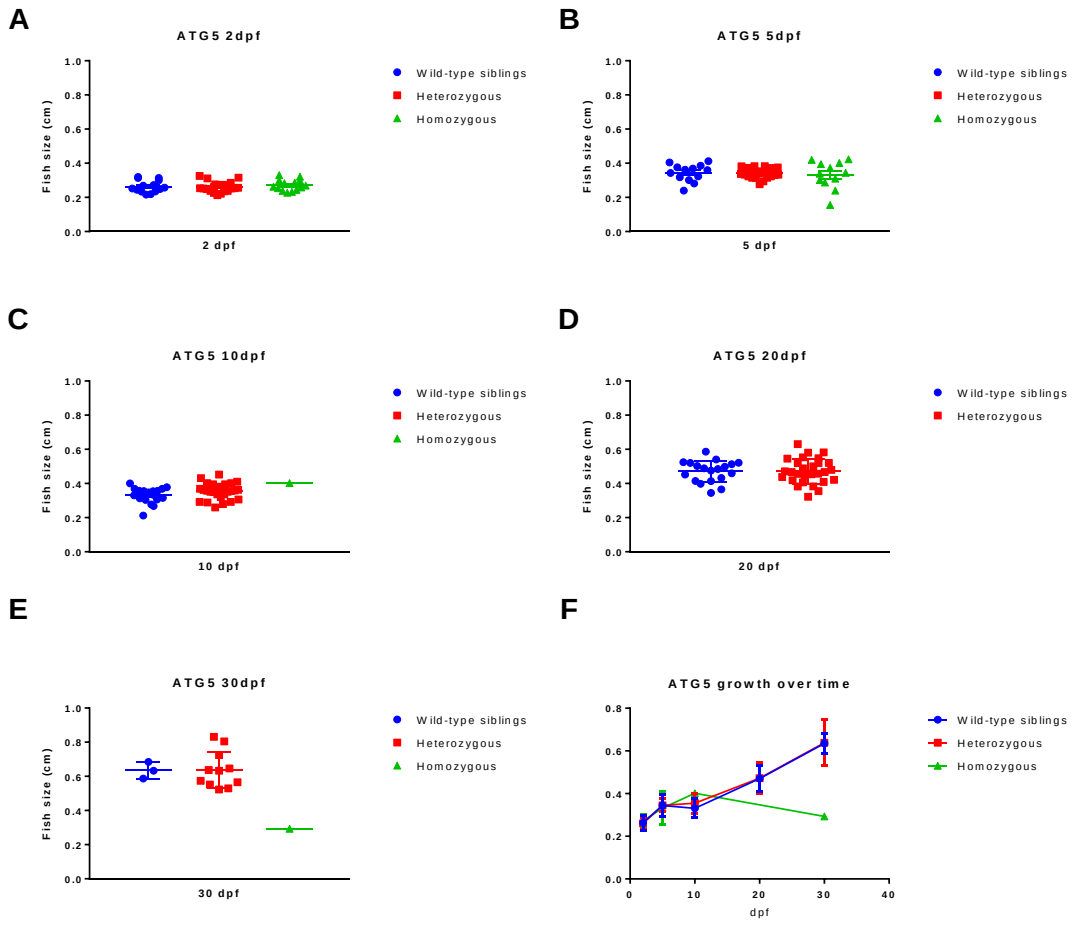

Figure 4.14 Autophagy *atg5* mutant zebrafish have a reduced size

The size of individual zebrafish larvae grouped by ATG3 genotype at different time points: **A** 2dpf (48 larvae), **B** 5dpf (48 larvae), **C** 10dpf (48 larvae), **D** 20dpf (47 larvae), **E** 30dpf (15 larvae), (Data collected in Singapore, n=1, Mann-Whitney T-test, ns, error bars +/-SD). **F** Average size of zebrafish grouped by genotype over time (Data collected in Singapore, n=1, error bars +/- SD).

In direct comparison to these data collected in IMCB, Singapore, are the size of autophagy mutants housed in Sheffield University's Aquarium (Fig. 4.15 and 4.16). These data represent three tanks containing 30 larvae raised until 10, 20 or 30dpf when size was measured, at or under 5dpf were not raised in tanks.

A clear size reduction is observed at 30dpf for *atg3* mutants in comparison to wild-type siblings, which is not apparent at 2, 5, 10 or 20 dpf (Fig. 4.15). On the other hand, *atg5* mutants have significantly reduced size at 20 and 30dpf, but not at 2, 5, or 10 dpf (Fig. 4.16). For both *atg3* and *atg5* heterozygous larvae no change in size is seen at any age.

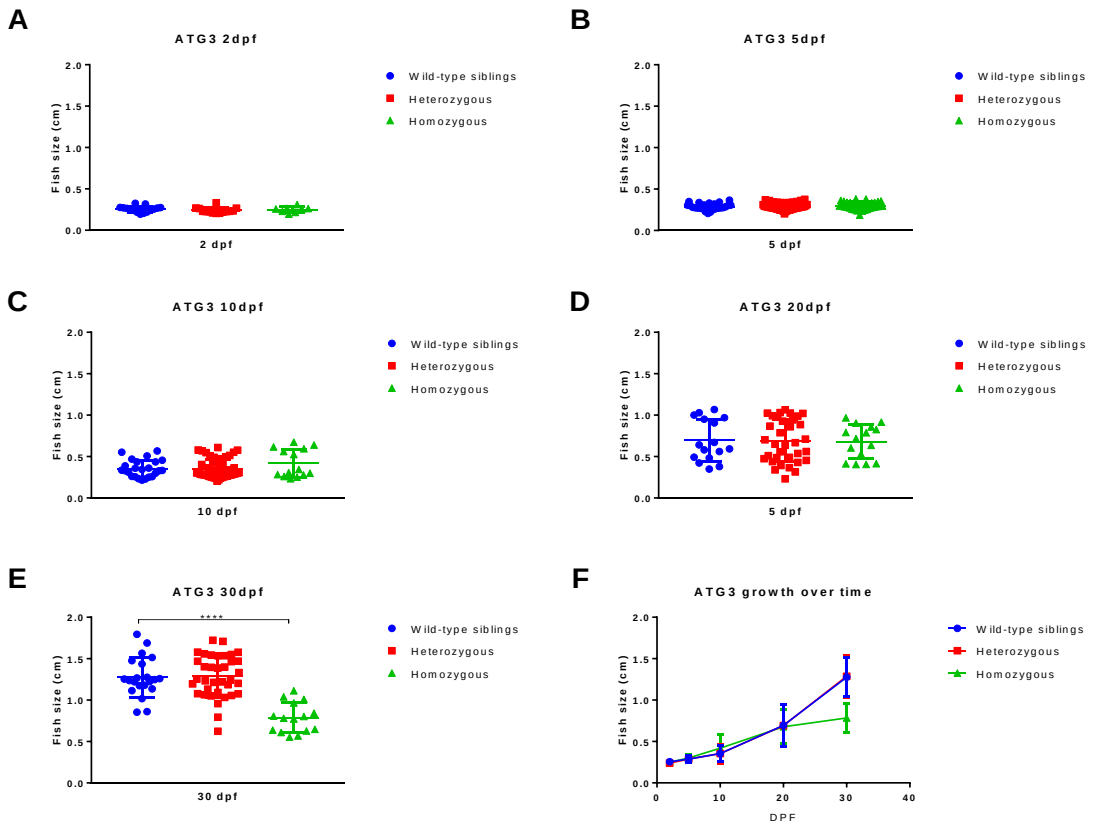

Figure 4.15 Autophagy *atg3* mutant zebrafish have a reduced size

The size of individual zebrafish larvae grouped by ATG3 genotype at different time points: **A** 2dpf (37 larvae), **B** 5dpf (126 larvae), **C** 10dpf (86 larvae), **D** 20dpf (65 larvae), **E** 30dpf (72 larvae), (Data collected at the University of Sheffield, n=3, Mann-Whitney T-test ****p<0.0001, error bars +/-SD). **F** Average size of zebrafish grouped by genotype over time (Data collected at the University of Sheffield, n=3).

Growth curves differ from larvae grown in IMCB in that for both *atg3* and *atg5* homozygous mutant's growth appears to match heterozygous and wild-type sibling growth until 20dpf, where growth becomes reduced (Fig. 4.15 F and Fig 4.16 F respectively). This change in growth is delayed in comparison to IMCB grown larvae which match growth only until 10dpf (Fig. 4.13 F and Fig. 4.14 F), for *atg3* and *atg5* respectively. This may represent a better environment for larvae growth at the University of Sheffield. Reduced size of homozygous fish from 10dpf, or 20dpf onwards is indicative of a lack of nutrients available for the fish to grow. This could be due to a lack of ability to recycle nutrients, or a feeding defect.

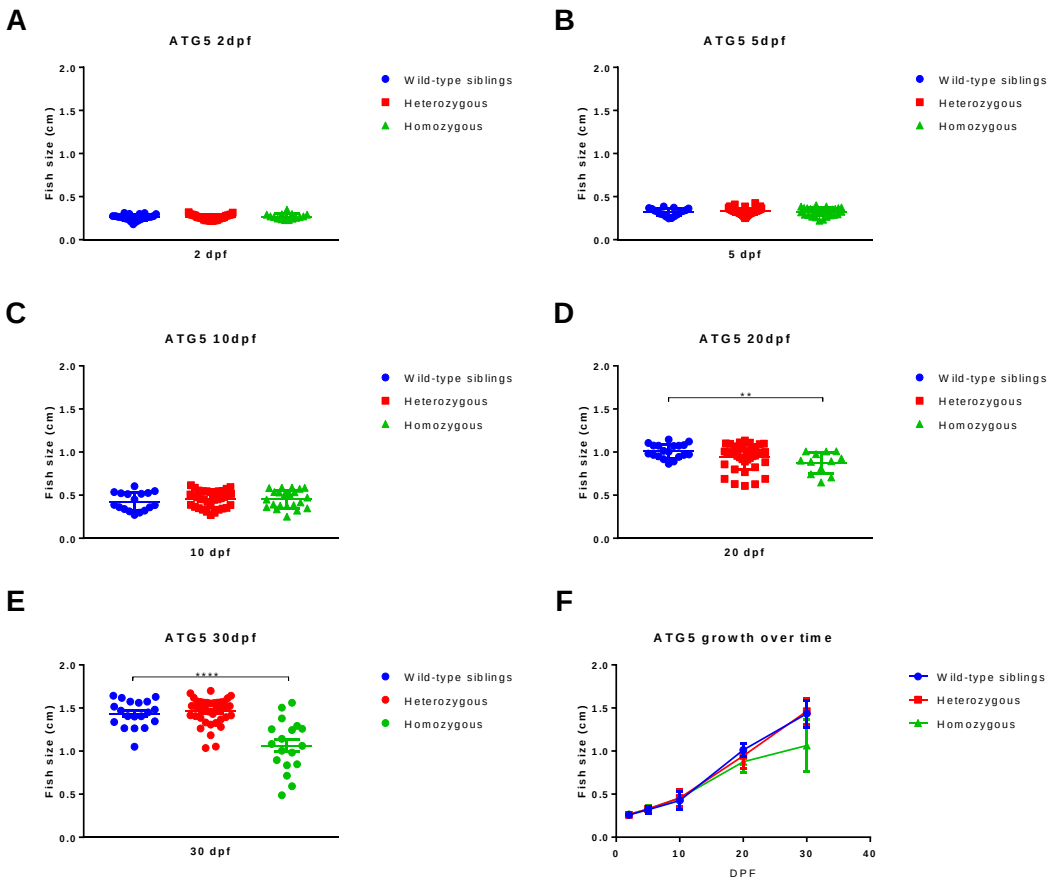

Figure 4.16 Autophagy *atg5* mutant zebrafish have a reduced size

The size of individual zebrafish larvae grouped by ATG5 genotype at different time points: **A** 2dpf (64 larvae), **B** 5dpf (111 larvae), **C** 10dpf (74 larvae), **D** 20dpf (71 larvae), **E** 30dpf (77 larvae), (Data collected at the University of Sheffield, n=3, Mann-Whitney T-test, **p<0.01, ****p<0.0001, error bars +/-SD). **F** Average size of zebrafish grouped by genotype over time (Data collected at the University of Sheffield, n=3).

The ability of zebrafish to feed would be expected to lead to a nutrient deficit which could be responsible for the inability of the zebrafish to grow normally. This may be an expected outcome of both *atg3* and *atg5* mutations, due to *Atg5* deficient mice which have a suckling defect (Kuma et al. 2004). Feeding was monitored at 15, 20, 25 and 30dpf at the Sheffield University. These time points were chosen as an age where larvae are fed a mixture of small dried food (a mix of Gemma 75 and Zebrafeed 100-200), and the larger sized live *Artemia* (brine shrimp) which are red. Importantly, larvae must have a properly developed mouth to hunt and eat *Artemia*. It is possible to directly observe if zebrafish are eating normally by observing whether any red colour from the *Artemia* are seen within the larvae's digestive system. For both *atg3* and *atg5* heterozygous in-crosses, at all time points, 100% of zebrafish were observed to have

eaten paramecia. As all fish were able to feed normally, this suggests that homozygous fish are able to feed normally, and therefore, any size difference is likely not caused by an inability to feed.

The potential that a lack of nutrients available for growth, potentially caused by the autophagy mutation, was next considered. A study on autophagy in zebrafish development using morpholinos suggested that cardiac tissue in zebrafish is lacking in amino acids (Lee et al. 2014), and this is suggested to be caused by a reduction in recycling of cellular components for which both *atg3* and *atg5* are required. To determine if the heart muscle was functioning normally in the larvae, the autophagy mutant lines were each crossed to the neutrophil specific traffic light Lc3 line, which includes a fluorescent GFP heart marker. Time-lapse imaging of the hearts of non-anesthetised fish at time points at 2dpf and 5dpf were analysed. After analysis, fish were genotyped and grouped.

The heart rate was not significantly different between homozygous, heterozygous or wild-type sibling *atg3* larvae at 2dpf (Fig 4.17 A) or at 5dpf (Fig 4.17 B). Similarly, there was no significant difference between *atg5* larvae of any genotype at 2dpf (Fig 4.18 A), or at 5dpf (Fig 4.18 B). This suggests that cardiac tissue at 2 and 5dpf in *atg3* and *atg5* mutants is functioning normally, and therefore does not suggest cardiac tissue is lacking amino acids. It would be useful to monitor the heart rate of larvae at later stages in development, for example after maternally contribution effects subside, unfortunately time restrictions did not allow for this.

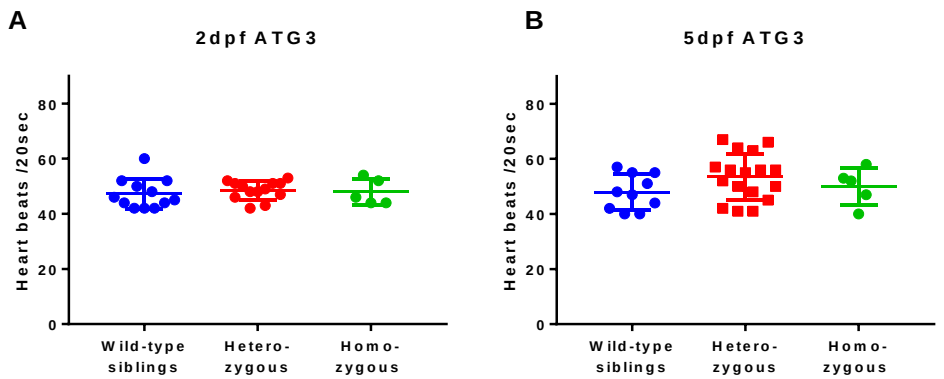

Figure 4.17 Autophagy *atg3* mutant heart rate is not changed

The heart beats (per 20 seconds) of individual zebrafish larvae grouped by *atg3* genotype at different time points: **A** 2dpf (n=3, 30 larvae, One-way ANOVA test (Kruskal-Wallis test), not-significant error bars +/-SD)., **B** 5dpf, (n=2, 32 larvae, One-way ANOVA test (Kruskal-Wallis test), not-significant error bars +/-SD).

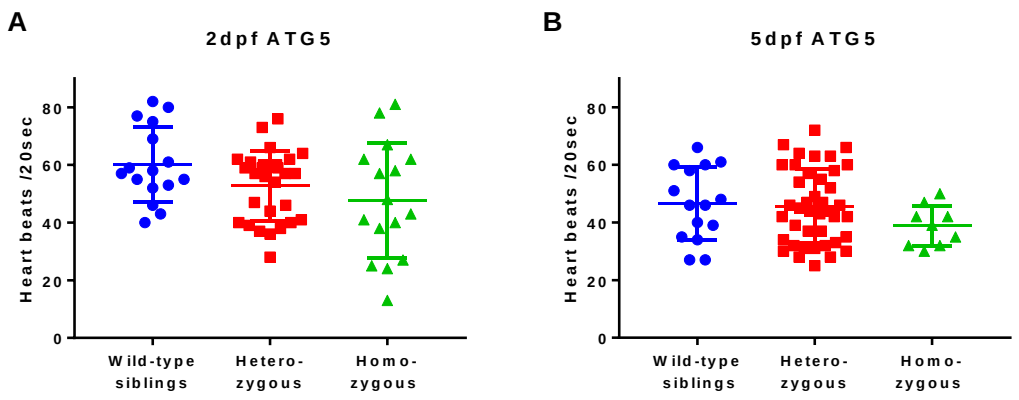

Figure 4.18 Autophagy *atg5* mutant heart rate is not changed

The heart beats (per 20 seconds) of individual zebrafish larvae grouped by *atg3* genotype at different time points: **A** 2dpf (n=4, 60 larvae, One-way ANOVA test (Kruskal-Wallis test), not-significant error bars +/-SD)., **B** 5dpf, (n=5, 65 larvae, One-way ANOVA test (Kruskal-Wallis test), not-significant error bars +/-SD).

4.2.9 Effect of starvation on survival of mutant fish

The survival defect in *atg3-/-* and *atg5-/-* mutant fish, in addition to the reduction in growth shown above, indicates that both zebrafish lines may have impaired autophagy, despite Lc3-II presence until at least 8dpf. Since *atg3-/-* and *atg5-/-* mouse models are lethal in the neonatal period, the corresponding fish models may be expected to cause death at an earlier stage than 30dpf. An explanation for this could be the difference in immediate starvation conditions experienced by the different models throughout development. Being mammals, mice risk immediate starvation after birth, which is usually avoided by suckling. In *atg5* deficient mice this immediate starvation, combined with a mutation-dependent suckling defect, places pressure on the autophagy pathway to provide essential nutrients (Kuma et al. 2004). Interestingly, even when the mouse mutants are force fed, to overcome the suckling defect, survival is only extended by a maximum of 25 hours (Kuma et al. 2004). In comparison, zebrafish do not experience starvation until 7dpf due to the presence of the yolk (Jardine & Litvak 2003). In addition, it might be that fish may not require autophagy so intensely due to a lower metabolic rate (van de Pol et al. 2017). For these reasons, the effect of withholding food from autophagy mutants may increase the demand on autophagy and therefore enhance the effect of the mutation on zebrafish survival.

Food was withheld from larvae from fertilisation to a maximum of 20dpf, where larvae would be expected to experience starvation from ~7-11dpf, when the yolk as a food source is fully depleted (animal work completed in Singapore was completed under the Institutional Animal Care and Use Committee (IACUC) guidelines, under locally ethically approved IACUC protocol number 140977). Dead larvae were collected and genotyped. In all cases, larvae did not survive beyond 16dpf (Fig. 4.19 A, B). Survival of larvae from the *atg3* heterozygous in-cross was not significantly different between wild-type siblings, heterozygous or homozygous larvae (Fig. 4.19 A). Survival of larvae from an *atg5* heterozygous in-cross was not significantly different in homozygous offspring compared to wild-type siblings and heterozygous fish, although more death events occurred ~4/5 days earlier than *atg3* mutants, primarily in *atg5* homozygous larvae (Fig. 4.19 B). These data suggest a defect in autophagy in *atg5* mutants, since *atg5* homozygous fish have earlier deaths under starvation conditions.

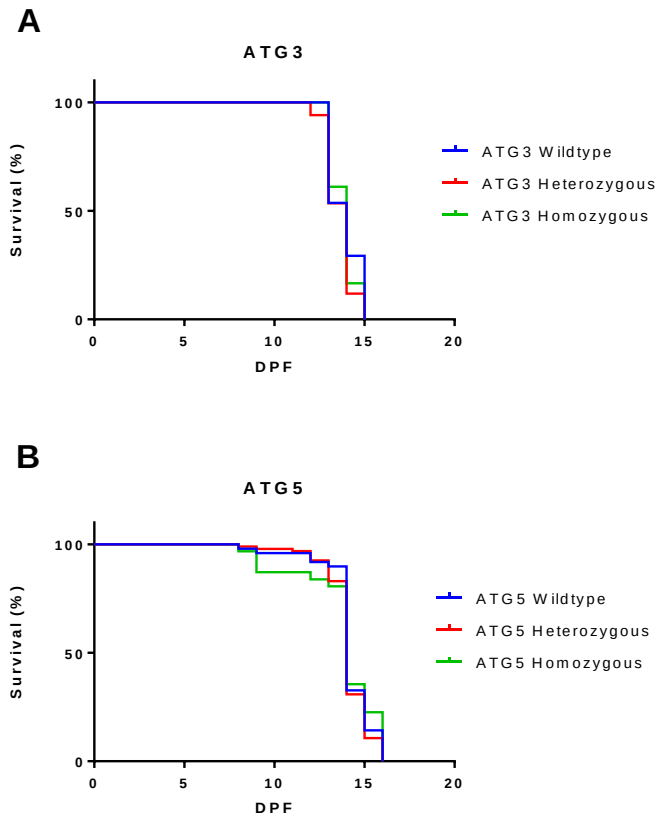

Figure 4.19 Autophagy mutant zebrafish survival under starvation conditions is not reduced

A Survival of *atg3* zebrafish grouped by genotype, food withheld (n=3, 178 larvae, no significance Log-Rank Mantel-Cox). **B** Survival of *atg5* zebrafish grouped by genotype, food withheld (n=3, 174 larvae, no significance Log-Rank Mantel-Cox). Completed at IMCB in Singapore.

4.2.10 Summary of characterisation of autophagy mutant zebrafish

Autophagy mutant fish show a clear survival defect. The cause of this defect may be a lack of available nutrients, as suggested by the reduction in homozygous mutant survival at 20dpf and reduced size in mutants after 20dpf. Indeed this is supported by earlier death of mutant larvae under starvation conditions, a traditional inducer of autophagy. However, Lc3-II, a marker of autophagosomes, is present in both autophagy mutants at 8dpf, indicating lipidation of Lc3, and perhaps some types of autophagy, are still functional in the homozygous mutants.

4.3 Discussion

4.3.1 Phenotype of autophagy mutants

The first aim of this chapter was to define any phenotype exhibited by autophagy mutant larvae. Determining that *atg3* and *atg5* homozygous mutants did not survive until adulthood highlights a severe survival defect. Indeed, further characterisation demonstrated that *atg3* and *atg5* homozygous mutants have significantly reduced survival by 20 and 30dpf respectively. Heterozygous fish for both *atg3* and *atg5* larvae survival matched wild-type survival. Corresponding murine autophagy deficient mice represent well studied, *in vivo* animal models, useful in comparison of potential phenotypes. Heterozygous mouse survival of each mutation was also normal (Kuma et al. 2004; Sou et al. 2008), indicating that a single allele of each gene is sufficient for autophagic requirements in both zebrafish and mice.

In zebrafish a clear survival phenotype is demonstrated, in that *atg3* and *atg5* homozygous fish are not able to survive as long as wild-type siblings, and suggests both mutations have delayed deleterious effects. A survival defect has also been demonstrated in *atg3* deficiency in *D. melanogaster*, where RNAi was used to block *atg3* function leading to a shorter lifespan (Tóth et al. 2008), indicating autophagy is important in animal survival. Interestingly, mutant survival in zebrafish (and in *atg3* deficient drosophila) survival is quite different to the corresponding *atg3* and *atg5* mouse mutants which are lethal earlier, in the neonatal period (Kuma et al. 2004; Sou et al. 2008). A potential explanation for the different timeframes of mortality in mouse and zebrafish models could be caused by differences in autophagy requirements during murine and zebrafish development. Alternatively, a significant lung defect is described for *atg5* deficient mice, which causes increased alveolar epithelial cell thickness which may present a barrier to gas exchange (Cheong et al. 2014). It is possible inefficient gas exchange in the lung could cause or contribute to an earlier death of murine autophagy mutants. Furthermore, the *atg5* deficient mice neonatal

death is rescued when *atg5* is expressed in neurons, indicating that the cause of death in mice may be caused by neuronal dysfunction (Yoshii et al. 2016).

The severe *atg3* or *atg5* homozygous survival defect is statistically significant by 20 or 30dpf respectively. Interestingly, expected mendelian ratios occur for both *atg3* and *atg5* heterozygous in-crosses, which concurs with corresponding mouse models (Kuma et al. 2004; Sou et al. 2008). Survival of homozygous larvae appears to be normal until 5-10dpf. It may be likely for both murine and zebrafish models that animal survival, until autophagy is under stress, is made possible through maternal contribution. In both *atg3* and *atg5* mutants wild-type coding mRNA (with no mutation) is present until at least 2dpf. For *atg5*-/- larvae, Atg5 protein was present at 2dpf. These data suggest maternal contribution enables functional protein production, and it would therefore be expected that autophagy could function normally.

In exception to this, two homozygous *atg5* mutants have been able to survive much later than other *atg5*-/- larvae, one until 226 dpf (at the time of writing). Interestingly, a single *atg5* deficient mouse was able to survive longer than most atg5 null mice, (9 days rather than 1). These rare animals suggest that genetic adaptations can occur which enable survival further than is otherwise possible. It would be interesting to study these animals to determine whether other autophagy-related genes are up-regulated which may compensate for a loss in *atg5.*

Mammals, including mice, after birth undergo immediate starvation, which may place autophagy, required to recycle nutrients needed in starvation conditions, under immediate pressure until feeding. Using GFP-LC3 reporter mice, it was determined that autophagy is used to a very low extent in the embryo, however within 30 minutes of birth the neonates have a massive up-regulation of autophagy, determined through huge up-regulation of GFP-LC3 “dots” only present in the mice after birth, rather than during the embryonic period (Kuma et al. 2004). It was then demonstrated that autophagy is responsible for providing amino acids (but not other potential nutrients such as blood glucose), through comparison of plasma level of amino acids in wild-type and *atg5* deficient mice, which were significantly reduced in autophagy deficient mice (Kuma et al. 2004). A reduction in amino acids has also been demonstrated in *atg3* and *atg7* deficient mice in a similar manner (Sou et al. 2008; Komatsu et al. 2005). Therefore, autophagy is key in providing amino acids in murine neonates throughout the immediate starvation experienced after birth.

On the other hand, zebrafish have a yolk-food source which is used as a food source until 5dpf when the larvae can begin to feed, although the yolk may supplement alternative food sources until 7dpf (Jardine & Litvak 2003). Zebrafish also have a lower

metabolic rate than mammals, primarily due to the fact that mammals must use comparatively much more energy to generate heat and for movement, whereas zebrafish do not need to generate heat, and swimming requires less energy (van de Pol et al. 2017). The yolk food source, and lower metabolic rate, may stop the immediate starvation and pressure on the autophagic system in zebrafish, which the *atg3*-/- and atg5-/- mice experience.

To test whether differences in growth are caused by a potential lack of nutrients caused by autophagy deficiency, particularly after ~7-11dpf when the yolk food source is depleted, the size of homozygous, heterozygous and wild-type siblings was measured.

For both *atg3* and *atg5* homozygous mutants at ages of 2dpf, 5dpf and 10dpf there was no significant difference in size in comparison to heterozygous and wild-type siblings. Data collected in IMCB in Singapore suggests that at 20dpf a reduction in size is seen for *atg3* homozygous mutants, and by 30dpf this is significantly reduced. A reduction in size is also seen for *atg5* homozygous larvae at 30dpf. The lack of viable homozygous fish at these later time points led to fewer data points for collection, but further highlights the homozygous survival defect. These data suggest that homozygous mutants are not able to grow normally, with growth affected after 10dpf, in line with yolk depletion. It is therefore tempting to suggest that growth is reduced due to a lack of cellular recycling through autophagy. Size analysis of autophagy mutants at The University of Sheffield highlighted a significant reduction in size at 30dpf for *atg3* homozygous larvae, and at 20 and 30dpf for *atg5* larvae. These data suggest that size is not reduced until after 20dpf, later than found at IMCB, Singapore.

Of note, there are some discrepancies in the size data collected in each aquariums used at IMCB in Singapore and at The University of Sheffield (TUOS) in the UK. Firstly, more homozygous mutants are viable at the 20dpf and 30dpf time points at TUOS in comparison to IMCB, suggesting improved survival of homozygous fish. Further supporting this, the size difference appears to be more pronounced at IMCB, with all homozygous fish at the 20 and 30dpf being smaller sized. At TUOS, there are some homozygous fish present at these later time points which are not clearly smaller in size. Improved survival and increased size of homozygous mutants could be caused by differences between the aquaria. In IMCB, there is potentially a higher pathogenic load in the water, with pathogen *Pseudoloma neurophilia* known to be present (Mohd Agus Bin Abdul Raman, personal communication). It is difficult to confirm whether pathogen load is different between aquaria, but any differences in pathogen load and the microflora may have an unknown impact on the development of the survival/growth phenotype. The presence of more pathogens may put increased pressure on fish, and

perhaps both autophagy homozygous fish are less able to deal with these pathogens, therefore highlighting size and survival defects to a greater degree than TUOS.

An explanation of why homozygous fish are smaller in size is a potential feeding defect. In fact, the corresponding *Atg5* autophagy mouse models have a suckling defect, which if force fed, does increase the lifespan of the mice for several hours (Kuma et al. 2004). This does suggest that a lack of nutrients is at least in part responsible for the murine neonatal deaths. It therefore could be possible that in zebrafish a feeding defect may also be present. To determine whether homozygous autophagy mutants had a feeding defect, paramecia which are red in colour, was observed in the digestive system by eye. In all cases all fish were seen to have eaten paramecia, irrespective of size and genotype. If all fish were able to eat paramecia, it is unlikely there is a feeding defect. However, to be sure this is true, further quantification is needed. In this case, the fact that all fish actively hunt and eat paramecia is very suggestive that feeding is normal.

A further consideration for differences in larval growth is the type of food which is available. In IMCB (Singapore) the larvae are provided with Zeigler larval (AHAB, USA) that ranges from 150 micron to 250 micron from 5-30dpf. In comparison TOUS aquarium fed larvae a mixture of small dried food from 50-100 microns (a mix of Gemma 75 and Zebrafeed 100-200), and the larger sized live *Artemia* (brine shrimp) in the same age range. It could be possible that the different availability of food offers different nutritional value, and leads to different growth rates, and perhaps improved growth in seen under the TOUS feeding regime. Further analysis of the growth rates according to feeding regime would be required to confirm this.

The survival and growth defects which appear to become important after the yolk food source is depleted are suggestive that after 10dpf, both *atg3* and *atg5* mutations become deleterious, perhaps due to lack of nutrients. For zebrafish, a feeding defect can likely be excluded, after visually determining that all fish are able to feed normally. To determine whether a lack of nutrients may be affecting cardiac tissue and therefore causing death in zebrafish, heart function was next studied.

Morpholino data show that *atg5* knockdown in zebrafish leads to defects in cardiac tissue development, and later, reduced survival (Lee et al. 2014). Furthermore, *atg5*-/- mice have defect in heart beat which is likely caused by a lack of available amino acids, presumably resulting from underprovided autophagy. In fact in wild-type mice, cardiac tissue was shown to increase autophagy use massively after birth (Kuma et al. 2004; Lee et al. 2014). It was therefore hypothesised that cardiac function may be changed in homozygous mutants, and this may be a cause of early death.

Heart function was studied by imaging a heterozygous in-cross of each autophagy mutant, which had previously been crossed to the traffic light Lc3 neutrophil line, which has a fluorescent heart marker. After imaging, heart rates were compared between genotype. At 2 and 5dpf, both *atg3* and *atg5* homozygous heart rates were not different in comparison to wild-type and heterozygous fish. Unfortunately, due to time restraints heart rates were not monitored at later time points. Although these data suggest that a cardiac defect is not caused by each *atg3* or *atg5* mutations, study at later time points is required, as maternal contribution, (shown here to be present in each mutant) may enable normal autophagy, amino acid production and ultimately survival until a later time point. Furthermore, analysis of the amino acid content of the blood plasma in autophagy mutants may by an important experiment to reveal whether zebrafish deficient in *atg3* or *atg5* lack have reduced amino acids, and whether this is turn could lead to a cardiac problems.

To further implicate the autophagy mutations as responsible for the survival defects and reduced growth, the autophagic system was put under additional pressure through larval starvation conditions. Fish survival was monitored until 20dpf, with starvation expected to start by 7-11dpf when the yolk is depleted. The maximum survival seen was 16dpf regardless of genotype. A significant reduction in survival was not seen for *atg3* or *atg5* homozygous mutants, however *atg5* homozygous fish did exhibit earlier death ~4/5 days before most deaths at 16dpf. Of note earlier *atg5* homozygous deaths were observed in each of the three repeats, it may be likely further analysis may lead to statistical significance. This may suggest that *atg5* is important for extended survival under starvation conditions. In non-suckling conditions *atg5*+/+ mice had significantly longer survival in comparison to *atg5*-/- which suggests that autophagy is important in providing nutrients under starvation conditions. As starvation is a common autophagy stressor which appears to enhance the survival defect, these data suggest the zebrafish *atg5* mutation is reducing autophagy perhaps leading to a lack of amino acids and subsequent death, although further analysis of nutrients (amino acids) available would be required to prove this hypothesis.

Additionally, a*tg5* independent autophagy is functional without LC3 lipidation (Nishida et al. 2009), which could occur in both *atg3* and *atg5* mutants, indicating that autophagy can be accomplished by alternative pathways. Atg5 independent autophagy may be essential to provide nutrients for larvae when classical autophagy is unable to. It would be very interesting to specifically target Atg5 independent autophagy in larval development to order to determine whether nutrients are provided through this pathway.

To conclude, both *atg3* and *atg5* homozygous mutants exhibit a clear survival defect. This survival defect may be caused by a lack of nutrients, normally made available via autophagy, leading to growth and cardiac defect which ultimately cause death. In fact, a clear growth defect is observed for both mutants, which is likely not caused by feeding defects. Furthermore, stressing autophagy through starvation appeared to enhance the survival defect in *atg5* homozygous larvae, associating lack of nutrients as a cause of the survival defect. However further analysis, focussing on amino acid availability, and cardiac function would be extremely useful for future investigation.

4.3.2 Autophagy mutation effects at the transcriptional and translational level

The second aim of this chapter was to determine whether *atg3* and *atg5* autophagy mutant fish are deficient in Atg3 or Atg5 protein respectively. The mutations expected effects were first analysed, predicting that both deletion mutations cause an early translation stop, leading to truncated and non-functional proteins.

The predicted Atg3-/- protein size was 71 amino acids in length, significantly shorter than the usual 317 amino acid protein. For the atg5-/-, the predicted protein size was 43 amino acids, also significantly shorter than the 275 normally translated. In both cases a large majority of the protein is predicted to be missing, leading to the deduction that the severely truncated protein would be non-functional. As an obvious example, the *atg5* mutation would lead to the loss of lysine 130 (Ohsumi et al. 1998), which is crucial for the conjugation of *atg5* to *atg12*, and required for autophagy. Furthermore, degradation of non-functional, miss-folded protein occurs under normal conditions, and this may remove any truncated protein which may be produced. For these reasons, the predicted mutation effects are likely to lead to missing, or non-functional proteins.

mRNA which has premature STOP codons are targeted for degradation through nonsense mediated decay (Wittkopp et al. 2009). This will reduce the amount of mRNA present in the mutant fish available for translation and reduces the likelihood that truncated protein will be translated from mutant mRNA. However, there is some debate on how efficient nonsense mediated decay is in zebrafish. Although all key genes required for non-sense mediated decay are present in zebrafish (Wittkopp et al. 2009). To determine whether mRNA either containing the deletion sites (wild-type), or missing the deletion sites (mutant) is present in both *atg3* and *atg5* mutants, the presence of mRNA (with or without the deletion site) was compared. Equally, this analysis enabled to comparison of maternally contributed mRNA, which would not contain the mutation site.

Firstly, wild-type fish were shown to have both expression of both *atg3* and *atg5* mRNA from the single cell stage, with no lapse in presence at any time point until at least 30dpf. Presence of *atg3* and *atg5* genes at the very early stages in development show that each gene is maternally contributed, considering that zygotic transcription does not start until ~3hpf (Kane & Kimmel 1993). The homozygous mutants were analysed using two pairs of primers, one over the mutation site and one away from the mutation site, with the aim to see a PCR product for primers only away from the mutation site. This is to determine whether "wild-type" maternal mRNA is present in the mutants. Indeed, for *atg3* and *atg5* homozygous larvae the presence of maternal mRNA is lost by 5dpf. Interestingly, the presence of mRNA containing the mutation is present at all ages, indicating that nonsense mediated decay is not effectively removing all the mRNA containing early translational stop in both *atg3* and *atg5* mutants, additionally agreeing with the suggestion that zebrafish nonsense mediated decay is not efficient.

It is important to note that the primers which were designed to cover the mutation site do not detect a loss of transcript, since the primers would not be able to bind due missing sequence (the missing mutation site). It is therefore likely that "mutant" cDNA is present in these larvae, which is also observed using the primer pair away from the mutation site. However these data do suggest wild-type cDNA (containing the mutation site) is not present in the homozygous larvae after 5dpf, (see appendix 3 for primer location on *atg3* and *atg5* cDNA sequences). It would be useful in the future to use additional primer binding sites, e.g. before, overlapping the mutation site (in addition to covering and after) the mutation site to enable improved understanding of what transcripts are present.

Maternal contribution may reduce deleterious effects through enabling normal Atg3 or Atg5 production until at least 2 dpf. This may partially explain why both corresponding mouse and zebrafish models survive past embryogenesis, since both models have maternal contribution. In a murine model it was demonstrated that an oocyte deficient in *atg5,* fertilised with *atg5*-/- sperm did not survive past the 4-8 cell stage (Tsukamoto et al. 2008). In this case maternally contributed *atg5* was not present, and clearly highlights that autophagy is important at very early stages in development, and specifically requires *atg5*. However, the lack of "wild-type" mRNA does not mean that protein, previously transcribed from maternally contributed mRNA is also absent, the protein may be long lived, and therefore provide longer lasting functional autophagy.

Unfortunately, an antibody which can recognise zebrafish Atg3 has not been described and my attempts at using an *ATG3* antibody raised against human protein were unsuccessful. Despite an antibody being unavailable for Atg3, it may be likely that due to the similar survival and size defects observed, in addition to only having a mutated

copy of mRNA after 2dpf, that protein is may not be present at 8dpf, as shown for *atg5*-/- larvae. To fully prove that the *atg3* mutation results in the loss of Atg3 protein, this would be a key experiment to complete in future.

The antibody used for the *atg5* western blots was made against the first 50 residues of the human ATG5 protein. Whilst the zebrafish protein has 81% identify to the human protein, for the first 50 residues, the expected mutation effect would lead to discrepancies by the 39th residue, with an expected STOP by the 43rd. This means that the antibody might not recognise any truncated protein produced. However, the wild-type full-length protein (determined by size) is shown to be recognised in the *atg5* western blots. If the mutation was not effective in stopping production of full length *atg5*, this protein would still be present at later stages. For this reason, the data showing Atg5 protein absence at 8dpf suggests that the *atg5* mutation is effective in causing a loss of Atg5 protein production.

The ATG5 antibody used recognised the ATG5-ATG12 complex, rather than ATG5 alone. This is because the ATG5-ATG12 complex contains a stable covalent bond, which is not broken during SDS-PAGE. Therefore, any free Atg5 should be recognised by the antibody, however, a band was not observed at the correct Atg5 size, suggesting in zebrafish *in vivo*, Atg5 is predominantly in complex with ATG12. In fact, free Atg5 (the full length form which can conjugate to ATG12) is not highly present in comparison to the ATG5-ATG12 complex, or a truncated Atg5 (used in apoptosis) during zebrafish development (Hu et al. 2011). It was suggested that Atg5 protein self-regulates *atg5* expression only when Atg5 protein levels are low, (Hu et al. 2011), and therefore Atg5 is likely to be in the complex rather than free in the cell. Ultimately, if Atg5 is not present, it cannot be found in complex with Atg12 either, and therefore using the Atg5-Atg12 complex as a marker for whether Atg5 is present is valid. Using this human ATG5 antibody, the presence of Atg5 protein was compared between *atg5* wild-type sibling, heterozygous and homozygous fish at 8dpf. The age of 8dpf was chosen as an age that any maternal contribution effects would have subsided. Indeed, at 8dpf it was shown that Atg5 protein was lost in homozygous mutants. It can be concluded that *atg5* homozygous fish are deficient in Atg5 protein by 8dpf.

The role of maternally contributed mRNA makes dissecting the mutation's deleterious effects difficult. I have shown that before 5dpf, maternally contributed mRNA is present in *atg5* homozygous fish and it is therefore likely functional Atg5 protein is present at early time points. To determine if this was true, Atg5 protein in wild-type siblings, heterozygous and homozygous was shown to be present at 2dpf. It does appear the amount of Atg5 protein may be reduced in homozygous mutants, suggesting less protein is present. However, the presence of Atg5 protein at early stages may account

for improved viability of the *atg5* homozygous mutants. This is supported by the fact that maternal contribution of *atg5* is required for development past the 4-8 cell stage in mice (Tsukamoto et al. 2008)

To conclude *atg5* homozygous fish have Atg5 protein present at 2dpf, which is present due to maternally contributed mRNA, but by 8dpf, homozygous mutants no longer have Atg5 protein. Although protein was not compared for *atg3* mutants, the maternally contributed wild-type mRNA is absent by 5dpf in homozygous fish, suggestive that Atg3 protein will be lost.

4.3.3 Autophagy mutation effects on autophagy

Although there is evidence that both *atg3* and *atg5* mutations are likely effective in inhibiting coding protein from being synthesised, especially so for *atg5* mutants, the effect each mutation has on autophagy is unknown. The next aim of this chapter was to ascertain whether autophagy is changed in *atg3* or *atg5* mutant larvae.

LC3 a widely used autophagosome marker, used to analyse autophagy. Therefore, Lc3 was used as a readout for any changed autophagy levels in each homozygous mutant. Two methods were used to analyse Lc3 in zebrafish, DNA traffic-light Lc3 injections, and Lc3 western blots. Furthermore, rapamycin and chloroquine treatments were used to simultaneously upregulate and block autophagy, to allow any changes in autophagic flux to be determined.

Firstly, (using traffic light Lc3) for both *atg3* and *atg5* homozygous mutants at 2dpf, no change in autophagic vesicle number was observed in comparison to wild-type siblings and heterozygous larvae, through analysis of both RFP or GFP positive vesicles, likely to be autophagosomes. Maternal contribution which is shown in this study to be present at 2dpf, is a likely explanation for the ability of zebrafish to produce Lc3-II marked vesicles at this age. Unexpectedly, the rapamycin and chloroquine treatment did not show a large increase in Lc3-associated vesicles. The ineffective drug treatments may be due to drug concentration (being too low), or that the drugs had expired. It is unlikely the drug concentration used was too low as the same concentration had previously been published as an effective working dose, and has been tried and tested within the lab. However there may be genetic and/or environmental differences (e.g. different aquaria) which may mean fish used in these experiments may respond differently to drugs. Fresh drugs, potentially at increased dosage are required to test this.

Assessing the ratio of RFP:GFP vesicles was used to investigate autophagic flux, where a high ratio indicates autophagy is functional. By comparing the ratio of RFP to GFP positive vesicles, it is possible to determine whether most Lc3-II marked vesicles

have become acidic (RFP). A higher ratio indicates autophagy is functional, whereas a lower ratio suggests autophagy has reduced functionality. No significant changes were found between this ratio, in *atg3* or *atg5* homozygous, heterozygous and wild-type siblings with or without rapamycin and chloroquine treatment. Similar to above, this indicates that autophagy is functional in all genotypes at 2dpf, likely caused by maternal contribution. Testing of fresh drugs may be useful for further analysis.

GFP-LC3 “dots” in heart tissue were absent in *atg3*-/- and *atg5*-/- mice (Sou et al. 2008; Kuma et al. 2004), suggesting a difference in LC3 production between model animals. It would be interesting to determine whether the cardiac tissue in zebrafish lack Lc3 puncta, and equally if the muscle tissue in mice do have LC3 puncta, which may represent tissue specific autophagy requirements. However, it is also possible that the different development and resulting autophagy stress could lead to differences in Lc3 presence.

Overall, the traffic light Lc3 data do conclusively demonstrate that Lc3-II is present in 2dpf homozygous mutants. After showing that maternal mRNA, is present in larvae at 2dpf for both *atg3* and *atg5* and for Atg5 protein is present, this result is somewhat expected as Lc3-II lipidation would be possible at this time point. Next a later stage of larvae development was analysed.

Western blot analysis was completed on larvae at 8dpf, clearly demonstrating that for both *atg3* and *atg5* homozygous mutants Lc3-II was present at equal, (if not slightly increased) levels in comparison to wild-type larvae. Importantly, the LC3 antibody is capable of recognising both LC3-I and LC3-II. Using a human control, of HEK 293 cells, in which both forms are recognised, in addition to a positive control of AB wild-type treated with NH_4Cl, known to increase LC3-II production (Hart & Young 1991), it is clear in the zebrafish Lc3-II is the protein being recognised. At very long exposures the higher Lc3-I band can be seen in zebrafish lysate, but due to the lower Lc3-II band being comparatively much brighter it is not often possible to clearly visualise.

Although there is evidence that the Lc3 band observed in the western blots is Lc3-II, it is possible this is not correct. Identifying a protein band as either Lc3-II, Lc3-I or Lc3 is difficult, especially since the antibody used can recognise all forms. The human form of Lc3-II may run at a different size to the zebrafish form and additionally prolonged NH_4Cl treatment (such as overnight treatment used in this study) may result in autophagy-inhibitory feedback loops which could result in an increase of Lc3-I. For these reasons the Lc3 band observed could be Lc3-I rather than Lc3-II. In order to fully confirm that the band observed is Lc3-II, using multiple durations of drug treatments which may be

expected to cause a build-up of Lc3-II at short durations, and a build-up of Lc3-I at long durations, would be very useful in confirming which form of Lc3 is being observed.

Homozygous *atg3* and *atg5* larvae having comparative levels of Lc3-II at 8dpf was unexpected, due to the absence of wild-type mRNA, and protein for Atg5, by this stage in development. This is in contrast to corresponding mouse models, where using mouse embryonic fibroblast (MEF) cells extracted from *atg3*-/- or *atg5*-/- mice, LC3-II presence was shown to be depleted by western blot analysis, and a band representing LC3-I was present (Kuma et al. 2004; Sou et al. 2008), a clear indication that autophagy is not functional. According to literature searches, there is not another protein which is known to physically lipidate LC3-I, as Atg3 does acting as an E2-like enzyme (Nath et al. 2014; Tanida et al. 2002). Similarly, Atg5 acting as an E3-like enzyme (in the ATG5-ATG12-ATG16 complex) is thought to be crucial for LC3-II production (Fujita et al. 2008). Furthermore, in *atg3* deficient mice, autophagosome-like structures were observed, which were determined to be the unclosed autophagosome-like vesicles, but not auto-lysosomes, which suggests autophagosome formation requires a functional LC3 conjugation system *in vivo* (Sou et al. 2008), this may suggest that autophagy conjugation systems are important in the closing of autophagosome and/or lysosome fusion, and not required for initiation or elongation steps of autophagy.

This suggests that an unidentified protein may be responsible lipidating Lc3-I in zebrafish. Lc3-II was present in cultured zebrafish cells taken from larvae injected with morpholinos targeting *atg5*, *atg7* or *beclin 1* (Lee et al. 2014), suggesting that Lc3-II can be produced in zebrafish autophagy mutants. Although this was completed using primary cell cultures which may reduce the effect of morpholinos, these data suggest that zebrafish cells may have alternative methods of Lc3-I lipidation. However, according to recent literature searches alternative Lc3 lipidation strategies are not described. Targeted approaches to examine a potential role of other E2 enzymes may lead to the discovery of how Lc3-II lipidation is occurring.

Of particular interest, a recent publication has demonstrated autolysosome formation in the absence of both the ATG5-ATG12 and LC3 conjugation systems, contrary to established belief, suggesting that *atg3* and *atg5* may not be essential for autolysosome formation (Tsuboyama et al. 2016). In *atg3* KO cells, which were deficient of LC3-II, lysosomal fusion could still occur, at a only slightly reduced speed (Tsuboyama et al. 2016). Although this does not explain the presence of Lc3-II in the autophagy deficient larvae, it highlights that Lc3 may not be an accurate autophagosome marker, and suggests that autophagy can occur in a process where Lc3-II may not be used (and therefore degraded through autophagy). Analysis using

syntaxin-17 (the autophagosome marker used in their study) may prove that autophagy occurs without Lc3-II involvement in zebrafish.

Furthermore, analysis of specific roles of other Lc3 homologues (such as GABARAP or GATE-16) may be important as key to determine the true importance of Lc3 lipidation. It may be discovered that these homologues are important in the LC3-II independent autophagy described by Tsuboyama et al 2016. For example, in *Atg3* deficient mice an increase in GATE-16 (non-lipidated) protein level is observed (Sou et al. 2008). This could suggest non-lipidated GATE-16 is performing a redundancy type role in autophagy deficient mice, which perhaps enables some autophagy processes to occur even when Lc3-I (or Lc3 homologue) lipidation cannot. Targeted deletion of GATE-16 (or other Lc3 homologues) in addition to ATG conjugation may affect the biogenesis of syntaxin-17 positive autophagosomes.

Importantly this current study only proves Atg5 protein is missing at 8dpf, not Atg3. Using larvae at later developmental ages, such as 10 - 30dpf for Lc3 western blots may highlight a reduction in Lc3-I lipidation, and provide evidence that maternally contributed Atg3 or Atg5 is longer lasting in fish, which presumably degrades over time leading to survival and growth defects. Indeed, Lc3 western blots on larval mutants at an age where survival and growth defects are observed would be extremely useful in determining if Lc3-II is lipidated via an alternative pathway.

Testing Lc3-II presence in larvae, after treatment with both rapamycin and chloroquine, was completed to investigate autophagic flux as mentioned above. Fish were grouped by genotype, with or without drug treatment. Independent of genotype, no large change in Lc3-II levels for the *atg3* larvae was observed. Similarly, for *atg5* over three biological repeats no large changes were seen, however for a single repeat in both wild-type siblings and heterozygous, both with drug treatment a large increase in Lc3-II levels were observed. This may represent that in these repeats the drug treatment was more effective. Although speculative, this may suggest that the homozygous larvae have reduced autophagy in the biological repeat where drug treatment appeared effective, since a single repeat showing more Lc3-II was not seen for homozygous larvae. As discussed above these results could indicate that the rapamycin and chloroquine were not consistently effective. It is however possible to conclude that at 8dpf Lc3-II is present in the larvae, however improved drug treatments are needed to analyse autophagic flux, for example using fresh drugs, or increased drug concentrations. If drug treatments were more effective under improved conditions, more lipidation of Lc3-I may be caused by rapamycin treatment, if autophagy mutants could not lipidate Lc3-I as effectively as wild-type siblings, a comparatively reduced amount of Lc3-II would be expected.

To determine how long lasting any residual Atg5 may be present for, assuming lipidation must be completed through Atg3/Atg5 dependant conjugation systems, analysis of Lc3-II presence in homozygous larvae at older ages, for example 20 or 30dpf, may highlight a difference in Lc3-II levels. This would be particularly interesting considering mutant survival is significantly longer than maternal contribution, and any residual Atg5 may be sufficient (in Lc3 lipidation) to meet the required autophagic demands in zebrafish development. This does assume that LC3-II is autophagy specific, when in fact LC3-II can mark single membranes in LC3 associated phagocytosis (LAP) (Sanjuan et al. 2007). However, LC3 must be lipidated in LAP which still raises the question of how Lc3-I is lipidated in zebrafish. Furthermore, both *atg3* and *atg5* are used in the lipidation of LC3-I which is trafficked to LAP phagosomes (Martinez et al. 2015). Although LC3-II levels may be expected to change in response to autophagy induction or blockage, because LC3 is not specific to autophagy and is not required for autophagosome formation (Tsuboyama et al. 2016), it is possible other un-identified factors are responsible for zebrafish Lc3-I lipidation, perhaps an alternative E2-like protein is able to lipidate Lc3-I as suggested above

Any blockage in autophagy conjugation systems would be expected to result in a loss of Lc3-II levels. The expected effect of each mutation was a reduction in Lc3 lipidation, since both *atg3* and *atg5* are key genes in the lipidation of Lc3. These expected results are not observed in either the *atg3* or *atg5* zebrafish mutants. The important roles of autophagy are diverse, including in development, infection, starvation and recycling, which may lead to high redundancy within the pathway. However, the importance of *atg3* and *atg5* are clearly represented in both zebrafish and murine deficient models reduced survival (Kuma et al. 2004; Sou et al. 2008). Furthermore, in the *atg5*-/- mouse model which does not receive any maternally contributed protein, the embryo does not survive past the 4-8 cell stage (Tsukamoto et al. 2008). *atg5* independent autophagy has previously been reported (Nishida et al. 2009), indicating a functional autophagy pathway which can circumvent classical autophagy components. It is important to consider that any mutation effect, is a single part of a large, interconnected and redundant system. For example, in *atg5*-independent autophagy, or in autophagosome formation which does not require LC3 lipidation (Nishida et al. 2009; Tsuboyama et al. 2016). This high redundancy may allow the zebrafish mutant to survive longer than expected, despite the importance of the specific gene which is mutated.

The presence of Lc3-II at similar levels is suggestive that autophagy is functional, perhaps high redundancy within the pathway may account for the lack of *atg3* or *atg5* dependant Lc3 lipidation, residual protein, or un-identified E2-like proteins as discussed above. For this reason, in addition to non-specificity, Lc3 is not a marker that can be

used to interpret autophagy function alone. To further verify autophagy as up-regulated and down-regulated, a combination of autophagy related markers, such as p62 or syntaxin-17, would be very useful to assess.

Despite the presence of Lc3-II, survival and growth defects in each autophagy mutant suggest that lack of *atg3* or *atg5* is causing autophagy related defects. The other method used to assess whether the autophagy mutants were in fact deficient in autophagy, was the study of survival under starvation conditions. As discussed above (section 4.3.1), for *atg5* homozygous mutants, earlier deaths under starvation conditions suggests that autophagy is deficient, although the reduced larval survival was not significant. In future comparison of amino acid availability in autophagy mutant larvae may provide evidence that survival and growth defects are caused by an autophagy mediated lack of amino acid supply, as shown for *atg3*, *atg5* and *atg7* mutant mice (Sou et al. 2008; Komatsu et al. 2005; Kuma et al. 2004). This would provide clear evidence of an autophagy mediated phenotype.

As described above, the yolk food source, and lower metabolic rate (due to no heat generation and swimming), may stop the immediate starvation and pressure on the autophagic system in zebrafish, which the *atg3*-/- and atg5-/- mice, as mammals experience (Jardine & Litvak 2003; van de Pol et al. 2017). Zebrafish may therefore have less reliance on autophagy during development, which may enable comparatively longer survival than autophagy deficient mammals, perhaps enables through the presence of residual protein. It is important to analyse Lc3-II levels at stages when autophagy mutants display the growth/survival defect (~20-30dpf), to determine if at later developmental stages Lc3-I lipidation is reduced and may be responsible for these phenotypes, perhaps through lack of amino acid recycling.

To conclude, using Lc3 as a marker of autophagy does not sufficiently prove any difference in autophagy levels in zebrafish larvae, although does provide evidence that Lc3-II is present at 2dpf and 8dpf, indicating that some autophagy is functional in the mutants. In fact these data raise a potentially very interesting question of exactly how Lc3-I is being lipidated in *atg3* and *atg5* deficient larvae when considering the key proteins involved in this step are missing, demonstrated conclusively for Atg5.

4.4 Chapter summary

Both *atg3* and *atg5* homozygous mutants display a severe survival defect at 20-30dpf, in addition to a growth defect starting at ~20dpf. Similar survival defects are displayed in other autophagy deficient models, suggestive that autophagy mutations are responsible for these phenotypes. Further analysis into amino acid availability and

cardiac function are required to validate this. Maternal contribution occurs for both mutants and may enable embryonic survival, however by 5dpf maternal mRNA is lost, and at 8dpf Atg5 protein is lost. These data suggest that each mutation is effective in causing *atg3* or *atg5* deficiency in zebrafish. Interestingly, Lc3-II is present at both 2dpf and 8dpf. Lc3-II presence at 2dpf may be enabled through maternal contribution, however at 8dpf (for *atg5* at least), Lc3-II is not expected. Further, investigation into how the lipidation Lc3-I is possible in these mutants presents an exciting opportunity for the future.

Chapter 5: Results chapter 3

Using zebrafish autophagy mutants to study the role of autophagy in *S. aureus* and *C. neoformans* infection

5.1 Chapter introduction

Autophagy is a cellular self-degradation process which has been implicated in the handling of several pathogens. Selective autophagy, specifically leading to the degradation of pathogens, is termed xenophagy. In some cases autophagy is important for ultimate degradation of the pathogen, however it is also possible that the pathogen exploits host cell autophagy to promote its own survival.

S. aureus has been shown to interact with host cell autophagy in multiple cell types. *S. aureus* is known to reside in autophagosomes with LC3 recruitment (Schnaith et al. 2007) and to interact with selective autophagy receptor p62 (Neumann et al. 2016). Whether host cell autophagy is beneficial for the bacteria or host cell is unclear, with evidence suggesting both (introduced in section 1.4.7). Differences in the role of host cell autophagy may be determined according to host cell type and bacterial virulence factor expression.

The role of host cell autophagy in *C. neoformans* infection has not been as well studied, although there is limited data suggesting that *C. neoformans* containing phagosomes can recruit autophagic components (Nicola et al. 2012). Furthermore, *C. neoformans* replication is reduced under conditions where host autophagy is non-functional (Qin et al. 2011; Nicola et al. 2012). Despite this, *C. neoformans* has never been visualised within a double-membrane vesicle. This may suggest that any role of autophagic components in cryptococcal infection is separate to autophagosome formation, although autophagosome formation cannot be ruled out. For both *S. aureus* and *C. neoformans*, there is evidence to suggest that host autophagy is beneficial for pathogen survival, however the mechanism of these interactions and the role they play in infection outcome are not fully characterised.

Zebrafish infection has been established for both *S. aureus* and *C. neoformans*. Importantly, tools available for studying autophagy in zebrafish are also established, with mutant and transgenic lines available. Initial *S. aureus* infection studies used morpholino experimental approaches to study autophagy gene expression. Morpholinos (phosphorodiamidate Morpholino oligomers) are short ~25bp oligomer molecules which are designed to bind and block access to RNA resulting in inhibition of protein production. Morpholinos were designed to target specific autophagy gene expression, and used to knock-down autophagy gene function at the translational level.

Although some potential changes in infection survival were suggested for an *atg16* knock-down, for key autophagy genes *atg3* and *atg5*, no change in infection survival was observed (PhD thesis, Lambein, 2015). Potential reasons for this could be the short-lived effects of morpholinos, off-target effects, or their true lack of efficacy. Therefore, morpholino based experiments do not adequately determine whether knock-down of specific autophagy genes affects survival during infection. For this reason autophagy mutant lines were established.

Hypothesis: Phagocyte control of *S. aureus* and *C. neoformans* infection, will be altered in *atg3-/-* and *atg5-/-* zebrafish in comparison to larvae with competent autophagy.

Chapter aims:

1) Establish if *S. aureus* is handled by the autophagy pathway, specifically in regards to the role of both *atg3* and *atg5*
2) Establish if *C. neoformans* is handled by the autophagy pathway, specifically in regards to the role of both *atg3* and *atg5*

This chapter aims to use autophagy zebrafish mutants in key autophagy genes, in addition to relevant autophagy transgenic lines, to dissect the role of host autophagy in response to *S. aureus* and *C. neoformans* infection.

atg3 and *atg5* autophagy mutants were established to test if key autophagy genes have an important role in the host-pathogen interaction of both *S. aureus*, and *C. neoformans* infection. Both *atg3* and *atg5* mutations lead to a survival defect and growth defect. However, because Lc3-II is present in the larvae, it is possible that some autophagy is functional. It is therefore significant that for the *atg5* mutants, by 8dpf, there is no detectable Atg5 protein within the zebrafish. This does indicate that the mutation is effective in stopping the production of Atg5 protein. Due to the similar phenotype of both mutants, it seems likely that the *atg3* mutation is also effective in this regard. Autophagy is known to be important in pathogen handling, or as a route of pathogen subversion. Here, using zebrafish lacking key autophagy genes, the role each gene plays in infection by either *S. aureus* or *C. neoformans* is examined.

5.2 Infection of autophagy mutants:

5.2.1 Inoculum dependant survival

Zebrafish models of infection of *S. aureus* and *C. neoformans* have been well established previously (Prajsnar et al. 2008; Bojarczuk et al. 2016), and the same infection protocols were followed. To ensure personal proficiency in infection, inoculum dependant survival curves were completed.

First, *C. neoformans* was injected at inocula of 0, 10, 100, 500 or 1000cfu at 2dpf and larval survival was monitored for 3 days. The range of infection inocula was chosen to be likely to cause different larval survival outcomes, as indicated by previously established *C. neoformans* infections (Bojarczuk et al. 2016). *S. aureus* was injected at inocula of 0, 1-600, 1200-1800 or 1800-2400cfu at 1dpf and survival monitored for 4 days. Grouped inocula were used, rather than exact inocula, due to the difficulties in calculating exact inoculum at the time of infection. The exact inoculum was determined subsequently through counting of colony forming units (of diluted injected doses) grown overnight, as described in the materials and methods. Different *S. aureus* inocula were chosen as likely to lead to differential survival outcomes as established previously (Prajsnar et al. 2008).

Survival of larvae was reduced when infected with *C. neoformans* at higher fungal inocula in comparison to reduced inocula. Survival of larvae infected with 500 and 1000cfu was significantly reduced in comparison to non-infected larvae (Fig. 5.1 A). *S. aureus* infection leads to large differences in larval survival, an inoculum lower than 1200cfu leads to a larval survival of more than 50%, whereas infection with more than 1200cfu leads to larval survival of less than 50%. Survival is significantly reduced for each infection dose, in comparison to non-infected fish (Fig. 5.1 B).

Importantly, these data show that zebrafish mortality is proportional to the pathogen load, and therefore it is the pathogen, rather than needle or handling related injuries, causing death, allowing the subsequent infection studies in autophagy mutants to exclude non-pathogen related death.

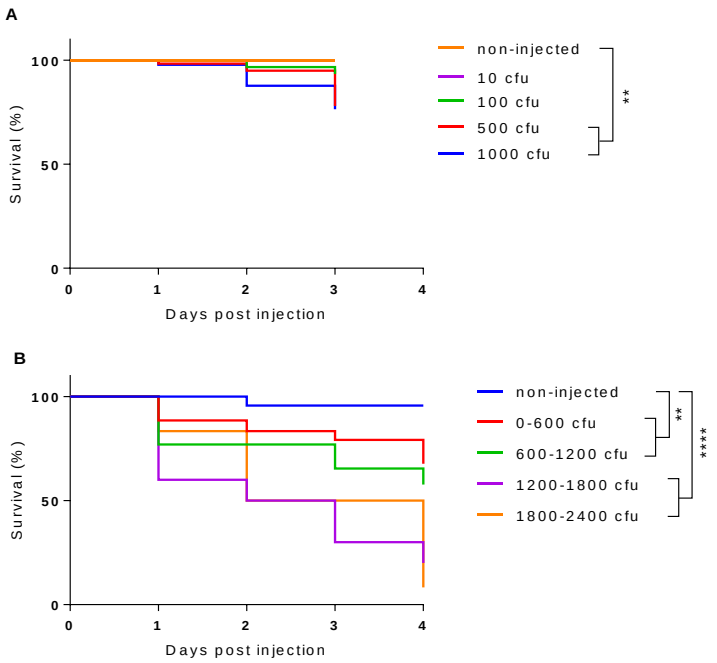

Figure 5.1 Larval survival of *C. neoformans* or *S. aureus* infection is dependent on inoculum

A Survival of AB wild-type fish infected with different inoculums of *C. neoformans* at 2dpf (** p<0.01, n=5 Log-Rank Mantel-Cox, 30-89 larvae per inoculum) **B** Survival of AB wild-type fish infected with different inocula of *S. aureus* at 1dpf (**p<0.01, ****p<0.0001, n=5, Log-Rank Mantel-Cox 23-96 larvae per inoculum).

5.2.2 Survival of autophagy mutants under infection

Survival of both *atg3* and *atg5* zebrafish lines was first examined, to determine if larval survival is changed in the homozygous mutants under infection conditions. Duration of infection was increased beyond 5dpf, to allow infection to be followed over a time period when protein derived from the maternal contribution should be absent from homozygous mutants (Fig. 4.6, above).

In the first instance, *C. neoformans* infection of autophagy mutants was followed over an extended duration, to investigate whether an obvious difference in survival would be seen. It might be expected that a different survival would be observed in 25% (representing the homozygous mutants) of a heterozygous in-cross, according to Mendelian genetics. *S. aureus* infection of *atg3* and *atg5* mutants was previously performed using abscess formation as an endpoint, with no difference in infection outcome observed (PhD thesis Lambein, 2015). Similarly, *C. neoformans* infection of larvae from a heterozygous in-cross of either *atg3* or *atg5* lines did not reveal any significant difference in survival in comparison to infected AB wild-type larvae (Fig. 5.2 A).

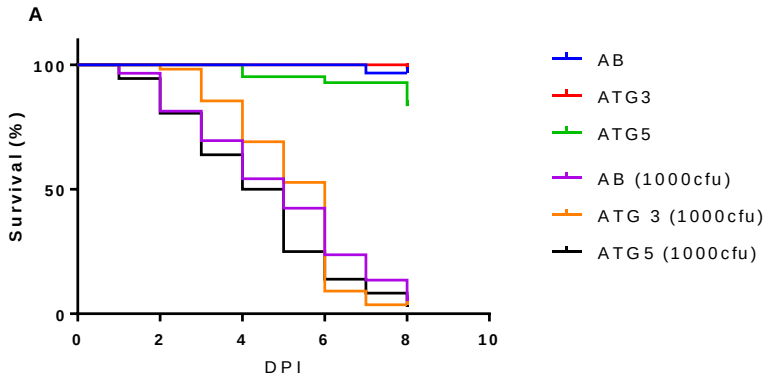

Figure 5.2 Larval survival is not reduced in *atg3* or *atg5* heterozygous in-crosses in *C. neoformans* infection

A Survival of *atg3* and *atg5* heterozygous fish in-crosses infected with 1000cfu KN99 *C. neoformans,* or without infection (not significant, n=3 Log-Rank Mantel-Cox, 36-62 larvae per group). Infection followed until 10dpf completed at IMCB in Singapore.

An obvious change in larval survival was not seen using heterozygous in-crosses of either autophagy zebrafish line. This suggests that a dramatic difference in survival was not observed for infected homozygous mutants. Next, survival of both *atg3* and *atg5* infected with *C. neoformans* or *S. aureus* was examined by genotype group, after larval death or experimental endpoint, to investigate any less dramatic changes in larval survival.

In all cases, non-infected larval survival was high, independent of genotype, demonstrating that larvae death is caused by infection. *C. neoformans* infection of an *atg3* heterozygous in-cross shows similar survival for all infected fish, including AB wild-type fish (Fig. 5.3 A), no significant difference in larval survival was observed for any infection genotype. Thus, survival of homozygous *atg3* fish in *C. neoformans* infection is not changed.

Survival of *atg5* homozygous larvae is significantly reduced compared to infected AB wild-type larvae, however is not significantly reduced in comparison to wild-type siblings in the *C. neoformans* infection of an *atg5* heterozygous in-cross (Fig. 5.3 B). Infected wild-type siblings are better controls than ABs, being closer genetically to the homozygous mutants. Therefore, survival is not changed for *atg5* homozygous mutants in *C. neoformans* infection.

Larval survival with infection of *S. aureus* was next considered. For both *atg3* and *atg5* heterozygous in-cross experiments, PBS control injections showed high larval survival. In both *atg3* and *atg5 S. aureus* infections larval survival was low, as compared to Figure 5.1 which show higher larval survival at 3dpf at comparative doses, than seen in these experiments, completed in IMCB.

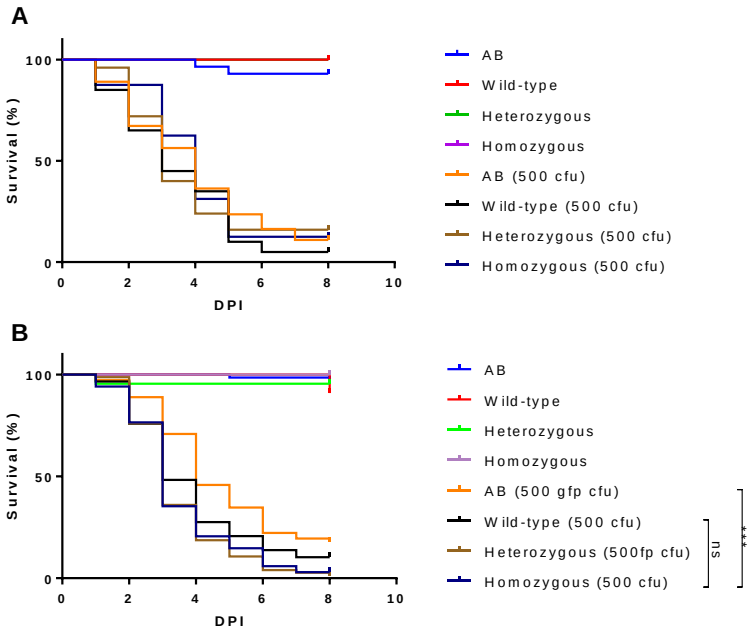

<u>Figure 5.3</u> Larval survival is not reduced for *atg3* or *atg5* mutants in *C. neoformans* infection

A Survival of *atg3* heterozygous fish in-crosses infected with 500cfu KN99 *C. neoformans,* or without infection (not significant, n=3 Log-Rank Mantel-Cox, 16-25 larvae per infected group). **B** Survival of *atg5* heterozygous fish in-crosses infected with 500cfu KN99 *C. neoformans,* or without infection (ns=not significant, ***p<0.001, n=3, Log-Rank Mantel-Cox 29-75 larvae per infected group). Infection followed until 10dpf completed at IMCB in Singapore.

Despite overall low larval survival, infection of the *atg3* heterozygous larvae shows that both homozygous and heterozygous fish have significantly better survival than wild-type siblings (Fig. 5.4 A). This indicates that *atg3* homozygous and heterozygous fish have improved survival in *S. aureus* infection. In contrast, survival of *atg5* homozygous zebrafish is not significantly different to wild-type siblings (Fig. 5.4 B). Therefore *atg5* homozygous fish do not have changed survival under *S. aureus* infection.

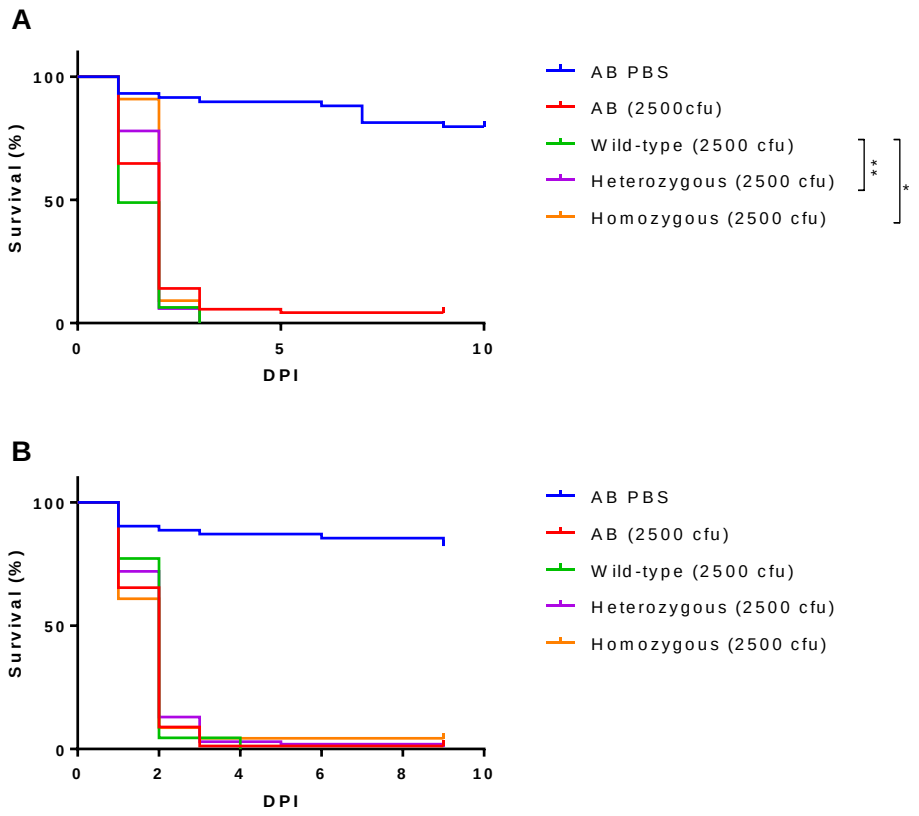

<u>Figure 5.4</u> Larval survival is improved for *atg3* but not *atg5* mutants in *S. aureus* infection

A Survival of *atg3* heterozygous fish in-crosses infected with ~2500cfu SH1000 GFP *S. aureus,* or control PBS infection (*p<0.05, **p<0.01, n=6, Log-Rank Mantel-Cox, 11-68 larvae per infection group). **B** Survival of *atg5* heterozygous fish in-crosses infected with ~2500cfu SH1000 GFP *S. aureus,* or control PBS infection (not significant, n=6, Log-Rank Mantel-Cox, 22-100 larvae per infection group). Infection followed until 10dpf completed at IMCB in Singapore.

Although an increase in larval survival was observed for both heterozygous and homozygous *atg3* larvae, no change was seen for *atg5* homozygous mutants in *S. aureus* infection. Infection with *C. neoformans* highlighted no change in infection outcome for either *atg3* or *atg5* autophagy mutant. I hypothesised that by putting

additional pressure on larval autophagy, any larval survival changes caused by infection may be amplified, which are not observed in the experimental conditions normally used.

5.2.3 Infection under starvation conditions

Starvation is a useful autophagy activator, which leads to an increase in autophagy, and increased turnover of autophagic machinery. Larval starvation (without infection), reduced the survival of *atg5* homozygous mutants, indicating that pressuring autophagy through lack of nutrients increases the pressure on autophagy, as shown above, (Fig. 4.19). A role of *atg3* and *atg5* in clearance of infection may become apparent through combined infection and lack of nutrients. Next, the survival of larvae under both infection and starvation conditions was investigated to determine if any survival changes are amplified.

A lower dose of each pathogen was used in these cases, 100cfu for *C. neoformans*, and 500cfu of *S. aureus*, to ensure that enough fish would survive until 7-11dpf when the yolk food source is depleted. An *atg3* or *atg5* heterozygous in-cross was used, with no AB wild-type controls. This was due to the valid wild-type siblings acting as control which are present in the heterozygous in-cross, this reduced the need to use AB wild-type fish in this procedure, (animal work completed in Singapore under the Institutional Animal Care and Use Committee (IACUC) guidelines, under locally ethically approved IACUC protocol number 140977).

Survival was not significantly different between *atg3* wild-type siblings, heterozygous or homozygous larvae in *C. neoformans* infection and starvation conditions (Fig. 5.5 A). Survival was also not significantly different between *atg5* wild-type siblings, heterozygous or homozygous larvae in *C. neoformans* infection and starvation conditions, (Fig. 5.5 B), however the *atg5* homozygous mutants show a (non-significant) trend towards reduced survival after 7dpf.

Only a small proportion of fish were able to survive until after 11dpf under *S. aureus* infection. For *atg3* starvation and *S. aureus* infection data, similar to the *C. neoformans* data, no significant difference was seen in larval survival between genotypes (Fig. 5.6 A). Larval survival was not significantly different between *atg5* homozygous, heterozygous or wild-type siblings in dual starvation and *S. aureus* infection (Fig. 5.6 B). Overall these data suggest for *atg3* homozygous fish, no significant changes in larval survival occur, for both *S. aureus* and *C. neoformans* infection.

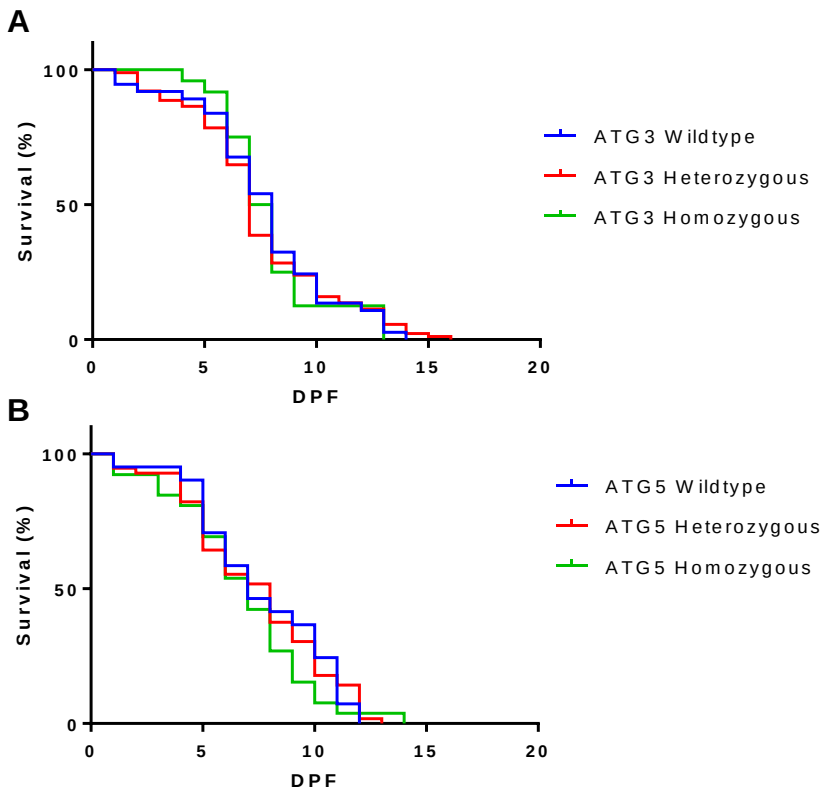

Figure 5.5 Autophagy mutant survival is not changed in *C.neoformans* infection in starvation conditions

A Larval survival from *atg3* heterozygous fish in-crosses infected with 100cfu *C. neoformans* (not significant, n=5, Log-Rank Mantel-Cox. 24-88 larvae per group). **B** Survival of *atg5* heterozygous fish in-crosses infected with 100cfu *C. neoformans* (not significant, n=4, Log-Rank Mantel-Cox, 26-56 larvae per group). Infection under starvation conditions followed until 20dpf completed at IMCB in Singapore.

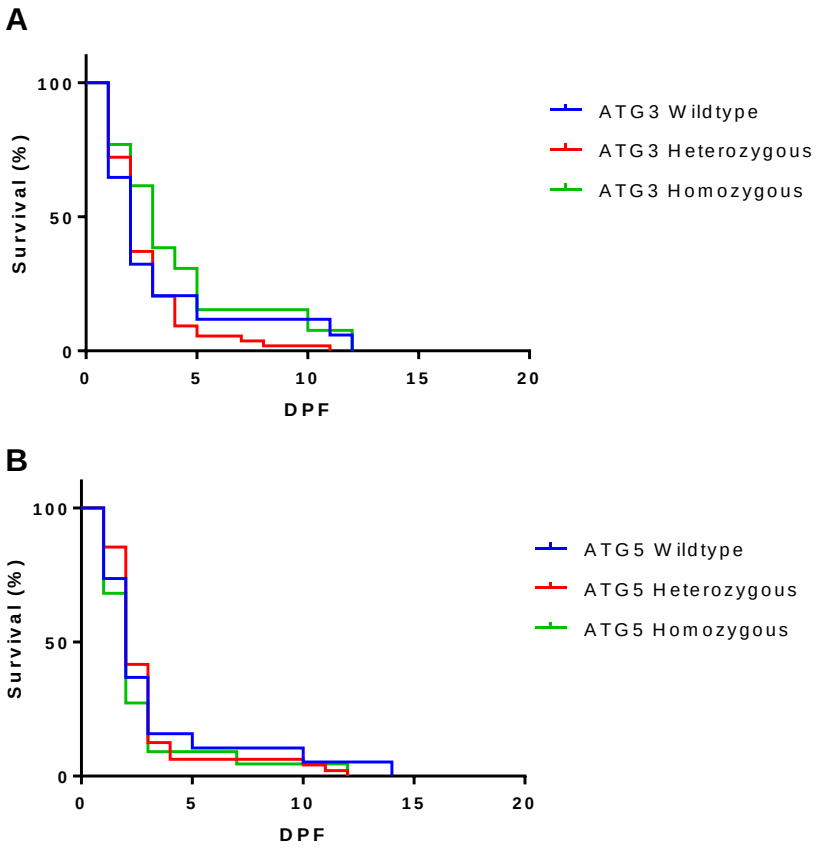

Figure 5.6 Autophagy mutant survival is not changed in *S. aureus* infection in starvation conditions

A Larval survival from *atg3* heterozygous fish in-crosses infected with 500cfu *S. aureus* (not significant, n=4, Log-Rank Mantel-Cox, 13-54 larvae per group). **B** Survival of *atg5* heterozygous fish in-crosses infected with 500cfu *S. aureus* (not significant, n=3, Log-Rank Mantel-Cox, 19-48 larvae per group). Infection under starvation conditions followed until 20dpf completed at IMCB in Singapore.

Under non-infection starvation conditions an earlier larvae death of ~4-5 days was seen for *atg5* homozygous larvae (Fig 4.19 above). For *atg5* homozygous fish, a trend towards reduced survival of larvae was seen after 7dpf in *C. neoformans* infection with starvation, which may be expected due to starvation conditions alone. No difference was seen in *atg5* homozygous larval survival for *S. aureus* infection with starvation. This may indicate a slight improvement in *atg5* homozygous larval survival during *S. aureus* infection, considering under non-infection starvation experiments, reduced survival is seen. However, due to the much earlier timeframe of death in *S. aureus* infection, this requires further investigation, perhaps using a lower dose to enable survival to later time points.

5.2.4 Infection at later time points

Data from starvation and infection survival experiments showed no significant changes in survival for the homozygous autophagy mutants. Both *atg3* and *atg5* homozygous mutants show reduced survival under normal feeding conditions by 20dpf (Fig. 4.4, above). I hypothesised that the effects of these mutations on responses to infection will be more prominent following infection at 20dpf.

These data remain preliminary, because although multiple repeats (of at least 4) were completed in all cases, the number of homozygous mutants viable at 20dpf was very low, leading to low numbers for analysis. Unfortunately, time constraints did not allow for further repeats.

Infection of 1000cfu *C. neoformans* at 20dpf led to similar survival between *atg3* homozygous, wild-type siblings and heterozygous larvae (Fig. 5.7 A). Similarly, survival

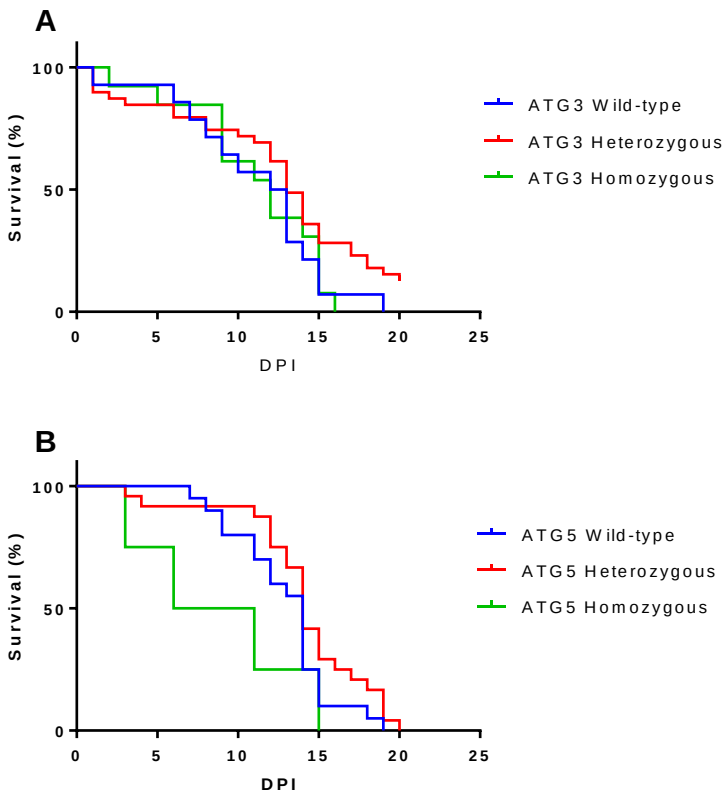

Figure 5.7 Autophagy mutant survival is not changed in *C.neoformans* infection at 20dpf

A Larval survival from *atg3* heterozygous fish in-crosses infected with 1000cfu *C. neoformans* (not significant, n=4, Log-Rank Mantel-Cox, 13-39 larvae per group). **B** Survival of *atg5* heterozygous fish in-crosses infected with 1000cfu *C. neoformans* (not significant, n=6, Log-Rank Mantel-Cox, 4-24 larvae per group). Infection at 20dpf followed until 40dpf completed at IMCB in Singapore.

of homozygous *atg5* mutant larvae was not significantly different to wild-type or heterozygous larval survival, although a (non-significant) trend towards reduced survival is shown for *atg5* homozygotes (Fig. 5.7 B).

Larval survival was not significantly different for *atg3* homozygous fish in comparison to wild-type or heterozygous fish, under infection of 2500cfu *S.aureus* (Fig. 5.8 A). On the other hand, for *atg5 S. aureus* infection at 20dpf, a difference was determined between homozygous mutants larval survival, and both wild-type siblings and heterozygous larvae (Fig. 5.8B). However, the homozygous group consists of a single fish so data from more homozygous fish would needed to confirm this result.

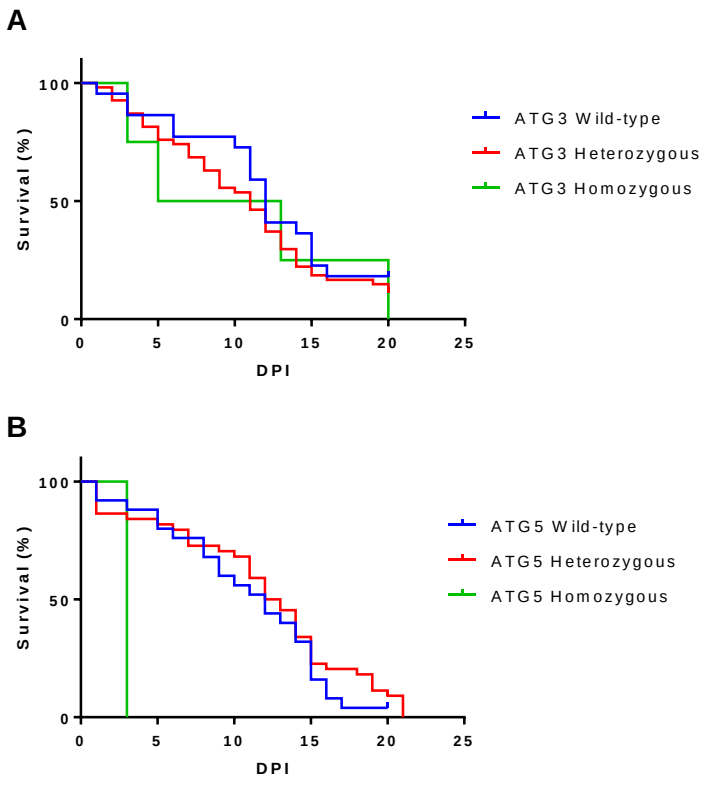

Figure 5.8 Autophagy mutant survival is not changed in *S. aureus* infection at 20dpf

A Larval survival from *atg3* heterozygous fish in-crosses infected with 2500cfu *S. aureus* (not significant, n=5, Log-Rank Mantel-Cox, 4-54 larvae per group). **B** Survival of *atg5* heterozygous fish in-crosses infected with 2500cfu *S. aureus* (n=4, Log-Rank Mantel-Cox, 1-44 larvae per group). Infection at 20dpf followed until 40dpf completed at IMCB in Singapore.

Overall, larvae survival was not drastically different for either *S. aureus* or *C. neoformans* infection in *atg3* or *atg5* mutants, a major change in survival outcome may have been expected if *atg3* or *atg5* play an important role in the outcome of host-pathogen interactions. However, an alternative reason why survival is not changed in infected larvae could be due two reasons. Firstly, early in infection maternal contribution may enable normal *atg3* or *atg5* levels in the larvae resulting in normal (not lacking *atg3* or *atg5*) host-pathogen handling. Secondly, later in development, the survival defect which is already causing homozygous death independently of infection may override any defects in handling of pathogens, leading to earlier death. For these reasons, using autophagy mutant larval survival outcome of infection alone to assess the role of *atg3* or *atg5* may not provide clear answers.

5.2.5 Fungal and bacterial burden

To determine if *C. neoformans* or *S. aureus* infection is able to cause death to a similar extent in autophagy deficient fish as wild-type fish, the fungal and bacterial burden within *atg3* and *atg5* larvae was compared. I hypothesised that if *atg3* or *atg5* are important in pathogen clearance, homozygous autophagy mutant larvae may have an increased fungal or bacterial burden during infection, in comparison to wild-type larvae. Additionally autophagy mutants may also have a lower pathogen burden which is able to cause to larval death.

The bacterial burden was measured in larvae at 0dpi (1dpf) to 4dpi (5dpf) in *atg3* and *atg5* after infection of 2500cfu of *S. aureus* into heterozygous in-crosses. There is no significant difference between *atg3* homozygous, heterozygous and wild-type siblings bacterial burden at any time point (Fig 5.9 A) indicating that bacterial burden is similar in all genotypes. The bacterial burden the day before death was compared to discover if a reduced bacterial burden in homozygous larvae may cause death in comparison to wild-type siblings. However, there was no significant difference between the bacterial burden preceding death between any *atg3* genotype (Fig 5.9 B). This indicates that *atg3* homozygous mutants do not have an increased bacterial burden during infection, and that a similar bacterial burden to wild-type siblings causes death.

Similarly, there is no significant difference between the bacterial burden of *atg5* homozygous, heterozygous and wild-type at any time point (Fig 5.9 C) indicating that bacterial burden is similar in all *atg5* genotypes. There was also no significant difference in the bacterial burden preceding death between any *atg5* genotype (Fig 5.9 D). This indicates that *atg5* homozygous mutants do not have an increased bacterial burden during infection, and larvae death is caused by a similar bacterial burden to wild-type siblings.

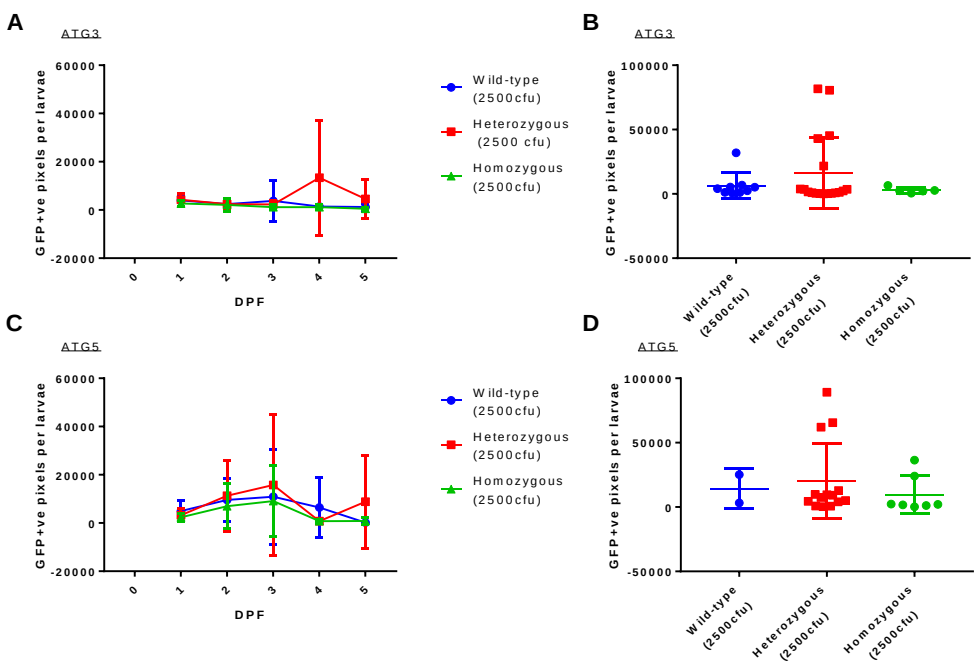

Figure 5.9 Lethal bacterial burden is not different for autophagy mutant larvae

2500cfu of GFP *S. aureus*, injected into *atg3* or *atg5* heterozygous in-crosses, imaged at 0dpi, 1dpi, 2dpi, 3dpi and 4dpi. GFP positive pixels represent the GFP positive bacteria within individual larvae. **A** Bacterial burden of *atg3* heterozygous fish, average at each time point (n=3, 63 larvae, +/- SD, not significant Two-way ANOVA, Tukey's test) **B** Bacterial burden of *atg3* heterozygous fish, of larvae which died on between 1dpi and 5dpi (n=3, 32 larvae, +/- SD, not significant One-way ANOVA, Kruskal-Wallis test) **C** Bacterial burden of *atg5* heterozygous fish, average at each time point (n=3, 37 larvae, +/- SD, not significant Two-way ANOVA, Tukey's test) **D** Bacterial burden of *atg5* heterozygous fish, of larvae which died on between 1dpi and 5dpi (n=3, 23 larvae, +/- SD, not significant One-way ANOVA, Kruskal-Wallis test)

Next, the fungal burden was measured in larvae at 0dpi (2dpf) to 3dpi (5dpf) in *atg3* and *atg5* after infection of 1000cfu of *C. neoformans* into heterozygous in-crosses. There is no significant difference between *atg3* homozygous, heterozygous and wild-type siblings fungal burden at 0dpf to 4dpf. However at 5dpf (3dpi) there is a significant decrease in fungal burden in *atg3* homozygous and *atg3* heterozygous larvae in comparison to wild-type siblings (Fig 5.10 A) indicating that fungal burden is similar in all genotypes until later in infection. This may suggest that host *atg3* is useful for fungal survival and growth. Furthermore, there was no significant difference between the fungal burdens preceding death between any *atg3* genotype (Fig 5.10 B). This indicates that *atg3* homozygous mutants do not have an increased fungal burden during early infection, but that a similar bacterial burden to wild-type siblings causes larvae death.

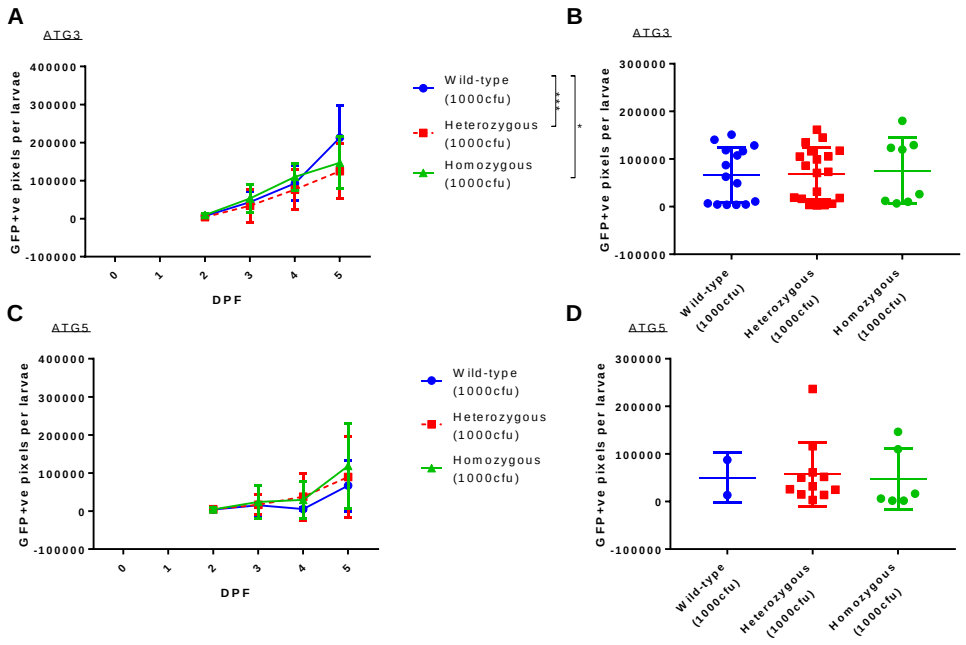

<u>Figure 5.10</u> Lethal fungal burden is not different for autophagy mutant larvae

1000cfu of GFP *C. neoformans*, injected into *atg3* or *atg5* heterozygous in-crosses, imaged at 0dpi, 1dpi, 2dpi and 3dpi. GFP positive pixels represent the GFP positive cryptococcal cells within individual larvae. **A** Fungal burden of *atg3* heterozygous fish, average at each time point (n=3, 64 larvae, +/- SD, *p<0.05, ***<p<0.001 Two-way ANOVA, Tukey's test at 5dpf) **B** Fungal burden of *atg3* heterozygous fish, of larvae which died on between 1dpi and 5dpi (n=3, 42 larvae, +/- SD, not significant One-way ANOVA, Kruskal-Wallis test) **C** Fungal burden of *atg5* heterozygous fish, average at each time point (n=3, 48 larvae, +/- SD, not significant Two-way ANOVA, Tukey's test) **D** Fungal burden of *atg5* heterozygous fish, of larvae which died on between 1dpi and 5dpi (n=3, 19 larvae, +/- SD, not significant One-way ANOVA, Kruskal-Wallis test)

There was no significant difference between the fungal burden of *atg5* homozygous, heterozygous and wild-type at any time point (Fig 5.10 C) indicating that fungal burden is similar in all *atg5* genotypes throughout infection. No significant difference in the fungal burden preceding death between any *atg5* genotype was observed (Fig 5.10 B). This indicates that *atg5* homozygous mutants do not have an increased fungal burden during infection, and homozygous larval death is caused by a similar fungal burden to wild-type siblings.

Analysis of the fungal and bacterial burden suggest that during infection both *atg3* and *atg5* are not important in controlling *S. aureus* or *C. neoformans* infection. Furthermore, these data suggest that host larvae deficient in *atg3* or *atg5* were not susceptible to infection at lower burdens than wild-type siblings.

ATG5 infection with 3-MA treatment

3-Methyladenine (3-MA) is an autophagy inhibitor (which acts to inhibit autophagy at the PI3K complex) which is known to inhibit ATG5-independent autophagy in addition to canonical macroautophagy (Juenemann & Reits 2012). To determine whether *atg5* independent autophagy is functional in *atg5* mutants, and therefore providing a route of autophagy mediated host clearance, any further potential changes in larval survival or fungal/bacterial burden, under both 3-MA treatment and infection were investigated.

In all cases an *atg5* heterozygous in-cross was used. No change in survival is seen between control *atg5* larvae and 3-MA treated larvae, suggesting 3-MA treatment does not kill larvae. However, a significant reduction in survival is observed for *S. aureus* infected larvae in comparison to both control and 3-MA treated larvae (Fig 5.11 A). This highlights that *S. aureus* is causing mortality of larvae. However, no significant difference between *atg5* homozygous, heterozygous or wild-type larvae treated with 3-MA and also infected with *S. aureus* was observed (Fig 5.11 B). As no change in survival is seen in homozygous larvae, this suggests that *atg5* independent autophagy is not crucial to larval survival of *S. aureus* infection. Of note, more repeats are required for this due to the low number of larvae within some genotype groups.

No change in survival was observed between *atg5* non-injected larvae, *atg5* larvae treated with 3-MA, or *atg5* larvae infected with *C. neoformans* (Fig 5.11 C). It may be expected that larvae infected with *C. neoformans* may have had a higher mortality. In *atg5* larvae treated with 3-MA and infected with *C. neoformans*, no significant difference in survival was observed between any genotype (Fig 5.11 D). This suggests that *atg5* independent autophagy is not important in larval survival of *C. neoformans* within *atg5* deficient fish.

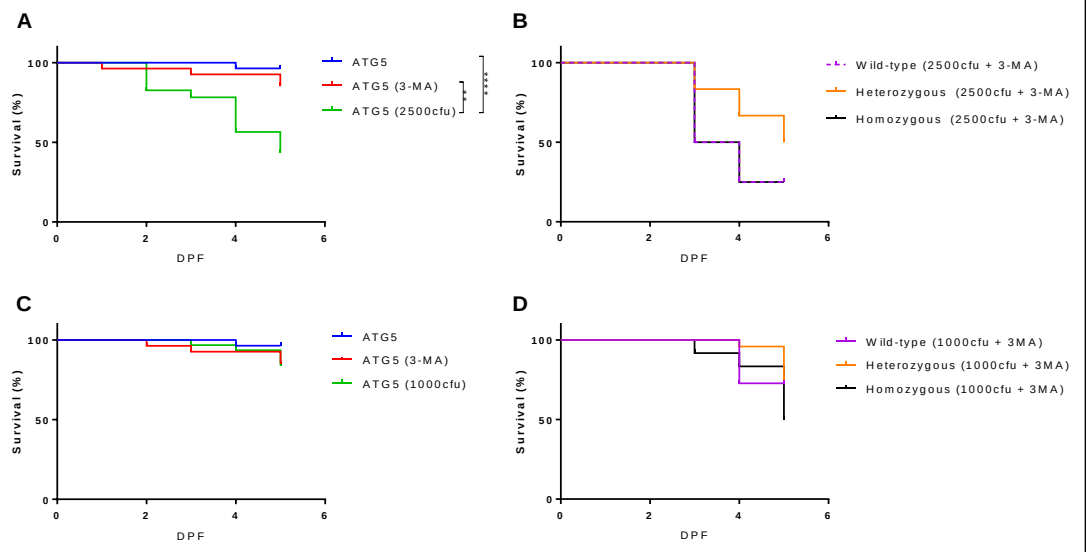

<u>Figure 5.11</u> No difference in survival in infected *atg5* autophagy mutant larvae treated with 3-MA

A Survival of *atg5* heterozygous fish, *atg3* larvae treated with 3-MA, or *atg3* infected with 2500cfu *S. aureus* (**p<0.01, ****p<0.001, n=3, Log-Rank Mantel-Cox, 23-28 larvae per group) **B** Survival of *atg5* heterozygous fish infected with 2500cfu *S. aureus* grouped by genotype (n=3, not significant Log-Rank Mantel-Cox, 4-12 larvae per group). **C** Survival of *atg5* heterozygous fish, *atg5* larvae treated with 3-MA, or *atg5* infected with 1000cfu *C. neoformans* (not significant, n=3, Log-Rank Mantel-Cox, 27-32 larvae per group). **D** Survival of *atg5* heterozygous fish infected with 1000cfu *C. neoformans* (not significant, n=3, Log-Rank Mantel-Cox, 11-24 larvae per group).

Preliminary data of the bacterial burden of *atg5 S. aureus* infected and 3-MA treated larvae, grouped by genotype over time highlights an increase in bacterial burden in homozygous larvae at 2dpf and 5dpf (Fig 5.12 A). This may represent larvae which are moribund due to extremely high bacterial burden, which in *S. aureus* infection can occur at 2dpf. To determine whether different extremes of bacterial burden causes different death outcomes between genotypes, the bacterial burden (the day before death) of larvae which died before 5dpf were compared. No significant difference in bacterial burden between *atg5* homozygous, heterozygous or wild-type siblings was found, (Fig 5.12 B) suggesting that all genotypes are equally susceptible to bacterial infection. Of note, limited data was collected due to time restrictions and further investigation may lead to statistical significance of a potential trend towards a higher bacterial burden in homozygous larvae.

Preliminary data of the fungal burden of *atg5 C. neoformans* infected and 3-MA treated larvae, grouped by genotype over time highlights an increase in fungal burden in all genotypes through the time course of infection to 5dpf, especially in homozygous and heterozygous larvae (Fig 5.12 C). This likely represents growth of fungal cells within the larvae over time. To determine whether different cases of fungal burden causes different death outcomes between genotypes, the fungal burden the day before death, in larvae which died before 5dpf, was compared.

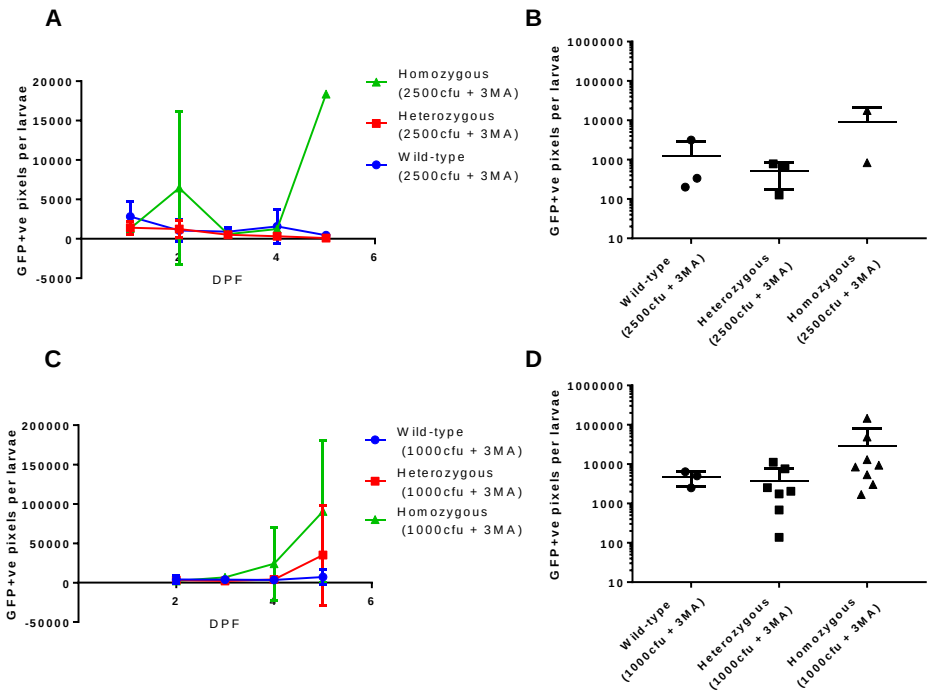

Figure 5.12 No difference in fungal or bacterial burden in *atg5* autophagy mutant larvae treated with 3-MA

A Bacterial burden of *atg5* heterozygous fish treated with 3-MA and infected with 2500cfu *S. aureus* (n=2, 3-5 larvae per group) **B** Bacterial burden from the day before death of *atg5* heterozygous fish treated with 3-MA and infected with 2500cfu *S. aureus* (n=2, not significant one-way ANOVA, 2-3 larvae per group) **C** Fungal burden of *atg5* heterozygous fish treated with 3-MA and infected with 1000cfu *C. neoformans* (n=3, 11-24 larvae per group) **D** Fungal burden from the day before death of *atg5* heterozygous fish treated with 3-MA and infected with 1000cfu *C. neoformans* (n=3, not significant one-way ANOVA, 3-8 larvae per group)

No significant difference in fungal burden between *atg5* homozygous, heterozygous or wild-type siblings was found, (Fig 5.12 D) suggesting that all genotypes are equally susceptible to *C. neoformans* infection. Similarly, further analysis may lead to statistical significance for an apparent trend towards a higher fungal burden observed in homozygous larvae.

5.2.6 *S. aureus* and *C. neoformans* handling by autophagy in neutrophils

Autophagy has been demonstrated to be involved in the host-pathogen interactions for both *S. aureus and C. neoformans* (see sections 1.4.7, 1.4.8). Analysis of mutant larval survival after infection with either *S. aureus* or *C. neoformans* provided limited insight into the role of autophagy during infection. This may be due to the multiple potential consequences of the autophagy mutations, which is clearly demonstrated with reduced survival under non-infection conditions. Therefore, pathogen interactions with the host were next examined at the cellular level.

The role of neutrophil autophagy was examined in both *S. aureus* and *C. neoformans* infections. A neutrophil specific traffic-light Lc3 reporter zebrafish line was infected with pathogen (2500cfu of *S. aureus* or 1000cfu of *C. neoformans*), at 2dpf, and images were acquired 2 hours post infection, and a further 24 hours later (26hpi), to allow changes in Lc3 recruitment/involvement in pathogen interactions to be compared.

Neutrophil handling of *S. aureus* involves Lc3 recruitment

The number of neutrophils which contain bacteria is significantly reduced from 0dpi to 1dpi (Fig 5.13 A, B), suggesting that neutrophils are able to efficiently degrade *S. aureus* or that the bacteria escapes from neutrophils. *S. aureus* is shown to reside in vesicles in the majority of cases, but can reside in the cytoplasm at both 0dpi and 1dpi (Fig 5.13 C). However, the vesicles which contain bacteria are significantly reduced in number by 1dpi, suggesting that bacteria are degraded before 1dpi (Fig 5.13 D). A limited number of bacteria were observed in the cytoplasm at 0dpi and 1dpi (Fig. 5.13 E), these may represent bacteria which have escaped the phagosome. These data highlight how *S. aureus* interacts with neutrophils in the first two days of infection, and suggests that the majority of bacteria is likely killed and degraded within the neutrophil after being phagocytosed.

The recruitment of Lc3 to *S. aureus* contained in neutrophil vesicles was next examined, to determine whether a difference in Lc3 recruitment occurs in autophagy deficient larvae. Unfortunately the number of cytoplasmic *S. aureus* was not analysed due to a lack of data points. Similarly, data was analysed for 0dpi, but not at 1dpi due to a lack of data points. This is likely due to the clearance of bacteria under normal circumstances, further repeats may enable analysis in the future.

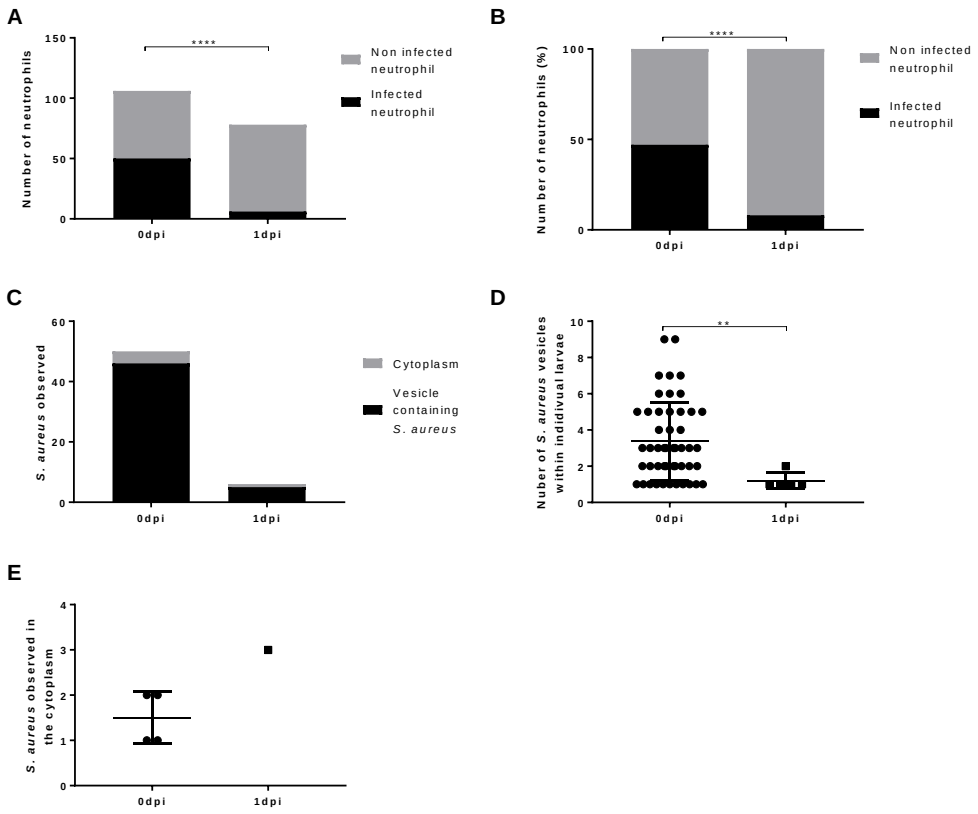

<u>Figure 5.13</u> Neutrophil handling of *S. aureus* results in bacterial clearance

2500cfu of GFP *S. aureus* injected into *Tg(LyzC:RFP.GFP.Lc3)*, larvae imaged in the CHT at 2hpi (0dpi) and 26hpi (1dpi). **A** The number of infected or non-infected neutrophils at 0dpi and 1dpi (****p<0.0001 Chi Square test, n=3, 17 0dpi larvae, 11 1dpi larvae) **B** The proportion of infected or non-infected neutrophils at 0dpi and (****p<0.0001 Chi Square test, n=3, 17 0dpi larvae, 11 1dpi larvae) **C** The location of *S. aureus*, either in a vesicle or in the cytoplasm (ns, Chi Square test, n=3, 17 0dpi larvae, 11 1dpi larvae) **D** The number of *S. aureus* events observed in a vesicle at 0dpi or 1dpi (**p<0.01 Mann-Whitney T-test, n=3, 17 0dpi larvae, 11 1dpi larvae) **E** The number of *S. aureus* events observed in the cytoplasm at 0dpi or 1dpi (n=3, 17 0dpi larvae, 11 1dpi larvae)

Lc3 association with *S. aureus* was investigated to highlight any role of autophagy (Lc3 recruitment) in bacterial clearance. Multiple Lc3 interactions were observed during *S. aureus* infection of the neutrophil specific Lc3 reporter larvae. *S. aureus* which had been phagocytosed was observed in neutrophil vesicles, with or without Lc3 marking the entire vesicle, as shown in Figure 5.14 A, B. Vesicles containing *S. aureus* may also have Lc3 puncta (Figure 5.14 C). Additionally, *S. aureus* was observed in the

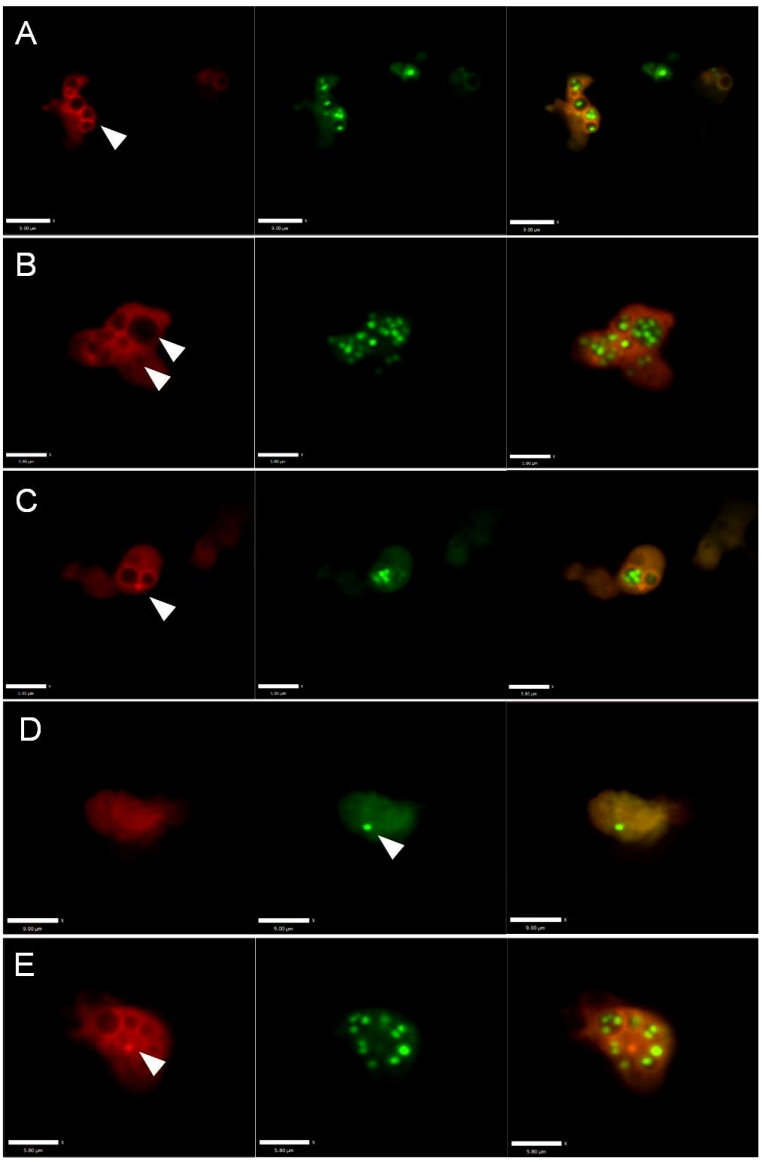

Figure 5.14 Lc3 can mark *S. aureus* vesicles or cytoplasmic bacteria

2500cfu of GFP *S. aureus* injected into *Tg(LyzC:RFP.GFP.Lc3)*, larvae imaged in the CHT at 2hpi (0dpi) and 26hpi (1dpi). White arrows point to specific examples, **A** *S. aureus* with Lc3 marking the entire vesicle, scale 9um **B** *S. aureus* without Lc3 marking the entire vesicle, scale 5.8um, **C** vesicle containing *S. aureus* with Lc3 puncta, scale 5.8um **D** *S. aureus* in the cytoplasm with no Lc3 co-localisation, scale 9um, **E** *S. aureus* in the cytoplasm with Lc3 co-localisation, scale 5.8um.

cytoplasm of the neutrophil, and these bacteria may also be co-localised with Lc3 puncta. (Figure 5.14 D, E). This highlights that Lc3 is involved in neutrophil handling of *S. aureus*, in multiple ways.

Lc3 is associated with the entire vesicle in the majority (77%) of vesicles containing bacteria at 0dpi, which is not significantly different at (50%) at 1dpi (Fig 5.15 A). This highlights that early in infection, Lc3 is recruited to the *S. aureus* vesicle in the majority of cases and therefore suggests that autophagy machinery is involved in the host neutrophils response to *S. aureus*. Vesicles containing *S. aureus* are significantly more likely to have Lc3 puncta associated at 0dpi, (Fig 5.15 B), although most bacteria is cleared by 1dpi. However, there is no significant change in the association of Lc3 puncta to *S. aureus* in the cytoplasm over time (Fig 5.15 C). Together these data suggest Lc3 associates with *S. aureus* vesicles, and due to the lack of *S. aureus* at 1dpi, likely marks vesicles before degradation or bacterial escape.

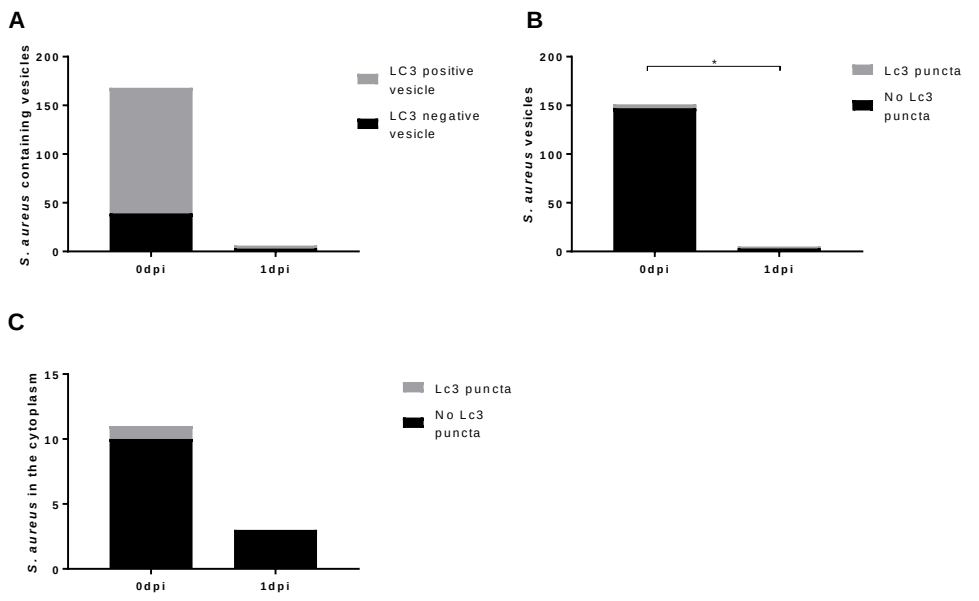

<u>Figure 5.15</u> Lc3 can associate to *S. aureus* in neutrophil infection

2500cfu of GFP *S. aureus* injected into *Tg(lyzC:RFP.GFP.Lc3)*, larvae imaged in the CHT at 2hpi (0dpi) and 26hpi (1dpi). **A** Lc3 association to the entire *S. aureus* vesicle at 0dpi and 1dpi (ns, Fisher's test, n =3, 17 0dpi larvae, 11 1dpi larvae) **B** The number of *S. aureus* vesicles with Lc3 puncta (*p<0.05, Fisher's test, n =3, 17 0dpi larvae, 11 1dpi larvae) **C** The number of *S. aureus* events in the cytoplasm with Lc3 puncta at 0dpi and 1dpi (ns, Fisher's test, n =3, 17 0dpi larvae, 11 1dpi larvae).

Neutrophil handling of *C. neoformans* involves Lc3 recruitment

Neutrophil handling of *C. neoformans* is not thought to be important in the infection outcome of cryptococcal infection, with macrophages thought to be key in fungal control. To determine whether neutrophils are important in the control of cryptococcal infection is the present study, *C. neoformans* was injected into *Tg(lyz:nsfB-mCherry)* larvae, which have the *nsfB* gene expressed in neutrophils. The *nsfB* gene encodes nitroreductase which converts pro-drug metronidazole into a cytotoxic metabolite which kills the cell it is expressed in, and therefore treatment of larvae with metronidazole can leads to specific ablation of neutrophils (Pisharath et al. 2007).

The ability of metronidazole treatment to ablate neutrophils was first confirmed, preliminary data shows at 3dpi a significant reduction in the number of neutrophils within each larvae is shown for metronidazole treated larvae in comparison to non-treated larvae (Fig. 5.16 A). However, preliminary data shows that at 3dpi the fungal burden was not changed in larvae treated with metronidazole (Fig. 5.16 B). These data suggest that neutrophil ablation does not affect fungal growth in zebrafish.

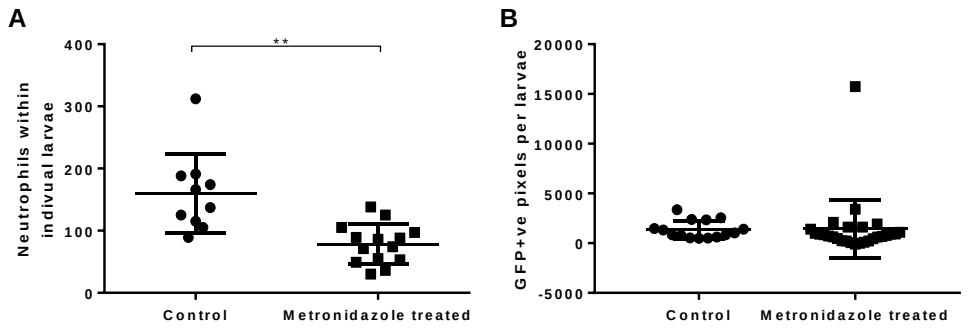

Figure 5.16 Neutrophil ablation does not alter fungal burden

1000cfu of GFP *C. neoformans* injected into *Tg(lyz:nsfB:mCherry)*, larvae imaged at 3dpi (5dpf)). **A** The number of neutrophils present 3dpi in control and metronidazole treated larvae (**p<0.01 Mann-Whitney t-test, n=2, 10-14 larvae per group) **B** The GFP positive pixels (fungal burden) at 3dpi in control and metronidazole treated larvae (ns, Mann-Whitney t-test, n=2, 15-27 larvae per group)

Multiple Lc3 interactions were observed after *C. neoformans* infection of the neutrophil specific Lc3 reporter larvae. Cryptococcal cells which had been phagocytosed were observed in neutrophil vesicles, with or without Lc3 marking the entire vesicle, as

shown in Figure 5.17 A, B. Vesicles containing cryptococci may also have Lc3 puncta (Figure 5.17 C). This highlights that Lc3 is involved in neutrophil handling of *C. neoformans*. Interestingly, in some cases *C. neoformans* was observed surrounded by RFP fluorescence, but not GFP (Fig 5.17 D). It is tempting to propose that this represents Lc3 on the acidic inside of a cryptococcal vesicle, perhaps resulting from a recently lysed neutrophil.

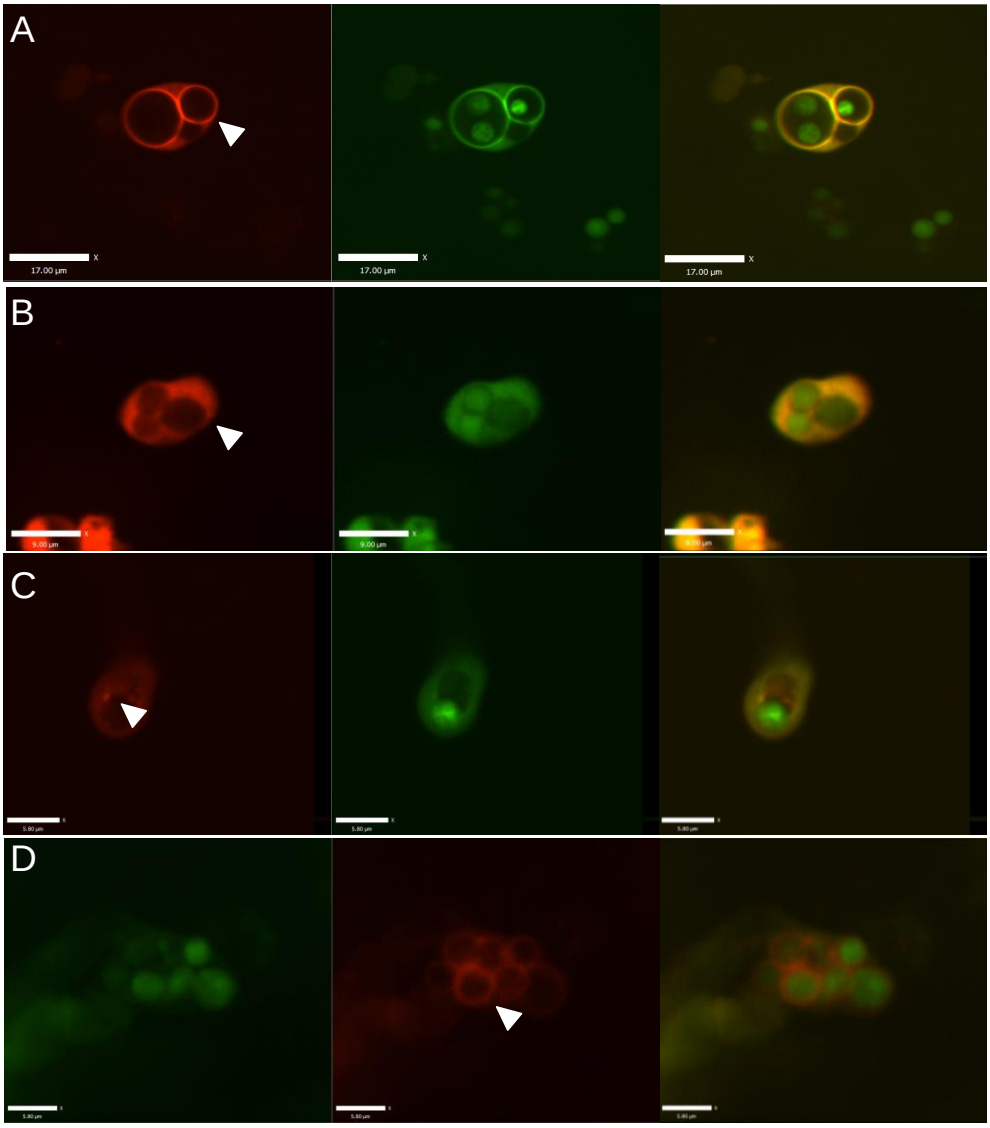

<u>Figure 5.17</u> Lc3 can mark *C. neoformans* vesicles

1000cfu of GFP *C. neoformans* injected into *Tg(LyzC:RFP.GFP.Lc3)*, larvae imaged in the CHT at 2hpi (0dpi) and 26hpi (1dpi). White arrows point at specific examples **A** *C.neoformans* with Lc3 marking the entire vesicle, scale 17um **B** *C. neoformans* without Lc3 marking the entire vesicle, scale 9um **C** vesicle containing *C. neoformans* with Lc3 puncta, scale 5.8um **D** *C. neoformans* was observed surrounded by RFP fluorescence, but not GFP, scale 5.8um.

A significant reduction of the number of neutrophils which contain cryptococcal cells is observed between 0dpi and 1dpi (Fig. 5.18 A, B), which may indicate fungal clearance from within the neutrophil, or an increase in overall neutrophil number. No significant increase in cryptococcal cells was observed within individual neutrophils (Fig 5.18 C) which suggests that intracellular growth or additional phagocytosis does not occur. Cryptococcal cells within RFP positive (but not GFP) vesicles, are observed on 0 and 1dpi, but more often on 1dpi, although not significantly (Fig. 5.18 D). The number of cryptococcal cells observed within a single RFP positive neutrophil is increased at 1dpi compared to 0dpi (Fig. 5.18 E). Together these data suggest that *C. neoformans* is phagocytosed by neutrophils during infection. The limited data on RFP positive vesicles

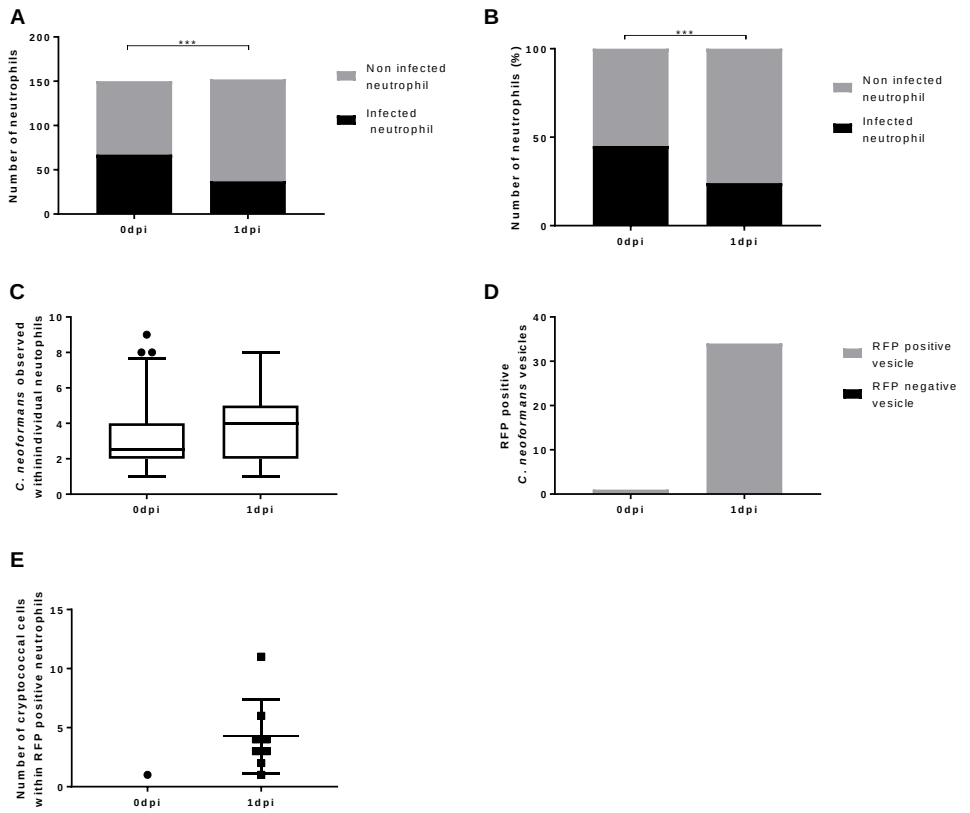

Figure 5.18 Neutrophil handling of *C. neoformans*

1000cfu of GFP *C. neoformans* injected into *Tg(LyzC:RFP.GFP.Lc3)*, larvae imaged in the CHT at 2hpi (0dpi) and 26hpi (1dpi). **A** The number of infected or non-infected neutrophils at 0dpi and 1dpi (***p<0.001 Fisher's test, n=3, 24 0dpi larvae, 14 1dpi larvae) **B** The proportion of infected or non-infected neutrophils at 0dpi and (***p<0.001 Fisher's test, n=3, 24 0dpi larvae, 14 1dpi larvae) **C** The number of cryptococcal cells observed within neutrophils at 0dpi and 1 dpi (ns, Mann-Whitney t-test, n=3, 24 0dpi larvae, 14 1dpi larvae) **D** The number of *C. neoformans* events observed in a RFP positive vesicle at 0dpi or 1dpi (ns Fisher's test, n=3, 24 0dpi larvae, 14 1dpi larvae) **E** The number of *C. neoformans* events observed in RFP vesicles 0dpi or 1dpi.

may suggest that a larger number of fungal cells within individual neutrophils, seen on 1dpi, results in the occurrence RFP positive neutrophils/vesicles.

Lc3 was observed to associate with entire cryptoccocal vesicles and as puncta which associate to the cryptococcal vesicle (Fig. 5.17). The number of cryptococcal vesicles marked by Lc3 significantly decreases from 0dpi to 1dpi (Fig. 5.19 A, B). Similarly, Lc3 puncta associated with cryptococcal vesicles is significantly decreased from 0dpi to 1dpi (Fig. 5.19 C). These data suggest that Lc3 mark cryptococcal vesicles early in infection, and perhaps suggests that Lc3 marked vesicles are degraded during infection.

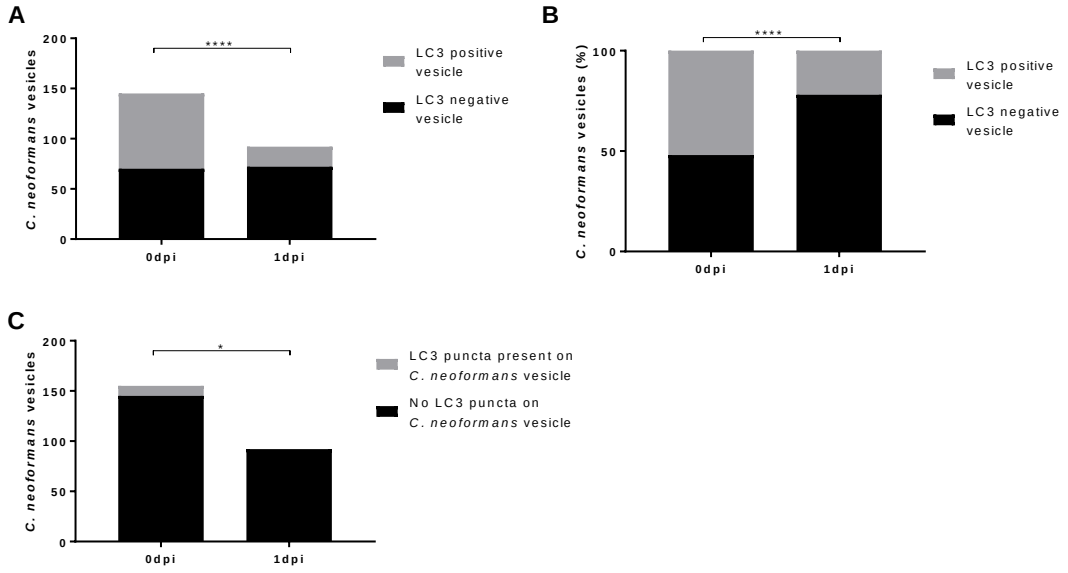

<u>Figure 5.19</u> Lc3 is present on *C. neoformans* vesicles during infection

1000cfu of GFP *C. neoformans* injected into *Tg(LyzC:RFP.GFP.Lc3)*, larvae imaged in the CHT at 2hpi (0dpi) and 26hpi (1dpi). **A** The number of Lc3 associated *C. neoformans* vesicles at 0dpi and 1dpi (****p<0.0001 Fisher's test, n=3, 24 0dpi larvae, 14 1dpi larvae) **B** The proportion of Lc3 associated to *C. neoformans* vesicles at 0dpi and 1dpi (****p<0.0001 Fisher's test, n=3, 24 0dpi larvae, 14 1dpi larvae) **C** The number of Lc3 puncta associated to *C. neoformans* vesicles at 0dpi and 1dpi (*p<0.05 Fisher's test, n=3, 24 0dpi larvae, 14 1dpi larvae)

Overall, it is clear that for both *S. aureus* and *C. neoformans* infection Lc3 can mark both pathogens' vesicles in neutrophils, and for both pathogens there is a reduction in Lc3 association throughout infection. This implicates autophagic machinery, Lc3, in the neutrophil host response to *S. aureus* and *C. neoformans* infections.

5.2.7 Infection of traffic light Lc3 reporter line in autophagy mutant background

To determine whether Lc3 association to *S. aureus* and *C. neoformans* in infection (within neutrophils) is important as a host defence or subversion by pathogens, the autophagy mutant lines were crossed into the traffic-light Lc3 line. The resulting lines, when in-crossed, allow visualisation of RFP.GFP.Lc3 in neutrophils, in addition to being *atg3* or *atg5* homozygous, heterozygous or wild-type siblings. The effects of the lack of *atg3* or *atg5* on Lc3 recruitment to each pathogen is next investigated.

Autophagy mutant neutrophil handling of *S. aureus*

Neutrophils were able to phagocytose *S. aureus* in *atg3* homozygous, heterozygous and wild-type siblings, no significant difference in the number of infected neutrophils between any genotype was found at each time point, however a significant reduction in infected neutrophils was observed between 0dpi and 1dpi for the same genotype group (Fig. 5.20 A, B). Similarly, neutrophils were able to phagocytose *S. aureus* in all *atg5* genotypes, at a similar rate within the same time points of 0dpi and 1dpi, but a significantly reduced number of infected neutrophils was observed for corresponding genotypes between 0dpi and 1dpi (Fig. 5.20 C, D). This suggests that neutrophils in *atg3* and *atg5* homozygous mutants phagocytose *S. aureus* at similar rates throughout the time infection time course, which includes a reduction of infected neutrophils at 1dpi from 0dpi, (which was also observed in the non-mutant background) (Fig 5.13 A, B above).

Lc3 recruitment is significantly reduced to *S. aureus* containing vesicles in neutrophils from *atg3* homozygous in comparison to wild-type siblings (Fig. 5.21 A, B). This suggests that Lc3 is not efficiently recruited to *S. aureus* vesicles when *atg3* is missing. Interestingly, the *atg3* heterozygous larvae also have significantly reduced Lc3 recruitment to *S. aureus* vesicles, this may suggest that heterozygous larvae have Lc3 recruitment defects. Lc3 recruitment is significantly reduced to *S. aureus* containing vesicles in neutrophils from *atg5* homozygous mutants, in comparison to both heterozygous and wild-type siblings (Fig. 5.21 C, D). This suggests that Lc3 recruitment does not efficiently mark *S. aureus* vesicles under *atg5* deficient conditions.

Although neutrophils in *atg3* or *atg5* homozygous appear to phagocytose at a similar rate throughout infection, leading to a similar number of infected vs non-infected neutrophils in comparison to wild-type siblings, any changes in Lc3 recruitment could be caused by differences in the amount of phagocytosed material and subsequent availability of Lc3. For example, if a neutrophil contained 6 *S. aureus* vesicles, fewer vesicles may be marked by Lc3 in comparison to a neutrophil containing 2 *S. aureus*

vesicles. The number of *S. aureus* vesicles within neutrophils was compared to determine whether neutrophils from *atg3* or *atg5* homozygous larvae phagocytose *S. aureus* in similar quantities.

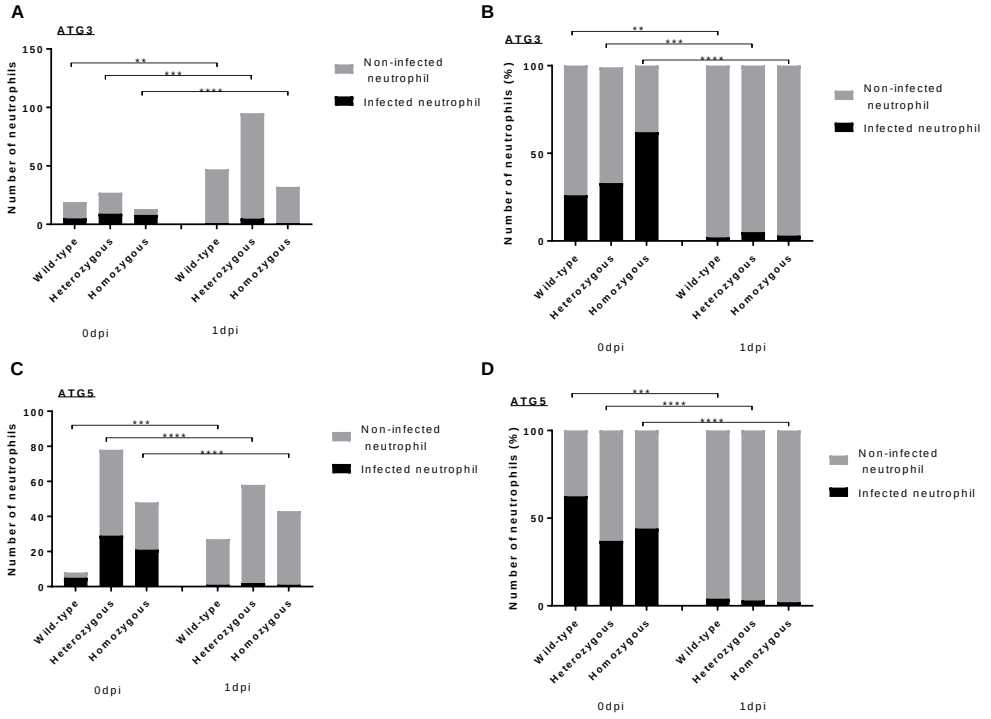

<u>Figure 5.20</u> Neutrophil handing is not changed in *S. aureus* infection in autophagy mutants

2500cfu of GFP *S. aureus* injected into an incross of either *atg3*$^{+/-}$* *Tg(LyzC:RFP.GFP.Lc3)*, or *atg5*$^{+/-}$**Tg(LyzC:RFP.GFP.Lc3)*, larvae imaged in the CHT at 2hpi (0dpi) and 26hpi (1dpi). **A** The number of infected or non-infected neutrophils in *atg3*$^{+/-}$* *Tg(LyzC:RFP.GFP.Lc3),* grouped by genotype at 0dpi and 1dpi (n=3, 17 larvae at 0dpi, and 20 larvae at 1dpi, **<p0.01, ***p<0.001, ****p<0.0001 Fisher's exact test) **B** The proportion of infected or non-infected neutrophils in *atg3*$^{+/-}$* *Tg(LyzC:RFP.GFP.Lc3),* grouped by genotype at 0dpi and 1dpi (n=3, 17 larvae at 0dpi, and 20 larvae at 1dpi, **<p0.01, ***p<0.001, ****p<0.0001 Fisher's exact test) **C** The number of infected or non-infected neutrophils in *atg5*$^{+/-}$* *Tg(LyzC:RFP.GFP.Lc3),* grouped by genotype at 0dpi and 1dpi (n=3, 24 larvae at 0dpi, and 19 larvae at 1dpi, ***p<0.001, ****p<0.0001 Fisher's exact test) **D** The proportion of infected or non-infected neutrophils in *atg5*$^{+/-}$* *Tg(LyzC:RFP.GFP.Lc3),* grouped by genotype at 0dpi and 1dpi (n=3, 24 larvae at 0dpi, and 19 larvae at 1dpi, ***p<0.001, ****p<0.0001 Fisher's exact test)

No significant difference in the number of *S. aureus* containing vesicles was observed for homozygous, heterozygous or wild-type siblings for either *atg3* (Fig. 5.22 A), or *atg5* larvae (Fig. 5.22 B). This suggests that the reduction Lc3 recruitment in autophagy mutants is not caused by differences in the amount of *S. aureus* phagocytosed.

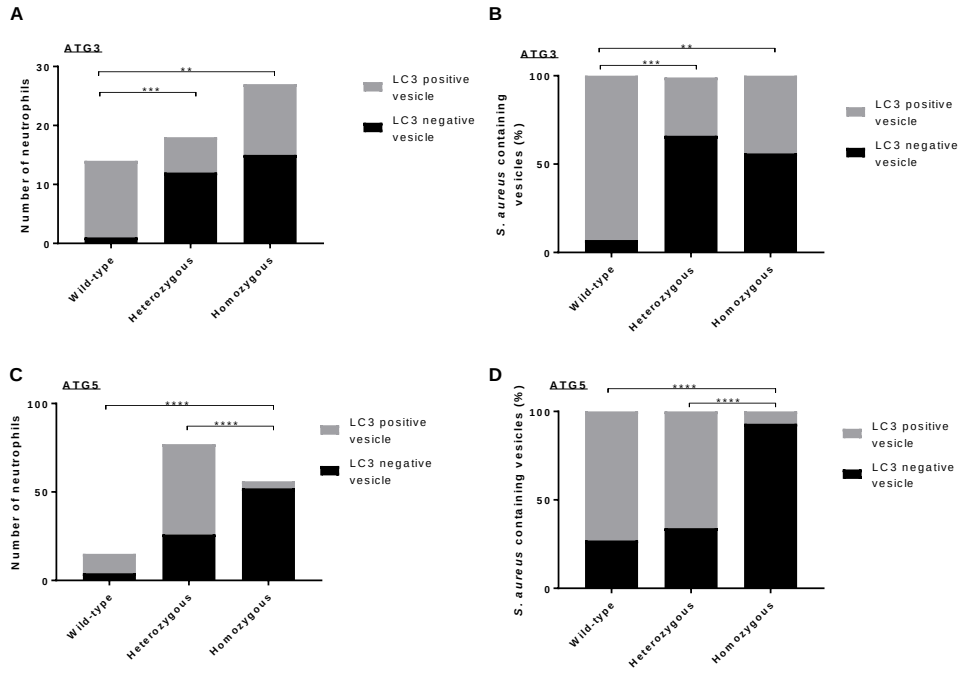

<u>Figure 5.21</u> Lc3 recruitment is reduced to *S. aureus* vesicles in autophagy mutants

2500cfu of GFP *S. aureus* injected into an incross of either *atg3*$^{+/-}$**Tg(LyzC:RFP.GFP.Lc3)*, or *atg5*$^{+/-}$**Tg(LyzC:RFP.GFP.Lc3)*, larvae imaged in the CHT at 2hpi (0dpi) and 26hpi (1dpi). **A** The number of *S. aureus* containing vesicles in neutrophils with or without Lc3 recruitment in *atg3*$^{+/-}$**Tg(LyzC:RFP.GFP.Lc3),* grouped by genotype at 0dpi (n=3, 17 larvae at 0dpi, ***p<0.001, ****p<0.0001 Fisher's exact test) **B** The proportion of *S. aureus* containing vesicles in neutrophils with or without Lc3 recruitment in *atg3*$^{+/-}$**Tg(LyzC:RFP.GFP.Lc3),* grouped by genotype at 0dpi (n=3, 17 larvae at 0dpi, **p<0.01, ***p<0.001 Fisher's exact test) **C** The number of *S. aureus* containing vesicles in neutrophils with or without Lc3 recruitment in *atg5*$^{+/-}$**Tg(LyzC:RFP.GFP.Lc3),* grouped by genotype at 0dpi (n=3, 24 larvae at 0dpi, ****p<0.0001 Fisher's exact test) **D** The proportion of *S. aureus* containing vesicles in neutrophils with or without Lc3 recruitment in in *atg5*$^{+/-}$**Tg(LyzC:RFP.GFP.Lc3),* grouped by genotype at 0dpi (n=3, 24 larvae at 0dpi, ****p<0.0001 Fisher's exact test)

Together these data suggest that a similar number and proportion of neutrophils phagocytose *S. aureus* throughout infection, and that the amount of *S. aureus* phagocytosed is similar for *atg3* or *atg5* larvae of homozygous, heterozygous and wild-type genotypes. This suggests that the reduction in Lc3 recruitment to *S. aureus* vesicles in neutrophils of *atg5* homozygous, and in *atg3* heterozygous and homozygous larvae, is not caused by differences in phagocytic ability of neutrophils. Although a reduction of Lc3 recruitment is observed in autophagy mutants, any potential differences in the outcome of *S. aureus* residing in Lc3 negative or Lc3

positive vesicles, for example increased bacterial survival or escape from vesicles/neutrophils, presents an exciting research area, which unfortunately could not be further investigated due to time restrictions.

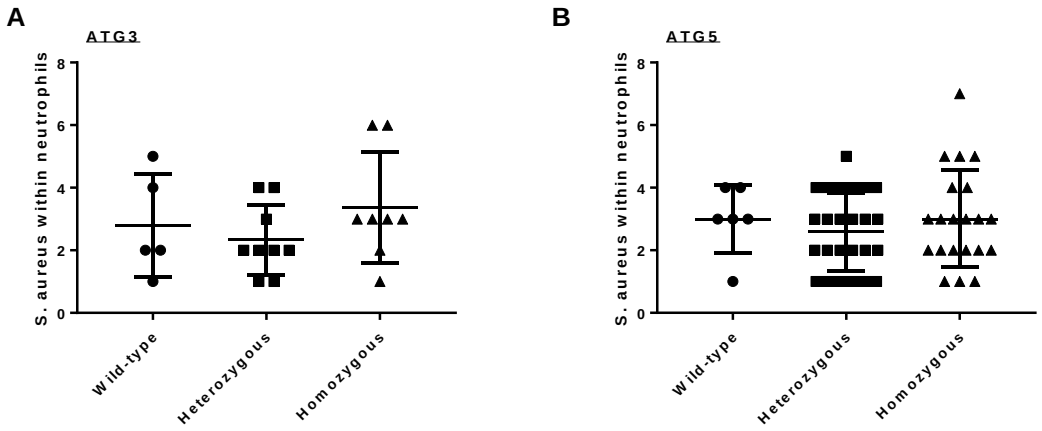

Figure 5.22 The number of *S. aureus* vesicles contained within neutrophils is not changed in autophagy mutants

2500cfu of GFP *S. aureus* injected into an incross of either *atg3*$^{+/-}$** *Tg(LyzC:RFP.GFP.Lc3)*, or *atg5*$^{+/-}$**Tg(LyzC:RFP.GFP.Lc3)*, larvae imaged in the CHT at 2hpi (0dpi). **A** The number of S. aureus vesicles contained within individual neutrophils from an in-cross of *atg3*$^{+/-}$**Tg(LyzC:RFP.GFP.Lc3)* grouped by genotype, imaged at 0dpi (n=3, 17 larvae, not significant, One-way ANOVA (Kruskal-Wallis test, +/- SD) **B** The number of S. aureus vesicles contained within individual neutrophils from an in-cross of *atg5*$^{+/-}$**Tg(LyzC:RFP.GFP.Lc3)* grouped by genotype, imaged at 0dpi (n=3, 24 larvae, not significant, One-way ANOVA (Kruskal-Wallis test, +/- SD)

Autophagy mutant neutrophil handling of *C. neoformans*

Neutrophils were able to phagocytose *C. neoformans* in *atg3* homozygous, heterozygous and wild-type siblings, no significant difference in the number of infected neutrophils between any genotype was found at each time point of 0dpi or 1dpi. However, for *atg3* heterozygous larvae a significant difference in the proportion of infected, non-infected and RFP-only positive neutrophils was observed between 0dpi and 1dpi, with a reduction in infected neutrophils (Fig. 5.23 A, B). The number of non-infected neutrophils is not significantly changed by 1dpi for homozygous and wild-type siblings, although an increase in RFP-only positive neutrophils was observed.

Neutrophils were able to phagocytose *C. neoformans* in all *atg5* genotypes, with no significant difference in the proportion of infected, non-infected or RFP-only positive neutrophils within the same time points of 0dpi or 1dpi in any genotype (Fig 5.23 C, D). For *atg5* homozygous, heterozygous and wild-type siblings, a significant change in the proportion of infected, non-infected or RFP-only positive neutrophils between 0dpi and 1dpi (for corresponding genotypes), was observed, with a reduction in infected neutrophils and increase in RFP-only neutrophils.

These data suggest that neutrophils in *atg3* and *atg5* homozygous mutants phagocytose *C. neoformans* at similar rates as neutrophils from wild-type and heterozygous larvae, throughout the time infection time course. This includes a reduction of infected neutrophils and increase in RFP-only positive neutrophils at 1dpi from 0dpi, (as observed in the non-mutant background) (Fig. 5.18 above).

The recruitment of Lc3 to *C. neoformans* vesicles within neutrophils was next examined, to determine whether a difference in Lc3 recruitment occurs in autophagy deficient larvae. There was a significant decrease in Lc3 marking of *C. neoformans* vesicles of *atg3* heterozygous and homozygous larvae in comparison to wild-type larvae at 0dpi, but not significant changes between genotypes at 1dpi (Fig. 5.24 A, B). However, between 0 and 1dpi, a significant decrease in Lc3 positive cryptococcal vesicles was observed only for wild-type larvae (Fig 5.24 A, B). These data suggest that early in infection *atg3* deficiency may reduce Lc3 marking of cryptococcal vesicles, but by 1dpi no difference is observed, despite a decrease in Lc3 positive vesicles observed over time for wild-type siblings.

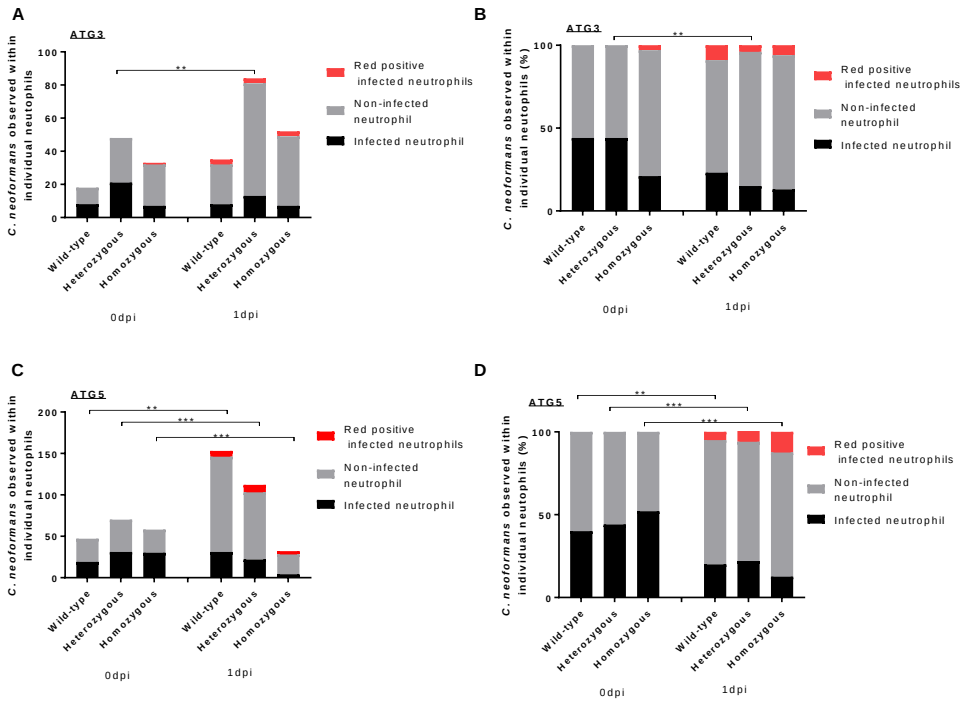

Figure 5.23 Neutrophil handing is not changed in *C. neoformans* infection in autophagy mutants

1000cfu of GFP *C. neoformans* injected into an incross of either *atg3*$^{+/-}$**Tg(LyzC:RFP.GFP.Lc3)*, or *atg5*$^{+/-}$**Tg(LyzC:RFP.GFP.Lc3)*, larvae imaged in the CHT at 2hpi (0dpi) and 26hpi (1dpi). **A** The number of infected or non-infected neutrophils in *atg3*$^{+/-}$**Tg(LyzC:RFP.GFP.Lc3),* grouped by genotype at 0dpi and 1dpi (n=3, 16 larvae at 0dpi, and 19 larvae at 1dpi, **<p0.01, Chi square test) **B** The proportion of infected or non-infected neutrophils in *atg3*$^{+/-}$**Tg(LyzC:RFP.GFP.Lc3),* grouped by genotype at 0dpi and 1dpi (n=3, 16 larvae at 0dpi, and 19 larvae at 1dpi, **<p0.01, Chi square test) **C** The number of infected or non-infected neutrophils in *atg5*$^{+/-}$* *Tg(LyzC:RFP.GFP.Lc3),* grouped by genotype at 0dpi and 1dpi (n=3, 32 larvae at 0dpi, and 19 larvae at 1dpi, **p<0.01, ***p<0.001, Chi square test) **D** The proportion of infected or non-infected neutrophils in *atg5*$^{+/-}$* *Tg(LyzC:RFP.GFP.Lc3),* grouped by genotype at 0dpi and 1dpi (n=3, 32 larvae at 0dpi, and 19 larvae at 1dpi, **p<0.01, ***p<0.001, Chi square test)

Similarly, a significant decrease in Lc3 marking of *C. neoformans* vesicles was seen for *atg5* heterozygous and homozygous larvae in comparison to wild-type larvae at 0dpi, but not significant changes between genotypes at 1dpi (Fig. 5.24 C, D). Again, between 0 and 1dpi, a significant decrease in Lc3 positive cryptococcal vesicles was observed only for wild-type larvae (Fig. 5.24 C, D). These data suggest that early in infection *atg5* deficiency may also reduce Lc3 marking of cryptococcal vesicles.

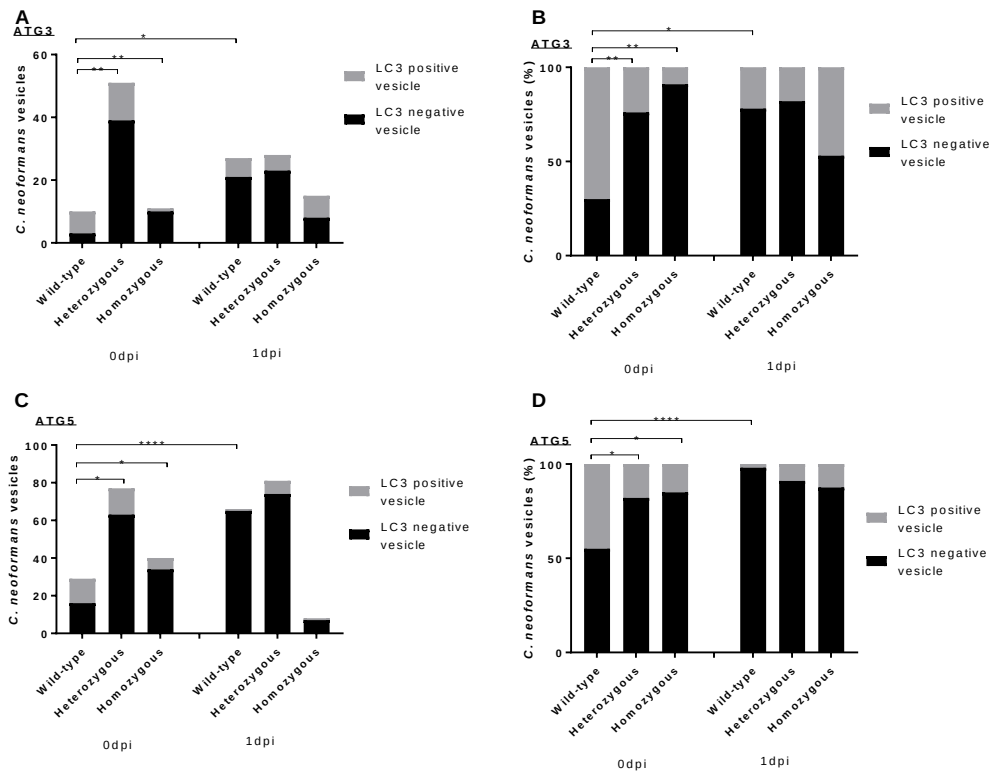

Figure 5.24 Lc3 recruitment is reduced to *C.neoformans* vesicles in autophagy mutants

1000cfu of GFP *C. neoformans* injected into an incross of either *atg3*$^{+/-}$**Tg(LyzC:RFP.GFP.Lc3)*, or *atg5*$^{+/-}$**Tg(LyzC:RFP.GFP.Lc3)*, larvae imaged in the CHT at 2hpi (0dpi) and 26hpi (1dpi). **A** The number of *C. neoformans* containing vesicles in neutrophils with or without Lc3 recruitment in *atg3*$^{+/-}$**Tg(LyzC:RFP.GFP.Lc3),* grouped by genotype at 0dpi and 1dpi (n=3, 16 larvae at 0dpi, and 19 larvae at 1dpi, *p<0.05, **p<0.01, Fisher's exact test) **B** The proportion of *C. neoformans* containing vesicles in neutrophils with or without Lc3 recruitment in *atg3*$^{+/-}$**Tg(LyzC:RFP.GFP.Lc3),* grouped by genotype at 0dpi and 1dpi (n=3, 16 larvae at 0dpi, and 19 larvae at 1dpi,, *p<0.05, **p<0.01, Fisher's exact test) **C** The number of *C. neoformans* containing vesicles in neutrophils with or without Lc3 recruitment in *atg5*$^{+/-}$**Tg(LyzC:RFP.GFP.Lc3),* grouped by genotype at 0dpi and 1dpi (n=3, 32 larvae at 0dpi, and 19 larvae at 1dpi, *p<0.05, ****p<0.0001 Fisher's exact test) **D** The proportion of *C. neoformans* containing vesicles in neutrophils with or without Lc3 recruitment in *atg5*$^{+/-}$**Tg(LyzC:RFP.GFP.Lc3),* grouped by genotype at 0dpi and 1dpi (n=3, 32 larvae at 0dpi, and 19 larvae at 1dpi, *p<0.05, ****p<0.0001 Fisher's exact test)

Neutrophils in *atg3* or *atg5* homozygous appear to phagocytose *C. neoformans* at 0dpi and 1dpi, leading to a similar number of infected vs non-infected neutrophils in comparison to wild-type siblings. The number of cryptococcal vesicles within individual neutrophils were compared to determine if any changes in Lc3 recruitment may be caused by differences in the amount of phagocytosed material and subsequent availability of Lc3.

No significant difference in the number of cryptococcal cells neutrophils contained was found for *atg3* or *atg5* larvae in any genotype, at 0dpi or 1dpi and at 1dpi in RFP positive neutrophils (Fig. 5.25 A, B). This suggests that the reduction of Lc3 marking of cryptococcal vesicles in autophagy mutants is not due to the amount of cryptococcal cells neutrophils contain.

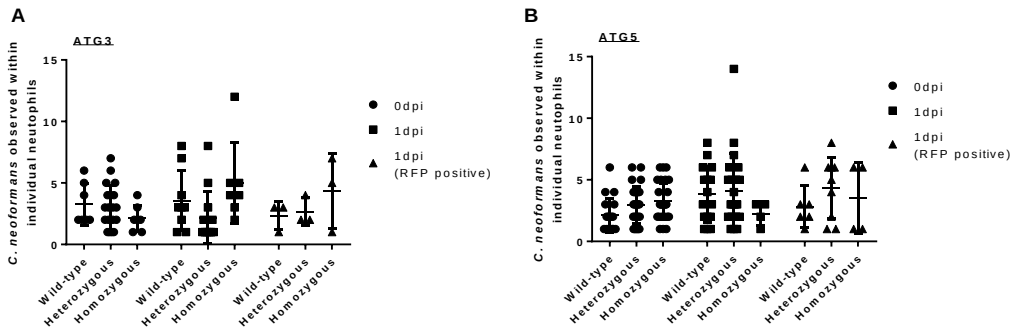

<u>Figure 5.25</u> The number of *C. neoformans* vesicles within neutrophils is not changed in autophagy mutants

1000cfu of GFP *C. neoformans* injected into an incross of either *atg3*$^{+/-}$**Tg(LyzC:RFP.GFP.Lc3)*, or *atg5*$^{+/-}$**Tg(LyzC:RFP.GFP.Lc3)*, larvae imaged in the CHT at 2hpi (0dpi) and 26hpi (1dpi). **A** The number of *C. neoformans* vesicles contained within individual neutrophils from an in-cross of *atg3*$^{+/-}$**Tg(LyzC:RFP.GFP.Lc3)* grouped by genotype, imaged at 0dpi and 1dpi (n=3, 16 larvae at 0dpi, and 19 larvae at 1dpi, not significant Two-way ANOVA, +/- SD) **B** The number of *C. neoformans* vesicles contained within individual neutrophils from an in-cross of *atg5*$^{+/-}$**Tg(LyzC:RFP.GFP.Lc3)* grouped by genotype, imaged at 0dpi and 1dpi (n=3, 32 larvae at 0dpi, and 19 larvae at 1dpi not significant, Two-way ANOVA, +/- SD)

Together these data suggest that a similar number and proportion of neutrophils phagocytose *C. neoformans* throughout infection, and that the number of cryptococcal cells phagocytosed is similar for *atg3* or *atg5* larvae of homozygous, heterozygous and wild-type genotypes. This suggests that the reduction in Lc3 recruitment to *C. neoformans* vesicles in neutrophils of *atg5* homozygous and heterozygous larvae, and in *atg3* heterozygous and homozygous larvae, at 0dpi, is not caused by differences in phagocytic ability of neutrophils.

A reduction of Lc3 recruitment to *C. neoformans* is observed in autophagy mutants at 0dpi. However, potential differences in the outcome of *C. neoformans* residing in Lc3 negative or Lc3 positive vesicles, for example in vomocytosis, or cryptococcal replication, presents an exciting future research area, which unfortunately could not be further investigated due to time restrictions.

5.2.8 Summary of infection of autophagy mutants

No significant change in larval survival is observed for either *atg3* or *atg5* larvae following *C. neoformans* infection. This was also observed for *atg5 S. aureus* infection. An increase of larval survival in *S. aureus* infection is seen for *atg3* homozygous and heterozygous fish. Next, further pressure was applied to the autophagy pathways through starvation. Under starvation conditions no significant changes in survival, after *S. aureus* and *C. neoformans* infection, was observed for *atg3* or *atg5* homozygous fish. Larval survival data may be complicated by off-target effects of the mutation which cause larval death without infection.

Fungal and bacterial burdens highlighted no significant difference between genotype and pathogen handling. However, preliminary data on fungal and bacterial burden with 3-MA treatment suggested an increase in pathogen load in *atg5* homozygous mutants, but requires further analysis.

Analysis of neutrophil cellular interactions may enable analysis which can circumvent the off target effects in both autophagy mutants which likely confounds larval survival analysis. A significant reduction in recruitment to Lc3 vesicles was observed for both autophagy mutants on the day of infection for both *S. aureus* and *C. neoformans* infection.

5.3 Chapter discussion

5.3.1 The role of host autophagy in handling of *S. aureus*

The first aim of this chapter was to establish whether *S. aureus* is handled by the autophagy pathway, specifically in regards to a role for both *atg3* and *atg5*. Although a reduction in autophagy levels in the mutants has not been clearly defined using Lc3 as an autophagy marker (chapter 4), it is still possible to use the autophagy mutants which do exhibit a clear phenotype linked to autophagy, to establish whether lack of *atg3* or *atg5* have any effect on pathogen handling.

Autophagy mutant survival of *S. aureus* infection

Firstly, inoculum dependant dose was shown to directly reduce larval survival infected with increasing numbers of *S. aureus* colony forming units. Previous data from a former lab member analysed the role of autophagy in *S. aureus* infection using bacterial loci as an endpoint of infection due to difficulties in genotyping fish after death. Using this end point, no change in bacterial infection was identified in *atg3* or *atg5* mutants (PhD thesis Lambein, 2015). However, by modifying the genotyping protocol for the *atg3* mutants to avoid a restriction site digest, genotyping of larvae which had died was

possible. Survival as an endpoint of infection may enable differences in fish survival during bacteraemia to be determined, which were not possible using the bacterial loci.

Using heterozygous in-crosses of each mutant, larval survival of bacterial infection of ~2500cfu was followed for 10dpf at IMCB. The infection time frame was extended from a maximum of 5dpf, to enable infection to be followed at time points after maternal contribution would end (see Chapter 4), where autophagic components may be under greater pressure. Of note, larval survival of *S. aureus* infection in autophagy mutants was overall very low irrespective of genotype, in comparison to the dose survival curves completed at the University of Sheffield. An explanation could be due to the difference in aquaria, as discussed above (see Chapter 4 discussion), where a higher pathogenic load or altered feeding regimes may explain differences between these experiments due to overall fish health and survival differences. However, the reduced survival of infected larvae meant that most fish did not survive longer than 4dpf, potentially when maternally contributed mRNA may still be present. It would be informative in future to use an even lower dose of *S. aureus*, or to infect at a later time, to enable the majority of fish to survive to a time point when maternal effects would have subsided.

There was no difference in survival of *atg5* heterozygous in-cross larvae infected with *S. aureus* between homozygous mutants, wild-type siblings or heterozygous larvae. On the other hand, *atg3* homozygous mutants and heterozygous larvae had significantly improved survival in comparison to wild-type siblings. Improved survival also seen in heterozygous, (not only homozygous) larvae suggests that normal *atg3* levels may be dependent on both alleles presence. These data suggest that *atg3* is important during *S. aureus* infection. It could be suggested that *S. aureus* uses autophagy which requires *atg3*, for its own survival, therefore when host autophagy is reduced *S. aureus* has reduced intracellular survival capabilities.

In an alternative *in vivo S. aureus* infection model, *S. aureus* infection in mice that were deficient in autophagy, specifically in ATG16 and LC3, an increase in lethality following bacterial infection was observed, despite a reduced bacterial burden (Maurer, Torres, et al. 2015). It was shown that a bacterial toxin (α-hemolysin) was responsible for lethality and autophagy enables tolerance (reduced susceptibility) of *S. aureus* (Maurer, Torres, et al. 2015). This suggests that host cell autophagy is beneficial for bacteria, since loss of autophagy reduced bacterial burden, (in agreement with the improved atg3 homozygous larvae survival after *S. aureus* infection data presented here), but equally autophagy is beneficial for the host enabling tolerance of a damaging toxin.

It has also been shown that host autophagy is required by *S. aureus* for improved bacterial replication and host bacterial control *in vitro*. This was demonstrated using mouse embryonic fibroblasts (MEFs) deficient in *atg5*-/-, whereby *S. aureus* had a reduced ability to replicate intracellularly in comparison to cells with *atg5* present (Schnaith et al. 2007). Interestingly, zebrafish that lack *atg5* did not have improved larval survival against *S. aureus* infection, suggesting that host *atg3* rather than *atg5* is important for bacterial survival in my model. This is interesting due to the closely related roles of *atg3* and *atg5* in the lipidation of LC3 and autophagosome formation. A similar effect on larval survival caused by *S. aureus* infection may be expected between *atg3* and *atg5* homozygous mutants.

However, an alternative study highlighted that autophagy was not useful for bacterial survival, where in *atg5*-/- MEFs had increased bacterial replication in comparison to *atg5*+/+ cells (Neumann et al. 2016). This indicates that the autophagy acting beneficially for *S. aureus* is likely very complex, where multiple factors may affect autophagy induction. A difference between these opposing studies is the bacterial strain used, which could cause these differences. Indeed, any differences in virulence factor expression could alter how host cell autophagy is affected by bacterial infection, such as the virulence factors controlled by the *agr* locus, which are required for host autophagy induction (Schnaith et al. 2007; O'Keeffe et al. 2015). It would be interesting to compare different *S. aureus* strains with and without certain virulence factor expressions effect on survival in autophagy mutants. It may be possible to observe opposing effects on larval survival depending whether toxins, such as α-hemolysin are present.

Importantly, general reduced survival in these experiments meant that the majority of larval infection did not overlap with time points in which larvae mutations may be fully effective, due to maternal contribution (see Chapter 4), so does not conclusively show that *atg3 or atg5* is important for *S. aureus* survival during infection.

Autophagy mutant survival of *S. aureus* infection with increased demand on the autophagy pathway

To investigate *S. aureus* infection when autophagy is under stress, fish were infected under starvation conditions, to place autophagy pathways under increased demand. Furthermore, larvae were infected with a lower dose of 500cfu in order to attempt to allow survival to later time points, specifically after maternal effects may have subsided. Despite the reduced inoculum, regardless of genotype, survival by 5dpf was only ~20%

for all infected fish, it would be informative in future experiments to inject with a further reduced inoculum.

For both *atg3* and *atg5* homozygous larvae, no change in survival was found in comparison to heterozygous and wild-type siblings after *S. aureus* infection and starvation. This suggests that autophagy is not important in the handling of *S. aureus* in zebrafish. Of note, the role of larval starvation, and the impact this may have on *S. aureus* virulence was not studied. It is possible that in autophagy deficient larvae have a reduced supply of nutrients, as are corresponding mouse models (Kuma et al. 2004; Sou et al. 2008), which are also unavailable for bacterial use, ultimately leading to a reduced bacterial virulence. It would be interesting to compare how bacterial survival and virulence is altered in nutrient deprived infection. In fact, in response to extreme nutrient starvation of *S. aureus,* ~99% bacterial death is observed with just a small proportion which are able to survive long term under starvation conditions. This small proportion of bacterial cells are able to become viable replicative cells when nutrients become available (Watson et al. 1998; Clements & Foster 1998). Therefore, it is possible that starvation of larvae, may also starve bacteria resulting in reduced bacterial virulence. To test this, starved or non-starved larvae could be homogenised, and *S. aureus* bacterial growth in non-starved and starved homogenate compared.

Both *atg3* and *atg5* homozygous mutants have reduced survival after 20dpf (chapter 4). The lack of either *atg3* or *atg5* is likely to have a more pronounced effect at this time, so infection at 20dpf was investigated. It is important to keep in mind that lethal mutation effects may override any potential change in survival due to *S. aureus* infection. *S. aureus* infection (2500cfu) of larvae at 20dpf highlighted no change in larval survival for both *atg3* and *atg5* homozygous mutants. Although *atg5* homozygous larvae may have reduced survival, but only a single homozygous larvae was infected. Unfortunately, after 20dpf, larval survival of *atg3* and *atg5* mutant homozygous larvae is reduced leading to difficulties in infecting enough homozygous larvae to gain statistically significant results. These data suggest that at time points where autophagy mutations become fatal, infection with *S. aureus* enhances mortality. Infection at 20dpf suggests that *atg5* autophagy mutant survival is reduced, but this may also be likely due to expected mutation effects at this time point. Indeed, if the homozygous larvae are already sick, infection with a pathogen is likely to further reduce survival. It is therefore not possible to conclude that this reduced survival is specifically caused by *S. aureus* and any change in host-pathogen interactions caused by the autophagy mutation.

To conclude, potential small changes in survival for are suggested, but overall *S. aureus* infection studies using the autophagy mutants are difficult to interpret. Early in infection, maternal contribution may effectively block any *atg3*-/- or *atg5*-/- specific effects, and equally later in infection the survival phenotype which is expected under non-infection conditions, may override any autophagy mutation effects. Larval survival analysis was not very informative as to the role of *atg3* and *atg5* mutations in *S. aureus* infection. To investigate the role further and avoid complication of survival at early and late stages of development, the rate of bacterial growth and the role of autophagy in mutants at a cellular level was next investigated.

Bacterial burden in autophagy mutants infected with *S. aureus*

The bacterial burden was compared between *atg3* or *atg5* homozygous, heterozygous and wild-type siblings during *S. aureus* infection. It may be expected that if host autophagy is important in the control of bacterial infection a larger bacterial burden would be present in homozygous larvae. However, for both *atg3* and *atg5* homozygous mutants, no significant difference in the bacterial burden was observed in comparison to heterozygous and wild-type siblings. This suggests that *atg3* and *atg5* are not important in the control of bacterial growth in the entire zebrafish. This may expected for bacteria which are able to survive extracellularly, where any alterations in autophagy would not affect bacterial growth. However, depletion of host cell (p62 mediated) autophagy through morpholino injection, was shown to increase zebrafish mortality and bacteria burden in *Shigella flexneri* infection (Mostowy et al. 2013), suggesting that autophagy knock-down in larvae can successfully allow observation of autophagy mediated pathogen handling at the organismal level.

Furthermore, the bacterial burden was compared between genotypes at the day before larval death, in order to determine whether the amount of bacteria present in larvae that causes death may be reduced for the homozygous autophagy mutants. However, there was no significant difference in the bacterial burden preceding larval death between any *atg3* or *atg5* genotype before 5dpf. This suggested that larvae deficient in *atg3* or *atg5* do not have increased susceptibility to *S. aureus* infection, and that deficient autophagy does not enable increased bacterial growth. Furthermore, the role of host cell autophagy as beneficial or detrimental for *S. aureus* is unclear, with data suggesting opposite observations (as discussed in section 1.4.7) and this may be due to the type of host cell *S. aureus* is invading, or the strain of *S. aureus*.

Of note these data were collected before 5dpf, and therefore may be unaffected due to maternal contribution. It would be very informative to investigate bacterial burden at

later time points, which was not possible as infection study at time points later then 5dpf were not approved in the UK. Overall it is not possible to confidently conclude that *atg3* and *atg5* deficiency does not alter bacterial burden in larvae, due to potential maternal contribution effects.

Autophagy mutant survival and bacterial burden of *S. aureus* infection with blocked *atg5*-independent autophagy

3-MA is an autophagy inhibitor, which inhibits PI3-Kinase activity, loss of which inhibits both classical autophagy and *atg5*-independent autophagy (Juenemann & Reits 2012). Additionally, *atg5*-independent autophagy has been linked to bacterial clearance. In intestinal epithelial cells *atg5*-independent autophagy is used to inhibit the survival of *Shigella flexneri* (Ra et al. 2016). In *Mycobacterium marinum* infection only a slight reduction in bacterial survival in *atg5*-/- MEFs was found. However, a role of *atg5*-independent autophagy in selective autophagy, in controlling sequestration of bacteria residing the cytoplasm has been demonstrated (Collins et al. 2009). It is therefore possible that despite *atg5* deficiency, some autophagy is still functional in the *atg5* homozygous mutants, which may be important in *S. aureus* clearance. However, no significant difference in larval survival of *S. aureus* infection with 3-MA treatment between any *atg5* genotype was shown. This suggests that *atg5*-independent autophagy does not play a role *S. aureus* infection control. However, larval survival analysis after infection, at a whole organism level, may not by informative because each autophagy mutation causes reduced survival independently of infection. Therefore, the bacterial burden was next analysed.

The bacterial burden of *atg5* homozygous mutants was significantly increased at both 2dpf and 5dpf in comparison to heterozygous and wild-type siblings. This suggests that *S. aureus* infection is not controlled in *atg5* homozygous mutants, also deficient in *atg5*–independent autophagy. In contrast, the bacterial burden, which caused larval death, was not significantly different between *atg5* genotypes, however additional analysis may lead to statistical significance for these preliminary data. Further analysis to examine whether 3-MA has any effect on bacterial virulence or viability is required to confirm these data.

These data suggest that *atg5* deficiency, coupled with *atg5*-independent autophagy inhibition leads to uncontrolled *S. aureus* infection. Therefore, host *atg5* and/or *atg5*-independent autophagy may be important in control of *S. aureus* infection. However, these conclusion require further investigation. For example, 3-MA is also able to block classical autophagy, presumably including any autophagy enabled through maternal

contribution at this age. It would be very useful to compare the bacterial burden in *atg5* homozygous larvae treated with alternative autophagy drugs, which will not affect induction of *atg5*-independent autophagy, in order to decipher whether *atg5*-independent autophagy alone is responsible for control of *S. aureus*.

To conclude, further analysis of bacterial burden, at later stages in infection may provide evidence that *atg3* or *atg5* is important in the control of *S. aureus* infection. However, preliminary data do indicate that *atg5* and/or *atg5*-indepednet autophagy is important in reducing bacterial burden, further work may provide interesting answer to exactly which type of autophagy is responsible.

Host neutrophil autophagy interactions with *S. aureus*

Cellular level interactions of *S. aureus* with the autophagosome marker Lc3-II in neutrophils were next examined, to potentially exclude off-target effects of each mutation, for example reduced larval survival. There is still potential that maternally encoded protein products could affect these experiments conducted at 2 and 3dpf. Neutrophils are a known intracellular niche for *S. aureus* (Prajsnar et al. 2012), so autophagy interactions could present a key host-pathogen interaction which may provide host protection, or that could be hijacked for the benefit of *S. aureus*.

Firstly *S. aureus* was injected into larvae with neutrophil specific traffic-light Lc3 expression, but not in an autophagy mutant background, to determine the normal neutrophil Lc3 interactions with *S. aureus*. The number of infected neutrophils is significantly reduced by 1dpi, (in comparison to 2hpi), with the majority of bacteria residing within a vesicle rather than cytoplasm at both time points. Finally, the number of intracellular bacteria within individual neutrophils significantly decreases over time.

Neutrophil degradation of the majority of bacteria has been previously demonstrated in the zebrafish infection model (Prajsnar et al. 2012), suggesting that most bacteria are expected to be degraded. These data indicate that throughout infection, *S. aureus* is phagocytosed by neutrophils, whereby bacteria are likely killed and degraded over time, as evidenced by the decrease in number of infected neutrophils and bacteria within them. However, although it is known that *S. aureus* successfully escapes the phagosome, there is currently no literature that addressed the dynamics of infection (e.g. how often and the speed of bacterial phagosome escape) so it has not been possible to compare the rates of phagosome escape of *S. aureus* that I have measured to other studies.

It is possible that bacterial cells are able to escape neutrophils through the use of multiple virulence factors (as introduced in Section 1.4.5). However, since only few

extracellular bacterial cells were observed at 1dpi (not quantified) it is more probable that bacterial degradation occurs. The limited number of bacteria observed in the cytoplasm may represent a small fraction of the bacterial population which have escaped the bacterial phagosome, and can persist in the neutrophil as described in *S. aureus* infection in zebrafish previously (Prajsnar et al. 2012).

The co-localisation of Lc3-II, that was shown to mark an entire staphylococcal vesicle, or as puncta on a vesicle to bacteria residing in the cytoplasm, determined that autophagic machinery is used in the host neutrophil response to *S. aureus*. In fact, the majority of bacteria that were resident in vesicles, were marked with Lc3 at 0dpi, clearly indicating that Lc3 can co-localise to *S. aureus*. Of note, the transgenic line over expresses the traffic light Lc3 construct, so although showing co-localisation can occur, it is not possible to conclude from these data whether endogenous Lc3 would mark so many vesicles. It is clear, however, that the autophagosome marker Lc3 co-localises to *S. aureus* in neutrophils which has been described before for non-professional phagocyte cells (Schnaith et al. 2007; Harada-Hada et al. 2014). Furthermore, an initial Lc3 recruitment, which is reduced over time was also observed for *S. aureus* in HeLa cells. Highest Lc3 recruitment of 90% was shown at 3hpi, and a reduction to basal levels in Lc3 recruitment seen by 5hpi (Schnaith et al. 2007). This is somewhat similar to data presented here but also utilises over expression of a GFP-LC3 vector. Using antibody staining of fixed samples in wild-type larvae or cells could confirm endogenous Lc3 acts in a similar manner. This Lc3 localisation to *S. aureus* may represent Lc3 recruitment to *S. aureus* containing autophagosomes, or to Lc3-assocaited phagosomes (LAP) as seen in *Shigella flexneri* infection of intestinal cells (Campbell-Valois et al. 2015). It is important to determine what type of vesicle *S. aureus* is residing in to be able to characterise whether LAP or autophagy is responsible for Lc3 co-localisation.

Very few bacteria were observed in neutrophils at 1dpi, suggesting bacteria are degraded by neutrophils, resultantly, it is difficult to conclude on any changes in Lc3 localisation over infection. A population bottleneck in *S. aureus* infection has been demonstrated in zebrafish, whereby a small number of bacterial cells evade immune cell degradation and are responsible for further uncontrolled infection. Therefore, it would be interesting to gather further data to examine whether Lc3 localisation to bacteria, particularly to bacteria resident in the cytoplasm, has any role in the bacterial population bottleneck process.

Autophagy involvement in Lc3 recruitment to *S. aureus* in neutrophils

To determine if *atg3* or *atg5* deficiency alters Lc3 recruitment to *S. aureus* vesicles at 0dpi, bacteria were injected into the neutrophil specific traffic light Lc3 line which was previously crossed to the *atg3* or *atg5* mutants. There was no difference in the number of neutrophils which were infected, or in the number of bacteria within neutrophils between *atg3* or *atg5* homozygous, heterozygous or wild-type siblings. This suggests that neutrophil ability to phagocytose are not detrimentally affected by either *atg3* or *atg5* deficiency. Therefore, since this presented data is early in infection (2hpi), any changes in bacterial survival/growth that may occur within autophagy deficient cells may not have been observed. Interestingly, when autophagy is blocked, either by 3-MA or by siRNA targeting *atg5* in human neutrophils, phagocytosis rates were reduced in pneumococcal infection (Ullah et al. 2017), although the mechanism behind this was not investigated. This suggests that autophagy can promote phagocytosis, but this is not suggested in the data presented in this study using *S. aureus* and may be caused by pathogen specific interactions. However, phagocytic ability was not directly studied in this study, and further analysis may provide better insight into the link between neutrophil autophagy and phagocytic ability.

A significant reduction of Lc3 localisation to *S. aureus* vesicles was found for *atg5* homozygous larvae in comparison to heterozygous and wild-type larvae at 0dpi. Furthermore, a significant reduction of Lc3 localisation to *S. aureus* vesicles was found for *atg3* homozygous and heterozygous larvae in comparison to wild-type larvae at 0dpi. These data highlight a reduction in Lc3 interactions with *S. aureus* (within a neutrophil) in autophagy deficient larvae, which have not been described before. Furthermore, it suggests that in autophagy deficient larvae, the recruitment of Lc3, and subsequent loss of Lc3, shown for zebrafish (above) and in HeLa cells (Schnaith et al. 2007) does not occur. This data is suggestive that both *atg3* and *atg5* mutants are not be able to efficiently produce Lc3-II, required for the marking of membranes, including *S. aureus* vesicles.

Importantly however, these data only highlight a reduction in Lc3 localisation to S. aureus in autophagy mutants. It is impossible to conclude that Lc3 recruitment is beneficial or detrimental for the bacteria. To determine if a lack of Lc3 recruitment to *S. aureus* is detrimental for the host, or bacteria, further analysis is required. For example, time lapse analysis following the fate of both the neutrophil, and bacteria in autophagy mutant larvae may reveal the role of host cell autophagy in *S. aureus* infection. Indeed, the outcome of altered autophagy interactions could present autophagy as a therapeutic target in treatment of infection. In order to circumvent larval survival issues, it might be useful to collect neutrophils from *atg5* larvae of different genotypes, and use

in vitro infection methodologies to examine the cellular interaction of Lc3 with *S. aureus*.

To conclude, Lc3 is shown to co-localise with *S. aureus* within neutrophils. The host Lc3 and *S. aureus* interaction may represent a host or pathogen derived interaction, future studies may reveal autophagy as a potential therapeutic target in *S. aureus* infection. A reduction in Lc3 recruitment to *S. aureus* in *atg3* and *atg5* mutants, which is not caused by defects in neutrophil phagocytosis, hints that autophagy could be manipulated to alter Lc3 interactions with *S. aureus*. However, it is important to determine whether Lc3 recruitment is beneficial to the host, or bacteria, and this presents an exciting research topic for the future.

5.3.2 The role of host autophagy in handling of *C. neoformans*

Alongside *S. aureus* infection, the other aim of this chapter was to determine whether *C. neoformans* is handled by the autophagy pathway, specifically in regards to the role of both *atg3* and *atg5*.

Autophagy mutant survival of *C. neoformans* infection

Inoculum dependant death was first proven to be responsible for reduced survival using wild-type larvae. This allows later experiments to exclude the possibility that handling related injuries cause larval mortality. A relatively high dose of 1000cfu is used for *C. neoformans* infection, which causes ~30-50% larval death at 3dpi, to enable visualisation of an increase or decrease in survival.

Survival of *C. neoformans* infection was increased to 10dpf (than the normal 5dpf endpoint) to extend infection time course until after the maternal contribution is expected to have stopped. Heterozygous in-crosses of either *atg3* or *atg5* homozygous mutants showed no significant difference in survival to AB wild-type fish. The aim was to determine whether an obvious survival change potentially expected in 25% of each heterozygous in-cross was identified. However, as only 25% of larvae were potentially homozygous, a non-obvious survival change may not be identified, as is likely in this case. Therefore, the survival assay was repeated with individually genotyped larvae.

To determine if *atg3* and *atg5* homozygous mutant survival of *C. neoformans* infection was changed, genotyping was performed (after infection experiments were completed) for each heterozygous in-cross. No change in survival was observed for *atg3* homozygous larvae in comparison to wild-type siblings and heterozygous larvae. Similarly, no significant change in survival was found between *atg5* homozygous larvae and wild-type siblings or heterozygous. Of note, the survival curves extend to 10dpf, (8dpi) later then maternal contribution, with survival reducing at a similar rate

independent of genotype over the entire time frame. This suggests that both *atg3* and *atg5* do not affect survival of *C. neoformans* infection, even after maternal contribution will have subsided, however Atg5 protein could be present until a maximum of 7dpf (see Chapter 4), at which point fungal burden may be so high that any differences in handling in autophagy mutants cannot be determined. These data are in contrast to a previous study that suggested that *C. neoformans* requires host cell autophagy (including *atg5*) for increased replication. This was demonstrated using RNAi to disrupt autophagy components in RAW 264.7 macrophages and led to decreased intracellular cryptococcal replication (Qin et al. 2011). A major difference between cellular and entire animal infections work is the ability of cryptococcal cells to survive and replicate outside of macrophages or other phagocytic cells. Furthermore, in myeloid cell specific *atg5*-/- mice no change in susceptibility to cryptococcal infection is observed (Nicola et al. 2012). This is in contrast to *Candida albicans* where mice showed increased susceptibility. Therefore, the murine model cryptococcal infection data agrees with data presented here, suggesting that at an entire organism level, *atg5* deficiency does not affect cryptococcal expansion.

This may be due to extracellular cryptococcal replication, which would not be controlled by myeloid cells. In zebrafish cryptococcal infection models, a shift from primarily extracellular to primarily intracellular resident cryptococci is seen at early stages of infection, although predominantly extracellular cryptococcal cell population is observed commonly later in infection (Bojarczuk et al. 2016). This might suggest that any influence that autophagy deficiency has on cryptococcal infection would be observed at early time points, however many cells are still extracellular. In the myeloid cell specific *atg5*-/- mice, a reduction in the activation of macrophages and inflammation was observed in the entire mouse lung following cryptococcal infection. It was also demonstrated that cryptococcal growth was increased in activated *atg5*-/- macrophages, (Nicola et al. 2012). Therefore, it is possible that where cryptococcal cells are residing intracellularly, activated macrophages may utilise autophagy in the host control of *C. neoformans*. It would be interesting to investigate the cellular interactions in both autophagy deficient mutants to determine if this is true in zebrafish, and for *atg3*.

Autophagy mutant survival of *C. neoformans* infection with increased demand on the autophagy pathway

To highlight any effects on larval survival autophagy deficiency causes, zebrafish autophagy was put under greater stress, using starvation conditions. Therefore, if autophagy mutations affect cryptococcal handling, this may be amplified due to an increase in autophagic machinery use in the entire larvae. A lower dose of 100cfu of *C.*

neoformans was used to enable larval survival to later stages of infection to after 10dpf, when starvation effects may begin (see Chapter 4). Homozygous *atg3* mutants showed no significant difference in larval survival in comparison to heterozygous and wild-type siblings. Equally, no significant difference in survival of *atg5* homozygous larvae in comparison to heterozygous and wild-type siblings was observed. However, further analysis could lead to statistical significance, where *atg5* homozygous mutants may have reduced survival after ~7-10dpf, this would be in keeping with the observed reduction in survival in non-infection starvation experiments, suggesting that *atg5* is not important in host-*C. neoformans* interactions. As discussed for *S. aureus* data above, starvation conditions may affect the nutrients available to *Cryptococcus*, and could therefore affect cryptococcal virulence or viability. *C. neoformans* growth is affected by nutrient availability. A lack of nutrients may also be expected in the *atg3* or *atg5* zebrafish mutants, much like the corresponding mouse models (Kuma et al. 2004; Sou et al. 2008), however this too requires further analysis. This may mean starvation of the larvae is also resulting in starvation of the pathogen and therefore analysis is required to determine if cryptococcal virulence is reduced. To test this, starved or non-starved larvae could be homogenised, and cryptococcal growth in non-starved and starved homogenate compared.

C. neoformans infection at 20dpf was completed to ascertain whether infection at later time points in development leads to changed mutant survival, where the mutation may be more effective since maternal contribution will have ablated. At 20dpf, a low number of viable homozygous larvae were present meaning further repeats are needed. Infection of *C. neoformans* with 1000cfu showed no change in survival for homozygous *atg3* larvae in comparison to heterozygous and wild-type siblings. This suggests that *atg3* is not important in *C. neoformans* infection. Comparison of *atg5* homozygous survival showed no significant change in survival in comparison to heterozygous and wild-type siblings, although further analysis may lead to statistical significance of reduced survival in homozygous larvae. Any reduced survival is likely caused by the deleterious effects of the mutation characterised above (see Chapter 4). Taking this into consideration, these data suggest *atg5* in not important in *C. neoformans* infection.

Similar to the *S. aureus* survival analysis above, larval survival of *C. neoformans* infection is not the most informative assay of host-pathogen interactions, and maternal contribution at early infection stages, in addition to survival defect after 20dpf, must be taken into consideration. However, in contrast to *S. aureus* infection, *C. neoformans* infection did progress at a constant rate with survival ~5% at 10dpf. This does allow stages between 5-10dpf for analysis free from survival and maternal effects. Although some small difference in survival are suggested, again no significant changes were

observed. Overall it is difficult to use survival of infection as a clear readout of autophagy if only subtle changes are occurring. No difference in cryptococcal infection using entire mice deficient in myeloid *atg5* is distinct from clear differences observed during cellular analysis of *atg5*-/- interactions with *C. neoformans* (Nicola et al. 2012). This suggests extracellular cryptococcal growth may conceal changes in infection outcome caused by autophagy handling at the cellular level in both zebrafish autophagy mutants. For this reason fungal growth dynamics and autophagy cellular interactions were next examined.

Fungal burden in autophagy mutants infected with *C. neoformans*

The fungal burden was compared between *atg3* or *atg5* homozygous, heterozygous and wild-type siblings during *C. neoformans* infection. It would be expected that if host autophagy is important in the control of cryptococcal infection a larger fungal burden would be present in autophagy mutant larvae.

In fact, at 5dpf, a significant decrease in fungal burden for *atg3* heterozygous and homozygous larvae, in comparison to wild-type siblings was observed. This suggested that host *atg3* is useful for fungal replication, and detrimental for the host. Indeed, it is reported that *C. neoformans* requires host cell autophagy for intracellular replication (Qin et al. 2011). It was recently demonstrated *in vivo* that cryptococcal infection leads to an increase in phosphorylation of both AMPKα or ULK-1 (both important in the initiation of autophagy), and that deletion of AMPKα in myeloid cells in mice leads to a reduction in fungal burden after infection (Pandey et al. 2017) suggesting that AMPKα, and therefore autophagy induction in myeloid cells increases susceptibility to cryptococcal infection.

However, for *atg5* homozygous mutants, no significant difference in the fungal burden was observed in comparison to heterozygous and wild-type siblings, suggesting *atg5* is not important in control of fungal growth. It is difficult to explain why *atg3,* but not *atg5,* is important in susceptibility to fungal growth, due to their intertwined roles in Lc3 lipidation and autophagosome formation. Furthermore, these experiments conducted at early developmental stages mean that maternal contribution may enable “normal” (*atg3* or *atg5*) autophagy function. However, the role of autophagy in promoting cryptococcal susceptibility may be *atg5*-independent. No change in cryptococcal susceptibility in myeloid *atg5* deficient mice was observed (Nicola et al. 2012), but was reduced in AMPKα myeloid deficient mice (Pandey et al. 2017). Therefore, *atg5*-independent autophagy in myeloid cells may be responsible for increased susceptibility to cryptococcal cells. The ability of *C. neoformans* to survive and replicate in the

extracellular environment, may further complicate this, as cellular autophagic control is not able to interact with extracellular fungal cells. For these reasons, it is likely that even if *atg3* or *atg5,* are both important in cryptococcal handing within phagocytes, it may not efficiently control fungal growth for the entire zebrafish, but may well be involved at the cellular level. Analysis of autophagy-cryptococcal interactions at the cellular level interactions are therefore required.

The fungal burden was also compared between mutant genotypes the day before larval death, to determine if the number of cryptococcal cells present in larvae causing death may be reduced for the homozygous autophagy mutants. No significant difference in the fungal burden preceding larval death between any *atg3* or *atg5* genotype before 5dpf was observed. This suggests that larvae deficient in *atg3* or *atg5* do not have increased susceptibility to cryptococcal infection, or that deficient autophagy does not enable increased fungal growth. Interestingly, previously published *in vitro* data suggest host autophagy is beneficial for cryptoccocal survival and replication (Qin et al. 2011). It would be interesting to examine the role of host cell autophagy on intracellular proliferation *in vivo* to enable further comparison.

These analysis were collected between 2dpf and 5dpf, and therefore may be still have functional autophagy proteins from maternal contribution (see Chapter 4). It would be very informative to investigate fungal burden at later time points, which was not possible as infection study at time points later then 5dpf were not ethically approved in the UK at the time and could not be completed at IMCB. Overall it is not possible to confidently conclude that *atg3* and *atg5* deficiency does or does not alter fungal burden in larvae, due to opposing *atg3* data and potential maternal contribution effects.

Autophagy mutant survival and fungal burden of *C. neoformans* infection with blocked *atg5*-independent autophagy

As described above, 3-MA is an autophagy inhibitor, which targets both classical and *atg5*-independent autophagy (Juenemann & Reits 2012). Although *atg5*-independent autophagy has been linked to bacterial clearance in intestinal cells (Ra et al. 2016), there are no publications on the role of *atg5*-independent autophagy in regards to fungal pathogens, although as suggested above *atg5*-independent autophagy may increase susceptibility to cryptococcal infection. It is possible that despite *atg5* deficiency, *atg5*-independent autophagy is functional in the *atg5* homozygous mutants, which may be useful in fungal clearance.

No significant difference in larval survival of *C. neoformans* infection with 3-MA treatment between any *atg5* genotype was observed. This suggests that *atg5*-independent autophagy does not play a role cryptococcal infection control. However,

as mentioned before, analysis at a whole organism level may not fully analyse any mutation and drugs effects, due to off target mutation effects, so the fungal burden was next analysed. The fungal burden of *atg5* homozygous mutants was not significantly different in comparison to heterozygous and wild-type siblings when treated with 3-MA, however, a trend towards increased fungal burden in homozygous (and to an extent heterozygous) larvae in comparison to wild-type larvae at 4 and 5dpf exists. Therefore, an increase in fungal burden at later time points is suggested. This suggests cryptococcal infection is not controlled in *atg5* homozygous mutants also deficient in *atg5*–independent autophagy and therefore suggests that *atg5* independent autophagy is beneficial for the host.

A preliminary comparison of the fungal burden preceding larval death was not significantly different between *atg5* genotypes. These data suggest that *atg5* deficiency, coupled with *atg5*-independent autophagy inhibition can block fungal growth as well as wild-type treated larvae. Therefore, host *atg5* and/or *atg5*-independent autophagy may be not important in control of *C. neoformans* infection. As described for corresponding *S. aureus* data, further investigation is required to determine whether *atg5*-independent autophagy alone is responsible for control of *C. neoformans*.

In conclusion, further investigation of fungal burden, at later stages in infection may provide evidence that *atg3* or *atg5* is important in the control of cryptococcal infection. However, preliminary data do indicate that *atg5* and/or *atg5*-independent autophagy is important in reducing *C. neoformans* burden, further work may provide interesting answers to exactly which type of autophagy is responsible, or if opposing roles are found.

Host neutrophil autophagy interactions with cryptococcal cells

In an attempt to analyse autophagy which may exclude potential off target effects of *atg3* or *atg5* mutations, cellular level interactions of *C. neoformans* with autophagosome marker Lc3-II in neutrophils were investigated. However, this still does not exclude the possibility that maternally encoded protein products could be present and affect these experiments conducted at 2 and 3dpf. Although macrophages, rather than neutrophils are considered a cryptococcal intracellular niche, there is evidence that neutrophils play a role in the control of cryptococcal infection. For example in myeloperoxidase mediated degradation of cryptococcal cells and in complement mediated responses to cryptococci (Sun et al. 2016b; Diamond et al. 1972). Despite this, neutrophil ablation data suggests that neutrophils are not required for control of fungal burden in these current experiments. While analysis within macrophages may have been ideal, suitable transgenic zebrafish lines were not available. Analysis of

cryptococcal-autophagy interactions within neutrophils, provides further evidence of cryptococcal interactions with neutrophils in a relatively under-studied (in relation to *C. neoformans*) innate immune cell.

The normal neutrophil Lc3 response to *C. neoformans* was first investigated by cryptococcal injection into larvae with neutrophil specific traffic-light Lc3 expression (not in an autophagy mutant background). The number of infected neutrophils, is significantly reduced at 1dpi, in comparison to 2hpi, although a similar number of neutrophils were analysed, suggesting that some neutrophils have degraded cryptococci, or that infected neutrophils were lysed. No significant increase in cryptococcal cells inside individual neutrophils over infection time course suggests none or limited fungal intracellular proliferation. These data suggest that neutrophils are able to effectively phagocytose cryptococcal cells, but that most cryptococcal cells are not degraded over time. In mouse models, clearance of intravascular cryptococcal cells has been shown require neutrophils (Sun et al. 2016a). Recent zebrafish cryptococcal infection data has also shown that neutrophils are important for clearance of intravascular cryptococcal cells (Davis et al. 2016). In fact, neutrophil mediated phagocytosis and killing of cryptococcal cells was shown to be important in the initial infection control, where neutrophil killing is superior to macrophage killing, and in control of cryptococcal cells which may escape from macrophage or endothelial cells later in infection (Davis et al. 2016). It may be likely that the reason more neutrophils are infected very early in infection is because most cryptococcal cells are extracellular, enabling neutrophil phagocytosis.

Of particular interest is the observation of “neutrophils” apparently containing cryptococcal cells, but in vesicles that are only RFP positive (rather than double GFP and RFP positive). It is tempting to speculate that this RFP fluorescent signal represents Lc3 on the inside of a cryptococcal phagosome, perhaps in cases where neutrophils have recently lysed, resulting in the loss of cytoplasmic GFP and RFP signal. The phagosome may retain its acidity resulting in the quenching of GFP signal and RFP signal remaining. Neutrophil phagosomes are not as acidic as macrophage phagosomes (Jankowski et al. 2002) and likely do not acidify enough to a pH less than 6 which is required to quench GFP (Murillo et al. 2001). It would be of interest to determine whether these RFP positive vesicles are acidic, perhaps by using pH sensitive dyes. This proposition may be supported by the observation that Lc3 molecules have been detected on cryptococcal cells which have escaped from macrophages non-lytically, however lipids which would represent a potential phagosome were not present on Lc3 positive cryptococcal cells (Nicola et al. 2012). It is unlikely that non-lytic escape is the cause of this interesting observation, since this

requires membrane fusion (Johnston & May 2010), which would not provide an acidic environment to provide just an RFP signal. A major difference is the cell type, of neutrophils used is this current study in comparison to most cryptococcal studies focussing on macrophages. It remains to be determined whether neutrophil lysis may be a major escape route for *Cryptococcus* from neutrophils, which may support this hypothesis. Interestingly, a small increase in the number of RFP only neutrophils is observed at 1dpi. Furthermore at 1dpi, an increase in the number of cryptococcal cells within RFP positive cells in observed. A large number of cryptococcal cells within the majority of RFP positive neutrophils may suggest that plasma membrane lysis could be caused by the physical presence of multiple cryptococcal cells. Time lapse imaging may provide good evidence of neutrophils lysis, which may also highlight a change from RFP/GFP signal to RFP signal alone. If this is proven correct, cryptococcal cells able to "hide" within host phagosomes in the extracellular environment may prevent phagocytosis and ultimately provide a possible "extra-cellular phagosome niche", which could potentially be an important stage in cryptococcal pathogenesis.

The co-localisation of Lc3-II to cryptococcal cells shown to mark an entire cryptococcal vesicles, or mark as puncta on cryptococcal vesicles, determined that autophagic machinery can mark cryptococcal phagosomes in the host neutrophil response to *C. neoformans*. This is consistent with other reports that Lc3 can mark cryptococcal vesicles (Nicola et al. 2012; Qin et al. 2011). A small majority of neutrophil cryptococcal vesicles were marked with Lc3 at 0dpi, however this was significantly reduced at 1dpi. Puncta were also significantly less likely to mark cryptococcal vesicles at 1dpi in comparison to 0dpi. These data suggest that an autophagy response occurs after phagocytosis of cryptococcal cells in neutrophils. A reduction of Lc3 marking of cryptococcal vesicles over time was also demonstrated in macrophage cells *in vitro,* whereby Lc3 marking was lost after 3hpi (Qin et al. 2011). This suggests an immediate autophagy response occurs, early after phagocytosis. Of note, the transgenic line over expresses the traffic light Lc3 construct, so although showing co-localisation can occur, it is not possible to conclude from this data whether endogenous Lc3 would mark as many vesicles. It would be very interesting to determine whether Lc3 recruitment in beneficial for the host or the fungal cell, and what outcome this may have on infection outcome.

To determine whether *atg3* or *atg5* deficiency alters Lc3 recruitment to cryptococcal vesicles at 0dpi and 1dpi, cryptococcal cells were injected into the neutrophil specific traffic light Lc3 line which was previously crossed to the *atg3* or *atg5* mutants. Importantly, no difference in the number of neutrophils which were infected, or to the number of yeast cells within neutrophils was found between *atg3* or *atg5* homozygous,

heterozygous or wild-type siblings at each individual time point. This suggests that phagocytosis occurs at a similar rate in neutrophils within larvae of all *atg3* or *atg5* genotypes throughout infection. However, between 0dpi and 1dpi, the number of infected neutrophils is decreased for all genotypes. This suggests that a reduction in phagocytosis occurs later in infection. Together these data suggest that the neutrophil's ability to phagocytose cryptococcal cells is not affected by either *atg3* or *atg5* deficiency. Therefore, any changes in Lc3 recruitment are likely not due to inability to phagocytose similar amounts of cryptococcal cells. Interestingly in macrophages, an *atg5* deficiency led to a reduction in phagocytic ability *in vitro* (Qin et al. 2011), highlighting potential different roles of autophagy between macrophages and neutrophils, although differences may also be caused by *in vitro* analysis, for example, RNAi may lead to off target effects which may reduce macrophage phagocytic ability. An additional difference is that Lc3 recruitment to *C. neoformans* only occurred in macrophages (J774.16 cells), when opsonised with antibody, and not with complement (Nicola et al. 2012). In zebrafish, the lack of an adaptive immune system at this larval age means that antibodies could not be present. Therefore, non-opsonised or complement opsonised cryptococcal cells are phagocytosed by neutrophils at this larvae age. This highlights that Lc3 recruitment to phagocytosed cryptococcal cells can occur without antibody involvement, in neutrophils.

A significant reduction of Lc3 localisation to cryptococcal vesicles was found for both *atg3* and *atg5* homozygous and heterozygous larvae in comparison to wild-type larvae at 0dpi. However, no significant difference between Lc3 localisation to cryptococcal vesicles was found for *atg3* or *atg5* homozygous and heterozygous larvae in comparison to wild-type larvae at 1dpi. The reduction of Lc3 co-localisation at 0dpf for *atg3* and *atg5* homozygous and heterozygous led to no significant change in Lc3 co-localisation between 0 and 1dpi, which was observed for wild-type larvae, and larvae not in either mutant back-ground. This suggests that autophagy deficiency in single or both alleles causes a reduction in Lc3 localisation to *C. neoformans* phagocytosed by neutrophils, early in infection. This has not been demonstrated previously. These data are suggestive that both *atg3* and *atg5* mutants are not be able to efficiently lipidate Lc3-I, required for the marking of membranes. Furthermore, in *atg3* deficient larvae, a reduced fungal burden was observed in comparison to wild-type siblings. Therefore, it is plausible that Lc3 recruitment is involved in the host degradation of cryptococcal cells, or conversely cryptococcal manipulation of cellular components. Importantly, these data only highlight a reduction in Lc3 localisation. In order to determine whether a lack of Lc3 recruitment to *C. neoformans* is detrimental for the host, or bacteria, and if Lc3 recruitment is involved as a LAP or autophagy marker, further analysis is required. Investigation may reveal a neutrophil niche, or even a neutrophil derived phagosomal

niche, for cryptococcal cells which may expand the current dogma that macrophages provide the primary intracellular niche in cryptococcal infection.

A relevant observation, or rather lack of observation, is that no double membrane vesicles, which are characteristic of autophagosomes, containing *C. neoformans* has so far been visualised. In fact, in macrophages only single-membrane vesicles have been observed to surround *C. neoformans*, and small double membrane vesicles observed only to fuse into this single membrane (Pandey et al. 2017; Nicola et al. 2012). This may suggest the mechanism of how autophagic machinery can be recruited to the single membrane, perhaps suggesting that LAP, rather than classical autophagy is involved in cryptococcal handling. Pathogenic fungus *Aspergillus fumigatus* was shown to be targeted to LAP, which is beneficial for the host. (Martinez et al. 2015). Furthermore, this may suggest that LAP (which requires both *atg3* and *atg5* for lipidation of Lc3-I which is subsequently trafficked to LAP-phagosomes) (Martinez et al. 2015), may be important in future studies, to determine exactly what role autophagy machinery is used for during cryptococcal infection.

To conclude, Lc3 is shown to co-localise with *C. neoformans* within neutrophils. The host Lc3 and cryptococcal co-localisation may represent a host or pathogen derived interaction, future studies may reveal autophagy as a mediator in a cryptococcal neutrophil niche. A reduction in Lc3 recruitment cryptococcal vesicles in *atg3* and *atg5* mutants, which is not caused by defects in neutrophil phagocytosis, suggests that autophagic machinery is involved in the neutrophil response to cryptococcal cells. However, it is important to determine whether Lc3 recruitment is beneficial to the host, or bacteria, and this presents an exciting research topic for the future.

Of note, only a limited number of publications focussing on the role of host cell autophagy in the pathogenesis of *C. neoformans* exist, and all focus on macrophages. While there appears to be an emerging role that cryptococcal cells benefit from host cell autophagy, there is also evidence that the activation state of the macrophages plays an important role in determining whether autophagy is truly beneficial for the cryptococcal cells (Nicola et al. 2012). As evidence is emerging that cryptococcal cells can survive and replicate within neutrophils, further analysis into the role of neutrophil autophagy, which may have different actions to macrophages, may provide interesting insights into the role of host autophagy in the pathogenesis of *C. neoformans*.

5.4 Chapter summary

Overall, larval survival and pathogen burden analysis of both *C. neoformans* and *S. aureus* infection did not provide any firm conclusions about the role of host cell autophagy either as a host defence, or in promoting improved pathogen survival. This

is likely due to the *atg3* and *atg5* zebrafish mutants survival defect, maternal contribution, and also the fact that both pathogens can reside extracellularly, which would not be affected by changes in host cell autophagy. However, within neutrophils, both pathogens had reduced Lc3-II co-localisation in comparison to wild-type controls, suggesting that *atg3* and *atg5* homozygous mutants have a reduction in Lc3-II production and/or ability to mark pathogen phagosomes. Further work is required to determine whether changes in Lc3-II marking of pathogen phagosomes is beneficial for the host or pathogen.

Chapter 6: Results chapter 4

Generation of a selective autophagy receptor reporter line

6.1 Chapter introduction

Autophagy is the process self-degradation of cellular components, usually engaged for cell homeostasis and survival, for example in starvation conditions. Autophagy machinery can also be employed in the selective degradation of unwanted cellular components including pathogens, termed xenophagy. This selective degradation requires the use of adapter molecules, (autophagy receptors) which are able to recognise and transport cargo, for example a bacterium, into contact with autophagic machinery, for degradation.

Many selective autophagy receptors (SARs) are able to recognise and bind to ubiquitinated cargo. Indeed, four SARs are known to be involved in recognition of ubiquitinated pathogens in mammals, including p62 (otherwise known as sequestosome 1, SQSTM1), optineurin (OPTN), (nuclear dot protein 52 kDa) NDP52 and TAX1BP1 (Tax1 Binding Protein 1) (Farré & Subramani 2016). SARs are able to bind to LC3 through a LC3-interacting region (LIR), and also to bind ubiquitin, enabling the recruitment of ubiquitinated pathogens for autophagic degradation. *In vivo* analysis of p62 localisation has not hitherto been possible, although *in vitro* systems to monitor autophagy molecules have been established (Larsen et al. 2010).

Neutrophils are a recognised intracellular niche for *S. aureus* (Prajsnar et al. 2012). Recent literature reports that p62 is able to recruit *S. aureus* residing in the cytoplasm to the autophagosome, but once within the autophagosome *S. aureus* is able survival, replicate and eventually to escape the autophagosome and/or host cell for its own survival (Neumann et al. 2016; Singh et al. 2017). It will be of interest to visualise the dynamics of p62 recruitment to *S. aureus,* during *in vivo* infection.

The role of xenophagy in clearance of fungal pathogens is not established, in fact, the term “xenophagy” is only used to describe clearance of bacterial and viral pathogens. It was recently reported that *C. neoformans* is able to manipulate the phagosome it resides in, within macrophages, to promote survival and potentially extracellular escape via vomocytosis (Smith et al. 2015). It was further demonstrated that LC3 was present on the surface of some cryptococcal cells which had escaped macrophage degradation (Nicola et al. 2012). Neutrophils are relatively less studied than macrophages in cryptococcal infection. However, neutrophils are able to kill *C. neoformans*, and may play a key role in intra-vasculature clearance of fungal cells (Sun et al. 2016a; Diamond et al. 1972). Although a role of autophagy in host cell control of cryptococcal infection

has not been demonstrated, it would be of interest to discover whether p62 is involved in the host control of cryptococcal infections within neutrophils.

Hypothesis: p62 is involved in the *in vivo* handling of *S. aureus* and *C. neoformans* in host neutrophils.

Chapter aims:

This chapter aims to create and use a zebrafish p62 reporter line to enable *in vivo* analysis of p62 interactions with pathogens, specifically within neutrophils.

1. Design and generate a zebrafish p62 reporter line
2. Determine whether the p62 reporter line shows a neutrophil specific expression, and if tagged GFP-p62 fusion protein acts in a similar manner to endogenous p62
3. Establish if p62 is employed by neutrophils in *in vivo S. aureus* infection
4. Establish if p62 is employed by neutrophils in *in vivo C. neoformans* infection

6.2 Zebrafish p62

To create a zebrafish p62 reporter line, it is important to determine whether human p62 gene structure and function is conserved in zebrafish. This ensures it is suitable as a tool for analysis of situations in which human p62 is known to interact with pathogens.

Autophagy receptor p62 (sequestosome 1, or SQSTM1) is found in both human and zebrafish genomes. In zebrafish, there is a single p62 gene, located on chromosome 14, which has two coding transcripts, and three non-protein coding transcripts (Silva et al. 2014; Mostowy et al. 2013). In comparison, in humans p62 is located on chromosome 5 and encodes six coding transcripts. A recent, thorough study compared human and zebrafish genomic sequences, transcripts, protein structure and predicted protein domain function (Silva et al. 2014). This study highlighted high similarity between zebrafish and human p62 protein structure and expression, and suggested they likely function in a similar manner. Indeed, the study concluded that zebrafish p62 would be a good model for human disease, specifically Paget's disease which is caused by mutations in p62 (Chamoux et al. 2009; Silva et al. 2014). Of particular interest, both the LIR and ubiquitin-associated (UBA) domains are conserved, with 41% and 81% identity respectively (Silva et al. 2014). This suggests that autophagy function is conserved and provides basis that generation of a zebrafish reporter line of p62 will provide a useful tool to study p62 function which may well be translatable to human studies.

6.3 Reporter line design and methodology

The Gateway system was chosen to generate a vector, which would encode a GFP-p62 reporter, easily inserted into the zebrafish genome through Tol2 transgenesis under the neutrophil-specific promoter l*yz*.

The Gateway™ system is completed through the generation of entry clones, through BP reactions, and the subsequent generation of expression clones through an LR reaction. Both BP and LR reactions are based on the use of “att” recombination sequences, which enable integration of required DNA sequences into specific locations on vectors. The “att” sites were originally isolated from DNA recombination sequences in bacteriophage λ, responsible for the location of integration sites of the viral genome into the host bacterial genome, through integrase enzyme activity. These “att” sites were optimised for recombination of PCR products and vectors for the Gateway system. Introduction of small variations in the “att” sequences enable site specific recombination, which are numbered 1-4 in the Gateway system. An example of multi-site Gateway three fragment assembly is shown in Fig 6.1 A.

The BP reaction places a required DNA sequence, for example a gene, into an entry vector. The “attB” sites are added by PCR onto the sequence to be inserted, flanking the insert. Corresponding “attP” sites are found on the selected 3’ entry clone. Recombination leads to the insertion of the sequence into the entry vector. The “attB” and “attP” sites recombine to create “attL” or “attR” sites located each side of the inserted sequence on the entry vector.

The LR reaction places the 5’, middle entry (ME), and 3’ vectors into a selected destination vector through the use of location specific complementary attL and attR sites (e.g. the attL3 on 3’ entry clone with the attR3 on the destination vector). Recombination by the LR clonase enzyme mix, results in the creation of the final expression clone.

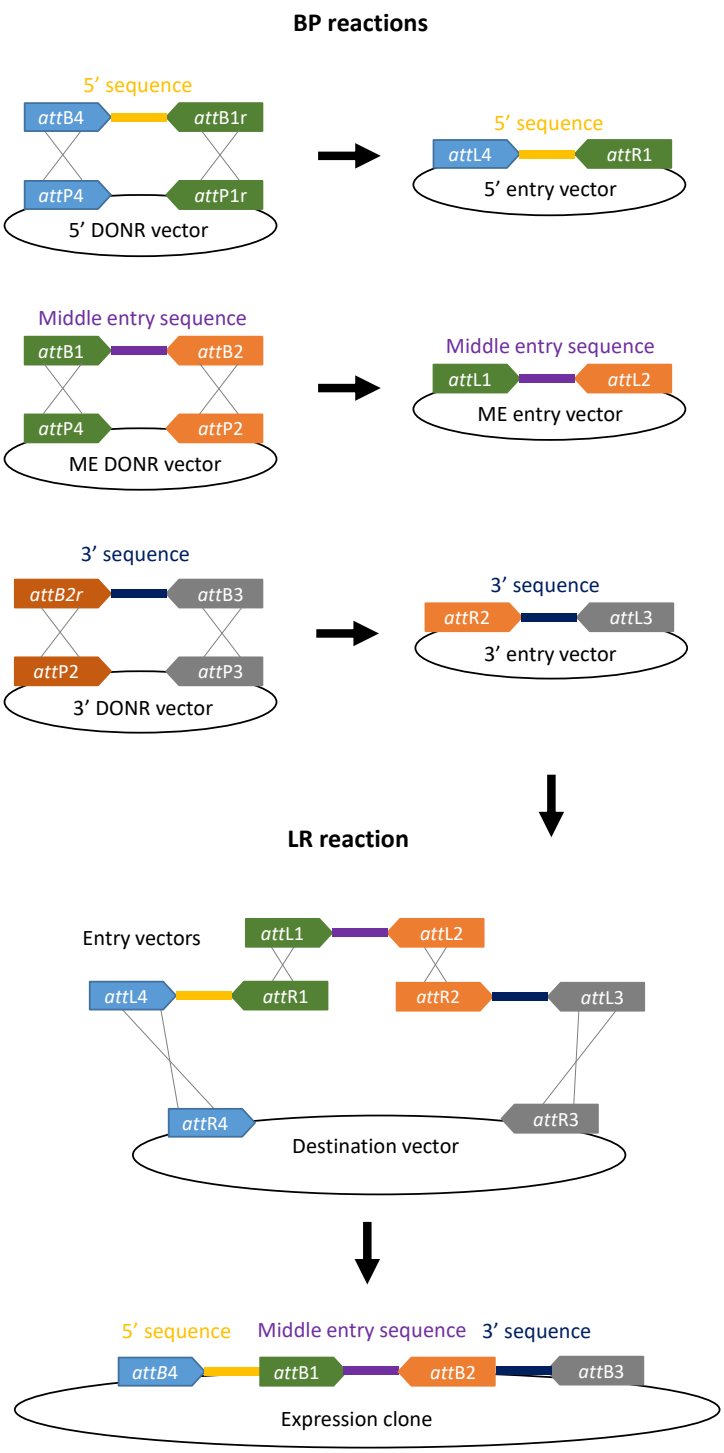

Figure 6.1 Gateway expression clone procedure

Experimental overview of generation of a three fragment destination vector, including entry clone generation by the BP reaction, and expression clone generation from LR reactions. Importantly the 5' sequence, middle entry sequence and 3' sequence (yellow, purple and dark blue respectively) are transferred from a PCR product into entry clones, and subsequently transferred into the expression clone

In the generation of a neutrophil specific, GFP p62 reporter line, the choice and order of entry vectors was carefully considered. The structure of the p62 protein, as shown in Figure 6.2, shows both LIR and UBA domains are closest to the 3' end of the sequence, in both human and zebrafish. Both LIR and UBA domains are important for the function of p62 in selective autophagy. To ensure the fusion tagged GFP would not sterically block p62 interactions at the LIR and UBA domains, it was decided to place the p62 gene in the 3' entry vector and GFP in the middle entry vector.

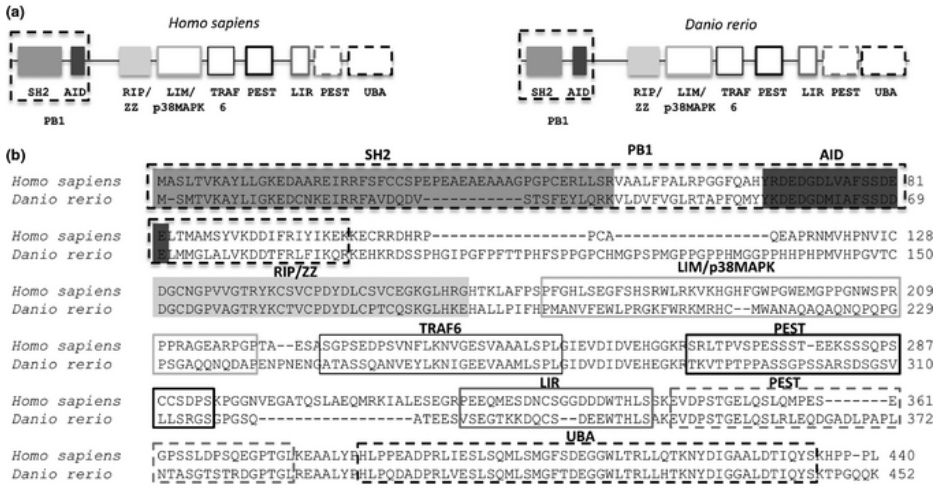

Figure 6.2 Protein structure of p62

Figure 5, Silva, I. A. L., Conceição, N., Michou, L. and Cancela, M. L. (2014), Can zebrafish be a valid model to study Paget's disease of bone?. J. Appl. Ichthyol., 30: 678–688. doi:10.1111/jai.12523. **A** Protein domain structure in human and zebrafish p62 genes, of note LIR and UBA domains **B** Protein sequence highlighting the similarity of residue sequences and related domain locations Permission for reproduction obtained see Appendix 2.

To enable expression of the fusion protein specifically within neutrophils, the *lyz* promoter was chosen to be used in the 5' entry vector. The *p5E-lyz* entry clone (Elks et al. 2011) and the *pME-GFP-nonstop* middle entry vectors were chosen. To ensure a fusion protein of GFP-p62, this middle entry vector was chosen as it did not contain a functional STOP codon. Therefore, it is expected that a protein will be translated from the GFP, through the small linker region, and to p62. The destination vector *pDestTol2CG*, was chosen which included Tol2 sites for integration into the genome, in addition to a GFP heart marker. The planned methodology is represented in Figure 6.3, and expected expression clone, *pDest(lyz:GFP.p62)* in Figure 6.4. The required p62 3' entry vector, and expression clone *pDest(lyz:GFP.p62)* were constructed following the Multisite Gateway™ three-fragment vector construction kit, as described in detail in the Appendix 1.

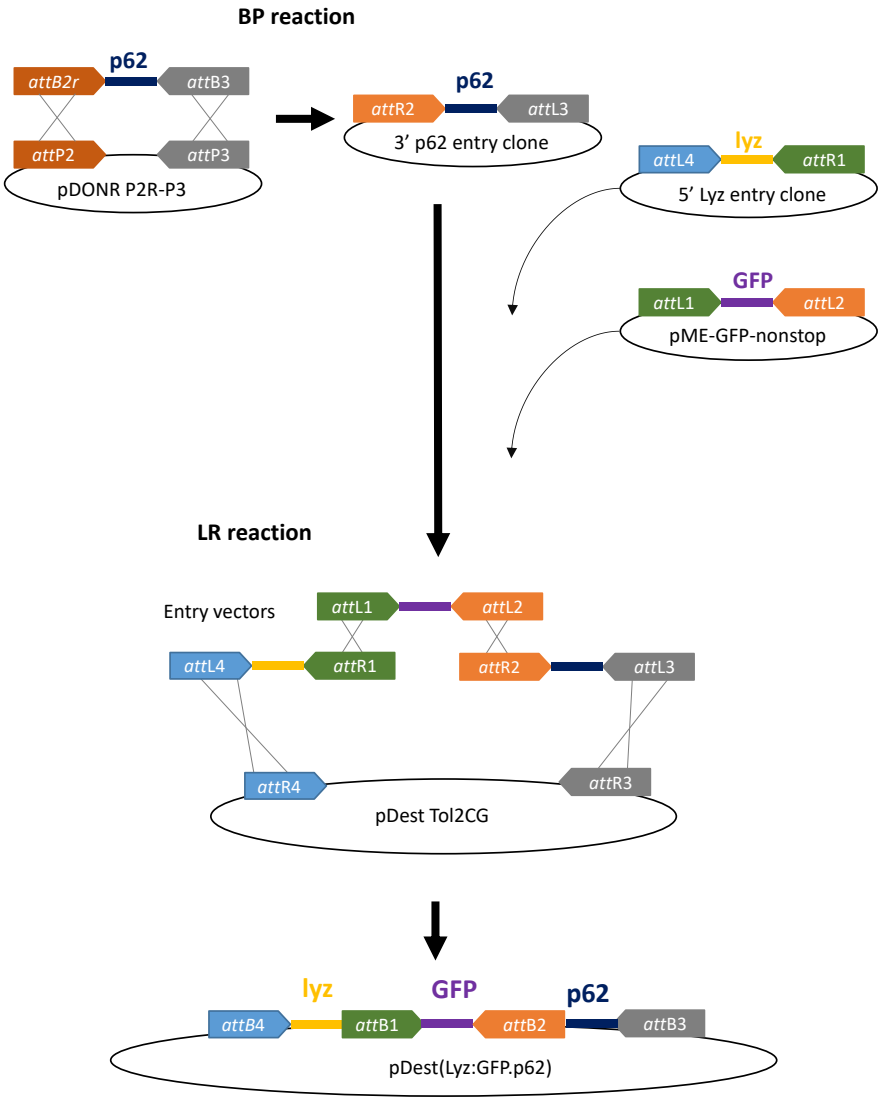

Figure 6.3 Gateway procedure followed in this project

Experimental procedure followed in this project with vectors used. The 3' p62 entry clone was generated by the BP reaction. The 5' entry clone (*lyz*) and middle entry clone (GFP) were previously created. Using the pDestTol2CG destination vector for the LR reaction, 5' *lyz* sequence, middle entry GFP sequence and 3' p62 sequence (yellow, purple and dark blue respectively) were transferred to create the expression clone.

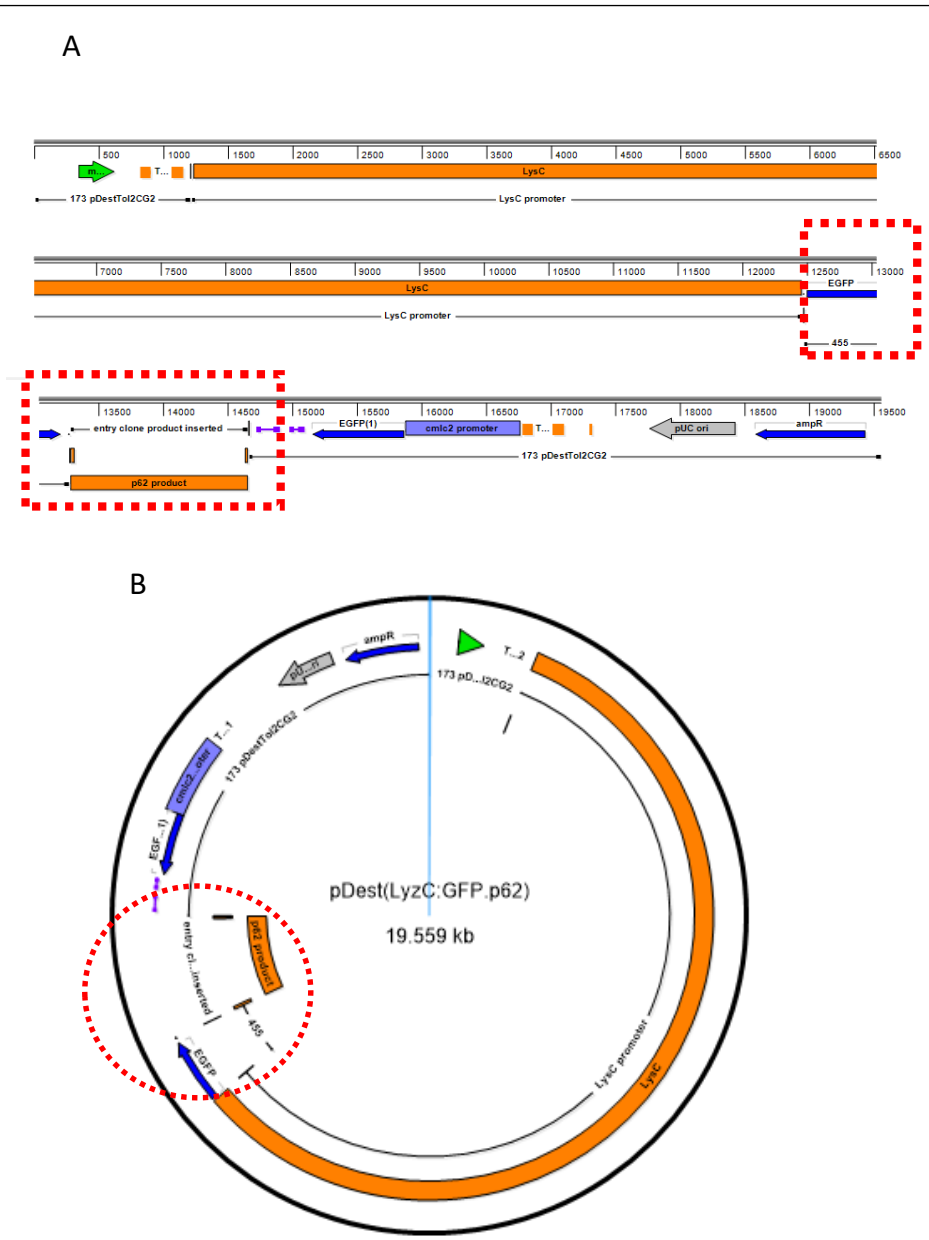

Figure 6.4 Expected *pDest(lyz:GFP.p62)* sequence

A Linear map of the expected *pDest(lyz:GFP.p62)* sequence, where the red box indicates the portion which will code for the fusion GFP-p62 protein (SeqBuilder DNASTAR Lasergene suite) **B** Circular map of the expected *pDest(lyz:GFP.p62)* sequence, where the red circle indicates the portion which will code for the fusion GFP-p62 protein (SeqBuilder DNASTAR Lasergene suite). Both maps highlight the *lyz* promoter, GFP and p62 sequence, in addition to the heart marker (cmlc2) driven GFP, and ampicillin (ampR) resistance gene sequence.

To ensure the final expression clone was correct in size (and sequence), a restriction site digest was performed. The NcoI enzyme is able to cut at four specific locations of the expected sequence of the *pDest(lyz:GFP.p62)* expression clone, marked in Fig 6.5 A. Following an NcoI digest, four fragments of 8703bp, 7482bp, 2043bp, and 1331bp in size are expected. The correct band sizes were observed after digestion of the *pDest(lyz:GFP.p62)* vector (Fig. 6.5 B). This suggests that the LR reaction worked as expected and yielded the correct expression clone. Additionally, sequencing was completed to cover each junction between entry vectors and those joining with the destination vector. In all cases, the expected sequence was confirmed. These data show the *pDest(lyz:GFP.p62)* expression clone was successfully generated.

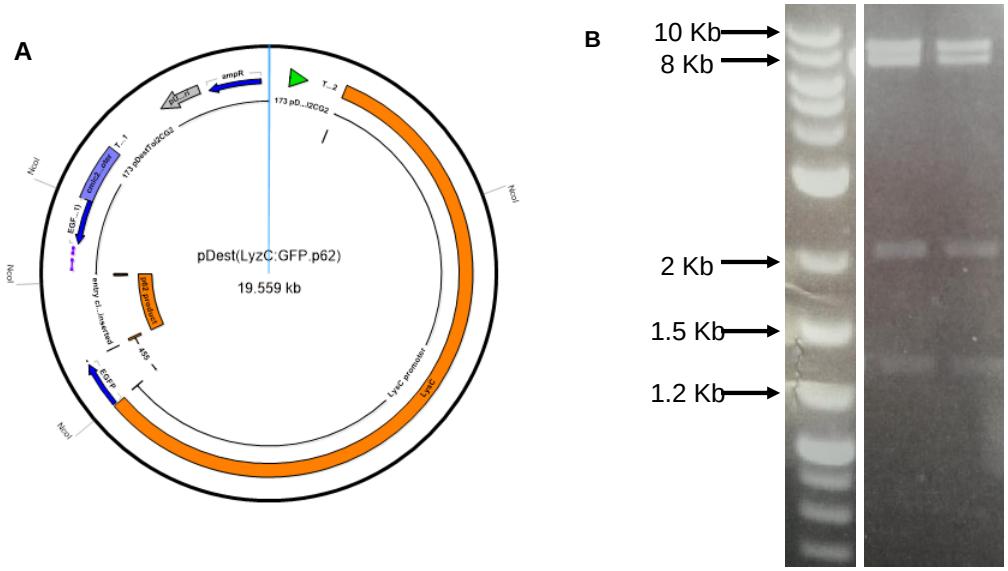

Figure 6.5 *pDest(lyz:GFP.p62)* restriction digest

A Schematic of the *pDest(lyz:GFP.p62)* construct, with NcoI restriction sites marked
B Nco1 digest: expected bands observed at 8703bp, 7482bp, 2043bp, and 1331bp

6.4 Tol2 synthesis and injection in F0

In order to insert *pDest(lyz:GFP.p62)* into the genome of zebrafish, Tol2 mediated transgenesis was used. Transposons (DNA transposable elements) are sequences of DNA which are able to move position in the genome. Movement of transposons within the genome can result in genomic change, such as a mutation. Transposase activity is responsible for the insertion of sequences into the genome and can be encoded by the transposon. Tol2 is a transposon, originating from in medaka fish. Tol2 encodes a transposase (Kawakami et al. 2000), and has been established as a useful transposon in the generation of zebrafish transgenic lines, due to its high rate of insertion into the

germ line. Tol2 is not found in zebrafish, therefore Tol2 mRNA in co-injected into the larvae to enable genomic integration, of sequences containing Tol2 transposon flanking sites. The backbone vector used in *pDest(lyz:GFP.p62)* contains Tol2 flanking sites at each side of the sequence to be integrated in the larvae genome.

To generate Tol2 mRNA, a *pT3Tol2* plasmid was used. The DNA *pT3Tol2* plasmid was linearised through a restriction site digest. Tol2 mRNA was generated by a transcription reaction (Ambion T3 mMessage Machine) from the linear *pT3Tol2* plasmid. Tol2 mRNA integrity was confirmed by Nanodrop and gel electrophoresis, and stored at -80ºC.

To generate a stable zebrafish line with *pDest(lyz:GFP.p62)* inserted into the genome. Tol2 mRNA and *pDest(lyz:GFP.p62)* were co-injected into a single cell (at the single cell stage) of wild-type AB larvae. A 1nl injection contained 30pg of Tol2 mRNA and 60pg of *pDest(lyz:GFP.p62)* (increased from the standard 30pg after the first test resulted in low transient expression). In addition a 1/10 dilution of phenol red in was used to confirm injection into the single cell was successful.

6.5 Transient expression

At 3 days after injection, larvae were screened on a fluorescence stereomicroscope to select larvae which had GFP transiently expressed within neutrophils. Presence of the GFP positive heart marker suggests that the integration of the *pDest(lyz:GFP.p62)* construct was successful. Larvae with a GFP positive heart were selected for further screening. GFP positive cells moving with the blood stream were observed in a small number of larvae, which were likely to be neutrophils. Static GFP positive cells located in the caudal haematopoietic tissue (CHT) were observed in some larvae were similarly believed likely to be neutrophils. In many cases, transient GFP expression was observed in the muscle somites, which is seen commonly in zebrafish transgenesis. Larvae with positive heart marker and high numbers of likely GFP positive neutrophils cells, were raised as potential *Tg(lyz:GFP.p62)* founders.

6.6 Founder screening and generation of stable line

Larvae which had been injected with *pDest(lyz:GFP.p62)* and raised as potential founders, were out-crossed to nacre wild-type. Resulting offspring from each pair were screened (as above section in 6.5) for GFP positive cells which were likely to be neutrophils. A single founder was identified in which ~70% of offspring contained GFP positive heart marker and single cells characteristic of neutrophils. The majority of resulting larvae from the founder and nacre cross were raised as an F1 generation of *Tg(lyz:GFP.p62)* line.

A small fraction of the F1 *Tg(lyz:GFP.p62)* were used for preliminary image analysis. A very small number of larvae were available for use, so infection with *S. aureus* and *C.*

neoformans was completed in just two larvae respectively. This assay was chosen to determine if phagocytosis occurs, with the hypothesis that phagocytosis events would establish that GFP positive cells were phagocytic cells. Indeed, phagocytosis was observed for both *S. aureus* and *C. neoformans* in GFP positive cells (Fig 6.6 A, B). Additionally, it was noticed that GFP puncta were present in both un-infected and infected phagocytic cells (Fig 6.6 A), with a uniform cytoplasmic GFP fluorescence seen in all GFP positive cells. These may represent p62 puncta at sites of autophagosomes within individual phagocytic cells. The uniform cytoplasmic GFP fluorescence may represent GFP-p62 not actively being used be the cell resulting in a cytoplasmic GFP distribution. Furthermore GFP puncta were seen co-localised with *S. aureus* within the cytoplasm of phagocytic cells (Fig. 6.6 A). Similarly, GFP puncta were present on what appear to be *C. neoformans* vesicles (Fig. 6.6 B). Vesicles were believed to be present due to the lack of GFP fluorescence in the location of individual cryptococcal cells.

These preliminary data suggest that the GFP positive cells are phagocytic cells. In addition, formation of GFP puncta within GFP positive cells may represent an interaction of GFP-p62 with autophagosomes and with pathogens.

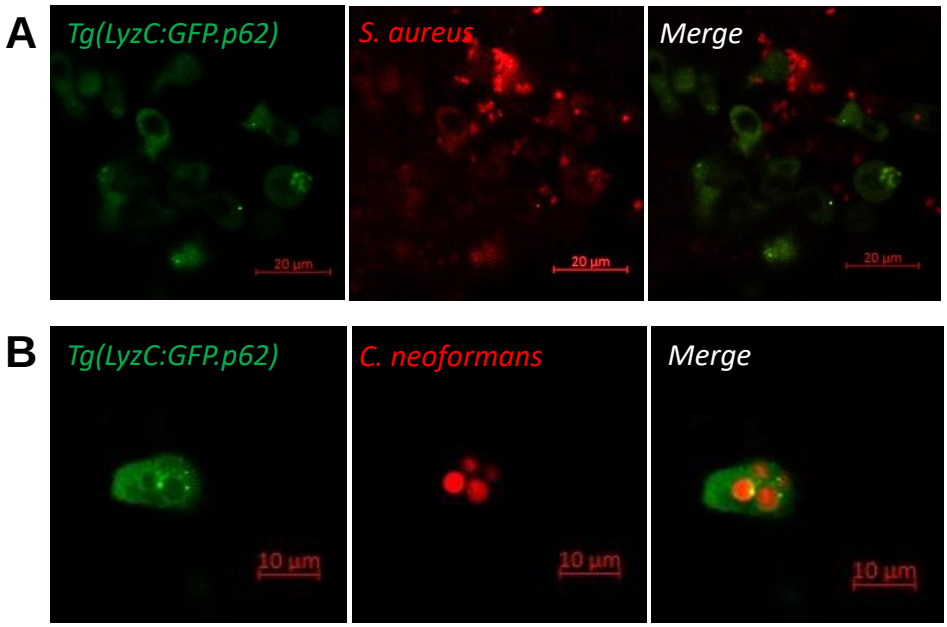

Figure 6.6 Phagocytosis of *S. aureus* and *C. neoformans*

Preliminary imaging of *Tg(lyz:GFP.p62)* F1 generation. **A** mCherry *S. aureus* infection into *Tg(lyz:GFP.p62)* F1 **B** mCherry *C. neoformans* infection *Tg(lyz:GFP.p62)* F1 generation

6.7 Characterisation of *Tg(lyz:GFP.p62)* transgenic line

It was next important to determine whether the generated *Tg(lyz:GFP.p62)* expressed protein specifically in neutrophils, and whether the tagged protein behaved as endogenous p62, before using the line for infection analysis. Characterisation is essential because it is possible that GFP fusion to p62 blocks function of the p62, perhaps sterically.

To determine whether the GFP-p62 was being expressed in neutrophils, an out-cross of the F1 generation of *Tg(lyz:GFP.p62)*, to a complementary neutrophil line, *Tg(lyz-nsfB-mCherry)*^{sh260} (Prajsnar et al. 2012), which expresses mCherry in the neutrophils was completed. High magnification imaging of both GFP and mCherry positive cells was completed in larvae. Comparison of the expression of GFP and mCherry neutrophils indicate a clear co-expression in neutrophils (Fig 6.7 A). The fluorescence intensity is derived from the *lyz* promoter, which may vary between individual neutrophils. Indeed, the fluorescence of GFP and mCherry intensity are matched within individual cells. Therefore, GFP fluorescence is being expressed specifically within neutrophils.

On the other hand, where GFP puncta are observed, no corresponding mCherry puncta are seen (Fig 6.7 B). This is suggests that GFP puncta are forming in a p62 dependant manner, rather than a consequence of expression. It is tempting to

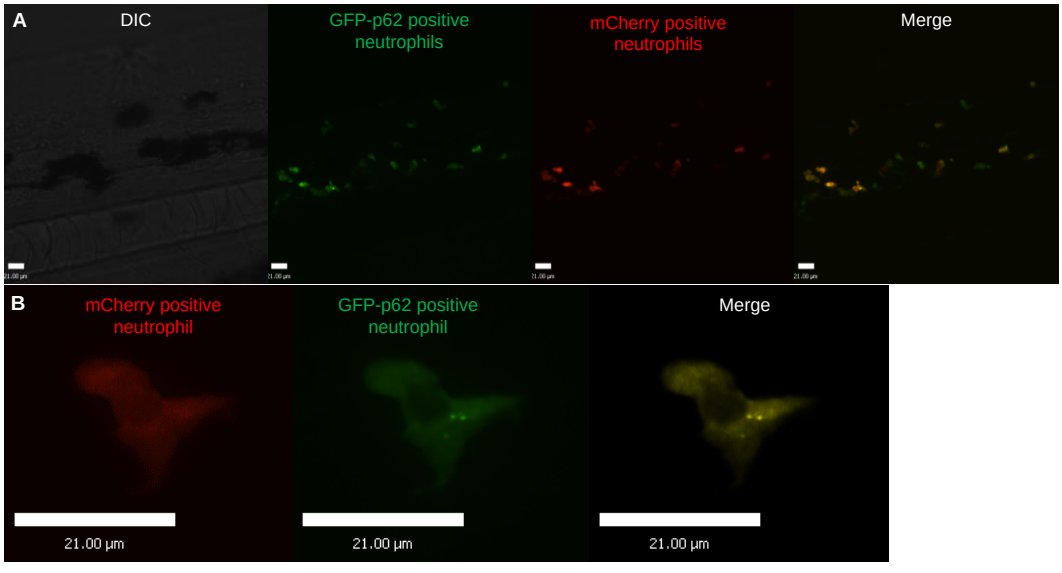

Figure 6.7 Neutrophil expression of GFP-p62

Imaging of *Tg(lyz:GFP.p62)* crossed to *Tg(lyz-nsfB-mCherry)*^{sh260} larvae **A** Co-localisation of both GFP and mCherry **B** A single neutrophil expressing both GFP and mCherry, with GFP puncta observed. All scale bars represent 21um.

speculate that the GFP puncta represent autophagosomes.

To determine whether the neutrophils were the only GFP positive cells, the number of double GFP and mCherry positive cells, or single colour cells were compared. In all cases, with a single exception, all cells were double GFP and mCherry positive (Fig 6.8 A). These data show GFP-p62 is expressed specifically within neutrophils.

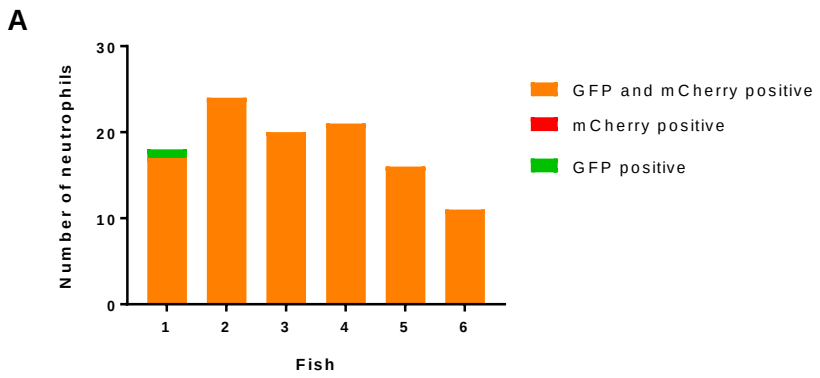

Figure 6.8 Neutrophil expression of GFP-p62

Imaging of *Tg(lyz:GFP.p62)* crossed to *Tg(lyz-nsfB-mCherry)*^{sh260} larvae **A** Fluorescence observed of GFP and mCherry within individual neutrophils, imaged a high magnification in the caudal haematopoietic tissue, using six representative larvae

Next, in order to determine whether the GFP tagged p62 was functional, *Tg(lyz:GFP.p62)* larvae were treated with autophagy influencing drugs. The aim was to determine whether GFP-p62 responded to changes in autophagy in a similar manner as expected of endogenous p62. Larvae were treated with either an autophagy blocker, BK8644 to block autophagy, or with rapamycin and chloroquine together (and each alone), to monitor autophagic flux. Larvae from the F1 generation were imaged after 24 hours of drug treatment, however it was noticed that fluorescence intensity was variable within individual fish, excluding the possibility of comparing fluorescence intensity between larvae in each drug treatment. In addition, fluorescence intensity would be dependent on expression of *lyz* promoter, rather than specifically p62, although a disappearance of GFP fluorescence may have represented an increase in autophagic flux. Therefore, the GFP-p62 puncta observed within neutrophils, were used as a measure of autophagy.

Puncta representing GFP tagged p62 were used a read-out of the effect of autophagy influencing drugs. The number of individual neutrophils containing puncta differs according to drug treatments (Fig 6.9 A), actual numbers were included to show that each treatment group had fairly similar neutrophil numbers. The same data is presented as percentage in Figure 6.9 B, to highlight the difference in ratio of neutrophils with/without puncta. Where autophagy is blocked by rapamycin and chloroquine, or BK8644, or chloroquine, no change in the number of neutrophil containing puncta in comparison to controls is shown. Similarly rapamycin treatment led to no change in the number of neutrophils containing puncta. A reduction may have been expected if autophagy is up-regulated and p62 molecules are used and degraded (Fig 6.9 B). These data do not suggest that GFP-p62 within neutrophils responded appropriately to autophagy influencing drugs, suggesting that GFP-p62 acts in a similar manner as endogenous p62.

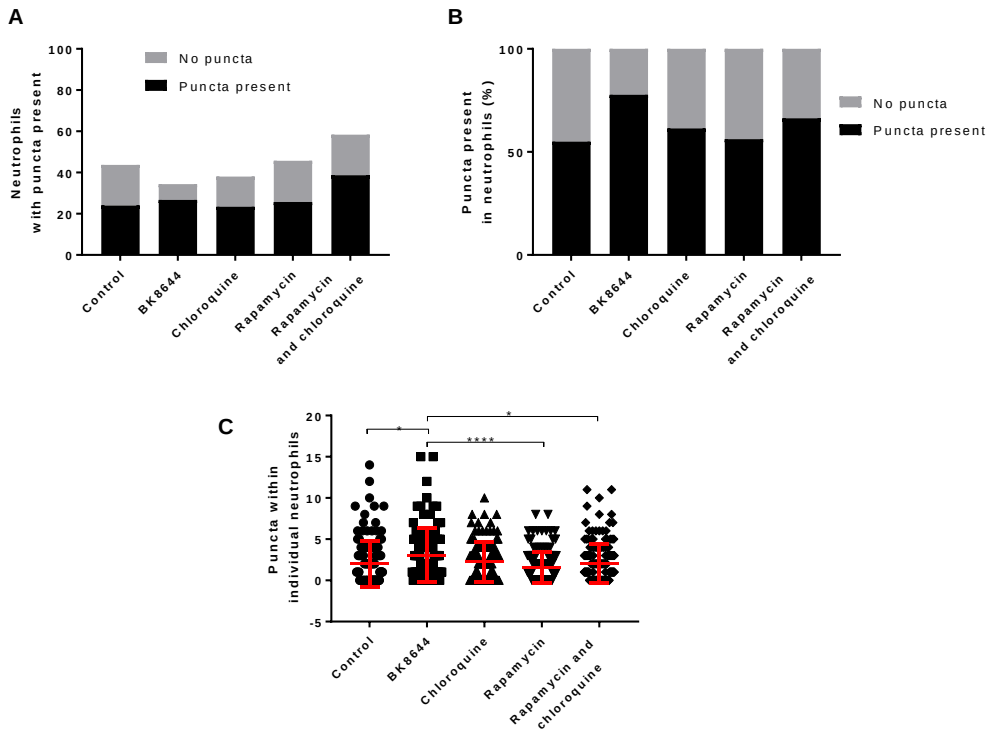

Figure 6.9 Neutrophil expression of GFP-p62 puncta

Imaging of *lyz*-GFP-p62 treated with autophagy influencing drugs **A** Actual number of neutrophils observed with puncta, treated with different autophagy influencing drugs (not-significant two-way ANOVA, n=3, 15-20 larvae per group) **B** Percentage of neutrophils with puncta present, treated with different autophagy influencing drugs (n=3, 15-20 larvae per group) **C** Number of puncta observed within individual neutrophils, in larvae treated with different autophagy influencing drugs (Error bars +/- SD, One-way ANOVA Tukey's multiple comparisons *p<0.05, ****p<0.001, n=3, 15-20 larvae per group).

I next examined the number of GFP-p62 puncta within individual neutrophils. Of note, in non-treated control larvae a large range of puncta were observed, between 0 and 14 puncta within individual neutrophils (Fig 6.9 C). Following treatment with autophagy inhibitor BK8644, the number of puncta in neutrophils observed is significantly increased in comparison to non-treated neutrophils (Fig 6.9 C). This is indicative that the GFP-p62 is not being degraded through autophagy, acting in a similar manner as endogenous p62 would be expected to behave. Rapamycin and chloroquine treatment, and chloroquine alone show a similar number of puncta in comparison to controls. Rapamycin had no change in puncta number in comparison to controls, but is significantly different to BK8644. This may be expected as rapamycin and BK8644 are expected to cause opposing effects on p62 a reduction and increase respectively. Ultimately, these data are suggestive that GFP-p62 is acting in a similar manner to endogenous p62.

Taken together, these data demonstrate that GFP-p62 in the *Tg(lyz:GFP.p62)* line is expressed specifically within neutrophils and suggests puncta formation/degradation responds to autophagy induction.

6.8 Verifying *Tg(lyz:GFP.p62)* as a fusion protein

The above analysis suggests that the GFP-p62 fusion protein is indeed influenced by autophagy drugs. To further confirm p62 is tagged with GFP a western blot (using an anti-GFP antibody) was performed. Zebrafish protein lysate from *Tg(lyz:GFP.p62)* larvae, AB wild-type, *Tg(mpx:eGFP)*^{i114} (neutrophil specific GFP) were compared. The expectation was that no GFP protein would be present in the AB wild-type, a single GFP band at ~27KDa for the *Tg(mpx:eGFP)*^{i114}, and a single band with a larger size of ~79KDa representing GFP tagged to p62 in the *Tg(lyz:GFP.p62)* larvae. The ~79KDa predicted size was calculated according to the coding sequence of the GFP-linker-p62 fusion protein.

A western blotting demonstrated that no GFP is present in AB wild-type larvae as expected (Fig. 6.10). In addition, a single GFP band at ~27KDa is observed for the *Tg(mpx:eGFP)*^{i114} larvae (Fig. 6.10), as expected of GFP present within neutrophils, but that is not tagged to another protein. However, multiple bands were observed for *Tg(lyz:GFP.p62)* larvae. A band representing the expected ~79KDa was not observed, although a larger size of ~125KDa was seen, in addition to ~62KDa, ~52KDa, ~46KDa, a large band at ~27KDa, and ~24KDa (Fig 6.10). The large band at ~27KDa likely represents the GFP heart marker protein, which is not a fusion protein.

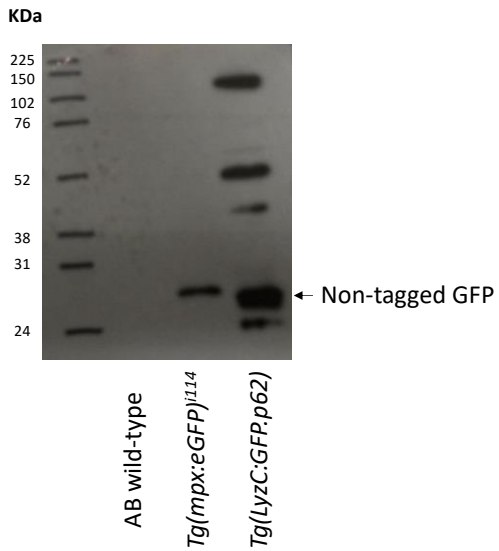

<u>Figure 6.10</u> GPF protein in *Tg(mpx:eGFP)*^{i114} and *Tg(lyz:GFP.p62)* larvae

Western blot using anti-GFP antibody on 5dpf AB wild-type, *Tg(mpx:eGFP)*^{i114} and *Tg(lyz:GFP.p62)* lysate. Protein ladder used Amersham full range RPN800E

Antibody company Abcam, advised that in western blots used on human brain protein samples, using their anti-p62 antibody (ab31545), four major bands were detected at 130KDa, 62KDa, 45KDa and 22KDa, with additional bands observed in rat lysate at 80KDa and 47KDa. This suggests that multiple p62 protein products exist. The products observed in human tissue appear to be similar, although not exact matches, to the protein product sizes observed in the *Tg(lyz:GFP.p62)* larvae. This suggests that the observation of multiple bands representing GFP-p62 may be expected in zebrafish.

6.9 Analysis of *S. aureus* interaction with p62

The *Tg(lyz:GFP.p62)* line was established in order to study *in vivo* p62 interactions with pathogens, specifically within neutrophils. The *Tg(lyz:GFP.p62)* larvae were injected with *S. aureus* to quantify any association with p62, with bacteria within vesicles or in the cytoplasm and whether any p62 associated handling of *S. aureus* changes over infection time course.

The *Tg(lyz:GFP.p62)* larvae were injected at 2dpf with 2,500cfu of *S. aureus*, and imaged at 2hpi, and 1dpi (~26hpi). Time points were chosen to compare initial pathogen interactions with GFP-p62 with any potential changes later in infection. An important initial observation showed that *S. aureus* is efficiently cleared by the larvae. The number of *S. aureus* events (where bacteria are observed within a neutrophil) decreases over time (Fig. 6.11 A). Furthermore, the proportion of infected neutrophils is significantly decreased over the infection time course (Fig. 6.11 B). Taken together these data suggest that neutrophils effectively degrade *S. aureus* during infection. Additionally, these data support the hypothesis that *S. aureus* goes through an immune cell mediated population “bottleneck”.

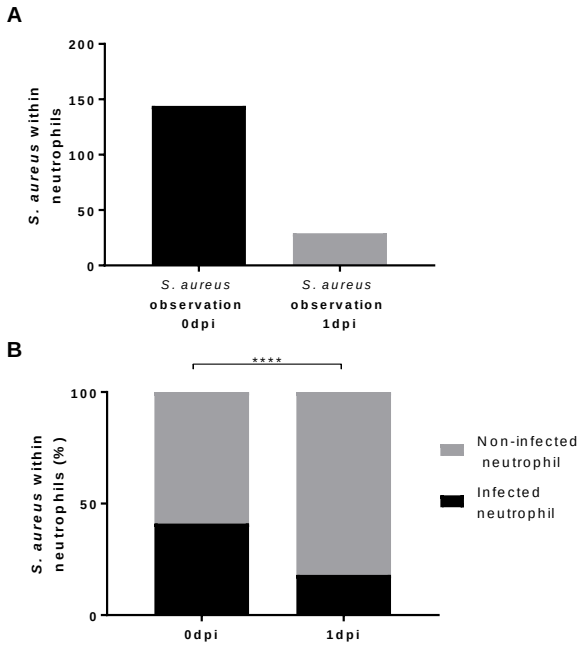

Figure 6.11 ***S. aureus*** **clearance over infection time course**

The *Tg(lyz:GFP.p62)* larvae were injected at 2dpf with 2,500cfu of mCherry *S. aureus*, and imaged at 0dpi (2hpi) and 1dpi (~26hpi). **A** The number of *S. aureus* events observed within neutrophils at 0dpi and 1dpi (n=3, 14 larvae at 0dpi, and 12 larvae at 1dpi) **B** Proportion of neutrophils infected or non-infected with *S. aureus* at 0dpi and 1dpi (****p<0.001, Fisher's exact test, n=3, 14 larvae at 0dpi, and 12 larvae at 1dpi)

The location of *S. aureus* within individual neutrophils was next examined. It is known that when *S. aureus* is phagocytosed, it will reside in a phagosome. However, *S. aureus* is capable of escaping the vesicle to reside in the cytoplasm. It is known that p62 is able to recruit to ubiquitinated pathogens, including *S. aureus*, but that this would only occur when *S. aureus* is free in the cytoplasm. Therefore, the location of *S. aureus* was examined.

It was possible to reason if *S. aureus* was possibly located in a vesicle, due to the presence of a "circular gap" in the disperse cytoplasmic GFP-p62 pattern (as discussed above), which most likely represents a vesicle (Fig. 6.12 A). Alternatively, where *S. aureus* was located in an area with diffuse cytoplasmic GFP-p62, it was considered to be cytoplasmic (Fig. 6.12 B).

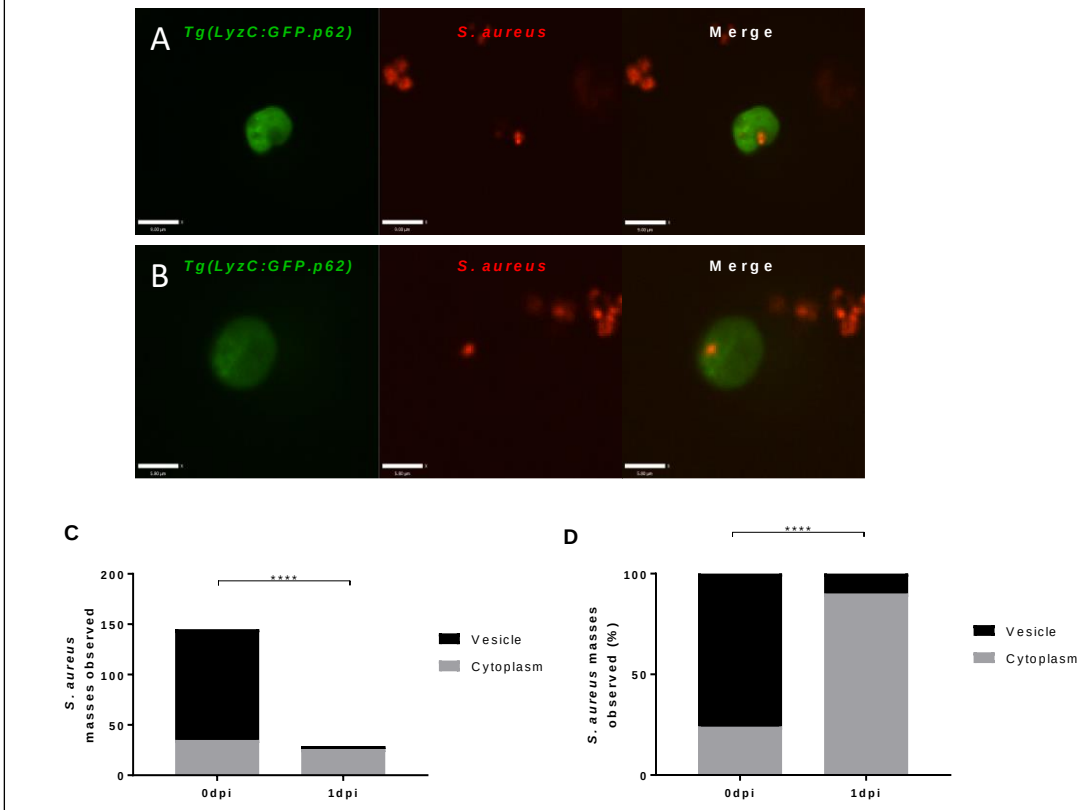

Figure 6.12 ***S. aureus*** **location within** ***Tg(lyz:GFP.p62)*** **neutrophils**

A Representative image of *S. aureus* observed within a likely "vesicle", scale 9um **B** representative image of *S. aureus* observed within the cytoplasm, scale 5.8um **C** The number of *S. aureus* events observed within vesicles or cytoplasm at 0dpi and 1dpi (****p<0.001, Fisher's exact test, n=3, 14 larvae at 0dpi, and 12 larvae at 1dpi) **D** proportion *S. aureus* events observed within vesicles or cytoplasm at 0dpi and 1dpi (****p<0.001, Fisher's exact test, n=3, 14 larvae at 0dpi, and 12 larvae at 1dpi).

The number of *S. aureus* masses located in a vesicle is reduced over infection, whereas the number located in the cytoplasm is relatively constant (Fig. 6.12 C). When considering the proportion of *S. aureus* observed in either the cytoplasm or a vesicle, a significant difference in location is observed over time (Fig. 6.12 D), a change of predominantly within a vesicle at 2hpi, to predominantly within the cytoplasm at 1dpi. These data suggest that whilst the majority of bacteria are degraded by the neutrophils, those which survive are found in the cytoplasm, indicating that bacterial survival is improved after escaping the phagocytic vesicle.

To determine if there is a role of p62 in the degradation of *S. aureus*, the co-localisation of GFP-p62 puncta with cytoplasmic bacteria (Fig. 6.13 A) and vesicles containing

bacteria (Fig. 6.13 B) was compared. In cases where *S. aureus* was located in a vesicle, multiple puncta, up to 6, were observed. However, in most cases 1 puncta was observed (Fig. 6.13 C). The bacteria had been recently phagocytosed, therefore it is likely they reside within a phagocytic vesicle. These GFP-p62 puncta may be located on phagosomes caused by LC3-associated phagocytosis (LAP), which recruits LC3 to the phagocytic vesicle. It is possible that these data represent GFP-p62 which can bind to LC3 present on an LAP vesicle. However, it is not possible with these data to determine whether p62 puncta are associating with an autophagosome or a phagocytic vesicle.

The change in presence of GFP-p62 puncta on *S. aureus* containing vesicles over time was examined. The majority of ~70% of *S. aureus* vesicles had GFP-p62 puncta associated at 0dpi (Fig. 6.13 D). However, at 1dpi only 3 *S. aureus* masses were observed within vesicles, with 2 clusters having GFP-p62 associated. No significant difference was found between GFP-p62 association at 0dpi and 1dpi (Fig. 6.13 D). These data show that most bacteria are either degraded within, or have escaped from the vesicle by 1dpi. An association with the majority of *S. aureus* containing vesicles at 0dpi may suggest that p62 may play a role in the degradation/escape of *S. aureus*, although further analysis is required.

The presence of GFP-puncta associated with cytoplasmic *S. aureus* was compared at 0dpi and 1dpi. At 0dpi, the majority of *S. aureus* in the cytoplasm are associated with p62, however at 1dpi, the majority do not associate with p62 (Fig. 6.13 E). These data could suggest that the minority of *S. aureus* which are not associated with GFP-p62 at 0dpi may survive intracellularly, whereas bacteria associated with GFP-p62 may be degraded. Taken together, these data suggest that p62 plays a role in clearance of *S. aureus* during *in vivo* infection.

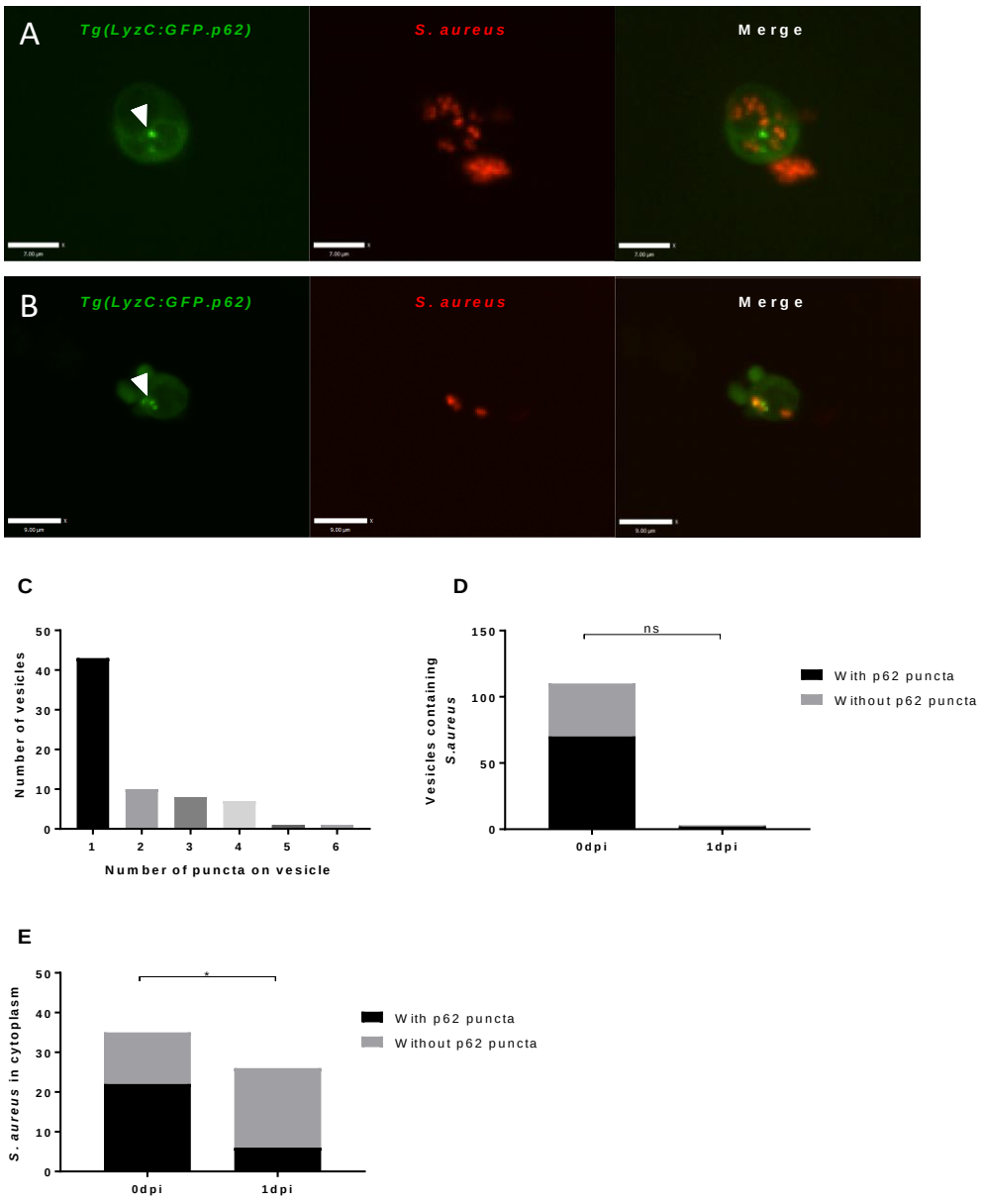

Figure 6.13 *S. aureus* co-localisation with GFP-p62

A Representative image of *S. aureus* observed within a likely "vesicle" with GFP-p62 puncta localisation, scale 7um **B** representative image of *S. aureus* observed within the cytoplasm with GFP-p62 puncta localisation, scale 9um **C** The number of p62 puncta observed on individual vesicles containing *S. aureus* at 0dpi **D** *S. aureus* within vesicles, co-localised with GFP-p62 at 0dpi and 1dpi (ns, Fisher's exact test, n=3, 14 larvae at 0dpi, and 12 larvae at 1dpi) **E** *S. aureus* in the cytoplasm, co-localised with GFP-p62 at 0dpi and 1dpi (*p<0.05, Fisher's exact test, n=3, 14 larvae at 0dpi, and 12 larvae at 1dpi)

To consider whether GFP-p62 puncta were being “used-up” in bacterial clearance, the number of cytoplasmic GFP-p62 puncta was compared between neutrophils containing *S. aureus*, and those which did not. I hypothesised that under conditions where autophagic machinery is used for bacterial clearance (e.g. infected neutrophils), GFP-p62 puncta would be degraded. At 0dpi, no significant difference was found in the number of cytoplasmic puncta in non-infected and infected neutrophils (Fig. 6.14 A). However, at 1dpi, a significantly larger number of puncta are observed in non-infected neutrophils in comparison to infected neutrophils. These data show a reduction in the number of GFP-p62 puncta in infected neutrophils occurs over time. This suggests that GFP-p62 is being degraded over time, potentially caused by an increase in autophagic turnover in infected neutrophils.

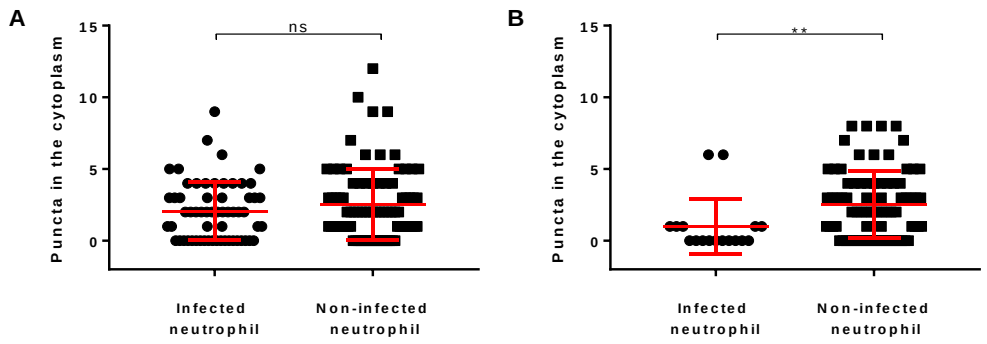

Figure 6.14 Cytoplasmic puncta in *S. aureus* infected and non-infected neutrophils

A GFP-p62 puncta in the cytoplasm of infected and non-infected at 0dpi (ns, Mann-Whitney test, n=3, error bars +/- SD, 14 larvae) **B** GFP-p62 puncta in the cytoplasm of infected and non-infected at 1dpi (**p<0.01, Mann-Whitney test, n=3, error bars +/- SD, 12 larvae)

Overall, these data demonstrate that in *S. aureus* infection, GFP-p62 puncta associate with bacteria. Neutrophils appear to be adept at clearance of most bacteria, degrading the majority by 1dpi, with largely cytoplasmic resident bacterial population observed at 1dpi. Cytoplasmic *S. aureus* may represent the small proportion of bacteria which survive in the neutrophil niche (Prajsnar et al. 2012). The proportion of bacteria which is cytoplasmic but not associated with GFP-p62 is increased by 1dpi. This may suggest that most bacteria are successfully captured and degraded through a p62-autophagy dependent mechanism.

6.10 Analysis of *C. neoformans* interaction with p62

The interaction of *C. neoformans* with GFP-puncta was next investigated. The larvae were injected with *C. neoformans* in order to quantify any association with p62 with cryptococcal cells within vesicles, and whether changes in p62 association with *C. neoformans* occur through the time course of infection. The *Tg(lyz:GFP.p62)* larvae were injected at 2dpf with 1000cfu of *C. neoformans*, and imaged at 2hpi, and 1dpi (~26hpi). Time points were chosen to compare initial pathogen-p62 interactions with any potential changes later in infection.

Unlike *S. aureus*, *C. neoformans* is not efficiently killed in the first 24 hours of infection and is only observed within "vesicles" (which lack GFP fluorescence as described above). In fact, the number of cryptococcal cells which are observed within neutrophils increases from 0dpi to 1dpi (Fig. 6.15 A). This may represent intracellular growth, or blood-stream growth which enables further phagocytosis of cryptococcal cells. There is

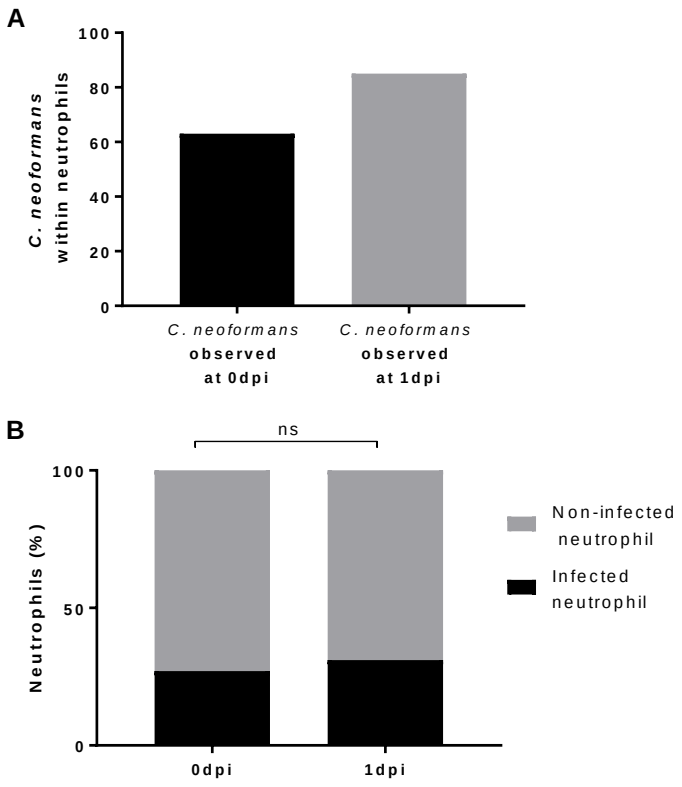

Figure 6.15 ***C. neoformans*** **growth *o*ver infection time course**

The *Tg(lyz:GFP.p62)* larvae were injected at 2dpf with 1000cfu of *C. neoformans*, and imaged at 2hpi, and 1dpi (~26hpi). **A** The number of *C. neoformans* events observed within neutrophils at 0dpi and 1dpi (n=3, 18 larvae at 0dpi, and 12 larvae at 1dpi) **B** Proportion of neutrophils infected or non-infected with *C. neoformans* at 0dpi and 1dpi (ns, Fisher's exact test, n=3, 18 larvae at 0dpi, and 12 larvae at 1dpi)

no significant change in the proportion of neutrophils which are infected at 0dpi and 1dpi, Fig. 6.15 B), at both 0dpi and 1dpi ~25% of neutrophils contain phagocytosed *C. neoformans*. This may suggest that intracellular proliferation of *C. neoformans* is increasing the number of cryptococcal cells observed in individual neutrophils in Figure 6.15 A.

I next compared the co-localisation of GFP-p62 puncta with *C. neoformans*. *C. neoformans* was observed with no GFP-p62 puncta within a “vesicle” (vesicle as described for *S. aureus*), or within cryptococcal vesicle which did have GFP-p62 puncta co-localisation (Fig. 6.16 A, B). The number of cryptococcal vesicles which have GFP-p62 puncta co-localisation is similar at 0dpi and 1dpi (Fig. 6.16 C). The same data (shown as a proportion) of cryptococcal vesicles with/without GFP-p62 puncta, shows that ~55% of vesicles have associated puncta. There is no significant change in puncta co-localisation to cryptococcal vesicles between 0dpi and 1dpi (Fig. 6.16 D). Taken together, these data show that GFP-p62 puncta localise to cryptococcal vesicles. However, no change in GFP-p62 association to cryptococcal vesicles over the time course of infection is observed, and may suggest that cryptococcal mediated manipulation of individual vesicles is preventing phagosome degradation.

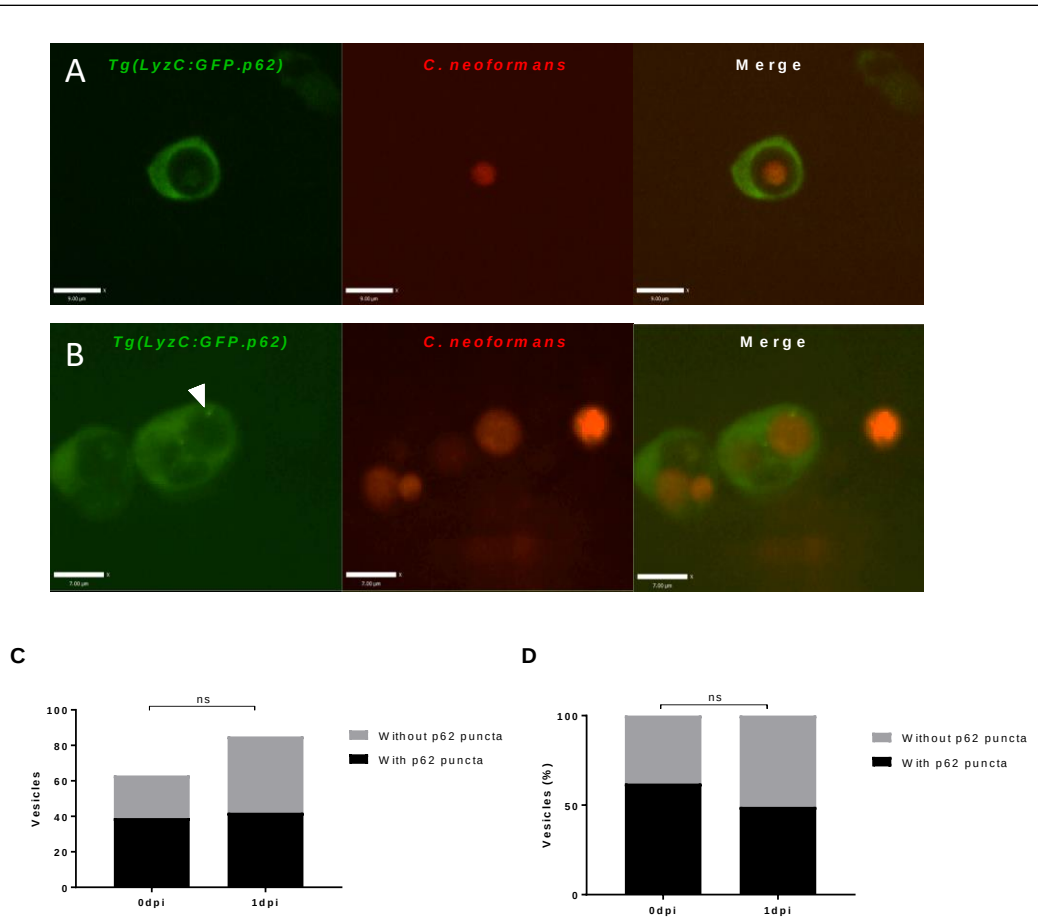

Figure 6.16 ***C. neoformans*** **co-localisation with GFP-p62**

A Representative image of *C. neoformans* observed within a likely "vesicle" with no GFP-p62 puncta localisation, scale 9um **B** representative image of *C. neoformans* observed within the cytoplasm with GFP-p62 puncta (white arrow) localisation, scale 7um **C** *C. neoformans* within vesicles, co-localised with GFP-p62 at 0dpi and 1dpi (ns, Fisher's exact test, n=3, 18 larvae at 0dpi, and 12 larvae at 1dpi) **D** Proportion of *C. neoformans* within vesicles, co-localised with GFP-p62 at 0dpi and 1dpi (ns, Fisher's exact test, n=3, 18 larvae at 0dpi, and 12 larvae at 1dpi)

The number of GFP-p62 puncta localised to individual cryptococcal vesicles was compared at 0dpi and 1dpi. The number of cryptococcal cells within individual vesicles was measured, to enable comparison of associated puncta in regards to size of the vesicle, where more cryptococcal cells increases the size of a vesicle. At 0dpi, a maximum of 3 cryptococcal cells are observed within an individual vesicle, with a single cell most often seen (Fig. 6.17 A). Furthermore, zero or a single puncta were most often observed, with multiple puncta occurring less frequently (Fig. 6.17 A).

At 1dpi, the maximum number of cryptococcal cells in an individual vesicle is 6 cells, likely representing intra-cellular growth during infection (Fig. 6.17 B). Similar to 0dpi, the majority of cryptococcal vesicles have a single or zero GFP-p62 puncta (Fig. 6.17 B). No change in the number of GFP-p62 puncta over infection (0dpi-1dpi) may suggest that cryptococcal cells manipulate their phagosome, which perhaps inhibits the ability of p62 to associate/dissociate at that location.

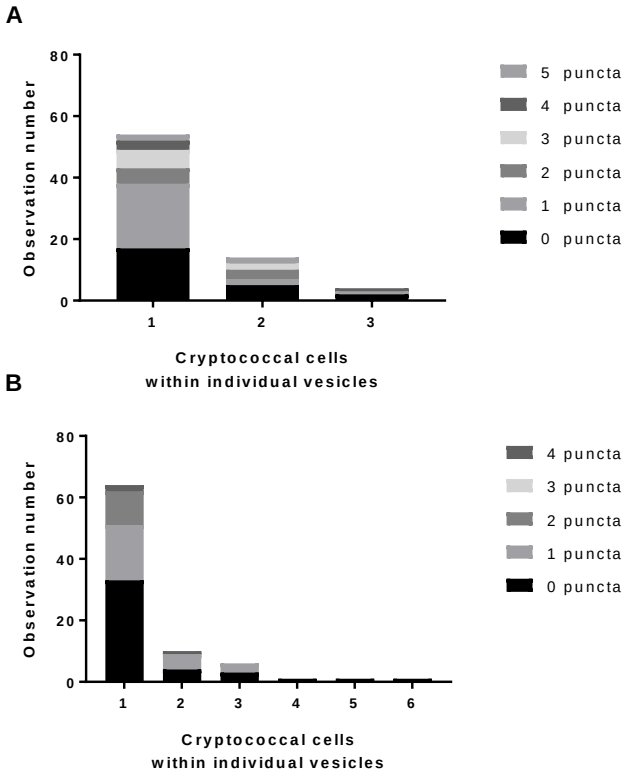

<u>Figure 6.17</u> Puncta on *C. neoformans* vesicles

The *Tg(lyz:GFP.p62)* larvae were injected at 2dpf with 1000cfu of *C. neoformans*, and imaged at 2hpi, and 1dpi (~26hpi). **A** GFP-p62 puncta on *C. neoformans* vesicles at 0dpi (n=3, 18 larvae) **B** GFP-p62 puncta on *C. neoformans* vesicles at 1dpi (n=3, 12 larvae)

Finally, the presence of GFP-p62 puncta in infected or non-infected neutrophils was compared, with the aim to determine whether puncta are “used-up” throughout infection. If puncta are “used-up” this may represent autophagy induction during cryptococcal infection. At 0dpi, unlike *S. aureus*, *C. neoformans* infection induces a significant reduction in the number of puncta in the cytoplasm of infected neutrophils (Fig. 6.18 A). Similarly, a significant reduction in GFP-p62 puncta presence in infected neutrophils was observed at 1dpi (Fig 6.18 B). Overall these data show that a GFP-p62

response does occur quickly in *C. neoformans* neutrophil infection, however, this response remains unchanged over the course of the infection.

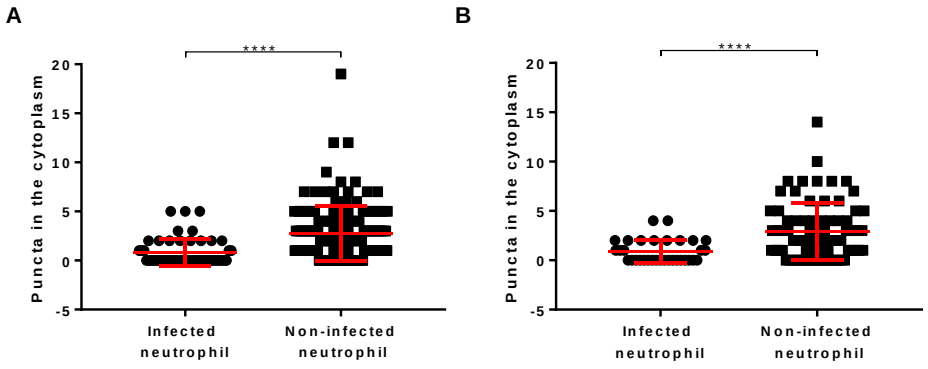

Figure 6.18 Cytoplasmic puncta in *C. neoformans* infected and non-infected neutrophils

A GFP-p62 puncta in the cytoplasm of infected and non-infected at 0dpi (****p<0.001, Mann-Whitney test, n=3, error bars +/- SD, 18 larvae) **B** GFP-p62 puncta in the cytoplasm of infected and non-infected at 1dpi (****p<0.001, Mann-Whitney test, n=3, error bars +/- SD, 12 larvae)

6.11 Chapter summary

The transgenic line *Tg(lyz:GFP.p62)* was generated through the Gateway™ Tol2 system, in order to examine whether p62 is involved in the neutrophil handling of *S. aureus* and *C. neoformans* infection *in vivo*. It was demonstrated that *Tg(lyz:GFP.p62)* was expressing GFP within neutrophils and that the GFP-p62 was successfully translated as a tagged protein. Furthermore, using GFP-p62 puncta as a read-out, it was shown that the tagged GFP-p62 likely responds in a similar as may be expected of endogenous p62.

Infection studies were next carried out, where an association of GFP-p62 was determined for both *S. aureus* and *C. neoformans*. For *S. aureus*, bacteria were efficiently degraded, however those which did survive until 1dpi were significantly less likely to associate with GFP-p62. This may indicate that p62 is involved in the clearance of *S. aureus* in neutrophils. While *C. neoformans* infection did induce a GFP-p62 association, the effect was constant between 2hpi and 1dpi. This may suggest that *C. neoformans* is manipulating the vesicle to enable survival, and this manipulation may inhibit p62 association.

6.12 Chapter discussion

The aim of this chapter was to design, generate and characterise a neutrophil specific GFP-p62 reporter line to enable analysis of *in vivo* interactions of p62 with pathogens.

6.12.1 Design and generation of a p62 reporter line

The design and generation of a p62 zebrafish reporter line was the initial aim in this chapter. A single p62 gene is encoded by zebrafish (Silva et al. 2014; Mostowy et al. 2013), meaning a single reporter was required for *in vivo* p62 analysis. Due to genome duplication events in zebrafish evolution, it is possible that multiple p62 genes may have been present, which could have evolved distinct functions in zebrafish requiring further analysis (Meyer & Schartl 1999). The p62 gene in zebrafish was confirmed in a recent study to be similar in gene sequence, structure, likely domain function and in expression (Silva et al. 2014). Furthermore, both LIR and UBA domains, important in the autophagy adapter function of p62, are present in the zebrafish p62 (Silva et al. 2014), therefore it is very likely that the zebrafish p62 gene will function as an autophagy receptor. Therefore I concluded that the zebrafish p62 gene would be useful in the analysis of p62 function, which could provide findings translational for human p62.

The Gateway™ and Tol2 transgenesis system was chosen to create the p62 reporter line. As a reporter line, the p62 protein would be a fusion protein with a fluorescent marker, in this case GFP. The structure of p62 gene was carefully considered. The location of the LIR and UBA domains are located at the 3' end of the p62 gene sequence. It is possible that placing a linker to a GFP protein at the 3' end of the p62 sequence, the GFP could sterically block LIR and UBA domain functions. Although this outcome is still potentially possible by placing the GFP protein on the 5' terminal, it was theorised there may be a reduced chance of this occurring. Furthermore, in all publications of a successful cell line expression of GFP-p62 fusion protein, it appears that the GFP was located on the 5' end of p62 (Larsen et al. 2010; Pankiv et al. 2007; Bjørkøy et al. 2005), further suggesting that LIR and UBA interactions can still occur with a GFP fusion at the 5' terminus. For these reasons the GFP was designed to be tagged to the 5' terminal of p62.

The Gateway™ and Tol2 system is a reliable and efficient method of creating reporter zebrafish lines. The 3' entry clone containing zebrafish p62 was created (as in appendix 1). Of note, a SNP led to a single residue alteration, albeit to a similar amino acid, is present in the p62 sequence used in this reported line. However, it is a

confirmed SNP in the zebrafish genome (appendix 1), and therefore is not expected to alter the function of p62.

The expression clone *pDEST(lyz:GFP.p62)* was created via the multisite Gateway™ three fragment assembly system, and inserted into the zebrafish genome through Tol2 mediated transgenesis. As described above, the *p5E-lyz* entry clone, *pME-GFP-nonstop* and generated *p3E-p62* were inserted into *pDestTol2CG* to create *pDEST(lyz:GFP.p62).* This was expected to produce neutrophil specific expression of GFP-p62 fusion protein, in addition to expression of GFP in the heart cells. Restriction digests of the *pDEST(lyz:GFP.p62),* (and sequencing of the plasmid) provided reliable evidence that the expression clone was the correct expected sequence and was therefore used for Tol2 transgenesis.

As described above, following Tol2 transgenesis, a high proportion of injected larvae expressed GFP in heart tissue and in neutrophil-like cells, this suggests that the transgenesis was successful. As a preliminary analysis of the F0 (Tol2 injected) generation, a limited number of larvae were infected with *C. neoformans* or *S. aureus*. This was completed to attempt to determine whether the GFP positive cells were likely to be neutrophils. As potential phagocytic cells, if the GFP positive cells were seen to engulf the pathogen, it would be suggested that the GFP fluorescence may be neutrophils (although could also be other phagocytic cells). Indeed, phagocytosis of each pathogen was observed, indicating the GFP cells were phagocytic cells. Additionally, a disperse cytoplasmic fluorescence and puncta fluorescence was observed within the GFP positive phagocyte cells, likely representing cytoplasmic GFP-62 not “in-use” whereas the puncta may represent sites of autophagosomes within individual phagocytic cells. Alternatively, puncta may represent aggregates of GFP-p62. However, a similar cytoplasmic and “dot” (puncta) fluorescence observation was seen for all *in vitro* studies using GFP-p62 (Larsen et al. 2010; Pankiv et al. 2007; Bjørkøy et al. 2005), suggesting that this type of expression is expected. Furthermore, antibody staining of endogenous p62 in HeLa cells also determined a puncta and cytoplasmic distribution of p62 (Bjørkøy et al. 2005). These observations suggest that Tol2 transgenesis was successful leading to the raising of these larvae as potential founders. Indeed, a founder was identified (screened by analysis of embryos resulting from an outcross to nacre wild-type larvae). Similarly, larvae from the founder fish expressed GFP in heart tissue and in neutrophil-like cells. It was therefore highly likely these cells, (as in the F0 generation), were phagocytic cells.

To conclude, successful design and generation of a neutrophil specific p62 reporter zebrafish line was completed. However, further characterisation was required to

determine whether the GFP signal in GFP expressing phagocytic cells, was truly a GFP-p62 fusion.

6.12.2 Characterisation of *Tg(lyz:GFP.p62)* reporter

After generation of the *Tg(lyz:GFP.p62)* reporter line, it was important to further characterise the GFP-p62 expression, specifically to determine whether the p62 reporter line has neutrophil specific expression, and if tagged GFP-p62 fusion protein acts in a similar manner as expected of endogenous p62.

Neutrophil specific GFP-p62 expression

Neutrophil specificity of GFP-p62 fluorescence was confirmed by crossing the *Tg(lyz:GFP.p62)* reporter line to a complementary fluorescently coloured neutrophil transgenic line. This cross was completed using a known mCherry neutrophil specific reporter (of nitroreductase gene *nfsB*), *Tg(lyz:nfsB.mCherry)*^{sh260}. A clear co-expression of GFP signal (GFP-p62) and mCherry signal (*nfsB*-mCherry) was observed, clearly demonstrating that GFP-p62 was being expressed within neutrophils. Indeed, only a single cell was observed with single GFP fluorescence, representing 0.92% of all compared cells. Furthermore, the intensity of cytoplasmic signal, either GFP or mCherry, was similar within individual cells, indicating that the fluorescence signal was being regulated by expression of the *lyz* promoter, as expected. These data suggest that GFP-p62 expressed within neutrophils.

Of note, the *lyz* promoter is largely neutrophil specific in zebrafish from 48hpf (Yang et al. 2012; Meijer et al. 2008), where before this age some macrophages may also express *lyz*. All experiments using this line were completed after 48hpf and therefore at these time-points GFP-p62 will be expressed only within neutrophils. However, comparing a *lyz* driven reporter line to another *lyz* driven reporter can only validate that expression in the same *lyz*-expressing cells is occurring. As some macrophages may express lyz, a comparison to alternative neutrophil promoter transgenic lines, such as *mpx* (neutrophil specific myeloperoxidase promoter) (Renshaw et al. 2006) may be useful. However, at 2dpf, *lyz* and *mpx* expression matched exactly (Meijer et al. 2008). It therefore may be better to test *Tg(lyz:GFP.p62)* neutrophil specificity using mpx histochemistry. However, these data suggest that GFP-p62 expression is specific to neutrophils.

Interestingly, puncta observed in GFP positive cells were GFP positive only, rather than both GFP (GFP-p62) and mCherry (*nfsB*-mCherry). This suggests that GFP puncta formation is independent of the *lyz* promoter. It is tempting to suggest puncta formation

is dependent on p62 protein functions. However, it is also possible that GFP-p62 may self-aggregate (independent of p62 protein function) and could therefore be the cause of GFP puncta formation. Interestingly, mCherry fusion proteins are thought to have an increased likelihood of self-aggregation in comparison to GFP fusion proteins (Voigt 2011). To examine whether GFP-p62 puncta are self-aggregating or dependent on p62 protein function, puncta were examined when autophagy influencing drugs were administered.

GFP-p62 response to autophagy induction or inhibition

In order to determine whether GFP-p62 responded to autophagy induction, or inhibition, *Tg(lyz:GFP.p62)* larvae were treated with autophagy inhibiting drugs, BK8644 or chloroquine, or with autophagy inducing drug rapamycin, or in combinded rapamycin and chloroquine treatment. The aim was to determine whether GFP-p62 puncta are affected by alterations in autophagy, to examine whether GFP-p62 puncta are self-aggregates or caused by p62 functions.

If GFP-p62 puncta are dependent on the autophagy function of p62, it may be expected where autophagy is inhibited, an increase in GFP-p62 puncta would be observed, since GFP-p62 would not be degraded by autophagy. Conversely, induction of autophagy may increase the rate of GFP-p62 degradation, and therefore a reduction in the number of GFP-p62 puncta may be expected.

Firstly, the number of neutrophils with puncta present in was compared between drug treatment groups. No change in the number of neutrophils containing puncta was seen between rapamycin, rapamycin and chloroquine treatment, BK8644, chloroquine alone, in comparison non-treated larvae. These results do not demonstrate the GFP-p62 puncta are being affected in terms of formation and degradation in response to autophagy influencing drugs.

The number of puncta within individual neutrophils was compared between treatment groups. A significant increase in the number of puncta inside individual neutrophils was observed after BK8644 treatment in comparison to non-treated larvae. No change was observed between non-treated, rapamycin and chloroquine treatment, chloroquine treatments. The BK8644 data do suggest that GFP-p62 puncta respond to autophagy influencing drugs, potentially in a manner similar to how endogenous p62 may be expected to. It would be useful in future to examine whether ubiquitin in present in the GFP-p62 puncta, which may indicate that the puncta are forming through a p62 mediated mechanism.

Importantly, autophagy is known to target protein aggregates for degradation. It is therefore possible that if the GFP-p62 is self-aggregating to form these puncta, the cellular clearance would also be affected an autophagy dependent manner leading to similar expected results. *In vitro* GFP-p62 fusion protein expression led to the observation of both cytoplasmic and “dot” (puncta) types of expression in all studies (Larsen et al. 2010; Pankiv et al. 2007; Bjørkøy et al. 2005). This suggests that puncta formation is not only seen *in vivo* as seen in this study, and may be an expected expression pattern of p62. As mentioned above antibody staining of endogenous p62 in HeLa cells also determined puncta and cytoplasmic distribution of p62 (Bjørkøy et al. 2005). Furthermore, *in vitro* expression of “dots” (puncta) was found to be dependent on the intact UBA domain in the fusion protein sequence. *In vitro* GFP-p62 constructs deficient in the UBA domain of p62, led to the observation of only cytoplasmic signal (Bjørkøy et al. 2005), suggesting puncta formation is dependent of p62 function. Interestingly, an increase in the number and size of *in vitro* GFP-p62 were observed when autophagy was inhibited (Bjørkøy et al. 2005), similar to data presented here. These data suggest that GFP-p62 puncta formation is caused by p62 function.

However, an important difference between some *in vitro* studies is that the cells are transiently expressing GFP-p62, (either due to tetracycline inducible expression of a stable line, or through transfection). In a stably expressing *in vitro* line, (expressed at approximately 4 fold higher than endogenous p62), an increase in puncta from 5 to 40% was observed (Bjørkøy et al. 2005). This may explain the large variation of GFP-p62 puncta observed in non-treated cells. In future it might be informative to analyse the rate of GFP-p62 expression in zebrafish in comparison to endogenous p62, perhaps by comparing puncta in wild-type larvae using anti-p62 antibodies. Furthermore, using live imaging of co-localisation to alternative autophagy markers, for example fluorescently tagged LC3, LAMP-1 or sytanxin-17 and the use of pH sensitive dyes, would enable visualisation of the interaction dynamics with multiple markers of autophagosomes/lysosomes. This would help determine that GFP-p62 puncta were truly marking autophagosomes, rather than protein aggregates.

To conclude, these data suggest that the GFP-p62 puncta are responding according to autophagy influence. However, they cannot definitely prove the GFP-p62 puncta are acting in a p62 manner.

GFP-p62 is a fusion protein

In order to determine that the GFP signal observed in the larvae was from correctly translated GFP-p62 fusion proteins, a western blot was used to analyse the size of the GFP proteins, or GFP tagged proteins in larvae. Wild-type control larvae had no GFP protein present as expected. Larvae from *Tg(mpx:eGFP)*^{i114} which express non-tagged GFP, had a single protein size present, at ~27KDa, the correct size of non-tagged GFP, also expected.

The expected size of a GFP-p62 fusion protein was calculated from the sequence, of ~79KDa. No protein was observed at ~79KDa in protein lysate collected from *Tg(lyz:GFP.p62)*, however GFP protein was identified at ~125KDam, ~62KDa, ~52KDa, ~46KDa, a large band at ~27KDa, and ~24KDa. The large band at ~27KDa likely represents the non-tagged GFP heart marker present in this line. As described above, antibody company Abcam advised that in western blots used on human brain protein samples, using their anti-p62 antibody (ab31545), four major bands were detected at 130KDa, 62KDa, 45KDa and 22KDa, with additional bands observed in rat lysate at 80KDa and 47KDa. This suggests that multiple p62 protein products exist, which are somewhat similar to protein sizes observed in zebrafish. Therefore, the observation of multiple bands representing GFP-p62 may be expected in zebrafish.

However, the reason that the expected band size of 79KDa is not present is not explained. Multiple factors can affect the running size of a protein which leads to difference in the predicated size and the size actually observed. For example, post-translational modification (such as phosphorylation), splice variants, relative charge and even formation of complexes. The occurrence of multiple sized proteins smaller than the expected 79kDa may be caused by splice variants, or potentially from transcription starting from in-frame internal methionine's which may lead to the formation of smaller protein products. It is unlikely smaller sized proteins are caused by degradation of GFP-p62 as a band sizes are discrete (rather than a smear expected when proteins are degraded). Further analysis into the splice variants and internal methionine transcription is required to fully understand the formation of smaller sized GFP-p62 proteins.

The ~125KDa size protein may be explained by dimerisation. p62 is known to form dimers, which could provide an explanation for the larger protein size observed, however the reducing western blot protocol may be expected to cause separation of these dimers. It has been reported that the p62 dimer, is highly stable, particularly in the presence of ubiquitin (Long et al. 2010). Furthermore, covalent bonds between p62 oligomers have been shown to form between the PB1 (Phox/Bem 1p) domains

(Donohue et al. 2014), which would be able to survive the western blotting protocol. It is therefore likely that the ~125kDa size protein represents p62 dimers. Additionally, the presence of the ~125KDa protein size suggests that the GFP-p62, in particular the PB1 domain, is able to act functionally as may be expected of endogenous p62.

To conclude, western blot analysis suggests that the *Tg(lyz:GFP.p62)* is in fact a GFP-p62 fusion protein, since the anti-GFP antibody used can only recognise proteins with GFP encoded, and multiple sized protein were recognised. Multiple p62 protein products have been observed human and rat samples, which appear somewhat similar in size to the GFP-p62, suggesting that forms of p62 are present in zebrafish. This includes p62 dimers, which are present in other animals. Together these data suggest that that the GFP-p62 fusion protein is successfully being produced within *Tg(lyz:GFP.p62)* larvae.

6.12.3 In vivo p62 co-localisation to *S. aureus* in neutrophils

The primary aim of this chapter was to use an *in vivo* zebrafish neutrophil reporter line to examine p62 interactions with intracellular pathogens. With the aim to determine whether p62 is employed by neutrophils in *in vivo S. aureus* infection, the host-pathogen interaction in *Tg(lyz:GFP.p62)* larvae were examined under *S. aureus* infection.

The number of neutrophils, which contain *S. aureus,* declined between 0dpi and 1dpi. This is very suggestive that neutrophils effectively degrade bacteria, or alternatively that *S. aureus* escapes neutrophils, perhaps through cell lysis. There was no observation that a large number of extracellular bacteria exist at 1dpi, suggesting that neutrophils effectively degrade *S. aureus* in the majority of cases. The presence of a small population of bacteria resident in neutrophils at 1dpi, supports the suggestion that a population bottleneck is caused in *S. aureus* infection. Whereby neutrophils provide an intraphagocyte niche in which a small proportion of bacteria reside, able to evade degradation, and finally escape and cause uncontrolled infection (Prajsnar et al. 2012). This assumes most bacteria and phagocytosed and degraded, as these current data suggest. Time-lapse analysis of *in vivo* cellular fates of neutrophils which contain bacteria at 1dpi may provide further evidence that bacteria are degraded or that bacteria can lyse the host cell. Alternatively, neutrophils could be collected through FACs sorting and infected *in vitro*, to enable individual cells to be monitored for the entire infection cycle, which may not be possible *in vivo*.

The location of *S. aureus* within the neutrophils was examined. The role of p62 in its ability to bind to ubiquitinated pathogens which are residing in the cytoplasm is established, so it was important to determine the location of the bacteria. As described

above, disperse cytoplasmic GFP-p62 signal was observed in neutrophil cells. In larvae which had been infected with *S. aureus*, circular “gaps” surrounding some bacteria were observed. I reasoned these “gaps” likely represent vesicles in which bacteria are contained but do not contain GFP-p62, due to the similarities in size and shape, as seen in other lines where the vesicle edges are clearly observed, for example traffic-light LC3 marked vesicles (see Chapter 5). It could be further reasoned that in an acidic environment GFP-p62 fluorescence would be quenched, so these “gaps” may also represent acidic vesicles. Importantly, the following data refers to these “gaps” as vesicles, despite the fact there are not fully proven to be vesicles. Further analysis to confirm vesicle identity is required, for example using electron microscopy, or use of pH sensitive dyes.

The majority of bacteria were resident in vesicles at 0dpi, but by 1dpi the majority of bacteria was resident in the cytoplasm (although most bacteria appear to have been degraded by 1dpi). Data using the traffic-light Lc3 line (see Chapter 5) agrees with this bacterial location data, further suggesting the “gaps” are truly vesicles. It is therefore likely that bacteria which escape from vesicles are able to survive longer, potentially by escaping vesical mediated degradation. In fact bacteria which escape vesicles, and represent the majority of bacteria at 1dpi, may be the bacteria which survive the population bottleneck in neutrophils (Prajsnar et al. 2012). To confirm this the fates of bacteria which are cytoplasmic residents could be compared with vesicle resident bacteria. Perhaps using time-lapse imaging both *in vivo* and *in vitro* may (as above), may provide evidence for this.

Importantly, an association of GFP-p62 puncta to *S. aureus* is clearly demonstrated in these data. Interestingly GFP-p62 is seen to localise both to *S. aureus* vesicles, and to cytoplasmic bacteria, which is unexpected as a role of p62 binding to ubiquitinated bacteria in the cytoplasm has been described, which no role of p62 being linked to *S. aureus* within vesicles. Ubiquitination of cargo for p62-mediated autophagy degradation is required for p62 to recognise and bind cargo, before interacting with autophagosome membranes through the LIR domain.

For bacteria within vesicles, ~70% of vesicles were co-localised with GFP-p62 puncta, although 1dpi this was not seen (which may in part be due to bacterial clearance). This data suggests that p62 presence on *S. aureus* vesicles is associated with bacterial degradation, however this does not show causality. To determine causality, perhaps *in vitro* analysis using cells deficient in p62, comparison of bacterial location (vesicle or cytoplasm) and survival may highlight a role of p62 in *S. aureus* vesicle degradation.

p62 has been well established as binding to ubiquitinated bacteria before localisation to LC3 marker autophagosomes, For example it has been demonstrated that p62 is involved in *Shigella flexneri* and *Listeria monocytogenes* autophagic degradation (Mostowy et al. 2011; Mostowy et al. 2010). It may be possible that the vesicles here represent autophagosomes, which have formed through selective autophagy pathways, after *S. aureus* has been ubiquitinated. In fact, recent literature reports that p62 is able to recruit *S. aureus* residing in the cytoplasm to an autophagosome (Neumann et al. 2016; Singh et al. 2017). This could suggest bacteria escape the phagosome after internalisation, p62 is recruited to ubiquitinated bacteria and autophagosomes are formed (which represent the GFP-p62 vesicles).

GFP-p62 marked vesicles may also represent phagosomes, since vesicles are observed soon after *S. aureus* infection, and not often at 1dpi. This could suggest p62 is being recruited to phagosomes, perhaps marked with LC3 through LAP, where p62 could potentially bind to through the LIR domain. However, the p62 LIR domain alone cannot target to LC3 positive membranes, shown when the LIR domain of p62, fused to GFP could not associate to LC3 marked membranes (Donohue et al. 2014), suggesting that multiple parts of the protein must be involved. Additionally, p62 is not recruited during LAP, for example, p62 is not recruited to *Listeria monocytogenes* LAP phagosomes (Lam et al. 2013). Therefore p62 recruitment is unlikely to represent LAP.

Despite this, a single incidence of p62 recruitment to a single-membrane has been described in the phagocytosis of red blood cells. Where single-membrane phagosome recruit LC3-II, p62, NDP52 and NBR1, all components of selective autophagy (Santarino et al. 2017). It was further suggested that the UBA, rather than LIR domain was required for the association of p62 with single membranes, perhaps to ubiquitinated components of the phagosome membrane. Indeed ubiquitin was found present on phagocytic cups which could enable p62 recruitment. Finally, p62 recruitment occurred before LC3-II recruitment to phagosomes, which may in part help to up-regulate autophagy pathways resulting in increased autophagy (Santarino et al. 2017). This suggests that p62 can recruit to phagosomes, independently of LC3-II. This might represent observations seen in this current analysis, and perhaps could be due to overexpression of GFP-p62. It might be useful to analyse the activity of the p62 and *lyz* promoters, perhaps through a promoter reporter system. Further investigation into whether *S. aureus* vesicles are single or double membrane structures is required to determine how GFP-p62 is being recruited, however if single-membrane vesicles are determined this may represent the first example of p62 recruitment to a pathogen (single membrane) phagosome.

For bacteria residing in the cytoplasm, GFP-p62 can co-localise to *S. aureus*, as expected in comparison to recent reports where p62 is shown to recruit ubiquitinated *S. aureus* to autophagosomes (Neumann et al. 2016; Singh et al. 2017). Interestingly, the association of GFP-p62 reduces over the infection time-course, perhaps suggesting that bacteria associated with GFP-p62 are being degraded, or can escape the autophagosome, this would be consistent with recent studies (Neumann et al. 2016; Singh et al. 2017). However, association does not prove causality, and (as above), time lapse analysis to visualise the degradation/escape of bacteria with/without GFP-p62 would be essential to determine whether GFP-p62 is leading to bacterial degradation.

To assess if GFP-p62 may be causing the degradation of *S. aureus*, the number of GFP-p62 puncta within infected and non-infected neutrophils was compared. Since p62 is degraded along with bacteria in selective autophagy, a reduced number of puncta may be expected within infected neutrophils. Indeed, at 1dpi, a reduction in GFP-p62 puncta was observed specifically within infected neutrophils. This suggests GFP-p62 is being degraded in infected neutrophils. It is possible that this is caused not by GFP-p62 recruitment to ubiquitinated bacteria, but by an increase in autophagy at the whole cell level, caused by *S. aureus* presence, which may be beneficial for the bacteria (Neumann et al. 2016; Singh et al. 2017). To prove GFP-p62 degradation is being caused specifically by targeting of bacteria, further analysis to allow visualisation of entire infection cycles, for example time-lapse, is required.

To conclude, GFP-p62 puncta associated with cytoplasmic bacteria as expected and also with bacteria within vesicles. Further analysis to determine exactly what vesicles bacteria are contained in, perhaps using multiple membrane markers (e.g. LC3-II, LAMP-1, Syntaxin-17), or electron microscopy to determine if it is single or double membrane is important. Together these data suggest cytoplasmic bacteria is targeted for autophagosome degradation by GFP-p62, which may represent the co-localisation to *S. aureus* containing vesicles. Furthermore, the likely degradation of most bacteria, suggests that those bacteria resident in the cytoplasm may be the source of the *S. aureus* population bottle-neck. Further analysis is required to determine whether the evasion of p62-autophagy dependent mechanism may be responsible for the *S. aureus* population bottleneck.

6.12.4 In vivo p62 co-localisation to *C. neoformans* in neutrophils

The next aim of this chapter was to determine whether p62 is employed by neutrophils during *in vivo* cryptococcal infection. Therefore host-pathogen interactions were examined in *Tg(lyz:GFP.p62)* larvae after *C. neoformans* infection. Importantly, extremely limited studies on the role of autophagy and selective autophagy exist for *C.*

neoformans or other fungal pathogens, which makes it difficult to interpret the data presented in this study.

During cryptococcal infection, the number of infected neutrophils was relatively constant, with ~25% of neutrophils infected at both 0dpi and 1dpi. In contract to *S. aureus* data, this suggests that *C. neoformans* in not effectively degraded by neutrophils, and cannot escape from neutrophils at 1dpi. Although cryptococcal cells are able to escape from macrophages by vomocytosis, a similar mechanism is not described for neutrophils. It might be likely cryptococcal cells escape neutrophils by lysis. Furthermore, all cryptococcal cells were observed within vesicles ("vesicles" as described as "gaps" above). Similarly, identification of the type of vesicle cryptococcal cells are in would be useful in the interpretation of this data.

It appears that cryptococcal cells are able to proliferate within the neutrophil, observed with a small increase in the number of cryptococcal cells within individual neutrophils. Coupled with the constant rate of ~25% of infected neutrophils, this increase in cryptococci may represent intracellular proliferation. Equally this may represent further phagocytosis events. In order to prove intracellular replication in neutrophils, time-lapse analysis is required. The presence of *C. neoformans* is able to reduce the killing ability of neutrophils, although the mechanism for this is currently unknown (Qureshi et al. 2011), this may enable the survival of cryptococcal cells within neutrophils.

Approximately 55% of all cryptococcal vesicles had associated GFP-p62 puncta at both 0dpi and 1dpi. Unlike *S. aureus*, it is unlikely that GFP-p62 is marking cryptococcal cells for degradation and then recruiting cryptococcal cells to autophagosome for degradation. This is because, cryptococcal cells have never been found within double-membrane vesicles, only within a single membrane vesicle, despite autophagosomes being seen in close proximity (Nicola et al. 2012; Pandey et al. 2017). It is therefore likely that the vesicles represent a single-membrane vesicle. As described above for *S. aureus*, there is some limited data to suggest that p62 is able to mark phagosomes in a UBA mediated binding mechanism to ubiquitinated products on the phagosome, before LC3-II is recruited (Santarino et al. 2017). If this is occurring for *C. neoformans* this would be the first evidence of fungal cells being targeted by selective autophagy within neutrophils. Clearly much more investigation is required, the type of vesicles *C. neoformans* is residing in must be confirmed. Additionally, over expression my lead to GFP-p62 accumulation, the levels of endogenous p62 recruitment could be compared by antibody staining.

Additionally, the fact that association does not change over the infection time course may suggest that the phagosome in not able to mature. It has been demonstrated that

in macrophages, cryptococcal cells can manipulate the phagosome to promote intracellular survival (Smith et al. 2015). Perhaps GFP-p62 is unable to either associate or dissociate when the phagosome is manipulated. If 25% of cryptococcal cells are able to promote their own survival within neutrophils, coupled with potential intracellular replication shown in this study, neutrophils may also present a niche in which cryptococcal cells can reside in.

The number of GFP-p62 puncta present in infected and non-infected neutrophils were compared. A significant reduction in the number of GFP-p62 puncta were present in infected neutrophils at both 0dpi and 1dpi. This suggests autophagy is induced immediately within infected neutrophils, leading to the degradation of GFP-p62. It has been shown that autophagy proteins are required for *C. neoformans* growth, of intracellular cryptococci within macrophages (Qin et al. 2011). Although contradictory evidence exists for whether autophagy is beneficial for the host or fungus (see section 1.6.8), it is tempting to suggest that host cell autophagy is induced in neutrophils upon infection, which leads to survival of cryptococcal cells within neutrophils, with the increased autophagy removing GFP-p62 puncta from the cell.

To conclude, GFP-p62 puncta associated with both cryptococcal cells, perhaps un-expectedly since they likely reside within single membrane vesicles. Further analysis is required to confirm a single membrane vesicle contains the cryptococcal cells, for example by electron microscopy. Due to the non-changing nature of the cryptococcal interactions described here, it would be interesting to follow infection over a long timescale, to determine whether GFP-p62 association leads to any differences in cryptococcal survival or host cell handling. Together these data suggest ~25% cryptococcal cells become marked by GFP-p62, in a static way, perhaps caused by cryptococcal manipulation of the phagosome. Further analysis is required to determine whether evasion of p62-autophagy is important in the outcome of cryptococcal-neutrophil interactions.

6.12.5 Chapter summary

In this chapter a neutrophil specific reporter line was designed and created using the Gateway™ and Tol2 transgenesis systems. The GFP-p62 fusion protein appears to be expressed exclusively within neutrophils, and responds to autophagy influencing drugs in an expected manner. Infection of the *Tg(lyz:GFP.p62)* with *S. aureus* suggested that p62 associates with cytoplasmic bacteria, leading to autophagosome recruitment. However, both *S. aureus* and *C. neoformans* within (what appear to be) vesicles, also have GFP-p62 recruitment. This may represent an initial observation of p62 recruitment

to pathogen vesicle membranes, although could also represent autophagosomes. Further analysis is required to determine whether GFP-p62 recruitment to pathogens in beneficial to the host or pathogen.

7.0 Overall discussion and future work

7.1 Intravascular cryptococcal proliferation leads to tissue invasion

Cryptococcal infection can cause cryptococcal meningitis, primarily in immunocompromised individuals. Cortical infarcts are observed in severe cases of cryptococcal meningitis, and are associated with increased lethality (Mishra et al. 2017). However, the physiological cause of cortical infarcts in cryptococcal meningitis is unknown. Clinical reports have shown that cryptococcal invasion of the brain occurs at sites of brain micro-capillaries which contain cryptococcal cells, and that cryptococcal infection causes vasculitis (Aharon-Peretz et al. 2004; Leite et al. 2004; Rosario et al. 2012). It is possible that vascular damage occurs at sites of cryptococcal growth in the brain. I therefore hypothesised that cortical infarcts (in cryptococcal meningitis) may be related to vascular damage caused by cryptococcal proliferation.

The data presented in this study show that cryptococcal cells become trapped in the vasculature (likely due to vessel size), in a mechanism similar to that reported in mice (Shi et al. 2010). Once trapped in the vasculature, localised cryptococcal proliferation causes vessel widening and damage. Subsequently, tissue invasion occurs at sites of cryptococcal proliferation. Tissue invasion may be enabled by damage to the vessel wall allowing escape or by another mechanism, likely to be transcytosis. Importantly my data suggest blood vessels become completely obstructed by resident cryptococcal cells, and that vessel wall integrity is lost through physical damage caused by cryptococcal proliferation. This may provide a physiological explanation for the cortical infarcts observed in cryptococcal meningitis.

This study also suggests that damage to the vasculature caused by cryptococcal proliferation provides an alternative route for cryptococcal cells to invade tissue. This may be of particular importance in crossing of the blood brain barrier by cryptococci. I propose that cryptococcal proliferation may be a mechanism for escaping the vasculature, which occurs in concert with alternative routes, for example by transcytosis or via a macrophage Trojan-horse (Charlier et al. 2009; Chen et al. 2003; Santiago-Tirado et al. 2017). Interestingly, tissue invasion was observed which did not damage vessel wall integrity, and is likely to be transcytosis. However, this occurred in this study only at sites of cryptococcal proliferation within the vasculature. This may suggest that intra-vascular cryptococcal proliferation also promotes transcytosis events, perhaps by promoting cryptococcal cell interactions with vascular endothelial cells. This is supported by the observation that cryptococcal invasion of the brain occurs in vessels with a high fungal burden (Tenor et al. 2015). It would be interesting to determine whether rates of cryptococcal transcytosis out of the vasculature are

determined by the number of cryptococcal cells (caused by proliferation) within the vessel.

An interesting observation was that vessel widening occurs at sites away from cryptococcal cells. This may represent vasculitis which is observed in cryptococcal meningitis (Leite et al. 2004). It was determined that vessel widening (away from cryptococcal sites) is likely caused by a cryptococcal factor, because I did not observe vessel widening at sites which were not obstructed by inert beads. However, a greater number of vessel blockage events may result in greater blood flow forces on unobstructed vessels resulting in increased growth/widening. It will be important to determine accurately whether vessel widening away from bead blockage can occur at higher bead inocula, as a major difference of cryptococcal cells in comparison to beads is their ability to proliferate and therefore cause vessel blockage in a larger number of intersegmental vessels. This may be assessed easily by injecting a much larger inocula of beads.

Cryptococcal mutants were used to test whether cryptococcal factors influence both cryptococcal vascular damage and may cause vessel widening at sites away from cryptococcal colonised vessels. All cryptococcal mutants examined were able to cause vessel damage at the site of cryptococcal proliferation, suggesting that cryptococcal proliferation is the major cause of vessel damage, rather than cryptococcal virulence factors. All cryptococcal mutants examined were also able to cause widening in vessels not colonised by *C. neoformans*. This suggests that the particular virulence factors which were examined do not affect the entire vasculature. In the future it would be exciting to examine many more cryptococcal virulence factors. If a cryptococcal mutant does not illicit a widening effect on vessels not colonised by *C. neoformans*, this may represent a virulence factor which may be a useful target in preventing vasculitis in cryptococcal meningitis. In turn, this may even reduce brain tissue invasion since vascular integrity may be improved in all vessels.

Overall, a clear mechanism of cryptococcal trapping, proliferation and tissue invasion through vascular damage is shown. These data may explain the presence of cortical infarcts in cryptococcal meningitis. Examining a potential role of cryptococcal virulence factors in causing widespread vascular damage may lead to therapeutic targets in the future to reduce clinical vasculitis in cryptococcal meningitis.

7.2 Characterisation of autophagy mutant zebrafish

Autophagy mutant zebrafish were generated to enable analysis of the role of autophagy in infection studies. It was important to first investigate whether the mutations were effective, and whether the mutations resulted in a loss of autophagy function. The genes *atg3* and *atg5* are both involved in ubiquitin-like conjugation processes, ultimately leading to LC3-I lipidation (Mizushima et al. 2001). Lc3-I lipidation is important in the formation of the autophagosome. Corresponding autophagy mice mutants are not able to produce lipidated Lc3, and have lower levels of amino acids (presumably due to lack of autophagy recycling of cellular components) (Kuma et al. 2004; Sou et al. 2008). Therefore, zebrafish mutants in key autophagy genes *atg3* or *atg5* were expected to result in an inability to lipidate Lc3-I, and be deficient in autophagy processes.

Maternally contributed mRNA was shown to be depleted by 5dpf for both *atg3* and *atg5* mutants. At 8dpf, *atg5* mutants did not have Atg5 protein. This suggests the mutations are effective in eliminating *atg3* or *atg5* expression. In the future it will be important to prove that Atg3 protein is also missing in zebrafish.

A clear survival defect and a growth defect were observed in both autophagy mutants, highlighting a clear phenotype. This differs from corresponding mouse mutants which are neonatal lethal (Kuma et al. 2004; Sou et al. 2008). As described in Chapter 4, differences in autophagy requirements between mammals and fish, for example differences in metabolic rate, may explain this. To prove these phenotypes are caused by a lack of autophagy, further work is required. Mouse mutant data suggest reduced amino acids may cause reduced survival (Kuma et al. 2004; Sou et al. 2008). It would be informative to examine amino acid levels in zebrafish throughout development, to determine if a reduction in amino acid availability corresponds to declining survival. Further analysis of organs/tissues which require a high autophagic turnover, for example cardiac tissue, may suggest a cause of death. Importantly, autophagy mutant zebrafish appear to be able to survive for a useful lifespan (in comparison to murine models). Therefore zebrafish autophagy mutants may enable *in vivo* study of autophagy which currently cannot be completed in mouse models.

It is expected that Lc3-I lipidation would not occur in zebrafish autophagy mutants. However, Lc3-II was observed at 2dpf and at 8dpf in both mutants. For *atg5* mutants (and likely for *atg3* mutants), this observation is difficult to explain, since by at least 8dpf (due to lack of Atg5 protein) larvae are not expected to be able lipidated Lc3-I. There are two possible explanations, either lipidation is performed by residual maternal Atg5, or lipidation is occurring via an Atg3 and Atg5 independent pathway.

The first explanation is that, Lc3-I lipidation is truly blocked in autophagy mutants, but due to maternal contribution, residual Atg5 is present in the larvae. Throughout development this is slowly used up leading to a delayed survival defect. To test this easily, Lc3 western blots through larval development after 8dpf and until 30dpf, could be used to determine if Lc3-II is reduced over time. This represents a key experiment that would be very informative for the future. Interestingly, in Chapter 5, at the cellular level, autophagy mutants appear to have a reduction in Lc3 marking of pathogen phagosomes. This might suggest that in cells which are actively using autophagy, any potential Atg5 protein (resulting from maternal contribution) is used up faster.

The alternative explanation is that Lc3 lipidation is not blocked in autophagy mutants. In this case for *atg5* (and likely *atg3*) this means that lipidation is occurring without the ubiquitin-conjugation systems. This raises a major question, of how Lc3-II is being produced in autophagy mutants. It may be useful to examine the potential roles of other E2-like enzymes in their ability to lipidate Lc3-I. If a separate enzyme was found to lipidate Lc3-I this could lead to a significant adjustment in the established autophagy pathway mechanisms.

To conclude, both autophagy mutations (for *atg5* and likely for *atg3*) successfully stop expression of key autophagy genes. A significant survival and growth defect caused by autophagy mutations is observed. To prove this phenotype is caused by autophagy deficiency analysis of amino acid levels is required. Furthermore, it is important to determine whether Lc3-I lipidation is truly present in autophagy mutants and if so, analysis of alternative lipidation mechanisms would be an exciting focus for the future.

7.3 Does autophagy have a role in *S. aureus* and *C. neoformans* handling?

S. aureus and *C. neoformans* are both able to reside intracellularly within host cells (Prajsnar et al. 2012; Levitz et al. 1999) and both pathogens have reduced replication when the host cell is deficient in autophagy (Diamond & Bennett 1973; Schnaith et al. 2007), suggesting autophagy is beneficial for pathogen growth. On the other hand, autophagy can degrade pathogens, which has been demonstrated to occur to *S. aureus* (Harada-Hada et al. 2014). Host cell autophagy appears to be either beneficial or detrimental depending on the strain of *S. aureus* and the type of cell the bacteria is residing in (discussed in section 1.4.7). There are limited data on the role of host cell autophagy in handling of *C. neoformans*. It is therefore unclear whether host cell autophagy is beneficial to the host or either invading pathogen.

Overall, using larval survival and bacterial/fungal burden as endpoints to monitor *S. aureus* or *C. neoformans* infection, I did not highlight autophagy deficiency as either

beneficial or detrimental to the pathogen or host. Importantly, both *S. aureus* and *C. neoformans* are capable of surviving intracellularly and extracellularly. It appears that using an entire organism may mask any changes in infection outcome caused by autophagy, which would only occur for intracellular pathogens. Analysis of exclusively intracellular pathogens is required, to exclude the contribution of extracellular pathogen infection dynamics. Overall I am not confident in concluding these data show autophagy deficiency does not affect *S. aureus* or *C. neoformans* infection.

An interesting observation was that Lc3-II can mark both *S. aureus* and *C. neoformans* vesicles in neutrophils soon after infection, and that this reduced over time. This suggests that Lc3-assisted phagocytosis (LAP) may play an important role in *S. aureus* and, particularly in *C. neoformans* infection, since cryptococcal cells are not known to reside in double-membrane vesicles. It the future, using electron microscopy to prove a single membrane structure is being marked with Lc3 will provide evidence that LAP is a host cell autophagy response to *S. aureus* and *C. neoformans*.

Autophagy mutant larvae showed a reduction in Lc3 recruitment to both pathogens in neutrophils. However, this shows only that a reduction of Lc3 recruitment occurs in autophagy mutant larvae. While this provides evidence the mutants are truly deficient in autophagy, it is impossible to conclude what a lack of Lc3 recruitment would cause, in terms of pathogen degradation or survival. Unfortunately it was not possible to analyse whether reduced recruitment leads to changes in cellular infection outcome. This represents vital experimental data which will help determine the role host cell autophagy plays in the control of intracellular pathogens.

After consideration of the data and progress (in terms of clearly determining how host cell autophagy affects intracellular pathogens) so far, it would be much more productive, and likely more successful, to focus on using time-lapse analysis of intracellular interactions of autophagy components with pathogens in autophagy mutants. Initial data suggests that Lc3 recruitment to pathogens is reduced in autophagy mutants. This opens an opportunity to discover what effect loss of Lc3 has on infection outcome, potentially enabling the role of autophagy in intracellular pathogen interactions to be determined. The zebrafish model was chosen specifically to enable *in vivo* analysis of host-autophagy pathogens and observe how these interactions occur. Using these advantages, future analysis could focus on further Lc3 interactions, and other autophagy markers, for example p62 using the transgenic line generated in this study (Chapter 6). In addition, it would be interesting to compare different cells, for example neutrophils, macrophages or endothelial cells to determine whether autophagy is utilised or subverted differently, depending on cell type.

7.4 Does p62-mediated selective autophagy target *S. aureus* and *C. neoformans* for degradation?

A zebrafish line was established, with a GFP-p62 neutrophil specific reporter, to enable analysis of p62 interactions with *S. aureus* and *C. neoformans*. Expression of GFP-p62 was shown to be neutrophil specific, and likely to act in a similar manner to endogenous p62. It would be informative to further analyse whether GFP-p62 is expressed at a similar level and is functionally similar to endogenous p62, in terms of promoter expression (since this line is likely over expressing GFP-p62), and in binding activity to ubiquitinated cargo and Lc3. It is important to keep in mind that although GFP-p62 can co-localise to pathogens, overexpression of GFP-p62 may enable more binding than would occur under normal circumstances. To determine whether binding activity is similar, co-localisation of pathogens, ubiquitin and Lc3 with p62 in wild-type and *Tg(lyz:GFP.p62)* larvae could be compared by antibody staining and imaging.

Interestingly, GFP-p62 was recruited to both *S. aureus* and *C. neoformans* that had been phagocytosed by neutrophils. This is expected for *S. aureus*, as p62 is known to recruit ubiquitinated staphylococci (which have escaped the phagosome) to an autophagosome (Neumann et al. 2016; Singh et al. 2017). In fact this co-localisation suggests that GFP-p62 is acting in the same way as endogenous p62. This would represent the first *in vivo* reporter line evidence of p62 recruitment to pathogens. It would be useful to determine if ubiquitination is occurring on *S. aureus* within neutrophils to further confirm this mechanism.

GFP-p62 appeared to be recruited to vesicles containing *S. aureus* or *C. neoformans*. Firstly, it is very important to determine whether these vesicles have a single membrane, by electron microscopy or membrane marker localisation. If it is determined that GFP-p62 is recruited to a single membrane containing pathogens, this may be the first report of this occurring. A single report of p62 binding to phagosomes (before LC3 recruitment in LAP) had been described for erythrocyte phagocytosis (Santarino et al. 2017). It has been suggested that p62 binding to a single membrane leads to increased LC3-II and ultimately, autophagy-mediated degradation (Santarino et al. 2017). It would be informative to prove p62 recruitment to phagosomal membranes occurs and to examine what role this may have in pathogen control.

Overall, these data only show co-localisation and do not provide evidence of the role p62 plays in host cell interactions with each pathogens. It would be particularly exciting to research this topic further, through use of zebrafish autophagy mutants. It may be possible to reduce GFP-p62 binding to pathogens or pathogen vesicles (in these

mutants), and determine whether p62 binding is dependent on Lc3-I lipidation. Equally, if p62 is able to bind phagosomes independently (in autophagy mutants), this would represent a new role of autophagy machinery in degradation of pathogens.

7.5 Thesis summary

The zebrafish infection model was used to analyse host-pathogen interactions with *S. aureus* and *C. neoformans*. This study has progressed the established tissue invasion mechanisms of *C. neoformans*, to include vascular damage caused by cryptococcal proliferation, and may even explain the occurrence of cortical infarcts in cryptococcal meningitis. It is demonstrated that autophagy components Lc3 and p62 are involved in neutrophil handling of *S. aureus* and *C. neoformans*. Despite this, the role of autophagy in handling *S. aureus* and *C. neoformans* and infection outcome is unclear. However, through characterisation of autophagy mutants and generation of a p62 reporter line, the next stages of future investigation, suggested above, are likely to provide informative data on the role of host cell autophagy in neutrophil handling of *S. aureus* and *C. neoformans*.

Reference List

Abe, Y. et al., 1998. Streptococcal and staphylococcal superantigen-induced lymphocytic arteritis in a local type experimental model: Comparison with acute vasculitis in the arthus reaction. *Journal of Laboratory and Clinical Medicine*, 131(1), pp.93–102.

Aharon-Peretz, J. et al., 2004. Cryptococcal meningitis mimicking vascular dementia. *Neurology*, 62(11), p.2135.

Al-Daccak, R., Mooney, N. & Charron, D., 2004. MHC class II signaling in antigen-presenting cells. *Current Opinion in Immunology*, 16(1), pp.108–113.

Alspaugh, J.A. & Granger, D.L., 1991. Inhibition of Cryptococcus neoformans replication by nitrogen oxides supports the role of these molecules as effectors of macrophage-mediated cytostasis. *Infection and immunity*, 59(7), pp.2291–6.

Altfeld, M. et al., 2000. T(H)1 to T(H)2 shift of cytokines in peripheral blood of HIV-infected patients is detectable by reverse transcriptase polymerase chain reaction but not by enzyme-linked immunosorbent assay under nonstimulated conditions. *Journal of acquired immune deficiency syndromes (1999)*, 23(4), pp.287–94.

Alvarez, M. & Casadevall, A., 2007. Cell-to-cell spread and massive vacuole formation after Cryptococcus neoformans infection of murine macrophages. *BMC immunology*, 8(16).

Amano, A., Nakagawa, I. & Yoshimori, T., 2006. Autophagy in innate immunity against intracellular bacteria. *Journal of biochemistry*, 140(2), pp.161–6.

Amer, A.O. & Swanson, M.S., 2005. Autophagy is an immediate macrophage response to Legionella pneumophila. *Cellular Microbiology*, 7(6), pp.765–778.

Anderson, J.M. & Van Itallie, C.M., 2009. Physiology and function of the tight junction. *Cold Spring Harbor perspectives in biology*, 1(2), p.a002584.

Arango Duque, G. & Descoteaux, A., 2014. Macrophage cytokines: involvement in immunity and infectious diseases. *Frontiers in immunology*, 5(491).

Arroyo, D.S. et al., 2013. Toll-like receptor 2 ligands promote microglial cell death by inducing autophagy. *The FASEB Journal*, 27(1), pp.299–312.

Asakawa, K. & Kawakami, K., 2008. Targeted gene expression by the Gal4-UAS system in zebrafish. *Development, Growth & Differentiation*, 50(6), pp.391–399.

Ashford, T.P. & Porter, K.R., 1962. Cytoplasmic components in hepatic cell lysosomes. *The Journal of cell biology*, 12, pp.198–202.

Auffray, C. et al., 2007. Monitoring of Blood Vessels and Tissues by a Population of Monocytes with Patrolling Behavior. *Science*, 317(5838), pp.666–70.

Axe, E.L. et al., 2011. Autophagosome formation from membrane compartments enriched in phosphatidylinositol 3-phosphate and dynamically connected to the endoplasmic reticulum. *The Journal of cell biology*, 182(4), pp.685–701.

Bakowska-Zywicka, K. & Tyczewska, A., 2009. Ribophagy–the novel degradation system of the ribosome. *Biotechnologia*, 1(84), pp.99–103.

Bayles, K.W. et al., 1998. Intracellular Staphylococcus aureus escapes the endosome and induces apoptosis in epithelial cells. *Infection and immunity*, 66(1), pp.336–42.

Ben-Ami, R. et al., 2010. Characterization of a 5-azacytidine-induced developmental Aspergillus fumigatus variant. *Virulence*, 1(3), pp.164–73.

Bera, A. et al., 2004. Why are pathogenic staphylococci so lysozyme resistant? The peptidoglycan O-acetyltransferase OatA is the major determinant for lysozyme resistance of Staphylococcus aureus. *Molecular Microbiology*, 55(3), pp.778–787.

Bhakdi, S. & Tranum-Jensen, J., 1991. Alpha-toxin of Staphylococcus aureus. *Microbiological reviews*, 55(4), pp.733–51.

Bjørkøy, G. et al., 2009. Chapter 12 Monitoring Autophagic Degradation of p62/SQSTM1. In pp. 181–197.

Bjørkøy, G. et al., 2005. p62/SQSTM1 forms protein aggregates degraded by autophagy and has a protective effect on huntingtin-induced cell death. *The Journal of Cell Biology*, 171(4).

Bojarczuk, A. et al., 2016. Cryptococcus neoformans Intracellular Proliferation and Capsule Size Determines Early Macrophage Control of Infection. *Scientific reports*, 6, p.21489.

Bokarewa, M., Jin, T. & Tarkowski, A., 2006. Staphylococcus aureus: Staphylokinase. *The International Journal of Biochemistry & Cell Biology*, 38(4), pp.504–509.

Botts, M.R. & Hull, C.M., 2010. Dueling in the lung: how Cryptococcus spores race the host for survival. *Current opinion in microbiology*, 13(4), pp.437–42.

Bovers, M., Hagen, F. & Boekhout, T., 2008. Diversity of the Cryptococcus neoformans-Cryptococcus gattii species complex. *Revista iberoamericana de micología*, 25(1), pp.S4-12.

Boya, P., Reggiori, F. & Codogno, P., 2013. Emerging regulation and functions of autophagy. *Nature cell biology*, 15(7), pp.713–20.

Brauweiler, A.M., Goleva, E. & Leung, D.Y.M., 2016. Interferon-γ Protects from Staphylococcal Alpha Toxin-Induced Keratinocyte Death through Apolipoprotein L1. *Journal of Investigative Dermatology*, 136(3), pp.658–664.

Brinkmann, V. et al., 2004. Neutrophil Extracellular Traps Kill Bacteria. *Science*, 303(5663), pp.1532–1535.

Bröker, B.M., Mrochen, D. & Péton, V., 2016. The T Cell Response to Staphylococcus aureus. *Pathogens*, 5(1).

Brown, A.F. et al., 2015. Memory Th1 Cells Are Protective in Invasive Staphylococcus aureus Infection L. S. Miller, ed. *PLOS Pathogens*, 11(11), p.e1005226.

Buchanan, K., 1998. What Makes Cryptococcus neoformans a Pathogen? *Emerging Infectious Diseases*, 4(1), pp.71–83.

Bukowski, M., Wladyka, B. & Dubin, G., 2010. Exfoliative toxins of Staphylococcus aureus. *Toxins*, 2(5), pp.1148–65.

Bussmann, J. & Schulte-Merker, S., 2011. Rapid BAC selection for tol2-mediated transgenesis in zebrafish. *Development*, 138(19), pp.4327–4332.

Campbell-Valois, F.-X. et al., 2015. Escape of Actively Secreting Shigella flexneri from ATG8/LC3-Positive Vacuoles Formed during Cell-To-Cell Spread Is Facilitated by IcsB and VirA. *mBio*, 6(3), pp.e02567-14.

Carnicer-Pont, D. et al., 2006. Risk factors for hospital-acquired methicillin-resistant Staphylococcus aureus bacteraemia: a case-control study. *Epidemiology and infection*, 134(6), pp.1167–73.

Chamoux, E. et al., 2009. The p62 P392L Mutation Linked to Paget's Disease Induces Activation of Human Osteoclasts. *Molecular Endocrinology*, 23(10), pp.1668–

1680.

Chan, S.N. & Tang, B.L., 2013. Location and membrane sources for autophagosome formation – from ER-mitochondria contact sites to Golgi-endosome-derived carriers. *Molecular Membrane Biology*, 30(8), pp.394–402.

Chang, T.-K. et al., 2013. Uba1 functions in Atg7- and Atg3-independent autophagy. *Nature Cell Biology*, 15(9), pp.1067–1078.

Chang, Y.C. & Kwon-Chung, K.J., 1994. Complementation of a capsule-deficient mutation of Cryptococcus neoformans restores its virulence. *Molecular and cellular biology*, 14(7), pp.4912–9.

Charlier, C. et al., 2009. Evidence of a Role for Monocytes in Dissemination and Brain Invasion by Cryptococcus neoformans. *Infection and Immunity*, 77(1), pp.120–127.

Chaturvedi, V., Wong, B. & Newman, S., 1996. Oxidative killing of Cryptococcus neoformans by human neutrophils. Evidence that fungal mannitol protects by scavenging reactive oxygen intermediates. *The Journal of Immunology*, 156(10), pp.3836–40.

Chayakulkeeree, M. et al., 2011. SEC14 is a specific requirement for secretion of phospholipase B1 and pathogenicity of Cryptococcus neoformans. *Molecular Microbiology*, 80(4), pp.1088–1101.

Chayakulkeeree, M. et al., 2012. SEC14 is a specific requirement for secretion of phospholipase B1 and pathogenicity of Crytococcus neoformans. , 80(4), pp.1088–1101.

Chen, S.C.A. et al., 2000. Purification and characterization of secretory phospholipase B, lysophospholipase and lysophospholipase/transacylase from a virulent strain of the pathogenic fungus Cryptococcus neoformans. *Biochemical Journal*, 347(2), pp.431–439.

Chen, S.H. et al., 2003. Cryptococcus neoformans induces alterations in the cytoskeleton of human brain microvascular endothelial cells. *Journal of Medical Microbiology*, 1134(52), pp.961–970.

Cheng, P.-Y., Sham, A. & Kronstad, J.W., 2009. Cryptococcus gattii isolates from the British Columbia cryptococcosis outbreak induce less protective inflammation in a murine model of infection than Cryptococcus neoformans. *Infection and immunity*, 77(10), pp.4284–94.

Cheong, H. et al., 2014. Analysis of a lung defect in autophagy-deficient mouse strains. *Autophagy*, 10(1), pp.45–56.

Chiang, H. et al., 1989. A role for a 70-kilodalton heat shock protein in lysosomal degradation of intracellular proteins. *Science*, 246(4928).

Clements, M. 0 & Foster, S.J., 1998. Starvation recovery of Staphylococcus aureus 8325-4. *Microbiology*, 144, pp.1755–1.

Codogno, P., Mehrpour, M. & Proikas-Cezanne, T., 2011. Canonical and non-canonical autophagy: variations on a common theme of self-eating? *Nature Reviews Molecular Cell Biology*, 13(1), p.7.

Coelho, C., Bocca, A.L. & Casadevall, A., 2014. The Tools for Virulence of Cryptococcus neoformans. In pp. 1–41.

Collins, C.A. et al., 2009. Atg5-Independent Sequestration of Ubiquitinated Mycobacteria L. Ramakrishnan, ed. *PLoS Pathogens*, 5(5), p.e1000430.

Colombo, M.I., 2005. Pathogens and autophagy: subverting to survive. *Cell death and differentiation*, 12 Suppl 2, pp.1481–3.

Crotzer, V.L. & Blum, J.S., 2010. Autophagy and adaptive immunity. *Immunology*, 131(1), pp.9–17.

Cuervo, A.M. & Dice, J.F., 1996. A Receptor for the Selective Uptake and Degradation of Proteins by Lysosomes. *Science*, 273(5274).

Cunnion, K.M. & Frank, M.M., 2003. Complement activation influences Staphylococcus aureus adherence to endothelial cells. *Infection and immunity*, 71(3), pp.1321–7.

Davis, J.M. et al., 2016. A Zebrafish Model of Cryptococcal Infection Reveals Roles for Macrophages, Endothelial Cells, and Neutrophils in the Establishment and Control of Sustained Fungemia. *Infection and immunity*, 84(10), pp.3047–62.

Davis, M.J. et al., 2015. Cryptococcus neoformans-induced macrophage lysosome damage crucially contributes to fungal virulence. *Journal of immunology*, 194(5), pp.2219–31.

Degenhardt, K. et al., 2006. Autophagy promotes tumor cell survival and restricts necrosis, inflammation, and tumorigenesis. *Cancer cell*, 10(1), pp.51–64.

Diamond, R.D. & Bennett, J.E., 1973. Growth of Cryptococcus neoformans within human macrophages in vitro. *Infection and immunity*, 7(2), pp.231–6.

Diamond, R.D., Root, R.K. & Bennett, J.E., 1972. Factors Influencing Killing of Cryptococcus neoformans by Human Leukocytes in vitro. *The Journal of Infectious Diseases*, 125(4), pp.367–376.

Dice, J.F., 1990. Peptide sequences that target cytosolic proteins for lysosomal proteolysis. *Trends in biochemical sciences*, 15(8), pp.305–9.

Dinges, M.M., Orwin, P.M. & Schlievert, P.M., 2000. Exotoxins of Staphylococcus aureus. *Clinical microbiology reviews*, 13(1), pp.16–34.

Donohue, E. et al., 2014. Induction of Covalently Crosslinked p62 Oligomers with Reduced Binding to Polyubiquitinated Proteins by the Autophagy Inhibitor Verteporfin. *PloS one*, 9(12), p.e114964.

Dorn, B.R., Dunn, W.A. & Progulske-Fox, A., 2001. Porphyromonas gingivalis traffics to autophagosomes in human coronary artery endothelial cells. *Infection and immunity*, 69(9), pp.5698–708.

Dryla, A. et al., 2005. Comparison of antibody repertoires against Staphylococcus aureus in healthy individuals and in acutely infected patients. *Clinical and diagnostic laboratory immunology*, 12(3), pp.387–98.

Dupont, N. et al., 2011. Autophagy-based unconventional secretory pathway for extracellular delivery of IL-1β. *The EMBO Journal*, 30(23), pp.4701–4711.

Ehrengruber, M.U., Geiser, T. & Deranleau, D.A., 1994. Activation of human neutrophils by C3a and C5A. Comparison of the effects on shape changes, chemotaxis, secretion, and respiratory burst. *FEBS letters*, 346(2–3), pp.181–4.

von Eiff, C. et al., 2001. Nasal Carriage as a Source of Staphylococcus aureus Bacteremia. *New England Journal of Medicine*, 344(1), pp.11–16.

Elks, P.M. et al., 2011. Activation of hypoxia-inducible factor-1α (Hif-1α) delays inflammation resolution by reducing neutrophil apoptosis and reverse migration in a zebrafish inflammation model. *Blood*, 118(3), pp.712–22.

Falugi, F. et al., 2013. Role of protein A in the evasion of host adaptive immune

responses by Staphylococcus aureus. *mBio*, 4(5), pp.e00575-13.

Fang, L. et al., 2014. TLR2 mediates phagocytosis and autophagy through JNK signaling pathway in Staphylococcus aureus-stimulated RAW264.7 cells. *Cellular Signalling*, 26(4), pp.806–814.

Farnoud, A.M. et al., 2015. The Granuloma Response Controlling Cryptococcosis in Mice Depends on the Sphingosine Kinase 1-Sphingosine 1-Phosphate Pathway. *Infection and immunity*, 83(7), pp.2705–13.

Farré, J.-C. & Subramani, S., 2016. Mechanistic insights into selective autophagy pathways: lessons from yeast. *Nature Reviews Molecular Cell Biology*, 17(9), pp.537–552.

Feldmesser, M. et al., 2000. Cryptococcus neoformans is a facultative intracellular pathogen in murine pulmonary infection. *Infection and immunity*, 68(7), pp.4225–37.

Fischer von Mollard, G. & Stevens, T.H., 1999. The Saccharomyces cerevisiae v-SNARE Vti1p is required for multiple membrane transport pathways to the vacuole. *Molecular biology of the cell*, 10(6), pp.1719–32.

Flesch, I.E., Schwamberger, G. & Kaufmann, S.H., 1989. Fungicidal activity of IFN-gamma-activated macrophages. Extracellular killing of Cryptococcus neoformans. *Journal of immunology (Baltimore, Md. : 1950)*, 142(9), pp.3219–24.

Floret, D., Delmas, C. & Cochat, P., 1989. Cerebellar infarction as a complication of pneumococcus meningitis. *The Pediatric Infectious Disease Journal*, 8(1), p.57.

Flory, C.M., Jones, M.L. & Warren, J.S., 1993. Pulmonary granuloma formation in the rat is partially dependent on monocyte chemoattractant protein 1. *Laboratory investigation; a journal of technical methods and pathology*, 69(4), pp.396–404.

Foley, J.E. et al., 2009. Targeted mutagenesis in zebrafish using customized zinc-finger nucleases. *Nature protocols*, 4(12), pp.1855–67.

Forsgren, A. & Nordström, K., 1974. Protein A from Staphylococcus aureus: the biological significance of its reaction with IgG. *Annals of the New York Academy of Sciences*, 236(1), pp.252–266.

Foster, T.J., 2005. Immune evasion by staphylococci. *Nature reviews. Microbiology*, 3(12), pp.948–58.

Franco, L.H. et al., 2017. The Ubiquitin Ligase Smurf1 Functions in Selective Autophagy of Mycobacterium tuberculosis and Anti-tuberculous Host Defense. *Cell Host & Microbe*, 21(1), pp.59–72.

Fromtling, R., Shadomy, H. & Jacobson, E., 1982. Decreased virulence in stable, acapsular mutants ofCryptococcus neoformans. *Mycopathologia*, 79(1), pp.23–9.

Fujita, N. et al., 2008. The Atg16L Complex Specifies the Site of LC3 Lipidation for Membrane Biogenesis in Autophagy. *Molecular Biology of the Cell*, 19(5), pp.2092–2100.

Garcia-Hermoso, D., Janbon, G. & Dromer, F., 1999. Epidemiological evidence for dormant Cryptococcus neoformans infection. *Journal of clinical microbiology*, 37(10), pp.3204–9.

Garro, A.P. et al., 2011. Eosinophils elicit proliferation of naive and fungal-specific cells in vivo so enhancing a T helper type 1 cytokine profile in favour of a protective immune response against Cryptococcus neoformans infection. *Immunology*, 134(2), pp.198–213.

Garro, A.P. et al., 2010. Rat eosinophils stimulate the expansion of Cryptococcus neoformans-specific CD4(+) and CD8(+) T cells with a T-helper 1 profile. *Immunology*, 132(2), pp.174–87.

Gates, M. a & Kozel, T.R., 2006. Differential localization of complement component 3 within the capsular matrix of Cryptococcus neoformans. *Infection and immunity*, 74(6), pp.3096–106.

Geunes-Boyer, S. et al., 2012. Surfactant protein D facilitates Cryptococcus neoformans infection. *Infection and immunity*, 80(7), pp.2444–53.

Geunes-Boyer, S. et al., 2009. Surfactant protein D increases phagocytosis of hypocapsular Cryptococcus neoformans by murine macrophages and enhances fungal survival. *Infection and immunity*, 77(7), pp.2783–94.

Gibson, R.H. et al., 2017. Mycophenolate mofetil increases susceptibility to opportunistic fungal infection independent of lymphocytes. *bioRxiv*.

Girardin, S.E. et al., 2003. Nod2 is a general sensor of peptidoglycan through muramyl dipeptide (MDP) detection. *The Journal of biological chemistry*, 278(11), pp.8869–72.

Glick, D., Barth, S. & Macleod, K.F., 2010. Autophagy: cellular and molecular mechanisms. *The Journal of pathology*, 221(1), pp.3–12.

Goldman, D.L. et al., 2001. Serologic Evidence for Cryptococcus neoformans Infection in Early Childhood. *Pediatrics*, 107(5), pp.e66–e66.

Goldsmith, J.R. & Jobin, C., 2012. Think small: zebrafish as a model system of human pathology. *Journal of biomedicine & biotechnology*, 2012, p.817341.

Goodyear, C.S. & Silverman, G.J., 2003. Death by a B cell superantigen: In vivo VH-targeted apoptotic supraclonal B cell deletion by a Staphylococcal Toxin. *The Journal of experimental medicine*, 197(9), pp.1125–39.

Grant, A.J. et al., 2008. Modelling within-Host Spatiotemporal Dynamics of Invasive Bacterial Disease D. A. Relman, ed. *PLoS Biology*, 6(4), p.e74.

Gratacap, R.L., Rawls, J.F. & Wheeler, R.T., 2013. Mucosal candidiasis elicits NF-κB activation, proinflammatory gene expression and localized neutrophilia in zebrafish. *Disease models & mechanisms*, 6(5), pp.1260–70.

Gray, C. et al., 2007. Ischemia Is Not Required for Arteriogenesis in Zebrafish Embryos. *Arteriosclerosis, Thrombosis, and Vascular Biology*, 27(10), pp.2135–2141.

Guidi-Rontani, C., 2002. The alveolar macrophage: the Trojan horse of Bacillus anthracis. *Trends in microbiology*, 10(9), pp.405–9.

Gutierrez, M.G. et al., 2005. Autophagy induction favours the generation and maturation of the Coxiella-replicative vacuoles. *Cellular Microbiology*, 7(7), pp.981–993.

Guttman, J.A. & Finlay, B.B., 2009. Tight junctions as targets of infectious agents. *Biochimica et Biophysica Acta (BBA) - Biomembranes*, 1788(4), pp.832–841.

van Hal, S.J. et al., 2012. Predictors of mortality in Staphylococcus aureus Bacteremia. *Clinical microbiology reviews*, 25(2), pp.362–86.

Hallett, A.F. & Cooper, R., 1980. Complement activation in Staphylococcus aureus bacteraemia. *Clinical and experimental immunology*, 40(2), pp.306–11.

Harada-Hada, K. et al., 2014. Phospholipase C-Related Catalytically Inactive Protein

Participates in the Autophagic Elimination of Staphylococcus aureus Infecting Mouse Embryonic Fibroblasts M. Komatsu, ed. *PLoS ONE*, 9(5), p.e98285.

Hare, R. & Thomas, C.G., 1956. The transmission of Staphylococcus aureus. *British medical journal*, 2(4997), pp.840–4.

Hart, P.D. & Young, M.R., 1991. Ammonium chloride, an inhibitor of phagosome-lysosome fusion in macrophages, concurrently induces phagosome-endosome fusion, and opens a novel pathway: studies of a pathogenic mycobacterium and a nonpathogenic yeast. *The Journal of experimental medicine*, 174(4), pp.881–9.

Harwood, C.G. & Rao, R.P., 2014. Host pathogen relations: exploring animal models for fungal pathogens. *Pathogens (Basel, Switzerland)*, 3(3), pp.549–62.

Hato, T. & Dagher, P.C., 2015. How the Innate Immune System Senses Trouble and Causes Trouble. *Clinical journal of the American Society of Nephrology : CJASN*, 10(8), pp.1459–69.

Haugen, R.K. & Baker, R.D., 1954. The pulmonary lesions in cryptococcosis with special reference to subpleural nodules. *American journal of clinical pathology*, 24(12), pp.1381–90.

Hayashi, F., Means, T.K. & Luster, A.D., 2003. Toll-like receptors stimulate human neutrophil function. *Blood*, 102(7), pp.2660–2669.

Hayes, J.B. et al., 2016. Modulation of Macrophage Inflammatory Nuclear Factor κB (NF-κB) Signaling by Intracellular Cryptococcus neoformans. *The Journal of biological chemistry*, 291(30), pp.15614–27.

He, C. & Klionsky, D., 2010. Analyzing autophagy in zebrafish. *Autophagy*, 6(5), pp.642–644.

He, W. et al., 2003. Phagocytic activity and monocyte chemotactic protein expression by pulmonary macrophages in persistent pulmonary cryptococcosis. *Infection and immunity*, 71(2), pp.930–6.

Herbomel, P., Thisse, B. & Thisse, C., 1999. Ontogeny and behaviour of early macrophages in the zebrafish embryo. *Development*, 126(17), pp.3735–45.

Hernandez, L.D. et al., 2003. A Salmonella protein causes macrophage cell death by inducing autophagy. *The Journal of cell biology*, 163(5), pp.1123–31.

Heyworth, P.G., Cross, A.R. & Curnutte, J.T., 2003. Chronic granulomatous disease. *Current Opinion in Immunology*, 15(5), pp.578–584.

Higgins, J. et al., 2006. Clumping factor A of *Staphylococcus aureus* inhibits phagocytosis by human polymorphonuclear leucocytes. *FEMS Microbiology Letters*, 258(2), pp.290–296.

Hosokawa, N. et al., 2009. Nutrient-dependent mTORC1 Association with the ULK1 – Atg13 – FIP200 Complex Required for Autophagy. , 20(m), pp.1981–1991.

von Hoven, G. et al., 2012. Modulation of translation and induction of autophagy by bacterial exoproducts. *Medical Microbiology and Immunology*, 201(4), pp.409–418.

Howe, K. et al., 2013. The zebrafish reference genome sequence and its relationship to the human genome. *Nature*, 496(7446), pp.498–503.

Hu, C. et al., 2012. Functional characterization of lipase in the pathogenesis of Staphylococcus aureus. *Biochemical and Biophysical Research Communications*, 419(4), pp.617–620.

Hu, Z., Zhang, J. & Zhang, Q., 2011. Expression pattern and functions of autophagy-related gene atg5 in zebrafish organogenesis. *Autophagy*, 7(12), pp.1514–27.

Huang, H. et al., 2006. Comparisons of community-associated methicillin-resistant Staphylococcus aureus (MRSA) and hospital-associated MSRA infections in Sacramento, California. *Journal of clinical microbiology*, 44(7), pp.2423–7.

Hwang, W.Y. et al., 2013. Efficient genome editing in zebrafish using a CRISPR-Cas system. *Nature Biotechnology*, 31(3), pp.227–229.

Hynes, W.L. & Walton, S.L., 2000. Hyaluronidases of Gram-positive bacteria. *FEMS Microbiology Letters*, 183(2), pp.201–207.

Ichimura, Y. et al., 2000. A ubiquitin-like system mediates protein lipidation. *Nature*, 408(6811), pp.488–492.

Itano, A.A. & Jenkins, M.K., 2003. Antigen presentation to naive CD4 T cells in the lymph node. *Nature Immunology*, 4(8), pp.733–739.

Izumikawa, K. et al., 2008. A case of pulmonary cryptococcosis followed by pleuritis in an apparently immunocompetent patient during fluconazole treatment. *Medical Mycology*, 46(6), pp.595–599.

Jaillon, S. et al., 2013. Neutrophils in innate and adaptive immunity. *Seminars in Immunopathology*, 35(4), pp.377–394.

Janeway, C.A.J. et al., 2001a. B-cell activation by armed helper T cells. In *Immunobiology: The immune system in health and disease. 5th Edition.* New York: Garland Science, p. Available from: https://www.ncbi.nlm.nih.gov/books.

Janeway, C.A.J. et al., 2001b. Induced innate responses to infection. In *Immunobiology: The immune system in health and disease. 5th Edition.* Garland Science, p. Available from: https://www.ncbi.nlm.nih.gov/books.

Janeway, C.A.J. et al., 2001c. T cell-mediated cytotoxicity. In *Immunobiology: The immune system in health and disease. 5th Edition.* Garland Science, p. Available from: https://www.ncbi.nlm.nih.gov/books.

Janeway, C.A.J. et al., 2001d. The complement system and innate immunity. In *Immunobiology: The immune system in health and disease. 5th Edition.* Garland Science, p. Available from: https://www.ncbi.nlm.nih.gov/books.

Jankowski, A., Scott, C.C. & Grinstein, S., 2002. Determinants of the phagosomal pH in neutrophils. *The Journal of biological chemistry*, 277(8), pp.6059–66.

Jardine, D. & Litvak, M.K., 2003. Direct yolk sac volume manipulation of zebrafish embryos and the relationship between offspring size and yolk sac volume. *Journal of Fish Biology*, 63(2), pp.388–397.

Jarvis, J.N. et al., 2013. The phenotype of the Cryptococcus-specific CD4+ memory T-cell response is associated with disease severity and outcome in HIV-associated cryptococcal meningitis. *The Journal of infectious diseases*, 207(12), pp.1817–28.

Jarvis, J.N. & Harrison, T.S., 2007. HIV - associated cryptococcal meningitis. *AIDS*, 21(16), pp.2119–29.

Jault, C., Pichon, L. & Chluba, J., 2004. Toll-like receptor gene family and TIR-domain adapters in Danio rerio. *Molecular Immunology*, 40(11), pp.759–771.

Jenkins, A. et al., 2015. Differential expression and roles of Staphylococcus aureus virulence determinants during colonization and disease. *mBio*, 6(1), pp.e02272-14.

Jin, J.-O. et al., 2014. BDCA1-positive dendritic cells (DCs) represent a unique human myeloid DC subset that induces innate and adaptive immune responses to Staphylococcus aureus Infection. *Infection and immunity*, 82(11), pp.4466–76.

Johnston, S. a & May, R.C., 2010. The human fungal pathogen Cryptococcus neoformans escapes macrophages by a phagosome emptying mechanism that is inhibited by Arp2/3 complex-mediated actin polymerisation. *PLoS pathogens*, 6(8), p.e1001041.

Juenemann, K. & Reits, E.A., 2012. Alternative Macroautophagic Pathways. *International Journal of Cell Biology*, 2012.

Kane, D.A. & Kimmel, C.B., 1993. The zebrafish midblastula transition. *Development (Cambridge, England)*, 119(2), pp.447–56.

Kanther, M. et al., 2011. Microbial colonization induces dynamic temporal and spatial patterns of NF-κB activation in the zebrafish digestive tract. *Gastroenterology*, 141(1), pp.197–207.

Kasper, L. et al., 2014. Identification of Candida glabrata Genes Involved in pH Modulation and Modification of the Phagosomal Environment in Macrophages A. T. Coste, ed. *PLoS ONE*, 9(5), p.e96015.

Kawakami, K., Shima, A. & Kawakami, N., 2000. Identification of a functional transposase of the Tol2 element, an Ac-like element from the Japanese medaka fish, and its transposition in the zebrafish germ lineage. *Proceedings of the National Academy of Sciences*, 97(21), pp.11403–11408.

Kelly, R.M. et al., 2005. Opsonic Requirements for Dendritic Cell-Mediated Responses to Cryptococcus neoformans. *Infection and immunity*, 73(1), pp.592–598.

Kiedrowski, M.R. et al., 2014. Staphylococcus aureus Nuc2 Is a Functional, Surface-Attached Extracellular Nuclease H. Rohde, ed. *PLoS ONE*, 9(4), p.e95574.

Kiertiburanakul, S. et al., 2006. Cryptococcosis in human immunodeficiency virus-negative patients. *International journal of infectious diseases : IJID : official publication of the International Society for Infectious Diseases*, 10(1), pp.72–8.

Kishore, U. et al., 2005. Surfactant proteins SP-A and SP-D in human health and disease. *Archivum immunologiae et therapiae experimentalis*, 53(5), pp.399–417.

Klas Kärre, K., Gustaf Ljunggren, H. & Piontek, G., 1986. Selective rejection of H-2-deficient lymphoma variants suggests alternative immune defence srategy. *J Immunol The Journal of Immunology by guest on August*, 319, pp.675–678.

Klebanoff, S.J. et al., 2013. Myeloperoxidase: a front-line defender against phagocytosed microorganisms. *Journal of leukocyte biology*, 93(2), pp.185–98.

Kleinfeld, K. et al., 2013. Vascular complications of fungal meningitis attributed to injections of contaminated methylprednisolone acetate. *JAMA neurology*, 70(9), pp.1173–6.

Klionsky, D., 2007. Autophagy: from phenomenology to molecular understanding in less than a decade. *Nature Reviews Molecular Cell Biology*, 8(8), pp.931–937.

Kloft, N. et al., 2010. Pro-autophagic signal induction by bacterial pore-forming toxins. *Medical Microbiology and Immunology*, 199(4), pp.299–309.

Kluytmans, J., van Belkum, a & Verbrugh, H., 1997. Nasal carriage of Staphylococcus aureus: epidemiology, underlying mechanisms, and associated risks. *Clinical microbiology reviews*, 10(3), pp.505–20.

Knorr, R.L., Lipowsky, R. & Dimova, R., 2015. Autophagosome closure requires

membrane scission. *Autophagy*, 11(11), pp.2134–2137.

Komatsu, M. et al., 2005. Impairment of starvation-induced and constitutive autophagy in Atg7-deficient mice. *The Journal of cell biology*, 169(3), pp.425–34.

Kondo, M. et al., 2003. Biology of hematopoietic stem cells and progenitors: Implications for Clinical Application. *Annual Review of Immunology*, 21(1), pp.759–806.

Kondo, M., 2010. Lymphoid and myeloid lineage commitment in multipotent hematopoietic progenitors. *Immunological reviews*, 238(1), pp.37–46.

Koyama, T., Yamada, M. & Matsuhashi, M., 1977. Formation of regular packets of Staphylococcus aureus cells. *Journal of bacteriology*, 129(3), pp.1518–23.

Kozel, T.R. & Mastroianni, R.P., 1976. Inhibition of phagocytosis by cryptococcal polysaccharide: dissociation of the attachment and ingestion phases of phagocytosis. *Infection and immunity*, 14(1), pp.62–7.

Kozel, T.R., Wilson, M. a & Murphy, J.W., 1991. Early events in initiation of alternative complement pathway activation by the capsule of Cryptococcus neoformans. *Infection and immunity*, 59(9), pp.3101–10.

Koziel, J. et al., 2009. Phagocytosis of Staphylococcus aureus by macrophages exerts cytoprotective effects manifested by the upregulation of antiapoptotic factors. *PloS one*, 4(4), p.e5210.

Krämer, H., 2013. Route to destruction: autophagosomes SNARE lysosomes. *The Journal of cell biology*, 201(4), pp.495–7.

Krueger, J. et al., 2011. Flt1 acts as a negative regulator of tip cell formation and branching morphogenesis in the zebrafish embryo. *Development (Cambridge, England)*, 138(10), pp.2111–20.

Kuballa, P. et al., 2012. Autophagy and the immune system. *Annual review of immunology*, 30, pp.611–46.

Kubli, D. a & Gustafsson, Å.B., 2012. Mitochondria and mitophagy: the yin and yang of cell death control. *Circulation research*, 111(9), pp.1208–21.

Kuma, A. et al., 2004. The role of autophagy during the early neonatal starvation period. *Nature*, 432(7020), pp.1032–1036.

Kumar, V. & Sharma, A., 2010. Neutrophils: Cinderella of innate immune system. *International Immunopharmacology*, 10(11), pp.1325–1334.

Kwan, K.M. et al., 2007. The Tol2kit: A multisite gateway-based construction kit forTol2 transposon transgenesis constructs. *Developmental Dynamics*, 236(11), pp.3088–3099.

Kwon-Chung, K. et al., 2002. (1557) Proposal to conserve the name Cryptococcus gattii against C. hondurianus and C. bacillisporus (Basidiomycota, Hymenomycetes, Tremellomycetidae). *Taxon*, 806(November), pp.804–806.

Kwon-Chung, K.J., 1976. Morphogenesis of Filobasidiella neoformans, the Sexual State of Cryptococcus neoformans. *Mycologia*, 68(4), p.821.

Kwon-Chung, K.J., Bennett, J.E. & Theodore, T.S., 1978. Cryptococcus bacillisporus sp. nov.: Serotype B-C of Cryptococcus neoformans. , 28(4).

Lam, G.Y. et al., 2013. Host and bacterial factors that regulate LC3 recruitment to Listeria monocytogenes during the early stages of macrophage infection. *Autophagy*, 9(7), pp.985–95.

Lamark, T. & Johansen, T., 2012. Aggrephagy: selective disposal of protein aggregates by macroautophagy. *International journal of cell biology*, 2012, p.736905.

Lambein, L., 2015. *An in vivo anti-staphylococcal drug screen using a zebrafish infection model implicates host autophagy in Staphylococcus aureus survival*. The University of Sheffield.

Lammie, G.A. et al., 2009. Tuberculous cerebrovascular disease: A review. *Journal of Infection*, 59(3), pp.156–166.

Lan, S. et al., 2001. Cerebral infarction in chronic meningitis: a comparison of tuberculous meningitis and cryptococcal meningitis. *QJM*, 94, pp.247–253.

Larsen, K.B. et al., 2010. A reporter cell system to monitor autophagy based on p62/SQSTM1. *Autophagy*, 66, pp.784–793.

Lee, E. et al., 2014. Autophagy is essential for cardiac morphogenesis during vertebrate development. *Autophagy*, 10(4), pp.572–587.

Lee, J.C. et al., 1987. Virulence studies, in mice, of transposon-induced mutants of Staphylococcus aureus differing in capsule size. *The Journal of infectious diseases*, 156(5), pp.741–50.

Lee, L.Y.L. et al., 2004. Inhibition of Complement Activation by a Secreted *Staphylococcus aureus* Protein. *The Journal of Infectious Diseases*, 190(3), pp.571–579.

Lee, S.C., Dickson, D.W. & Casadevall, A., 1996. Pathology of cryptococcal meningoencephalitis: analysis of 27 patients with pathogenetic implications. *Human pathology*, 27(8), pp.839–47.

Leite, A.G.B. et al., 2004. Cerebral Infarction Related to Cryptococcal Meningitis in an HIV-Infected Patient: Case Report and Literature Review. *www.bjid.com.br BJID The Brazilian Journal of Infectious Diseases*, 88(2), pp.175–179.

Lev, S. et al., 2017. Pho4 Is Essential for Dissemination of Cryptococcus neoformans to the Host Brain by Promoting Phosphate Uptake and Growth at Alkaline pH. *mSphere*, 2(1).

Levine, B., Mizushima, N. & Virgin, H., 2011. Autophagy in immunity and inflammation. *Nature*, 469(7330), pp.323–335.

Levitz, S.M. et al., 1997. Chloroquine induces human mononuclear phagocytes to inhibit and kill Cryptococcus neoformans by a mechanism independent of iron deprivation. *The Journal of clinical investigation*, 100(6), pp.1640–6.

Levitz, S.M. et al., 1999. Cryptococcus neoformans resides in an acidic phagolysosome of human macrophages. *Infection and immunity*, 67(2), pp.885–90.

Li, H. et al., 1999. The structural basis of t cell activation by superantigens. *Annual Review of Immunology*, 17(1), pp.435–466.

Li, Q. et al., 2010. Central nervous system cryptococcoma in immunocompetent patients: a short review illustrated by a new case. *Acta Neurochirurgica*, 152(1), pp.129–136.

Li, Y. et al., 2017. Pattern recognition receptors in zebrafish provide functional and evolutionary insight into innate immune signaling pathways. *Cellular & molecular immunology*, 14(1), pp.80–89.

Li, Y. & Hu, B., 2012. Establishment of Multi-Site Infection Model in Zebrafish Larvae for Studying Staphylococcus aureus Infectious Disease. *Journal of Genetics and*

Genomics, 39(9), pp.521–534.

Lieschke, G.J. et al., 2001. Morphologic and functional characterization of granulocytes and macrophages in embryonic and adult zebrafish. *Blood*, 98(10), pp.3087–96.

Liu, G.Y. et al., 2005. Staphylococcus aureus golden pigment impairs neutrophil killing and promotes virulence through its antioxidant activity. *The Journal of experimental medicine*, 202(2), pp.209–15.

Llewelyn, M. & Cohen, J., 2002. Superantigens: microbial agents that corrupt immunity. *The Lancet Infectious Diseases*, 2(3), pp.156–162.

Long, J. et al., 2010. Dimerisation of the UBA Domain of p62 Inhibits Ubiquitin Binding and Regulates NF-κB Signalling. *Journal of Molecular Biology*, 396(1), pp.178–194.

López, P. et al., 2013. Influence of Atg5 Mutation in SLE Depends on Functional IL-10 Genotype S. Assassi, ed. *PLoS ONE*, 8(10), p.e78756.

Lowy, F., 1998. Staphylococcus aureus infections. *New England Journal of Medicine*, 339(8), pp.520–532.

Lucitti, J.L. et al., 2007. Vascular remodeling of the mouse yolk sac requires hemodynamic force. *Development (Cambridge, England)*, 134(18), pp.3317–26.

Ma, H. et al., 2009. The fatal fungal outbreak on Vancouver Island is characterized by enhanced intracellular parasitism driven by mitochondrial regulation. *Proceedings of the National Academy of Sciences of the United States of America*, 106(31), pp.12980–5.

Ma, T. et al., 2015. Atg5-independent autophagy regulates mitochondrial clearance and is essential for iPSC reprogramming. *Nature Cell Biology*, 17(11), pp.1379–1387.

Majka, S.M. et al., 2002. Cryptococcus neoformans pulmonary granuloma formation is associated with matrix metalloproteinase-2 expression. *Medical Mycology*, 40(3), pp.323–328.

Mambula, S.S. et al., 2000. Human neutrophil-mediated nonoxidative antifungal activity against Cryptococcus neoformans. *Infection and immunity*, 68(11), pp.6257–64.

Mandell, G.L., 1975. Catalase, superoxide dismutase, and virulence of Staphylococcus aureus. In vitro and in vivo studies with emphasis on staphylococcal--leukocyte interaction. *The Journal of clinical investigation*, 55(3), pp.561–6.

Martinez, F.O. & Gordon, S., 2014. The M1 and M2 paradigm of macrophage activation: time for reassessment. *F1000prime reports*, 6, p.13.

Martinez, J. et al., 2015. Molecular characterization of LC3-associated phagocytosis reveals distinct roles for Rubicon, NOX2 and autophagy proteins. *Nature cell biology*, 17(7), pp.893–906.

Marzella, L., Ahlberg, J. & Glaumann, H., 1981. Autophagy, heterophagy, microautophagy and crinophagy as the means for intracellular degradation. *Virchows Archiv B Cell Pathology Including Molecular Pathology*, 36(1), pp.219–234.

Mathai, B., Meijer, A. & Simonsen, A., 2017. Studying Autophagy in Zebrafish. *Cells*, 6(3), p.21.

Maurer, K., Reyes-Robles, T., et al., 2015. Autophagy mediates tolerance to Staphylococcus aureus alpha-toxin. *Cell host & microbe*, 17(4), pp.429–40.

Maurer, K., Torres, V.J. & Cadwell, K., 2015. Autophagy is a key tolerance mechanism

during *Staphylococcus aureus* infection. *Autophagy*, 11(7), pp.1184–1186.

McAdow, M., Missiakas, D.M. & Schneewind, O., 2012. Staphylococcus aureus secretes coagulase and von Willebrand factor binding protein to modify the coagulation cascade and establish host infections. *Journal of innate immunity*, 4(2), pp.141–8.

McDevitt, D. et al., 1994. Molecular characterization of the clumping factor (fibrinogen receptor) of Staphylococcus aureus. *Molecular microbiology*, 11(2), pp.237–48.

McQuiston, T., Luberto, C. & Del Poeta, M., 2010. Role of host sphingosine kinase 1 in the lung response against Cryptococcosis. *Infection and immunity*, 78(5), pp.2342–52.

Meijer, A.H. et al., 2008. Identification and real-time imaging of a myc-expressing neutrophil population involved in inflammation and mycobacterial granuloma formation in zebrafish. *Developmental & Comparative Immunology*, 32(1), pp.36–49.

Meijer, A.H., van der Vaart, M. & Spaink, H.P., 2014. Real-time imaging and genetic dissection of host-microbe interactions in zebrafish. *Cellular Microbiology*, 16(1), pp.39–49.

Merle, N.S. et al., 2015. Complement System Part II: Role in Immunity. *Frontiers in immunology*, 6, p.257.

Meyer, A. & Schartl, M., 1999. Gene and genome duplications in vertebrates: the one-to-four (-to-eight in fish) rule and the evolution of novel gene functions. *Current Opinion in Cell Biology*, 11(6), pp.699–704.

Mijaljica, D., Prescott, M. & Devenish, R.J., 2011. Microautophagy in mammalian cells Revisiting a 40-year-old conundrum. *www.landesbioscience.com Autophagy Autophagy*, 6737(7), pp.673–682.

Mishra, A.K. et al., 2017. Cerebrovascular injury in cryptococcal meningitis. *International Journal of Stroke*, p.174749301770624.

Mitchell, T.G. & Perfect, J.R., 1995. Cryptococcosis in the era of AIDS--100 years after the discovery of Cryptococcus neoformans. *Clinical microbiology reviews*, 8(4), pp.515–48.

Mizushima, N., 2007. Autophagy: process and function. *Genes & development*, 21(22), pp.2861–73.

Mizushima, N. et al., 2008. Autophagy fights disease through cellular self-digestion. *Nature*, 451(7182), pp.1069–1075.

Mizushima, N. et al., 2001. Dissection of autophagosome formation using Apg5-deficient mouse embryonic stem cells. *The Journal of cell biology*, 152(4), pp.657–68.

Mizushima, N., 2004. Methods for monitoring autophagy. *The international journal of biochemistry & cell biology*, 36(12), pp.2491–502.

Mizushima, N. et al., 2007. The Atg12-Atg5 conjugate has a novel E3-like activity for protein lipidation in autophagy. *The Journal of biological chemistry*, 282(52), pp.37298–302.

Mizushima, N., Yoshimori, T. & Levine, B., 2010. Methods in mammalian autophagy research. *Cell*, 140(3), pp.313–26.

Mizushima, N., Yoshimori, T. & Ohsumi, Y., 2011. The role of Atg proteins in autophagosome formation. *Annual review of cell and developmental biology*, 27,

pp.107–32.

Moore, F.E. et al., 2012. Improved Somatic Mutagenesis in Zebrafish Using Transcription Activator-Like Effector Nucleases (TALENs) J. L. Bonkowsky, ed. *PLoS ONE*, 7(5), p.e37877.

Moreno, S.E. et al., 2006. IL-12, but Not IL-18, Is Critical to Neutrophil Activation and Resistance to Polymicrobial Sepsis Induced by Cecal Ligation and Puncture. *The Journal of Immunology*, 177(5).

Morrow, C.A. & Fraser, J.A., 2013. Is the nickel-dependent urease complex of Cryptococcus the pathogen's Achilles' heel? *mBio*, 4(4), pp.e00408-13.

Mostowy, S. et al., 2010. Entrapment of Intracytosolic Bacteria by Septin Cage-like Structures. *Cell Host & Microbe*, 8(5), pp.433–444.

Mostowy, S. et al., 2011. p62 and NDP52 proteins target intracytosolic Shigella and Listeria to different autophagy pathways. *The Journal of biological chemistry*, 286(30), pp.26987–95.

Mostowy, S. et al., 2013. The Zebrafish as a New Model for the In Vivo Study of Shigella flexneri Interaction with Phagocytes and Bacterial Autophagy S. R. Blanke, ed. *PLoS Pathogens*, 9(9), p.e1003588.

Murillo, J., Vinatzer & Jackson, 2001. The effect of pH on green fluorescent protein. *Molecular Biology Today*, 2(1), pp.1–4.

Murphy, K., 2012. *Janeway's ImmunoBiology* 8th Editio. E. Lawrence et al., eds., New York: Garland Science.

Nagl, M. et al., 2002. Phagocytosis and killing of bacteria by professional phagocytes and dendritic cells. *Clinical and diagnostic laboratory immunology*, 9(6), pp.1165–8.

Naito, T., Kuma, A. & Mizushima, N., 2013. Differential contribution of insulin and amino acids to the mTORC1-autophagy pathway in the liver and muscle. *The Journal of biological chemistry*, 288(29), pp.21074–81.

Nakatogawa, H. et al., 2009. Dynamics and diversity in autophagy mechanisms: lessons from yeast. *Nature Reviews Molecular Cell Biology*, 10(7), pp.458–467.

Nath, S. et al., 2014. Lipidation of the LC3/GABARAP family of autophagy proteins relies on a membrane-curvature-sensing domain in Atg3. *Nature cell biology*, 16(5), pp.415–24.

Neumann, Y. et al., 2016. Intracellular *Staphylococcus aureus* eludes selective autophagy by activating a host cell kinase. *Autophagy*, 12(11), pp.2069–2084.

Ngamskulrungroj, P. et al., 2012. The primary target organ of Cryptococcus gattii is different from that of Cryptococcus neoformans in a murine model. *mBio*, 3(3).

Nguyen-Chi, M. et al., 2014. Transient infection of the zebrafish notochord with E. coli induces chronic inflammation. *Disease models & mechanisms*, 7(7), pp.871–82.

Ní Eidhin, D. et al., 1998. Clumping factor B (ClfB), a new surface-located fibrinogen-binding adhesin of Staphylococcus aureus. *Molecular microbiology*, 30(2), pp.245–57.

Nicod, L.P., 2005. Lung defences: an overview. *European Respiratory Review*, 14(95), pp.45–50.

Nicola, A.M. et al., 2012. Macrophage autophagy in immunity to Cryptococcus neoformans and Candida albicans. *Infection and immunity*, 80(9), pp.3065–76.

Nicola, A.M. et al., 2011. Nonlytic exocytosis of Cryptococcus neoformans from macrophages occurs in vivo and is influenced by phagosomal pH. *mBio*, 2(4), pp.e00167-11.

Nielsen, K. et al., 2003. Sexual cycle of Cryptococcus neoformans var. grubii and virulence of congenic a and alpha isolates. *Infection and immunity*, 71(9), pp.4831–41.

Nishida, Y. et al., 2009. Discovery of Atg5/Atg7-independent alternative macroautophagy. *Nature*, 461(7264), pp.654–658.

Noverr, M.C. et al., 2003. Role of PLB1 in pulmonary inflammation and cryptococcal eicosanoid production. *Infection and immunity*, 71(3), pp.1538–47.

Nygaard, T.K. et al., 2016. Interaction of Staphylococci with Human B cells T. Msadek, ed. *PLOS ONE*, 11(10), p.e0164410.

O'Halloran, D.P., Wynne, K. & Geoghegan, J.A., 2015. Protein A is released into the Staphylococcus aureus culture supernatant with an unprocessed sorting signal. *Infection and immunity*, 83(4), pp.1598–609.

O'Keeffe, K.M. et al., 2015. Manipulation of Autophagy in Phagocytes Facilitates Staphylococcus aureus Bloodstream Infection. *Infection and immunity*, 83(9), pp.3445–57.

O'Riordan, K. & Lee, J.C., 2004. Staphylococcus aureus capsular polysaccharides. *Clinical microbiology reviews*, 17(1), pp.218–34.

Oehlers, S.H. et al., 2011. The inflammatory bowel disease (IBD) susceptibility genes NOD1 and NOD2 have conserved anti-bacterial roles in zebrafish. *Disease models & mechanisms*, 4(6), pp.832–41.

Ohsumi, Y. et al., 1998. A protein conjugation system essential for autophagy. *Nature*, 395(6700), pp.395–398.

Oller, A.R., Province, L. & Curless, B., 2010. Staphylococcus aureus recovery from environmental and human locations in 2 collegiate athletic teams. *Journal of athletic training*, 45(3), pp.222–9.

Olszewski, M.A. et al., 2004. Urease expression by Cryptococcus neoformans promotes microvascular sequestration, thereby enhancing central nervous system invasion. *The American journal of pathology*, 164(5), pp.1761–71.

Onodera, J. & Ohsumi, Y., 2005. Autophagy Is Required for Maintenance of Amino Acid Levels and Protein Synthesis under Nitrogen Starvation. *Journal of Biological Chemistry*, 280(36), pp.31582–31586.

Orr, M.E. & Oddo, S., 2013. Autophagic/lysosomal dysfunction in Alzheimer's disease. *Alzheimer's research & therapy*, 5(5), p.53.

Palmer, G.E., Askew, D.S. & Williamson, P.R., 2008. The diverse roles of autophagy in medically important fungi. *Autophagy*, 4(8), pp.982–988.

Pandey, A. et al., 2017. Global Reprogramming of Host Kinase Signaling in Response to Fungal Infection. *Cell Host & Microbe*, 21(5), p.637–649.e6.

Pankiv, S. et al., 2007. p62/SQSTM1 binds directly to Atg8/LC3 to facilitate degradation of ubiquitinated protein aggregates by autophagy. *The Journal of biological chemistry*, 282(33), pp.24131–45.

Pappas, P.G., 2013. Cryptococcal infections in non-HIV-infected patients. *Transactions of the American Clinical and Climatological Association*, 124, pp.61–79.

Park, B.J. et al., 2009. Estimation of the current global burden of cryptococcal meningitis among persons living with HIV/AIDS. *AIDS (London, England)*, 23(4), pp.525–30.

Park, Y.-D. et al., 2014. A role for LHC1 in higher order structure and complement binding of the Cryptococcus neoformans capsule. *PLoS pathogens*, 10(5), p.e1004037.

Park, Y.-D. et al., 2010. Mating pheromone in Cryptococcus neoformans is regulated by a transcriptional/degradative “futile” cycle. *The Journal of biological chemistry*, 285(45), pp.34746–56.

Parker, D. & Prince, A., 2012. Staphylococcus aureus induces type I IFN signaling in dendritic cells via TLR9. *Journal of immunology (Baltimore, Md. : 1950)*, 189(8), pp.4040–6.

Parng, C. et al., 2002. Zebrafish: A Preclinical Model for Drug Screening. *ASSAY and Drug Development Technologies*, 1(1), pp.41–48.

Passoni, G. et al., 2017. Imaging of viral neuroinvasion in the zebrafish reveals that Sindbis and chikungunya viruses favour different entry routes. *Disease Models & Mechanisms*.

Pauli, N.T. et al., 2014. Staphylococcus aureus infection induces protein A-mediated immune evasion in humans. *The Journal of experimental medicine*, 211(12), pp.2331–9.

Perfect, J.R., 2006. Cryptococcus neoformans: the yeast that likes it hot. *FEMS yeast research*, 6(4), pp.463–8.

Perobelli, S.M. et al., 2015. Plasticity of neutrophils reveals modulatory capacity. *Brazilian Journal of Medical and Biological Research*, 48(8), pp.665–675.

Persson, C., 2015. Staphylococcus aureus and primary lysis of eosinophils. *Clinical & Experimental Allergy*, 45(2), pp.488–489.

Pichon, N. et al., 2008. Fatal-stroke syndrome revealing fungal cerebral vasculitis due to Arthrographis kalrae in an immunocompetent patient. *Journal of clinical microbiology*, 46(9), pp.3152–5.

Pisharath, H. et al., 2007. Targeted ablation of beta cells in the embryonic zebrafish pancreas using E. coli nitroreductase. *Mechanisms of development*, 124(3), pp.218–29.

Pizarro-Cerdá, J. et al., 1998. Brucella abortus transits through the autophagic pathway and replicates in the endoplasmic reticulum of nonprofessional phagocytes. *Infection and immunity*, 66(12), pp.5711–24.

van de Pol, I., Flik, G. & Gorissen, M., 2017. Comparative Physiology of Energy Metabolism: Fishing for Endocrine Signals in the Early Vertebrate Pool. *Frontiers in endocrinology*, 8, p.36.

Poon, A. et al., 2012. ATG5, autophagy and lung function in asthma. *Autophagy*, 8(4), pp.694–695.

Popovic, D. & Dikic, I., 2012. The molecular basis of selective autophagy. *Biochemist*, (April), pp.24–30.

Prajsnar, T.K. et al., 2008. A novel vertebrate model of Staphylococcus aureus infection reveals phagocyte-dependent resistance of zebrafish to non-host specialized pathogens. *Cellular microbiology*, 10(11), pp.2312–25.

Prajsnar, T.K. et al., 2012. A privileged intraphagocyte niche is responsible for

disseminated infection of Staphylococcus aureus in a zebrafish model. *Cellular microbiology*, 14(10), pp.1600–19.

Price, M.S. et al., 2011. Cryptococcus neoformans requires a functional glycolytic pathway for disease but not persistence in the host. *mBio*, 2(3), pp.e00103-11.

Prince, L.R. et al., 2012. Staphylococcus aureus induces eosinophil cell death mediated by α-hemolysin. *PloS one*, 7(2), p.e31506.

Prouty, M.G. et al., 2003. Zebrafish- Mycobacterium marinum model for mycobacterial pathogenesis. *FEMS Microbiology Letters*, 225(2), pp.177–182.

Py, B., Lipinski, M. & Yuan, J., 2007. Autophagy limits Listeria monocytogenes intracellular growth in the early phase of primary infection. *Autophagy*, 3(2), pp.117–125.

Qi, L.S. et al., 2013. Repurposing CRISPR as an RNA-Guided Platform for Sequence-Specific Control of Gene Expression. *Cell*, 152(5), pp.1173–1183.

Qin, Q.-M. et al., 2011. Functional analysis of host factors that mediate the intracellular lifestyle of Cryptococcus neoformans. *PLoS pathogens*, 7(6), p.e1002078.

Qiu, Y. et al., 2012. Immune Modulation Mediated by Cryptococcal Laccase Promotes Pulmonary Growth and Brain Dissemination of Virulent Cryptococcus neoformans in Mice C. Valery, ed. *PLoS ONE*, 7(10), p.e47853.

Qureshi, A. et al., 2011. Cryptococcus neoformans modulates extracellular killing by neutrophils. *Frontiers in microbiology*, 2(September), p.193.

Ra, E.A. et al., 2016. TRIM31 promotes Atg5/Atg7-independent autophagy in intestinal cells. *Nature Communications*, 7, p.11726.

Rahman, M.M. & McFadden, G., 2011. Modulation of NF-κB signalling by microbial pathogens. *Nature reviews. Microbiology*, 9(4), pp.291–306.

Rajasingham, R. et al., 2017. Global burden of disease of HIV-associated cryptococcal meningitis: an updated analysis. *The Lancet Infectious Diseases*.

Renshaw, S.A. et al., 2006. A transgenic zebrafish model of neutrophilic inflammation. *Blood*, 108(13).

Renshaw, S. a & Trede, N.S., 2012. A model 450 million years in the making: zebrafish and vertebrate immunity. *Disease models & mechanisms*, 5(1), pp.38–47.

Rhodes, J., Wicker, L. & Urba, W., 1980. Genetic control of susceptibility to Cryptococcus neoformans in mice. *Infection and immunity*, 29(2), p.494.

Rigby, K.M. & DeLeo, F.R., 2012. Neutrophils in innate host defense against Staphylococcus aureus infections. *Seminars in immunopathology*, 34(2), pp.237–59.

Rivera, J., Zaragoza, O. & Casadevall, A., 2005. Antibody-Mediated Protection against Cryptococcus neoformans Pulmonary Infection Is Dependent on B Cells. *Infection and Immunity*, 73(2), pp.1141–1150.

Rocha, J.D.B. et al., 2015. Capsular polysaccharides from Cryptococcus neoformans modulate production of neutrophil extracellular traps (NETs) by human neutrophils. *Scientific Reports*, 5(1), p.8008.

Rock, R.B. et al., 2008. Central nervous system tuberculosis: pathogenesis and clinical aspects. *Clinical microbiology reviews*, 21(2), p.243–61, table of contents.

Rogov, V. et al., 2014. Interactions between autophagy receptors and ubiquitin-like proteins form the molecular basis for selective autophagy. *Molecular cell*, 53(2),

pp.167–78.

Rollason, J. et al., 2008. Epidemiology of community-acquired meticillin-resistant Staphylococcus aureus obtained from the UK West Midlands region. *The Journal of hospital infection*, 70(4), pp.314–20.

Romagnani, S., 2000. T-cell subsets (Th1 versus Th2). *Annals of Allergy, Asthma & Immunology*, 85(1), pp.9–21.

Rong, Y. et al., 2011. Spinster is required for autophagic lysosome reformation and mTOR reactivation following starvation. *Proceedings of the National Academy of Sciences of the United States of America*, 108(19), pp.7826–31.

Rosario, M., Song, S.X. & McCullough, L.D., 2012. An unusual case of stroke. *The neurologist*, 18(4), pp.229–32.

Sahu, R. et al., 2011. Microautophagy of cytosolic proteins by late endosomes. *Developmental cell*, 20(1), pp.131–9.

Sancak, Y. et al., 2008. The Rag GTPases bind raptor and mediate amino acid signaling to mTORC1. *Science (New York, N.Y.)*, 320(5882), pp.1496–501.

Sanjuan, M.A. et al., 2007. Toll-like receptor signalling in macrophages links the autophagy pathway to phagocytosis. *Nature*, 450(7173), pp.1253–1257.

Santarino, I.B. et al., 2017. Involvement of the p62/NRF2 signal transduction pathway on erythrophagocytosis. *Scientific reports*, 7(1), p.5812.

Santiago-Tirado, F.H. et al., 2017. Trojan Horse Transit Contributes to Blood-Brain Barrier Crossing of a Eukaryotic Pathogen. *mBio*, 8(1).

Schindler, D. et al., 2012. Dendritic cells are central coordinators of the host immune response to Staphylococcus aureus bloodstream infection. *The American journal of pathology*, 181(4), pp.1327–37.

Schlesinger, L.S. et al., 2002. Mycobacterium tuberculosis-infected human macrophages exhibit enhanced cellular adhesion with increased expression of LFA-1 and ICAM-1 and reduced expression and/or function of complement receptors, FcγRII and the mannose receptor. *Microbiology*, 148(10), pp.3161–3171.

Schmid, D., Pypaert, M. & Münz, C., 2007. Antigen-Loading Compartments for Major Histocompatibility Complex Class II Molecules Continuously Receive Input from Autophagosomes. *Immunity*, 26(1), pp.79–92.

Schnaith, A. et al., 2007. Staphylococcus aureus subvert autophagy for induction of caspase-independent host cell death. *The Journal of biological chemistry*, 282(4), pp.2695–706.

Schröder, A. et al., 2006. Live cell imaging of phagosome maturation in Staphylococcus aureus infected human endothelial cells: small colony variants are able to survive in lysosomes. *Medical Microbiology and Immunology*, 195(4), pp.185–194.

Schurch, S., Lee, M. & Gehr, P., 1992. Pulmonary surfactant: Surface properties and function of alveolar and airway surfactant. *Pure and Applied Chemistry*, 64(11), pp.1745–1750.

Schwandner, R. et al., 1999. Peptidoglycan- and lipoteichoic acid-induced cell activation is mediated by toll-like receptor 2. *The Journal of biological chemistry*, 274(25), pp.17406–9.

Selders, G.S. et al., 2017. An overview of the role of neutrophils in innate immunity,

inflammation and host-biomaterial integration. *Regenerative biomaterials*, 4(1), pp.55–68.

Serba, J., 2016. *In vivo imaging of host-pathogen interactions in Staphyloccocus aureus infection*. The University of Sheffield.

Shamri, R., Xenakis, J.J. & Spencer, L.A., 2011. Eosinophils in innate immunity: an evolving story. *Cell and tissue research*, 343(1), pp.57–83.

Shaw, R.J. et al., 2004. The LKB1 tumor suppressor negatively regulates mTOR signaling. *Cancer Cell*, 6(1), pp.91–99.

Shi, C.-S. & Kehrl, J.H., 2008. MyD88 and Trif target Beclin 1 to trigger autophagy in macrophages. *The Journal of biological chemistry*, 283(48), pp.33175–82.

Shi, M. et al., 2010. Real-time imaging of trapping and urease-dependent transmigration of Cryptococcus neoformans in mouse brain. *Journal of Clinical Investigation*, 120(5), pp.1683–1693.

Shibuya, K. et al., 2005. Granuloma and cryptococcosis. *Journal of infection and chemotherapy : official journal of the Japan Society of Chemotherapy*, 11(3), pp.115–22.

Shpilka, T. et al., 2011. Atg8: an autophagy-related ubiquitin-like protein family. *Genome Biology*, 12(7), p.226.

Siafakas, A.R. et al., 2007. Cell wall-linked cryptococcal phospholipase B1 is a source of secreted enzyme and a determinant of cell wall integrity. *The Journal of biological chemistry*, 282(52), pp.37508–14.

Siboo, I.R. et al., 2001. Clumping factor A mediates binding of Staphylococcus aureus to human platelets. *Infection and immunity*, 69(5), pp.3120–7.

Silva, I.A.L. et al., 2014. Can zebrafish be a valid model to study Paget's disease of bone? *Journal of Applied Ichthyology*, 30(4), pp.678–688.

Silverman, G.J. et al., 2000. A B cell superantigen-induced persistent "Hole" in the B-1 repertoire. *The Journal of experimental medicine*, 192(1), pp.87–98.

Sim, R.B. & Tsiftsoglou, S.A., 2004. Proteases of the complement system. *Biochemical Society transactions*, 32(Pt 1), pp.21–7.

Singh, A. et al., 2017. TBK1 regulates p62/sqstm1 mediated autophagic clearance of intracellular ubiquitinated Staphylococcus aureus in human epithelial cells. *Translational genetics and genomics*, [online fi.

Sinha, B. et al., 1999. Fibronectin-binding protein acts as Staphylococcus aureus invasin via fibronectin bridging to integrin α5β1. *Cellular Microbiology*, 1(2), pp.101–117.

Sinha, B. et al., 2000. Heterologously expressed Staphylococcus aureus fibronectin-binding proteins are sufficient for invasion of host cells. *Infection and immunity*, 68(12), pp.6871–8.

Smith, L.M., Dixon, E.F. & May, R.C., 2015. The fungal pathogen *C ryptococcus neoformans* manipulates macrophage phagosome maturation. *Cellular Microbiology*, 17(5), pp.702–713.

Sofer, A. et al., 2005. Regulation of mTOR and cell growth in response to energy stress by REDD1. *Molecular and cellular biology*, 25(14), pp.5834–45.

Sonoda, N. et al., 1999. Clostridium perfringens enterotoxin fragment removes specific claudins from tight junction strands: Evidence for direct involvement of claudins in

tight junction barrier. *The Journal of cell biology*, 147(1), pp.195–204.

Soong, G. et al., 2015. Methicillin-Resistant *Staphylococcus aureus* Adaptation to Human Keratinocytes. *mBio*, 6(2), pp.e00289-15.

Sou, Y. et al., 2008. The Atg8 conjugation system is indispensable for proper development of autophagic isolation membranes in mice. *Molecular biology of the cell*, 19(11), pp.4762–75.

Strasser, J.E. et al., 1999. Regulation of the macrophage vacuolar ATPase and phagosome-lysosome fusion by Histoplasma capsulatum. *Journal of immunology (Baltimore, Md. : 1950)*, 162(10), pp.6148–54.

Strømhaug, P.E. & Seglen, P.O., 1993. Evidence for acidity of prelysosomal autophagic/endocytic vacuoles (amphisomes). *The Biochemical journal*, 291, pp.115–21.

Subramaniam, K. et al., 2009. IgM $^{+}$ Memory B Cell Expression Predicts HIV-Associated Cryptococcosis Status. *The Journal of Infectious Diseases*, 200(2), pp.244–251.

Summerton, J. & Weller, D., 1997. Morpholino Antisense Oligomers: Design, Preparation, and Properties. *Antisense and Nucleic Acid Drug Development*, 7(3), pp.187–195.

Sun, D., Zhang, M., Liu, G., Wu, H., Li, C., et al., 2016a. Intravascular clearance of disseminating Cryptococcus neoformans in the brain can be improved by enhancing neutrophil recruitment in mice. *European journal of immunology*, 46(7), pp.1704–14.

Sun, D., Zhang, M., Liu, G., Wu, H., Zhu, X., et al., 2016b. Real-Time Imaging of Interactions of Neutrophils with Cryptococcus neoformans Demonstrates a Crucial Role of Complement C5a-C5aR Signaling G. S. Deepe, ed. *Infection and Immunity*, 84(1), pp.216–229.

Sun, D. & Shi, M., 2016. Neutrophil swarming toward Cryptococcus neoformans is mediated by complement and leukotriene B4. *Biochemical and Biophysical Research Communications*, 477(4), pp.945–951.

Syme, R. et al., 2002. Primary dendritic cells phagocytose Cryptococcus neoformans via mannose receptors and Fcγ receptor II for presentation to T lymphocytes. *Infection and …*, 70(11), pp.5972–5981.

Takata, S. et al., 2011. [A case of secondary pulmonary cryptococcosis presenting with multiple cystic shadows]. *Nihon Kokyuki Gakkai zasshi = the journal of the Japanese Respiratory Society*, 49(4), pp.315–20.

Takeuchi, O., Hoshino, K. & Akira, S., 2000. Cutting Edge: TLR2-Deficient and MyD88-Deficient Mice Are Highly Susceptible to Staphylococcus aureus Infection. *The Journal of Immunology*, 165(10).

Taneja, J. et al., 2008. Cryptococcal granulomas in an immunocompromised HIV-negative patient. *Indian journal of pathology & microbiology*, 51(4), pp.553–5.

Tanida, I., 2011. Autophagy basics. *Microbiology and immunology*, 55(1), pp.1–11.

Tanida, I. et al., 2002. Human Apg3p/Aut1p homologue is an authentic E2 enzyme for multiple substrates, GATE-16, GABARAP, and MAP-LC3, and facilitates the conjugation of hApg12p to hApg5p. *The Journal of biological chemistry*, 277(16), pp.13739–44.

Taylor, A.L., Watson, C.J.E. & Bradley, J.A., 2005. Immunosuppressive agents in solid organ transplantation: Mechanisms of action and therapeutic efficacy. *Critical*

Reviews in OncologyHematology, 56, pp.23–46.

Tenor, J.L. et al., 2015. Live Imaging of Host-Parasite Interactions in a Zebrafish Infection Model Reveals Cryptococcal Determinants of Virulence and Central Nervous System Invasion. *mBio*, 6(5), pp.e01425-15.

Thomsen, I.P. et al., 2017. Monoclonal Antibodies Against the Staphylococcus aureus Bicomponent Leukotoxin AB Isolated Following Invasive Human Infection Reveal Diverse Binding and Modes of Action. *The Journal of Infectious Diseases*, 215(7), pp.1124–1131.

Thurston, T.L.M. et al., 2009. The TBK1 adaptor and autophagy receptor NDP52 restricts the proliferation of ubiquitin-coated bacteria. *Nature immunology*, 10(11), pp.1215–21.

Torda, A., Kumar, R.K. & Jones, P.D., 2001. The pathology of human and murine pulmonary infection with Cryptococcus neoformans var. gattii. *Pathology*, 33(4), pp.475–8.

Torraca, V. et al., 2014. Macrophage-pathogen interactions in infectious diseases: new therapeutic insights from the zebrafish host model. *Disease models & mechanisms*, 7(7), pp.785–97.

Tóth, M.L. et al., 2008. Longevity pathways converge on autophagy genes to regulate life span in Caenorhabditis elegans. *Autophagy*, 4(3), pp.330–8.

Tseng, H.-K. et al., 2012. Identification of Genes from the Fungal Pathogen Cryptococcus neoformans Related to Transmigration into the Central Nervous System K. Nielsen, ed. *PLoS ONE*, 7(9), p.e45083.

Tsenova, L. et al., 1999. Tumor necrosis factor alpha is a determinant of pathogenesis and disease progression in mycobacterial infection in the central nervous system. *Proceedings of the National Academy of Sciences of the United States of America*, 96(10), pp.5657–62.

Tsompanidou, E. et al., 2012. The sortase A substrates FnbpA, FnbpB, ClfA and ClfB antagonize colony spreading of Staphylococcus aureus. *PloS one*, 7(9), p.e44646.

Tsuboyama, K. et al., 2016. The ATG conjugation systems are important for degradation of the inner autophagosomal membrane. *Science*, 354(6315).

Tsukamoto, S. et al., 2008. Autophagy Is Essential for Preimplantation Development of Mouse Embryos. *Science*, 321(5885), pp.117–120.

Tucker, S.C. & Casadevall, A., 2002. Replication of Cryptococcus neoformans in macrophages is accompanied by phagosomal permeabilization and accumulation of vesicles containing polysaccharide in the cytoplasm. *Proceedings of the National Academy of Sciences of the United States of America*, 99(5), pp.3165–70.

Tuomanen, E.I. et al., 1989. Reduction of inflammation, tissue damage, and mortality in bacterial meningitis in rabbits treated with monoclonal antibodies against adhesion-promoting receptors of leukocytes. *The Journal of experimental medicine*, 170(3), pp.959–69.

Ueki, S. et al., 2013. Eosinophil extracellular DNA trap cell death mediates lytic release of free secretion-competent eosinophil granules in humans. *Blood*, 121(11), pp.2074–2083.

Ullah, I., Ritchie, N.D. & Evans, T.J., 2017. The interrelationship between phagocytosis, autophagy and formation of neutrophil extracellular traps following infection of human neutrophils by Streptococcus pneumoniae. *Innate immunity*, 23(5),

pp.413–423.

Usategui-Martín, R. et al., 2015. Polymorphisms in autophagy genes are associated with paget disease of bone. *PloS one*, 10(6), p.e0128984.

Vandenesch, F., Lina, G. & Henry, T., 2012. Staphylococcus aureus hemolysins, bi-component leukocidins, and cytolytic peptides: a redundant arsenal of membrane-damaging virulence factors? *Frontiers in cellular and infection microbiology*, 2, p.12.

Velagapudi, R. et al., 2009. Spores as infectious propagules of Cryptococcus neoformans. *Infection and immunity*, 77(10), pp.4345–55.

Villena, S.N. et al., 2008. Capsular polysaccharides galactoxylomannan and glucuronoxylomannan from Cryptococcus neoformans induce macrophage apoptosis mediated by Fas ligand. *Cellular microbiology*, 10(6), pp.1274–85.

Voelz, K. et al., 2010. Automated analysis of cryptococcal macrophage parasitism using GFP-tagged cryptococci. *PloS one*, 5(12), p.e15968.

Voelz, K. et al., 2014. “Division of labour” in response to host oxidative burst drives a fatal Cryptococcus gattii outbreak. *Nature communications*, 5, p.5194.

Voelz, K., Lammas, D. a & May, R.C., 2009. Cytokine signaling regulates the outcome of intracellular macrophage parasitism by Cryptococcus neoformans. *Infection and immunity*, 77(8), pp.3450–7.

Voelz, K. & May, R.C., 2010. Cryptococcal interactions with the host immune system. *Eukaryotic cell*, 9(6), pp.835–46.

Voigt, C.A., 2011. *Synthetic biology* 1st ed., Academic Press.

Wang, Y., Aisen, P. & Casadevall, a, 1995. Cryptococcus neoformans melanin and virulence: mechanism of action. *Infection and immunity*, 63(8), pp.3131–6.

Wardenburg, J.B., Williams, W.A. & Missiakas, D., 2006. Host defenses against Staphylococcus aureus infection require recognition of bacterial lipoproteins. *Proceedings of the National Academy of Sciences*, 103(37), pp.13831–13836.

Watson, S.P., Clements, M.O. & Foster, S.J., 1998. Characterization of the starvation-survival response of Staphylococcus aureus. *Journal of bacteriology*, 180(7), pp.1750–8.

Wecke, J. et al., 1982. Cell wall degradation of Staphylococcus aureus by lysozyme. *Archives of Microbiology*, 131(2), pp.116–123.

Weidberg, H. et al., 2010. LC3 and GATE-16/GABARAP subfamilies are both essential yet act differently in autophagosome biogenesis. *The EMBO journal*, 29(11), pp.1792–1802.

Weiss, G. & Schaible, U.E., 2015. Macrophage defense mechanisms against intracellular bacteria. *Immunological reviews*, 264(1), pp.182–203.

Wenzel, R.P. et al., 1995. The significance of nasal carriage of Staphylococcus aureus and the incidence of postoperative wound infection. *The Journal of hospital infection*, 31(1), pp.13–24.

Wild, P. et al., 2011. Phosphorylation of the autophagy receptor optineurin restricts Salmonella growth. *Science*, 333(6039), pp.228–233.

Wilkinson, R. et al., 2013. A method for high-throughput PCR-based genotyping of larval zebrafish tail bio[sies. *www.BioTechniques.com*, 55(6), pp.314–316.

Willett, C.E. et al., 1999. Early hematopoiesis and developing lymphoid organs in the

zebrafish. *Developmental dynamics : an official publication of the American Association of Anatomists*, 214(4), pp.323–36.

Williamson, P.R. et al., 2017. Cryptococcal meningitis: epidemiology, immunology, diagnosis and therapy. *Nature Reviews Neurology*, 13(1), pp.13–24.

Wittkopp, N. et al., 2009. Nonsense-mediated mRNA decay effectors are essential for zebrafish embryonic development and survival. *Molecular and cellular biology*, 29(13), pp.3517–28.

Woehl, J.L. et al., 2014. The extracellular adherence protein from Staphylococcus aureus inhibits the classical and lectin pathways of complement by blocking formation of the C3 proconvertase. *Journal of immunology (Baltimore, Md. : 1950)*, 193(12), pp.6161–6171.

Wong, B. et al., 1990. Production of the hexitol D-mannitol by Cryptococcus neoformans in vitro and in rabbits with experimental meningitis. *Infection and immunity*, 58(6), pp.1664–70.

Wozniak, K.L., Kolls, J.K. & Wormley, F.L., 2012. Depletion of neutrophils in a protective model of pulmonary cryptococcosis results in increased IL-17A production by γδ T cells. *BMC immunology*, 13(1), p.65.

Wozniak, K.L., Vyas, J.M. & Levitz, S.M., 2006. In vivo role of dendritic cells in a murine model of pulmonary cryptococcosis. *Infection and immunity*, 74(7), pp.3817–24.

Wright, J.R., 2004. Host defense functions of pulmonary surfactant. *Biology of the neonate*, 85(4), pp.326–32.

Xu, L. & Luo, Z.-Q., 2013. Cell biology of infection by Legionella pneumophila. *Microbes and infection*, 15(2), pp.157–67.

Xu, Y., Jagannath, C. & Liu, X., 2007. Toll-like receptor 4 is a sensor for autophagy associated with innate immunity. *Immunity*, 27(1), pp.135–144.

Yamaoka, H. et al., 1996. Intravascular granuloma induced by intravenous inoculation of Cryptococcus neoformans. *Mycopathologia*, 133(3), pp.149–58.

Yang, C.-T. et al., 2012. Neutrophils exert protection in the early tuberculous granuloma by oxidative killing of mycobacteria phagocytosed from infected macrophages. *Cell host & microbe*, 12(3), pp.301–12.

Yang, Z. et al., 2006. Atg22 Recycles Amino Acids to Link the Degradative and Recycling Functions of Autophagy. , 17(December), pp.5094–5104.

Yazdanbakhsh, M. et al., 1986. Bactericidal action of eosinophils from normal human blood. *Infection and immunity*, 53(1), pp.192–8.

Yilmaz, M. et al., 2016. Mortality predictors of Staphylococcus aureus bacteremia: a prospective multicenter study. *Annals of clinical microbiology and antimicrobials*, 15, p.7.

Yogev, O. et al., 2013. eIF4EBP3L Acts as a Gatekeeper of TORC1 In Activity-Dependent Muscle Growth by Specifically Regulating Mef2ca Translational Initiation D. L. Stemple, ed. *PLoS Biology*, 11(10), p.e1001679.

Yona, S. et al., 2013. Fate mapping reveals origins and dynamics of monocytes and tissue macrophages under homeostasis. *Immunity*, 38(1), pp.79–91.

Yoshii, S. et al., 2016. Systemic Analysis of Atg5-Null Mice Rescued from Neonatal Lethality by Transgenic ATG5 Expression in Neurons. *Developmental Cell*, 39(1), pp.116–130.

Yu, L. et al., 2010. Termination of autophagy and reformation of lysosomes regulated by mTOR. *Nature*, 465(7300), pp.942–6.

Yu, Z.-Q. et al., 2012. Dual roles of Atg8-PE deconjugation by Atg4 in autophagy. *Autophagy*, 8(6), pp.883–92.

Zaragoza, O., Taborda, C.P. & Casadevall, A., 2003. The efficacy of complement-mediated phagocytosis of Cryptococcus neoformans is dependent on the location of C3 in the polysaccharide capsule and involves both direct and indirect C3-mediated interactions. *European journal of immunology*, 33(7), pp.1957–67.

Zhang, M. et al., 2016. Real-time in vivo imaging reveals the ability of neutrophils to remove Cryptococcus neoformans directly from the brain vasculature. *Journal of Leukocyte Biology*, 99(3), pp.467–473.

Zhang, S. & Cui, P., 2014. Complement system in zebrafish. *Developmental & Comparative Immunology*, 46(1), pp.3–10.

Ziegler, C. et al., 2011. The dynamics of T cells during persistent Staphylococcus aureus infection: from antigen-reactivity to in vivo anergy. *EMBO molecular medicine*, 3(11), pp.652–66.

Zou, P.F. et al., 2015. Higher antiviral response of RIG-I through enhancing RIG-I/MAVS-mediated signaling by its long insertion variant in zebrafish. *Fish & Shellfish Immunology*, 43(1), pp.13–24.

Appendix 1

Generation of the 3' entry vector p3E-p62

In order to have a stable p62 cDNA sample which could be preserved, and used for any further experiments, a sample was inserted into a vector for long term storage. It would be important if an exact copy of the cDNA sample was required during the experimental procedure or in the future.

Primers were designed to cover the start ATG and the stop TAG, to enable amplification through PCR of the entire zebrafish p62 transcript, excluding the un-translated regions. It was important to exclude the 5' UTR (which contains ribosome binding sites) to ensure that once the p62 product was integrated into the zebrafish genome, translation of just the p62 section would not occur. Using zebrafish cDNA, kindly gifted by Dr Abraha G. Kahsay (IMCB, Singapore), p62 was amplified. Larvae of 5dpf were used to collect RNA and subsequently synthesise cDNA. 5dpf was used as a time point when it is known p62 is expressed in zebrafish larvae at least by 48hpf (Yogev et al. 2013). The PCR product was run on a gel to determine whether the correct size product had been amplified. Indeed, the correct expected band size was observed, at 1360bp, corresponding to the entire p62 transcript, excluding the UTR's (Fig A1).

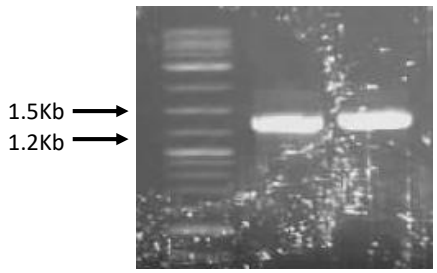

Figure A1 Amplification of zebrafish p62

PCR product size of 1360bp seen for PCR amplification of p62 from zebrafish cDNA (Ladder: 2-Log ladder N32200S, Forward: ATGTCGATGACAGTGAAA GCTTAC, Reverse: CTACTTCTGTTGTCCTGGTGTTTTG).

To enable safe storage and easy amplification of the PCR product, it was inserted into a pGEMTEasy vector (Fig. A2 A). To enable ligation into the vector an A-tailing reaction was first completed. After ligation into the pGEMTEasy (which contains an ampicillin resistance gene) vector, the reaction product was transformed into competent cells, and then plated out on an LB agar plate. The agar plate contained ampicillin, to be selective for the pGEMTEasy colonies only. Additionally X-Gal solution was added to the plate, to enable selection of vectors which had the PCR product

inserted, through the colour produced by individual colonies. White colonies are formed when insertion of the PCR product is into, and therefore disrupting, the coding sequence of β-galactosidase. When β-galactosidase is not disrupted, blue colonies are formed, through production of a blue pigment caused by hydrolysis of X-gal on the plate, indicative that the PCR product is not inserted.

Colonies which had an insert (white) were chosen. A PCR using T7 and SP6, primer sites present on the pGEMTEasy vector, on either side of the insertion site, to amplify the insertion was completed to determine the size of the insertion and if this correlated with the size of the P62 product (Fig. A2 B).

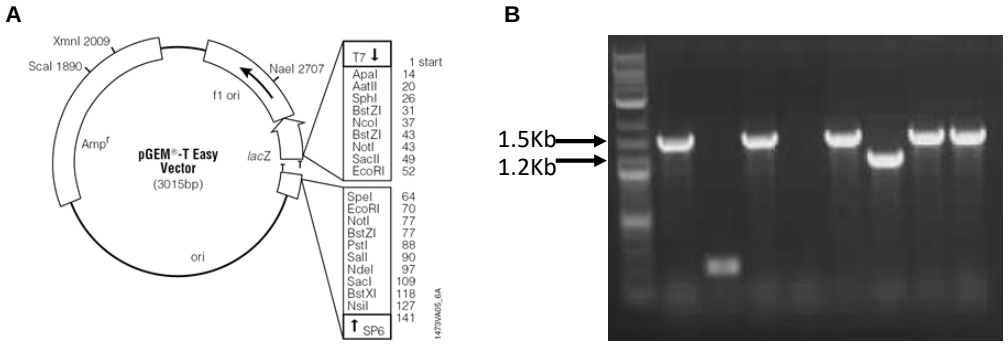

Figure A2 Insertion of zebrafish p62 into pGEMTEasy

A Schematic of the pGEMTEasy vector (pGEM-T and pGEM-T-Easy vector systems protocol PDF Revised 6.15, TM042). **B** PCR product size of ~1510bp seen for PCR amplification of p62 from pGEMTEasy vector in lanes 1, 3, 5, 7 and 8 (Ladder: 2-Log ladder N32200S)

The sequence of the inserted PCR products were next examined, it is important the sequence is the same as in cDNA. The PCR products of lanes 1,3,5,7 and 8 (Fig. A2 B), which represent the correct size of 1510bp p62 were next sequenced, using either T7 or SP6 primers to enable sequencing of each end of the insertion.

The vector chosen matched the expected sequence exactly, aside from a single base change. The vector chosen had a single residue alteration, GA**C** to GA**A,** resulting in a Aspartic acid (Asp, D) change to a Glutamic acid (Glu, E), this change is to a very similar residue in terms of residue structure and properties, both are amino acids with electrically charged side chains, and both are acidic, (Fig A3).

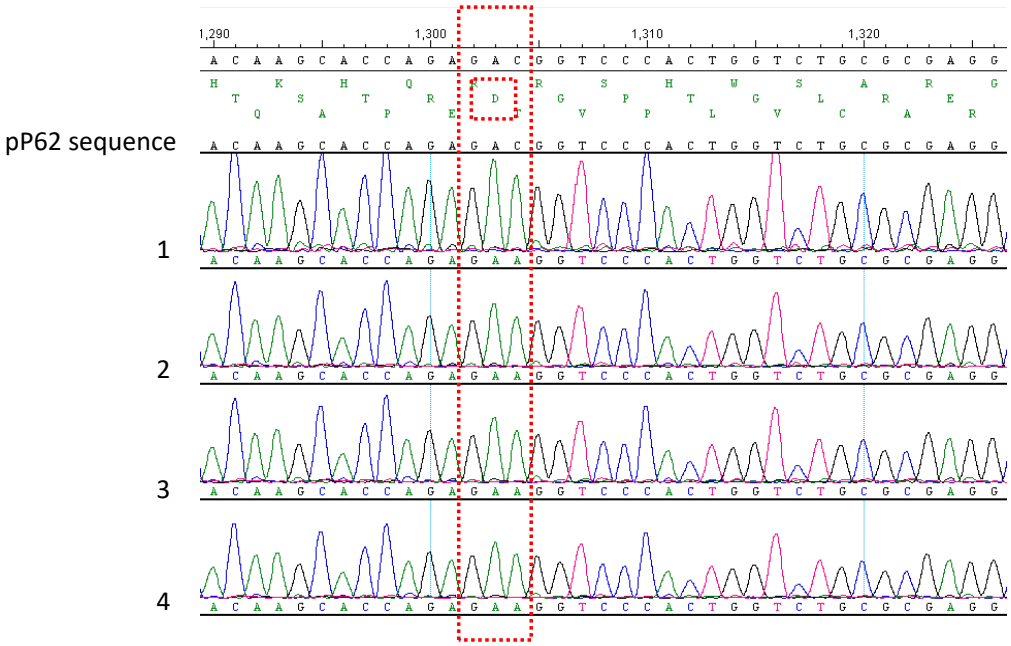

Figure A3 Aspartic acid to Glutamic acid change in zebrafish cDNA

The known p62 sequence (ENSDARG00000075014) compared to sequencing data (1-4). 1-2 represent PCR products made using G2 GoTaq polymerase. 3-4 represent PCR products made using primestar polymerase. Large red box highlights the GAC (Asp, D, small red box) codon, which is shown to be GAA in 1-4 PCR products.

In all PCR products, this residue change was observed. Due to the presence of this Asp to Glu change in all PCR products, it is likely this is not a PCR based error. To be sure, a separate polymerase enzyme was tested, with the (Asp to Glu) change seen in all PCR products (Fig A3). This divergence from expected p62 sequence may represent a Single Nucleotide Polymorphism (SNP). Indeed, a missense SNP (C to A), has been recorded (rs504189497 SNP, Ensembl). Therefore, this p62 sequence was chosen to be used for the generation of a p62 reporter line. Next an entry clone using the Gateway system was generated from this p62 sequence.

Entry vector generation

To enable generation of a neutrophil specific, GFP-p62 fusion protein, a 3-prime entry vector containing p62 was generated. To do this, a p62 PCR product with flanking “attB” sites is required for the BP reaction into the selected 3’ entry clone (*pDonrP2r-P3*). Therefore, attB primers were designed according to the Gateway protocol, to cover each end of the p62 sequence. The pGEMTEasy vector with the selected and sequenced p62 insertion was used for PCR amplification of p62 product with flanking attB sites present in the primers, and the size of the product was confirmed by gel electrophoresis.

The att-site flanked p62 size was correct, this product could be used in the BP reaction. Reaction was completed according to Gateway™ protocol, with 50 femtomoles of both attB PCR products and the donor vector, pDonrP2r-P3. The BP reaction resulted in insertion of the attB flanked p62 product in the donor vector, and creation of resultant corresponding L and R sites, known as the entry clone; as shown in the schematic (Fig. 6.1). It was next necessary to isolate a single copy of the entry clone, and confirm the sequence of the p62 and surrounding L and R sites were intact.

The BP reaction products were transformed into One-shot TOP10 competent cells, and plated onto the kanamycin containing LB agar plate, to select entry clones (since the pDonrP2r-P3 contains a kanamycin resistance gene). Resultant single colonies were chosen for PCR amplification, using M13 forward and reverse primers, which are either side of the insert (Fig A4 A), to create a PCR product suitable for sequencing analysis. Sequencing analysis enabled a single clone to be selected, which had the same (Asp to Glu) difference as found in the original pGEMTEasy p62 insertion (Fig A4 B), in addition to a second change. The new change is a TT**T** to TT**C**, both of which code for phenylalanine (Phe, F), (Fig A4 C). The second change results in coding for the same residue, so would not alter protein structure so was considered acceptable for use. Therefore, a suitable 3' entry clone for p62 was created.

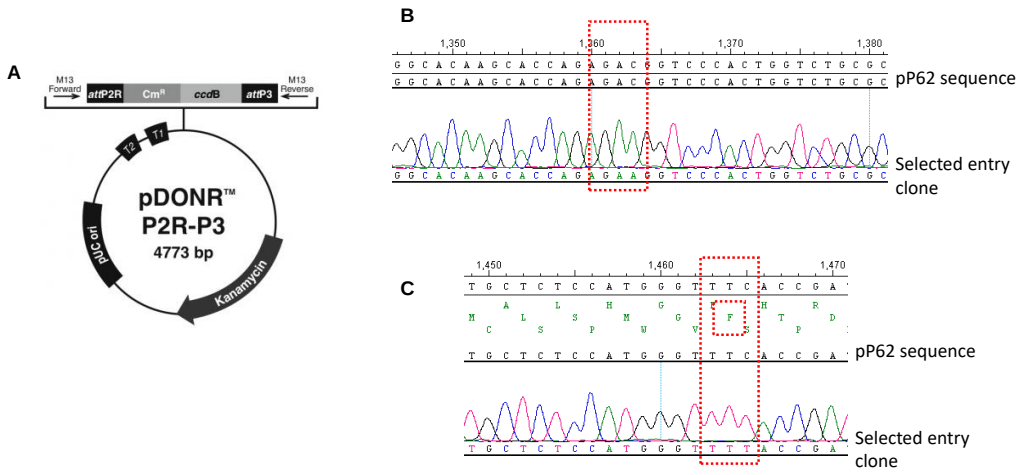

Figure A4 Entry vector sequencing

A Schematic of the pDonrP2r-P3 (Multisite Gateway® Three-Fragment Vector Construction Kit. Using Gateway® Technology to simultaneously clone multiple DNA fragments. Catalog number 12537-023. Revision date 3 January 2012. Publication Part number 25-0541 MAN0000299). **B** Aspartic acid to glutamic acid (red box) change in zebrafish cDNA sequenced from selected entry clone in comparison to the known p62 sequence (ENSDARG00000075014) **C** The base pair change of TTC to TTT found in the entry clone in comparison to the known p62 sequence (ENSDARG00000075014).

Generation of the expression clone pDest(lyz:GFP.p62)

After generation of the 3' p62 entry clone, all components required for assembly into the destination vector were available. As described in Figure 6.3, the destination vector used was *pDestTol2CG*, the 5' entry clone used was *p5E-lyz*, the middle entry clone was *pME-GFP-nostop*, and the generated *p3E-p62* vector was used for the 3' entry clone.

The LR reaction places the 5', ME, and 3' vectors into the destination vector through the use of location specific "att" recombination sequences. The "att" sites were originally in DNA recombination sequences in bacteriophage λ, responsible for the location of integration sites of the viral genome into the host bacterial genome, through integrase enzyme activity. These "att" sites were optimised for recombination of PCR products and vectors for the Gateway system. Small variations in the "att" sequences enable site specific recombination, which are numbered 1-4 in the Gateway system. These complementary attL and attR sites (e.g. the attL3 on 3' entry clone with the attR3 on the destination vector) are recombined by the LR clonase enzyme mix, resulting in the creation of the final destination vector, in this case *pDest(lyz:GFP.p62)*.

The LR reaction was completed according to Gateway™ protocol, with 10 femtomoles of *p5E-lyz*, *pME-GFP-nostop*, *p3E-p62*, and 20 femtomoles of *pDestTol2CG*. The LR

reaction product was transformed into TOP10 competent cells. Ampicillin resistance in the destination vector enables selection of vector after transformation. The *ccd*B gene is a “suicide gene” which inhibits the growth of *E. coli*. The *ccd*B is present between each “att” site on the destination vector and is removed when recombination is successful. Therefore any vectors where recombination has not been successful cannot grow due to the presence of the *ccdB* gene.

Selected colonies were grown overnight in Amp+ve LB enabling collection *pDest(lyz:GFP.p62)* through an mini prep (axyprep). The vector was confirmed *as pDest(lyz:GFP.p62)* with a restriction site digest (Fig 6.5) and sequencing.

Appendix 2

A reproduction license was obtained for the reproduction of a figure from (Silva et al. 2014). The first page of the reproduction license in shown below.

JOHN WILEY AND SONS LICENSE TERMS AND CONDITIONS

Aug 30, 2017

This Agreement between Sheffield University -- Josie Gibson ("You") and John Wiley and Sons ("John Wiley and Sons") consists of your license details and the terms and conditions provided by John Wiley and Sons and Copyright Clearance Center.

License Number	4178911427430
License date	Aug 30, 2017
Licensed Content Publisher	John Wiley and Sons
Licensed Content Publication	Journal of Applied Ichthyology
Licensed Content Title	Can zebrafish be a valid model to study Paget\'s disease of bone?
Licensed Content Author	I. A. L. Silva,N. Conceição,L. Michou,M. L. Cancela
Licensed Content Date	Jul 25, 2014
Licensed Content Pages	11
Type of use	Dissertation/Thesis
Requestor type	University/Academic
Format	Print and electronic
Portion	Figure/table
Number of figures/tables	1
Original Wiley figure/table number(s)	Figure 5
Will you be translating?	No
Title of your thesis / dissertation	In vivo imaging and analysis of host-pathogen interactions of intracellular pathogens

Appendix 3

Zebrafish cDNA sequence of for *atg3* and *atg5*

atg3 cDNA sequence with RT-PCR primer sites marked

```
  1 ATGCAGAACGTGATAAACTCGGTGAAAGGCACTGCTCTGGGGGTCGCGGAGTTTTTGACG  60
  1 ATGCAGAACGTGATAAACTCGGTGAAAGGCACTGCTCTGGGGGTCGCGGAGTTTTTGACG  60
  1 -M--Q--N--V--I--N--S--V--K--G--T--A--L--G--V--A--E--F--L--T-  20

 61 CCAGTTTTGAAGGAATCTAAATTTAAAGAAACTGGGGTTATAACTCCAGAGGAGTTTGTT 120
 61 CCAGTTTTGAAGGAATCTAAATTTAAAGAAACTGGGGTTATAACTCCAGAGGAGTTTGTT 120
 21 -P--V--L--K--E--S--K--F--K--E--T--G--V--I--T--P--E--E--F--V-  40

121 GCAGCAGGAGATCATCTGGTTCATCACTGTCCCACATGGAAATGGGCATCTGGAGAAGAA 180
121 GCAGCAGGAGATCATCTGGTTCATCACTGTCCCACATGGAAATGGGCATCTGGAGAAGAA 180
 41 -A--A--G--D--H--L--V--H--H--C--P--T--W--K--W--A--S--G--E--E-  60

181 GCAAAGGTGAAGCCCTATCTGCCCAATGACAAACAGTTCCTATTAACTCGAAACGTTCCA 240
181 GCAAAGGTGAAGCCCTATCTGCCCAATGACAAACAGTTCCTATTAACTCGAAACGTTCCA 240
 61 -A--K--V--K--P--Y--L--P--N--D--K--Q--F--L--L--T--R--N--V--P-  80

241 TGTTATAAGCGCTGTAAACAGATGGAGTACTCAGATGAGCTGGAGGCCATCATAGAAGAG 300
241 TGTTATAAGCGCTGTAAACAGATGGAGTACTCAGATGAGCTGGAGGCCATCATAGAAGAG 300
 81 -C--Y--K--R--C--K--Q--M--E--Y--S--D--E--L--E--A--I--I--E--E- 100

301 GACGATGGAGATGGCGGATGGGTGGACACCTTTCATAACTCGGGTGTTACAGGGGTGACT 360
301 GACGATGGAGATGGCGGATGGGTGGACACCTTTCATAACTCGGGTGTTACAGGGGTGACT 360
101 -D--D--G--D--G--G--W--V--D--T--F--H--N--S--G--V--T--G--V--T- 120

361 GAAGCTGTTCGGGAAATCTCATTGGATAATAAGGATAATATGAATATGAATGTGAAGACG 420
361 GAAGCTGTTCGGGAAATCTCATTGGATAATAAGGATAATATGAATATGAATGTGAAGACG 420
121 -E--A--V--R--E--I--S--L--D--N--K--D--N--M--N--M--N--V--K--T- 140

421 GGTGCCTGTGGAAATAGTGGAGATGACGATGATGATGAAGAAGGAGAGGCGGCAGACATG 480
421 GGTGCCTGTGGAAATAGTGGAGATGACGATGATGATGAAGAAGGAGAGGCGGCAGACATG 480
141 -G--A--C--G--N--S--G--D--D--D--D--D--E--E--G--E--A--A--D--M- 160

481 GAAGAATATGAAGAAAGTGGACTTTTGGAAACAGATGATGCCACTCTTGACACAAGTAAA 540
481 GAAGAATATGAAGAAAGTGGACTTTTGGAAACAGATGATGCCACTCTTGACACAAGTAAA 540
161 -E--E--Y--E--E--S--G--L--L--E--T--D--D--A--T--L--D--T--S--K- 180

541 ATGGCTGATTTAAGTAAAACTAAGGCCGAAGCTGGAGGGGAAGATGCCATTCTACAGACA 600
541 ATGGCTGATTTAAGTAAAACTAAGGCCGAAGCTGGAGGGGAAGATGCCATTCTACAGACA 600
181 -M--A--D--L--S--K--T--K--A--E--A--G--G--E--D--A--I--L--Q--T- 200

601 AGAACTTATGACCTGTATATCACATATGACAAATATTACCAGACCCCAAGACTATGGCTG 660
601 AGAACTTATGACCTGTATATCACATATGACAAATATTACCAGACCCCAAGACTATGGCTG 660
201 -R--T--Y--D--L--Y--I--T--Y--D--K--Y--Y--Q--T--P--R--L--W--L- 220

661 TTTGGATATGATGAGGACAGACAGCCTCTAACTGTGGATCAGATGTATGAAGACATCAGC 720
661 TTTGGATATGATGAGGACAGACAGCCTCTAACTGTGGATCAGATGTATGAAGACATCAGC 720
221 -F--G--Y--D--E--D--R--Q--P--L--T--V--D--Q--M--Y--E--D--I--S- 240

721 CAGGATCATGTTAAAAAAACCGTCACCATTGAGAATCACCCTAATCTCCCTCCACCTGCT 780
721 CAGGATCATGTTAAAAAAACCGTCACCATTGAGAATCACCCTAATCTCCCTCCACCTGCT 780
241 -Q--D--H--V--K--K--T--V--T--I--E--N--H--P--N--L--P--P--P--A- 260

781 ATGTGCTCCGTACATCCATGCAGACACGCTGAGGTGATGAAAAAGATTATCGAGACTGTG 840
781 ATGTGCTCCGTACATCCATGCAGACACGCTGAGGTGATGAAAAAGATTATCGAGACTGTG 840
261 -M--C--S--V--H--P--C--R--H--A--E--V--M--K--K--I--I--E--T--V- 280

841 GCGGAAGGAGGAGGTGAACTCGGGGTCCATATGTATCTTCTGATTTTCCTGAAATTTGTG 900
841 GCGGAAGGAGGAGGTGAACTCGGGGTCCATATGTATCTTCTGATTTTCCTGAAATTTGTG 900
281 -A--E--G--G--G--E--L--G--V--H--M--Y--L--L--I--F--L--K--F--V- 300

901 CAAGCTGTCATTCCAACAATAGAGTACGATTACACAAGGCATTTCACCATGTAG       954
901 CAAGCTGTCATTCCAACAATAGAGTACGATTACACAAGGCATTTCACCATGTAG       954
301 -Q--A--V--I--P--T--I--E--Y--D--Y--T--R--H--F--T--M--*-       317
```

***atg3* mutation site**
primers away from mutation site
primers over mutation site

atg5 cDNA sequence with RT-PCR primer sites marked

```
  1 ATGATAATGGCAGATGACAAGGATGTGCTTCGAGATGTTTGGTTTGGAAGGATACCCGCC  60
  1 ATGATAATGGCAGATGACAAGGATGTGCTTCGAGATGTTTGGTTTGGAAGGATACCCGCC  60
  1 -M--I--M--A--D--D--K--D--V--L--R--D--V--W--F--G--R--I--P--A-  20

 61 TGTTTCACACTGTCTCCAGACGAAACCACAGAGAGAGAGGCAGAACCCTACTATCTGCTC 120
 61 TGTTTCACACTGTCTCCAGACGAAACCACAGAGAGAGAGGCAGAACCCTACTATCTGCTC 120
 21 -C--F--T--L--S--P--D--E--T--T--E--R--E--A--E--P--Y--Y--L--L-  40

121 CTCCCACGGGTCAGTTACCTGACACTAGTCACTGATAAAGTCAAGAAACATTTTCTCAAA 180
121 CTCCCACGGGTCAGTTACCTGACACTAGTCACTGATAAAGTCAAGAAACATTTTCTCAAA 180
 41 -L--P--R--V--S--Y--L--T--L--V--T--D--K--V--K--H--F--L--K-  60

181 GTCATGAAGGCAGAGGATGTGGAGGAAATGTGGTTTGAACACGAGGGAACGCCTCTTAAA 240
181 GTCATGAAGGCAGAGGATGTGGAGGAAATGTGGTTTGAACACGAGGGAACGCCTCTTAAA 240
 61 -V--M--K--A--E--D--V--E--E--M--W--F--E--H--E--G--T--P--L--K-  80

241 TGGCACTATCCCATTGGTGTGTTGTTCGACCTCCATGCTTCAAACTCCGCTCTGCCCTGG 300
241 TGGCACTATCCCATTGGTGTGTTGTTCGACCTCCATGCTTCAAACTCCGCTCTGCCCTGG 300
 81 -W--H--Y--P--I--G--V--L--F--D--L--H--A--S--N--S--A--L--P--W- 100

301 AATATCACAGTGCACTTCAAGAACTTCCCAGAACAAGACTTGCTTCACTGCTCAACAAAC 360
301 AATATCACAGTGCACTTCAAGAACTTCCCAGAACAAGACTTGCTTCACTGCTCAACAAAC 360
101 -N--I--T--V--H--F--K--N--F--P--E--Q--D--L--L--H--C--S--T--N- 120

361 TCTGTGATAGAAGCACATTTCATGTCTTGCATTAAAGAGGCCGATGCACTCAAACATAAA 420
361 TCTGTGATAGAAGCACATTTCATGTCTTGCATTAAAGAGGCCGATGCACTCAAACATAAA 420
121 -S--V--I--E--A--H--F--M--S--C--I--K--E--A--D--A--L--K--H--K- 140

421 GGCCAGGTCATCAACGATATGCAGAAGAAAGACCATAAACAACTGTGGATGGGTCTGCAG 480
421 GGCCAGGTCATCAACGATATGCAGAAGAAAGACCATAAACAACTGTGGATGGGTCTGCAG 480
141 -G--Q--V--I--N--D--M--Q--K--K--D--H--K--Q--L--W--M--G--L--Q- 160

481 AATGATAAATTTGACCAGTTCTGGGCCATGAATCGCAAACTCATGGAGTATCCCACCGAA 540
481 AATGATAAATTTGACCAGTTCTGGGCCATGAATCGCAAACTCATGGAGTATCCCACCGAA 540
161 -N--D--K--F--D--Q--F--W--A--M--N--R--K--L--M--E--Y--P--T--E- 180

541 GAGGGAGGCTTTCGGTATATCCCCTTTAGAATATATCAGACTATGAGTGACAGACCATTC 600
541 GAGGGAGGCTTTCGGTATATCCCCTTTAGAATATATCAGACTATGAGTGACAGACCATTC 600
181 -E--G--G--F--R--Y--I--P--F--R--I--Y--Q--T--M--S--D--R--P--F- 200

601 ATCCAGACGCTCTTCCGACCAGTGTCTTCTGAAGGCCAAGCGCTTACACTGGGAGACCTG 660
601 ATCCAGACGCTCTTCCGACCAGTGTCTTCTGAAGGCCAAGCGCTTACACTGGGAGACCTG 660
201 -I--Q--T--L--F--R--P--V--S--S--E--G--Q--A--L--T--L--G--D--L- 220

661 CTGAAGGAGCTGTTTCCTGCTGCCATTGAGGATGAGCCAAAGAAATTCCAGGTTATGATT 720
661 CTGAAGGAGCTGTTTCCTGCTGCCATTGAGGATGAGCCAAAGAAATTCCAGGTTATGATT 720
221 -L--K--E--L--F--P--A--A--I--E--D--E--P--K--K--F--Q--V--M--I- 240

721 CACGGCATTGAACCCCTGCTAGAGACGCCCATCCAGTGGCTAAGTGAACACTTGAGCCAC 780
721 CACGGCATTGAACCCCTGCTAGAGACGCCCATCCAGTGGCTAAGTGAACACTTGAGCCAC 780
241 -H--G--I--E--P--L--L--E--T--P--I--Q--W--L--S--E--H--L--S--H- 260

781 CCCGACAACTTTCTCCACATCAGCATCATCCCTGCACCGAGTGACTGA             828
781 CCCGACAACTTTCTCCACATCAGCATCATCCCTGCACCGAGTGACTGA             828
261 -P--D--N--F--L--H--I--S--I--I--P--A--P--S--D--*-             275
```

***atg5* mutation site**
primers away from mutation site
primers over mutation site